APPLICATION OF HYDROGEN BONDING IN ASYMMETRIC HYDROGENATION

By

JIALIN WEN

A dissertation submitted to the

Graduate School-New Brunswick

Rutgers, The State University of New Jersey

In partial fulfillment of the requirements

For the degree of

Doctor of Philosophy

Graduate Program in Chemistry and Chemical Biology

Written under the direction of

Professor Xumu Zhang

And approved by

_____

_____

_____

_____

New Brunswick, New Jersey

October, 2016

ABSTRACT OF THE DISSERTATION

Application of Hydrogen Bonding in Asymmetric Hydrogenation

By JIALIN WEN

Dissertation Director:

Xumu Zhang

Hydrogen bonding has been widely observed in biosynthesis and enzyme catalysis. It plays an important role in such fields as molecular recognition, supramolecular chemistry and small molecule catalysis. A new concept of organocatalysis emerged in recent two decades. Hydrogen bonding is the keystone for thiourea catalysis or phosphoric acid catalysis. With high turnover numbers and excellent enantioselectivity, transition metal catalysis not only is the arts in academia, but also find its merit in industrial application. Homogeneous hydrogenation, among many successful transition metal catalyzed reactions, has been serving the synthetic communities for many years, both in academia or in industry. The success of secondary interaction and hydrogen bonding offer us an alternative: the combination of hydrogen bonding and steric hindrance help to create a chiral environment in which substrates could be reduced efficiently.

Guided by this rationale, a ferrocene-based bisphosphine/thiourea ligand, ZhaoPhos was synthesized in our group. It was applied in the asymmetric hydrogenation of nitroolefins with hydrogen bonding between the ligand and substrates. Thiourea-carbonyl hydrogen bonding is another model of non-covalent interaction. Therefore, the asymmetric hydrogenation of unsaturated carbonyl compounds is also practical. Besides neutral compounds, ionic unsaturated substrates could form non-covalent interactions with thiourea through anion binding as well. It makes the asymmetric reduction of iminium ions and *N*-heteroaromatics (quinolines, isoquinolines and indoles) possible. These type of unsaturated compounds were challenging for traditional transition metal catalyzed hydrogenation. They could now be achieved with high enantioselectivity with a rhodium/ZhaoPhos complex. An outer-sphere mechanism involving hydride transfer was proposed since these substrates were thought to lack of coordinating ability to the metal center.

As a traditional catalytic system, rhodium/bisphosphine complexes have been applied to catalyze hydrogenation of C=C bonds in a long time. The application in hydrogenation of non- or weak coordinating unsaturated compounds changed our view towards of this class of complexes. In the meanwhile, the role of hydrogen bonding is still a mechanistically unexplored area: what is the geometry of the ligand-substrate complex? How does the hydrogen bonding influence the activation energy in the transition state? Many in-depth studies are needed in the future.

Acknowledgement

I express my sincere gratitude to Professor Xumu Zhang. He accepted me as his graduate student four years ago when I was experiencing a very hard time in my Ph.D. study in Rutgers. In the Zhang Group, Xumu respects group members and gives us autonomy in research. He has a broad knowledge in both organometallic and organic chemistry. As a good educator, he always encourages us to explore more in the chemistry. We had a wonderful time in discussing and troubleshooting. Xumu is a highly self-motivated scholar, his hard-working and devoted attitude sets a vivid example to us, whipping us to become immersed in chemistry. With many-year experience in ligand design and sharp intuition, Xumu always helped us overcome difficulties.

I am also grateful to Professor Alan Goldman and Professor Ralf Warmuth. Alan is an expert in organometallic chemistry and always be rigorous to science. During my graduate study, each time we have a meeting he would get the point and came up with sharp questions. I took Ralf's organic spectroscopy course when I was in my second year in Rutgers. He is an encouraging educator and his course is practical with skills in NMR and MS analysis. He also enlightened me to take entropy into consideration in catalysis when I was preparing my qualification presentation. Before that, I underestimated the role of entropy, treating enthalpy as the main issue.

I would like to thank Professor Hong Yan of Nanjing University. She led me into the real world of researching chemistry. As an undergraduate student, I began to learn to do

and think as a chemist since I joined her group in 2009. The Yan group is warm family, in which I had a happy time.

After I joined the Zhang group, I was welcomed by the former group members. Dr. Kexuan Huang and Dr. Mingxin Chang were the senior student and they were instructive to beginners like me. I was lucky since Kexuan and Mingxin shared their knowledge and experience with me. Mr. Shaodong Liu, Renchang Tan Bin Qian and Ms. Lin Yao helped me a lot: we frequently discussed on latest scientific topics and brainstormed when facing a tough problem. In addition, I am grateful to their being accompany with me during routine lab work.

I want to convey my gratefulness to Dr. Qingyang Zhao and Mr. Jun Jiang. Qingyang was doing the pioneering work in the cooperative catalysis with transition metal and thiourea hydrogen bonding. He guided me to explore a new field in asymmetric catalysis. Qingyang is a hard-working and brilliant scholar. It is a great pleasure to work with him. Mr. Jun Jiang is also my collaborator. I could not finish my research before the defense without him.

I appreciate the help from Mr. Yang Gao and Mr. Tian Zhou of the Goldman group. Yang is experienced with organometallic chemistry and his technical support enable me to gain mechanistic study. Tian is good at computational modeling: he helped me to gain the geometry of the reactive complex.

At last, I appreciate the support and love from my parents and my girlfriend. I shared my feeling with them every day, no matter happiness and sadness. They encouraged me,

they supported me and they love me. When I was suffering the darkest days, it was them who stood beside me. I gain faith, courage and confidence from them.

Dedication

谨以此论文献给我的父母　温陟良、钟秀芬

和我的未婚妻　刘畅

TABLE OF CONTENT

ABSTRACT OF THE DISSERTATION II

ACKNOWLEDGEMENT IV

LIST OF TABLES X

LIST OF FIGURES XI

LIST OF SCHEMES XII

CHAPTER ONE ..... - 1 -

BACKGROUND INTRODUCTION: THE DEVELOPMENT OF BISPHOSPHINE LIGANDS FOR ASYMMETRIC HYDROGENATION AND HYDROGEN BONDING IN ASYMMETRIC CATALYSIS .. - 1 -

1.1 INTRODUCTION TO THE DEVELOPMENT OF BISPHOSPHINE LIGANDS FOR ASYMMETRIC HYDROGENATION . - 1 -

1.2 HYDROGEN BONDING AS A SECONDARY INTERACTION IN CATALYST DESIGN ..... - 8 -

1.3 THE DEVELOPMENT OF A NOVEL BISPHOSPHINE-THIOUREA CATALYST AND THE PRELIMINARY ..... - 12 -

CHAPTER TWO ..... - 18 -

RHODIUM CATALYZED ASYMMETRIC HYDROGENATION OF *N*-UNPROTECTED IMINIUMS VIA THIOUREA-CHLORIDE ANION BINDING ..... - 18 -

2.1 INTRODUCTION ..... - 18 -

2.2 METHOD DEVELOPMENT ..... - 20 -

2.3 SUBSTRATE SCOPE OF *N*-UNPROTECTED IMINES ..... - 22 -

2.4 MECHANISTIC STUDY ..... - 23 -

2.5 SUMMARY ..... - 26 -

2.6 EXPERIMENTAL SECTION ..... - 27 -

CHAPTER THREE ..... - 43 -

STRONG BRØNSTED ACID PROMOTED ASYMMETRIC HYDROGENATION OF ISOQUINOLINES AND QUINOLINES CATALYZED BY A RH-THIOUREA CHIRAL PHOSPHINE COMPLEX VIA ANION BINDING ..... - 43 -

3.1 INTRODUCTION ..... - 43 -

3.2 METHOD DEVELOPMENT ..... - 45 -

3.3 SUBSTRATE SCOPE ..... - 47 -

3.4 NMR STUDY FOR EVIDENCE OF INTERACTION BETWEEN LIGAND AND SUBSTRATE ..... - 50 -

3.5 CONTROL EXPERIMENTS TO EVALUATE EACH UNIT IN ZHAOPHOS ..... - 51 -

3.6 DEUTERIUM LABELLING EXPERIMENTS AND PROPOSED MECHANISM ..... - 52 -

3.7 CONCLUSIONS ..... - 56 -

3.8 EXPERIMENTAL SECTION ..... - 57 -

CHAPTER FOUR 87

RHODIUM CATALYZED ASYMMETRIC SYNTHESIS OF CHIRAL INDOLINES: THE COOPERATION

OF TRANSITION METAL, BRØNSTED ACID AND THIOUREA ANION BINDING 87

4.1 INTRODUCTION 87
4.2 METHOD DEVELOPMENT 90
4.3 SUBSTRATE SCOPE 95
4.4 MECHANISTIC STUDY 96
4.5 NONLINEAR EFFECT 100
4.5 SUMMARY 102
4.6 EXPERIMENTAL SECTION 102

CHAPTER FIVE 124

RHODIUM CATALYZED ASYMMETRIC HYDROGENATION OF A, B-UNSATURATED CARBONYL COMPOUNDS VIA A THIOUREA HYDROGEN BONDING 124

5.1 INTRODUCTION 124
5.2 METHOD DEVELOPMENT 126
5.3 SUBSTRATE SCOPE 128
5.3 MECHANISTIC SDUTIES 130
5.4 CONCLUSION 133
5.5 EXPERIMENTAL SECTION 133

PUBLICATIONS 155

List of tables

Table 2.1 Optimization of conditions…….….…19
Table 2.2 Hydrogen pressure, temperature and catalyst loading…….……20
Table 2.3 Influence from additives…….....21
Table 2.4 Substrates Scope Screening…….……22
Table 2.5 Ligands study and control experiments…….……23
Table 2.6 Substrates study and control experiments…….…...24
Table 3.1, Optimization of condition……...45
Table 3.2 Counterion effect……46
Table 3.3 Substrate scope for isoquinolines……47
Table 3.4 Substrate scope for quinolines……48
Table 3.5. Ligand evaluation and control experiment…….…51
Table 4.1 Condition optimization for 2-methylindole……90
Table 4.2 Brønsted acid screening for 2,3-disustituted indole……91
Table 4.3 Substrate scope for asymmetric hydrogenation of indoles……...93
Table 4.4 Control experiments and ligand evaluation……96
Table 4.5 Counterion effects……97
Table 4.6. Nonlinear effects for Rh/ZhaoPhos catalyzed asymmetric hydrogenation of indole……99
Table 5.1 Condition optimization……125
Table 5.2 Substrate scope of hydrogenation of α,β-unsaturated amides…….127
Table 5.3 Substrate scope of hydrogenation of α,β-unsaturated esters and ketone…….128
Table 5.4 Ligand evaluation and control experiment……...130

List of figures

Figure 1.1 Early milestones in asymmetric hydrogenation……2
Figure 1.2 Atropisometric biaryl bisphosphine ligands…….….3
Figure 1.3 Some successful chiral bisphosphine ligands before 2000……3
Figure 1.4 Successful P-chiral ligands……4
Figure 1.5 Ferrocene-based chiral bisphsphine ligands…….....5
Figure 1.6 Secondary interaction between ligand and substrate via electrostatics…….8
Figure 1.7 Chiral phosphoric acid and thiourea: two wide-applied motives in small-molecule catalysis…….……10
Figure 2.1 ^{1}H NMR spectra of **ZhaoPhos** with tetrabutylammonium chloride (TBAC)…...26
Figure 3.1 NMR study for the interaction of ZhaoPhos and **3a**……...……49
Figure 4.1. Chiral Brønsted acid catalysis versus thiourea anion binding with simple Brønsted acid……...…….87
Figure 4.2 ZhaoPhos and cooperative catalysis of transition metal, Brønsted acid and thiourea anion binding……89

List of schemes

Scheme 1.1 Steric hindrance as an important factor that controls enantioselectivity….6
Scheme 1.2 Two diastereomers of catalyst-substrate complexes: secondary coordination…….7
Scheme 1.3 A novel thiourea-bisphosphine ligand: strategy of hydrogen bonding and cooperative catalysis…….....12
Scheme 1.4 Synthetic route to prepare ZhaoPhos…….12
Scheme 1.5 Asymmetric hydrogenation of nitroolefins: a preliminary example of ZhaoPhos……...13
Scheme 2.1 Chiral amine in drugs and asymmetric hydrogenation of umprotected imines with iridium/f-BINAPHINE…….18
Scheme 2.2 Extension of our Rh/Bisphosphine-Thiourea catalytic system……19
Scheme 3.1 Asymmetric hydrogenation of quinolines and isoquinolines……...44
Scheme 3.2 Deuterium labeling experiment and proposed transformation path…….53
Scheme 3.3 Outer-sphere mechanism for hydrogenation of *N*-heteroaromatics…….55
Scheme 4.1 Asymmetric hydrogenation of unprotected indole……...88
Scheme 4.2. Leveling effect of HCl in solutions…….92
Scheme 4.3. Deuterium labeling experiments…….98
Scheme 4.4 Equilibrium scheme for nonlinear effect……100

Chapter One

Background introduction: the development of bisphosphine ligands for asymmetric hydrogenation and hydrogen bonding in asymmetric catalysis

1.1 Introduction to the development of bisphosphine ligands for asymmetric hydrogenation

1.1.1 Brief history of ligands for asymmetric hydrogenation

Asymmetric hydrogenation has been proved one of the most powerful methods for chiral synthesis. Since the discovery of Wilkinson's complex[1], organometallic complexes have shown great potential and practical application in hydrogenation, both in academia and in industry. The step of theoretical study and discovery of ligands has been boosted especially in last 20 years. Although the neutral Wilkinson's catalyst $[RhCl(PPh_3)_3]$ and the cationic RhL_2^+ catalyst (developed by Schrock and Osborn later) showed impressive activity in hydrogenation of unsaturated organic compounds, enantioselectivity remained a problem in front of increasing demands of chiral bio-active molecules. In 1968, Knowles and Horner opened the door of asymmetric hydrogenation by replacing the triphenylphosphine of the Wilkinson's catalyst with chiral

monophosphines. The enantioselectivity of their attempt, however, was poor. Later, Kagan developed first bisphosphine ligand DIOP with several significant applications in asymmetric hydrogenation, proving that chirality from the backbone could offer better selectivity[2-4]. DIOP was a milestone for C2-symmetry ligand. Sooner afterwards, Knowles discovered DIPAMP[5-6], which was successfully applied in industrial synthesis of L-DOPA[7].

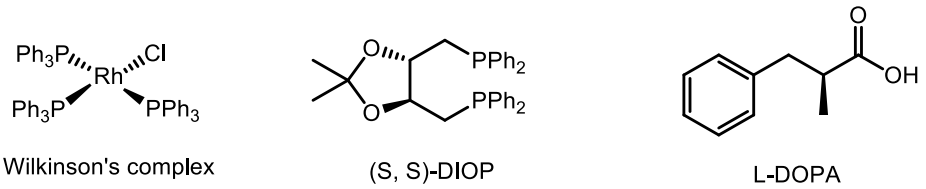

Figure 1.1 Early milestones in asymmetric hydrogenation

Another milestone of asymmetric hydrogenation is the discovery of BINAP. In 1980s, Noyori reported an atropisomeric bisphosphine ligand BINAP with C2-symmetry[8]. It was firstly applied in Rh-catalyzed asymmetric hydrogenation of α-(acylamino)acrylic acids[9]. The real breakthrough, however, was its application in Ru chemistry. Noyori and Takaya developed BINAP-Ru dicarboxylic acid complex and applied it in hydrogenation of various functionalized olefins[10]. Another breakthrough of BINAP was made in 1990s, when Noyori discovered that BINAP-Ru diamine complexes were efficient catalyst for asymmetric hydrogenation of unfunctionalized ketones[11]. Inspired by Noyori's outstanding work, chemists made a series of modifications on the BINAP system. Many excellent ligands were reported in the meanwhile or afterwards, like H8-BINAP[12-13], SEGPHOS[14], BIFAP[15]. Zhang's group developed a series of TunaPhos[16], and thoroughly studied the relationship of dihedral angel and the enantioselectivity.

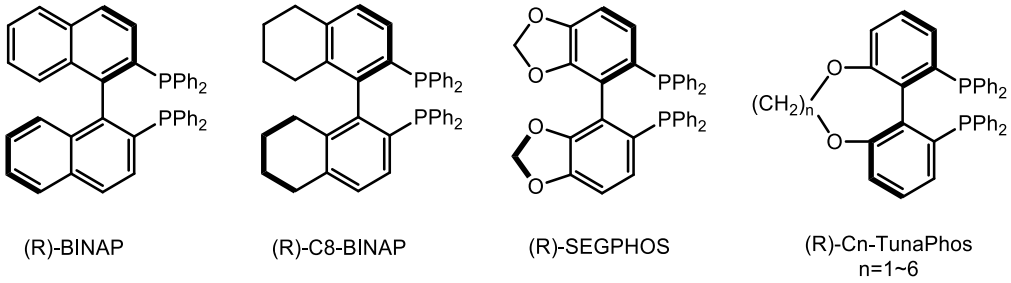

Figure 1.2 Atropisometric biaryl bisphosphine ligands

Many other bisphosphine ligands have been developed in the asymmetric hydrogenation history. One of the most famous ligands is DuPhos[17], which was first reported by Burk in early 1990's. DuPhos and its analogue BPE could catalyze Rh-hydrogenation of many substrates with extremely high efficiency and impressive enantioselectivity, such enamides, as α-(acylamino)acrylic acids, enol acetates, β-keto esters, unsaturated carboxylic acids and itaconic acids[18]. Afterwards, chemists have developed a series of modified DuPhos ligands. BASPHOS[19], CnrPhos[20], BINAPHANE[21] and PennPhos[22] are good examples of them.

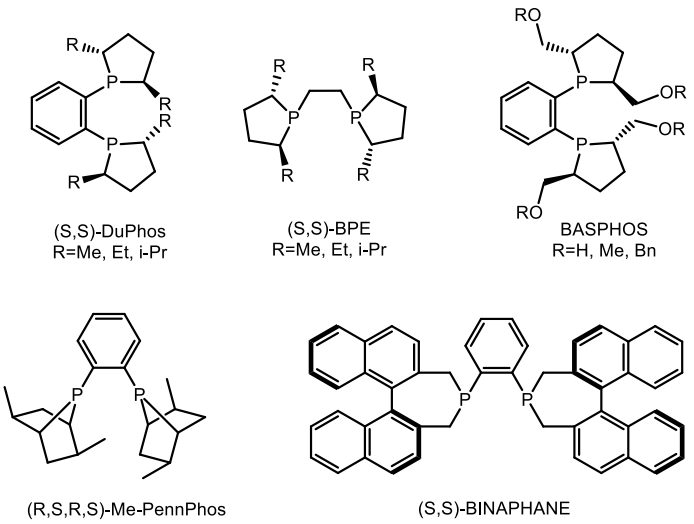

Figure 1.3 Some successful chiral bisphosphine ligands before 2000.

Another class of chiral ligands are P-chiral phosphine ligands. The discovery of new P-chiral phosphine ligands has been very slow since the first discover of DIPAMP[5],

which was developed by Knowles over 30 years ago. This is mainly due to the difficulty of synthesis. However, several excellent ligands with P-chirality have shown huge potential use in synthesis. From BisP*[23], MiniPhos[24], BIPNOR[25], they show good enantioselectivity in asymmetric Rh-hydrogenation of useful substrates, such as α-dehydroamino acids, enamides, α-(acylamino)cinnamic acids, and β-(acylamino) acrylates. Zhang's group have developed a series of rigid P-chiral phosphine ligands. TangPhos[26], DuanPhos[27] and ZhangPhos[28], bearing similar structure, could render different performance towards various substrates due to different steric and electronic effects.

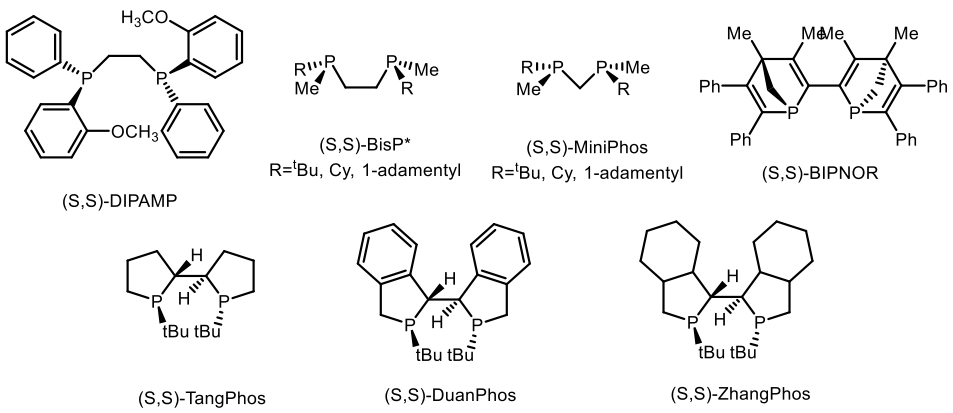

Figure 1.4 Successful P-chiral ligands

Another group are ligands with ferrocene backbone. The first ferrocene-based ligand, TRAP[29-30], was developed by Ito. Modification was done on TRAP, which led to a series of efficient ligands. Togni and Spindler reported a class of non-C2-symmetrical ferrocene-based bisphosphine ligand: Josiphos[31]. This family of ligands not only show effectiveness in academic research, but have excellent industrial application. PPF-tBu has been applied in commercial asymmetric hydrogenation for (+)-biotin[32], while XyliPhos in Ir-catalyzed hydrogenation for synthesis of (S)-metolachlor[33]. Zhang has

reported several C2-symmetric ferrocene-base ligands, such as f-binaphane[34].

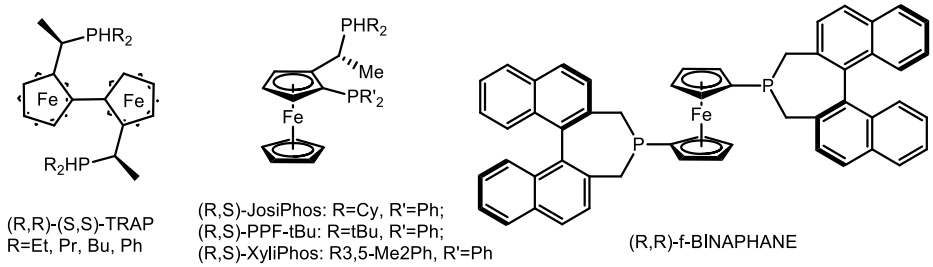

Figure 1.5 Ferrocene-based chiral bisphsphine ligands

1.1.2 Trends in ligand design

The pillar of asymmetric hydrogenation is chiral ligands and therefore the design of new ligand is always a demand. Today, chemists have developed thousands of chiral ligands. However, only a few of these ligands could offer both efficiency and selectivity for industrial application. In addition, there are no universal excellent catalysts for all different types of substrates. Two main problems manacle the application of transition metal catalyzed asymmetric hydrogenation: (1) limited substrate scope, (2) high catalyst loading. The demand of new effective ligands is greatly in need.

In order to create suitable chiral environment, ligand designers have been sailing towards two different directions to achieving high enantioselectivity: 1) increasing the steric hindrance and the rigidity of the ligand skeleton; 2) introducing secondary interaction to enlarge the energetic difference of two diastereometic catalyst-substrate complexes in the transition state.

In a long time, the strategy for ligand design has been focused on steric effect: by introducing proper steric hindrance, high enantioselectivity is achieved. A good example of the first strategy is the development of spiro scaffold. The success of BINAP inspired chemists to develop a new generation of bisphosphine ligands with large steric

hindrance. Bisphosphine ligands with spirobiindane and spirobifluorene[35] scaffolds were synthesized in the recent decade. Crystalline analysis[35] of palladium/ bisphosphine complex Pd(II)Cl_2(P-P) revealed the tendency of increasing P-Pd-P bite angles from BIANP to SDP and SFDP (Scheme 1.1). Another benefit from large steric hindrance is the rigidity of ligands. Like the evolution from TangPhos to DuanPhos and then ZhangPhos, increasing steric hindrance renders high rigidity of the ligand, thus strengthening the coordinating ability and increasing enantioselectivity. In the case of ruthenium catalyzed asymmetric hydrogenation of α,β-unsaturated carboxylic acid, we could clearly observe the positive correlation of the enantioselectivity with steric hindrance[35].

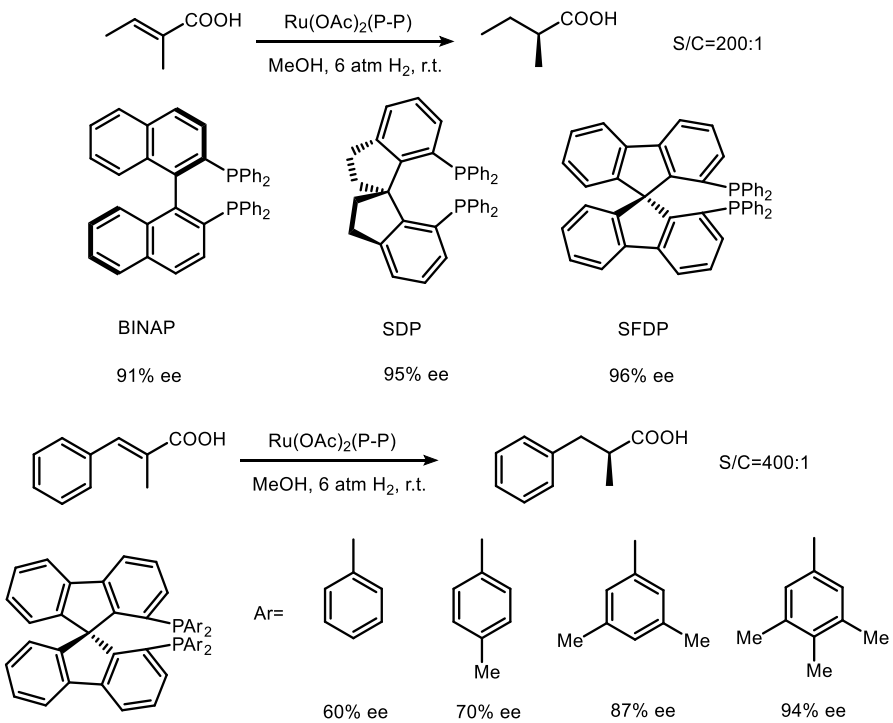

Scheme 1.1 Steric hindrance as an important factor that controls enantioselectivity.

Another guideline is secondary interaction. Secondary interaction is not rare in asymmetric hydrogenation. In the classic Rh catalyzed asymmetric hydrogenation of

ethyl-α-acetamidocinnamate, Halpern[36] conducted a series of experimental research to explore the origin of enantioselectivity. Solid evidence from X-ray crystal structure of the Rh(I)(P-P)/enamide complex revealed the existence of secondary interaction: the oxygen atom from the acetyl group coordinates with the cationic Rh(I) metal while the C=C bond coordinates, forming a co-planar complex. Other than Rh catalyzed hydrogenation of acetamides, this type of bischelate coordination of substrate to the transition metal has been found in many hydrogenation cases, such as Ir or Ru catalyzed

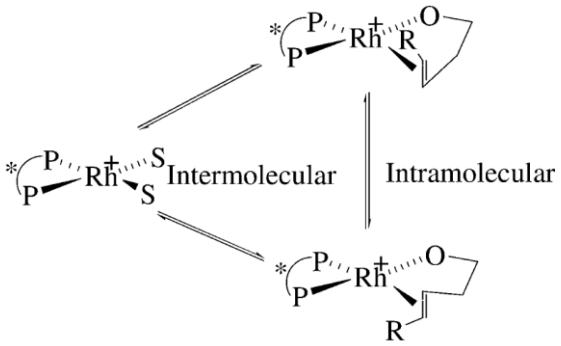

hydrogenation of unsaturated carboxylic acids.

Scheme 1.2 Two diastereomers of catalyst-substrate complexes: secondary coordination.

Ligand-substrate interaction is another strategy for high enantioselectivity. With this type of interaction, the difference in energy of different conformers that coordinate with the metal center is enlarged. Trifer[37] and ChenPhos[38], which were developed by Chen, are good examples of non-covalent secondary interaction. When catalyzing the hydrogenation of α-substituted carboxylic acids, a charge-charge interaction is formed between the tertiary ammonium on TriFer and ChenPhos and the carboxylate anion.[39] Hydrogen bond is also believed to be responsible for the remarkable enantioselectivity

in Rh catalyzed hydrogenation of allylic alcohol.

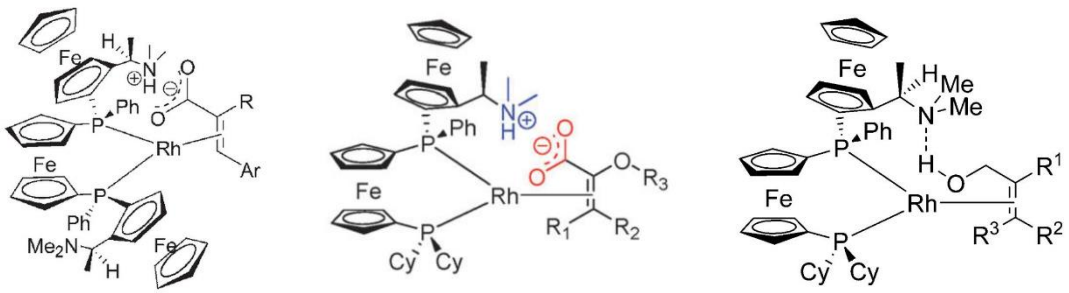

Figure 1.6 Secondary interaction between ligand and substrate via electrostatics.

The pursuit of high rigidity and large steric hindrance will bring a problem: the synthetic difficulty and long synthetic route of the ligand will dramatically increase its cost for application. Poor accessibility becomes a major obstacle for many synthetic methodologies. Zhou developed a series of spiro-based ligands[35]: C2-bisphosphine ligands, P-N ligands and tri-dented P-N-N ligands. They highly efficient for the asymmetric hydrogenation of simple ketones and imines with remarkable enantioselectivities. The major problem that keeps the catalysts from being widely applied is the accessibility. The key precursor of spiro-base ligands is the optically pure SPINOL, which requires seven steps[40] in the synthetic route. In addition, resolution with a cinchonidine derivative is needed. The optimized overall yield is about 11%. From chiral SPINOL, many steps lead to the reactive ligands. Industry is seeking for efficient catalysts with low cost and this is why chemical practitioners are keeping developing novel catalytic methods.

1.2 Hydrogen bonding as a secondary interaction in catalyst design

Hydrogen bond[41] (H-bond) is one of the most commonly observed and studied non-covalent interaction in nature. Recent two decades have seen the boost of the application

of H-bonding in small molecule catalysis. A concept of organocatalysis[42-43] emerged in recent years and the core idea of this transition metal-free lies on non-covalent interactions, such as electrostatics, H-bonding, cation-π interaction or π-π stacking[44-48]. Pioneering studies involving hydrogen donor catalysts revealed an interesting conclusion that in some cases, H-bonding shows comparative activating ability to Lewis acids. Aimed to develop a strategy to activate the electrophile for the electrophile-nucleophile reactions, H-bonding is designed to lowering the lowest unoccupied molecular orbital (LUMO) [49-52], and therefore decrease the energy barrier in the transition states.

Two families of organocatalysis involving this non-covalent interaction are thiourea and phosphoric acid. While the bifunctional activation sites within phosphoric acids are the P=O and O-H group, thiourea is highly tunable: many secondary interactions could be incorporated with covalent bonds (Figure). We envision that the incorporation of transition metal and thiourea will be a good solution for a bifunctional catalysis. In thiourea organocatalysis, other non-covalent interaction, such as electrostatics or cation-π, serves as a secondary interaction. We attempt to apply thiourea H-bonding as a secondary interaction. It seems to be meaningless to distinguish the primary or the secondary interaction.

Many non-covalent interaction models have been established in the mechanistic studies of thiourea catalyzed organic reactions. Carbonyl, imine, halide anion, sulfonate and phosphonate anion are good hydrogen acceptors and their binding with thiourea has been studied, both qualitatively and quantitatively. Nucleophilic addition, conjugate

addition, ring opening, rearrangement, Friedel-Crafts Reaction, Diels-Alder reaction are among successful examples of small molecule catalysis with thiourea as the hydrogen donor. Although the activating potency and directionality is weaker than metal Lewis acids, hydrogen bond is softer and more tolerate to functional groups. With appropriate conformation and geometry, H-bonding can also activate electrophiles efficiently.

Anion binding, a subsidiary of H-bonding, originated in anion recognition and supramolecular chemistry, has been employed in asymmetric catalysis[48, 53-54]. Not like the pattern of activating the electrophile in thiourea-carbonyl H-bonding, anion binding behaves differently: it establishes an association between an active reactant and the thiourea catalyst. Electrostatics usually connects the cationic reactant and the chiral catalyst, thus introducing chirality in the product. Similarly, a secondary interaction is commonly responsible for high enantioselectivity and reactivity.

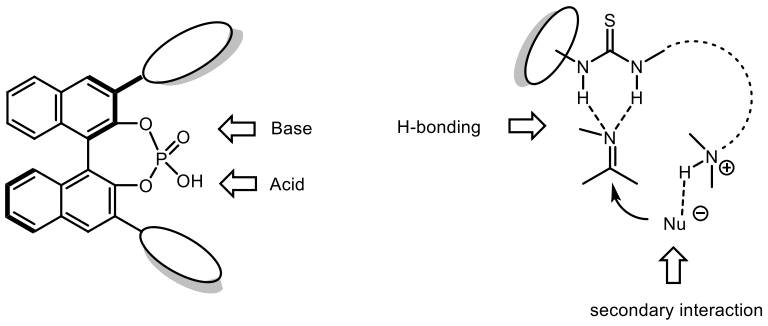

Figure 1.7 Chiral phosphoric acid and thiourea: two wide-applied motives in small-molecule catalysis.

The strategy of cooperative catalysis emerged in recent years, aiming to combine two or more catalytic centers to achieve a single reaction.[55-59] Recently, several breakthroughs were made with the application of this strategy in several kinds of reactions, such as Pararov reaction[60], hydrogenation[61], hydroformylation[62-64] and Diels-

Alder reaction[65]. The combination of thiourea/urea derivatives and simple Brønsted acids offers a similar effect to chiral phosphoric acids, but it can render a broader acidity range. Moreover, tunable substituents on bifunctional thiourea/urea catalysts can introduce many kinds of secondary interactions.[44-48] By establishing a bridge between the thiourea and the conjugate base anion of the Brønsted acid, anion binding makes the chiral catalyst associate with a protonated substrate. This strategy combines the essences of both approaches. Transition metal catalysis, with high turnover numbers and potent reactivity, plays a crucial role in synthetic chemistry. It shows a very broad application in pharmaceutical and fine chemical industries. The integration of transition metal catalysis and small molecule organocatalysis has shown its potential in the synthetic chemistry communities.[58-59] We envision that certain kinds of reactions could be catalyzed by the cooperative catalysis of transition metal, Brønsted acid and thiourea anion binding.

As quoted by R. Knowles and E. Jacobsen[66], in order to achieve high enantioselectivity, “small molecule catalysts are designed to introduce steric hindrance to increase the transition state energy of one diastereomer of the two catalyst-substrate complexes; while macromolecule catalysis is to lowering the energy of transition state for one enantiomer.” Non-covalent interactions, such as hydrogen bonding, cation-π or anion-π interaction, π-π stacking are easily found in enzyme catalysis. With remarkably high enantioselectivity and efficiency, the latter strategy deserves more attention in catalytic organic reactions.

This thesis is mainly focused on H-bonding as a second interaction, aiming to explore

its application of in asymmetric hydrogenation.

1.3 The development of a novel bisphosphine-thiourea catalyst and the preliminary examples of its application.

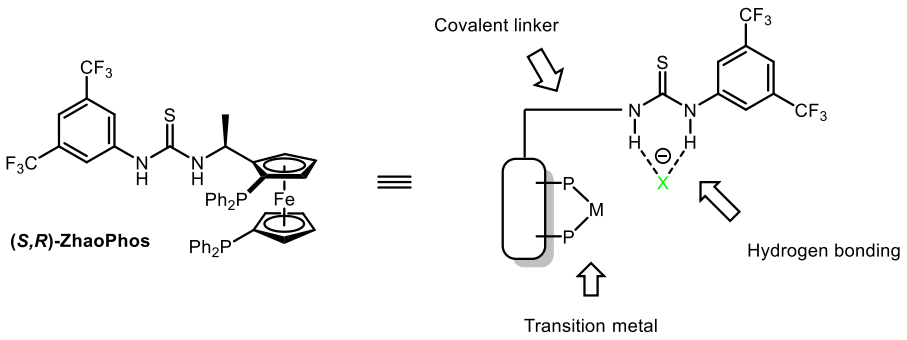

Scheme 1.3 A novel thiourea-bisphosphine ligand: strategy of hydrogen bonding and cooperative catalysis.

Guided by such strategies as cooperative catalysis and H-bonding effect, we recently designed and synthesized a ferrocene-based bisphosphine-thiourea catalyst, ZhaoPhos[67]. Previous successful examples involved non-covalent interactions between catalytically reactive units, such as ion pair and hydrogen bond. Within ZhaoPhos, a covalent linker connects the transition metal unit and the thiourea moiety. The length the linker is believed to be crucial for high efficiency and selectivity.

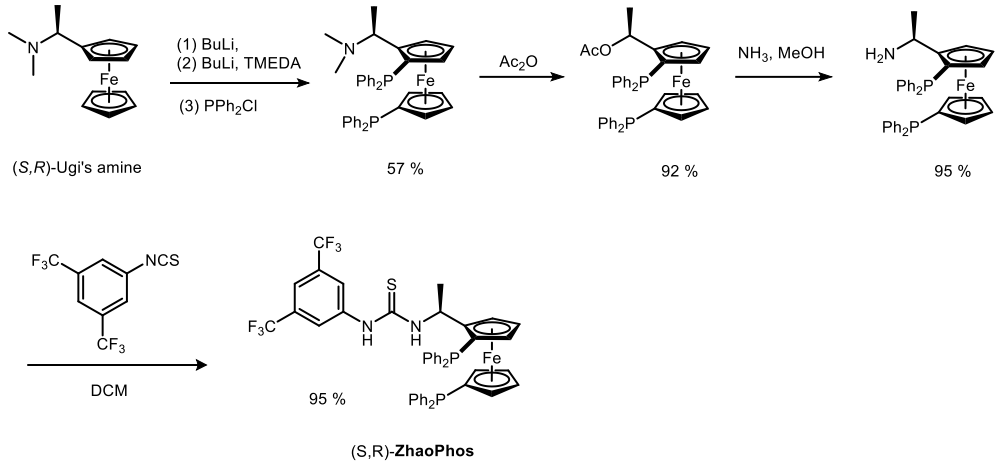

Scheme 1.4 Synthetic route to prepare ZhaoPhos.

Preparation of ZhaoPhos is readily reported in the preliminary work in our group by Dr. Qingyang Zhao.[67] From commercially available chiral Ugi's amine, only four steps are required to synthesize this ligand (Scheme 1.4). This route is mature: a 10-gram-scale preparation can easily proceed with good repeatability.

ZhaoPhos has been successfully applied in asymmetric hydrogenation of nitroolefins with remarkable enantioselectivity. Control experiments were conducted to confirm the cooperation of thiourea and the ferrocene-based bisphosphine ligand. Based on reports in organocatalysis, a thiourea-nitro interaction was proposed. This secondary interaction was believed to bring dual benefit: (1) activate the conjugate C=C bonding by hydrogen bonding; (2) create a suitable chiral environment and therefore help to obtain good enantioselectivity.

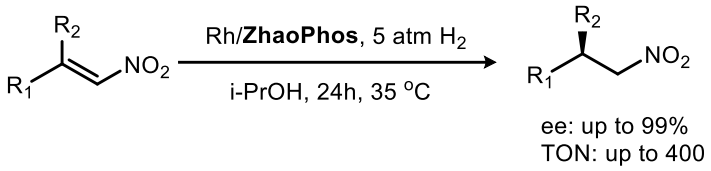

Scheme 1.5 Asymmetric hydrogenation of nitroolefins: a preliminary example of ZhaoPhos.

By applying this synthetic route, a series of ferrocene-based bisphosphine-thiourea ligands have been successfully prepared. Conjugate nitroolefins with various substituents on β-position have been successfully reduced. Control experiments support the assumption that thiourea and bisphosphine cooperate within a catalyst molecule. The covalent linker is crucial for effective catalysis.

The preliminary results inspired us to explore its broader application of this strategy in asymmetric catalysis.

1. Osborn, J. A.; Jardine, F. H.; Young, J. F.; Wilkinson, G., *J. Chem. Soc. A* **1966**, 1711.
2. Kagan, H. B.; Dang, T. P., *Chem. Commun.* **1971**, 481.
3. Kagan, H. B.; Dang, T. P., *J. Am. Chem. Soc.* **1972,** *94*, 6429.
4. Kagan, H. B.; Langlois, N.; Dang, T. P., *J. Organomet. Chem.* **1975,** *90*, 353.
5. Vineyard, B. D.; Knowles, W. S.; Sabacky, M. J.; Bachman, G. L.; Weinkauff, D. J., *J. Am. Chem. Soc.* **1977,** *99*, 5946.
6. Knowles, W. S., *Acc. Chem. Res.* **1983,** *16*, 106.
7. Knowles, W. S., *J. Chem. Educ.* **1986,** *63*, 222.
8. Miyashita, A.; Yasuda, A.; Takaya, H.; Toriumi, K.; Ito, T.; Souchi, T.; Noyori, R., *J. Am. Chem. Soc.* **1980,** *102*, 7932.
9. Miyashita, A.; Takaya, H.; Souchi, T.; Noyori, R., *Tetrahedron* **1984,** *40*, 1245.
10. Noyori, R.; Ohta, M.; Hsiao, Y.; Kitamura, M.; Ohta, T.; Takaya, H., *J. Am. Chem. Soc.* **1986,** *108*, 7117.
11. Ohkuma, T.; Ooka, H.; Hashiguchi, S.; Ikariya, T.; Noyori, R., *J. Am. Chem. Soc.* **1995,** *117*, 2675.
12. Zhang, X.; Mashima, K.; Koyano, K.; Sayo, N.; Kumobayashi, H.; Akutagawa, S.; Takaya, H., *Tetrahedron Lett.* **1991,** *32*, 7283.
13. Zhang, X.; Mashima, K.; Koyano, K.; Sayo, N.; Kumobayashi, H.; Akutagawa, S.; Takaya, H., *J. Chem. Soc., Perkin Trans. 1* **1994**, 2309.
14. Saito, T.; Yokozawa, T.; Ishizaki, T.; Moroi, T.; Sayo, N.; Miura, T.; Kumobayashi, H., *Adv. Synth. Catal.* **2001,** *343*, 264.
15. Sollewijn Gelpke, A. E.; Kooijman, H.; Spek, A. L.; Hiemstra, H., *Chem. Eur. J.* **1999,** *5*, 2472.
16. Zhang, Z.; Qian, H.; Longmire, J.; Zhang, X., *J. Org. Chem.* **2000,** *65*, 6223.
17. Burk, M. J.; Harlow, R. L., *Angew. Chem., Int. Ed. Engl.* **1990,** *29*, 1462.
18. Burk, M., *J. Acc. Chem. Res.* **2000,** *33*, 363.
19. Holz, J.; Heller, D.; Stürmer, R.; Börner, A., *Tetrahedron Lett.* **1999,** *40*, 7059.
20. Marinetti, A.; Buzin, F. X.; Ricard, L., New Chiral Dichlorophosphines and Their Use in the Synthesis of Phosphetane Oxides and Phosphinic Chlorides. *J Org Chem* **1997,** *62* (2), 297-301.
21. Xiao, D.; Zhang, Z.; Zhang, X., *Org. Lett.* **1999,** *1*, 1679.
22. Jiang, Q.; Jiang, Y.; Xiao, D.; Cao, P.; Zhang, X., *Angew. Chem., Int. Ed. Engl.* **1998,** *37*, 1100.
23. Imamoto, T.; Watanabe, J.; Wada, Y.; Masuda, H.; Yamada, H.; Tsuruta, H.; Matsukawa, S.; Yamaguchi, K., *J. Am. Chem. Soc.* **1998,** *120*, 1635.
24. Yamanoi, Y.; Imamoto, T., Methylene-Bridged P-Chiral Diphosphines in Highly Enantioselective Reactions. *J Org Chem* **1999,** *64* (9), 2988-2989.
25. Robin, F.; Mercier, F.; Ricard, L.; Mathey, F.; Spagnol, M., *Chem. Eur. J.* **1997,** *3*, 1365.
26. Tang, W.; Zhang, X., *Angew. Chem., Int. Ed. Engl.* **2002,** *41*, 1612.
27. Liu, D.; Zhang, X., Practical P-Chiral Phosphane Ligand for Rh-Catalyzed Asymmetric Hydrogenation. *European Journal of Organic Chemistry* **2005,** *2005* (4), 646-649.
28. Zhang, X.; Huang, K.; Hou, G.; Cao, B.; Zhang, X., Electron-Donating and Rigid P-Stereogenic Bisphospholane Ligands for Highly Enantioselective Rhodium-Catalyzed Asymmetric Hydrogenations. *Angewandte Chemie* **2010,** *122* (36), 6565-6568.
29. Sawamura, M.; Kuwano, R.; Ito, Y., *J. Am. Chem. Soc.* **1995,** *117*, 9602.
30. Sawamura, M.; Hamashima, H.; Sugawara, M.; Kuwano, N.; Ito, Y., *Organometallics* **1995,** *14*, 4549.
31. Togni, A.; Breutel, C.; Schnyder, A.; Spindler, F.; Landert, H.; Tijani, A., *J. Am. Chem. Soc.* **1994,**

116, 4062.

32. McGarrity, J.; Spindler, F.; Fuchs, R.; Eyer, M., *Chem. Abstr.* **1995,** *122*, P81369q.

33. Blaser, H. U.; Buser, H. P.; Coers, K.; Hanreich, R.; Jalett, H. P.; Jelsch, E.; Pugin, B.; Schneider, H. D.; Spindler, F.; Wegmann, A., *Chimia* **1999,** *53*, 275.

34. Xiao, D.; Zhang, X., *Angew. Chem., Int. Ed. Engl.* **2001,** *40*, 3425.

35. Xie, J.-H.; Zhou, Q.-L., Chiral Diphosphine and Monodentate Phosphorus Ligands on a Spiro Scaffold for Transition-Metal-Catalyzed Asymmetric Reactions. *Accounts of Chemical Research* **2008,** *41* (5), 581-593.

36. de Vries, J. G.; Elsevier, C. J., *The handbook of homogeneous hydrogenation*. Wiley-VCH: 2007.

37. Chen, W.; McCormack, P. J.; Mohammed, K.; Mbafor, W.; Roberts, S. M.; Whittall, J., Stereoselective Synthesis of Ferrocene-Based C2-Symmetric Diphosphine Ligands: Application to the Highly Enantioselective Hydrogenation of α-Substituted Cinnamic Acids. *Angewandte Chemie International Edition* **2007,** *46* (22), 4141-4144.

38. Chen, W.; Spindler, F.; Pugin, B.; Nettekoven, U., ChenPhos: Highly Modular P-Stereogenic C1-Symmetric Diphosphine Ligands for the Efficient Asymmetric Hydrogenation of α-Substituted Cinnamic Acids. *Angewandte Chemie International Edition* **2013,** *52* (33), 8652-8656.

39. Yao, L.; Wen, J.; Liu, S.; Tan, R.; Wood, N. M.; Chen, W.; Zhang, S.; Zhang, X., Highly enantioselective hydrogenation of [small alpha]-oxy functionalized [small alpha],[small beta]-unsaturated acids catalyzed by a ChenPhos-Rh complex in CF3CH2OH. *Chemical Communications* **2016,** *52* (11), 2273-2276.

40. Xie, J.-H.; Wang, L.-X.; Fu, Y.; Zhu, S.-F.; Fan, B.-M.; Duan, H.-F.; Zhou, Q.-L., Synthesis of Spiro Diphosphines and Their Application in Asymmetric Hydrogenation of Ketones. *Journal of the American Chemical Society* **2003,** *125* (15), 4404-4405.

41. Pihko, P. M., *Hydrogen Bonding in Organic Synthesis*. Wiley: 2009.

42. Jacobsen, E. N.; MacMillan, D. W. C., Organocatalysis. *Proceedings of the National Academy of Sciences* **2010,** *107* (48), 20618-20619.

43. MacMillan, D. W. C., The advent and development of organocatalysis. *Nature* **2008,** *455* (7211), 304-308.

44. Doyle, A. G.; Jacobsen, E. N., Small-Molecule H-Bond Donors in Asymmetric Catalysis. *Chemical Reviews* **2007,** *107* (12), 5713-5743.

45. Zhang, Z.; Schreiner, P. R., (Thio)urea organocatalysis-What can be learnt from anion recognition? *Chemical Society Reviews* **2009,** *38* (4), 1187-1198.

46. Takemoto, Y., Development of Chiral Thiourea Catalysts and Its Application to Asymmetric Catalytic Reactions. *Chemical and Pharmaceutical Bulletin* **2010,** *58* (5), 593-601.

47. Taylor, M. S.; Jacobsen, E. N., Asymmetric Catalysis by Chiral Hydrogen-Bond Donors. *Angewandte Chemie International Edition* **2006,** *45* (10), 1520-1543.

48. Brak, K.; Jacobsen, E. N., Asymmetric Ion-Pairing Catalysis. *Angewandte Chemie International Edition* **2013,** *52* (2), 534-561.

49. Schreiner, P. R.; Wittkopp, A., H-Bonding Additives Act Like Lewis Acid Catalysts. *Organic Letters* **2002,** *4* (2), 217-220.

50. Pihko, P. M., Activation of Carbonyl Compounds by Double Hydrogen Bonding: An Emerging Tool in Asymmetric Catalysis. *Angewandte Chemie International Edition* **2004,** *43* (16), 2062-2064.

51. Huynh, P. N. H.; Walvoord, R. R.; Kozlowski, M. C., Rapid Quantification of the Activating Effects of Hydrogen-Bonding Catalysts with a Colorimetric Sensor. *Journal of the American Chemical Society*

2012, *134* (38), 15621-15623.

52. Walvoord, R. R.; Huynh, P. N. H.; Kozlowski, M. C., Quantification of Electrophilic Activation by Hydrogen-Bonding Organocatalysts. *Journal of the American Chemical Society* **2014,** *136* (45), 16055-16065.

53. Phipps, R. J.; Hamilton, G. L.; Toste, F. D., The progression of chiral anions from concepts to applications in asymmetric catalysis. *Nat Chem* **2012,** *4* (8), 603-614.

54. Mahlau, M.; List, B., Asymmetric Counteranion-Directed Catalysis: Concept, Definition, and Applications. *Angewandte Chemie International Edition* **2013,** *52* (2), 518-533.

55. Rueping, M.; Koenigs, R. M.; Atodiresei, I., Unifying Metal and Brønsted Acid Catalysis—Concepts, Mechanisms, and Classifications. *Chemistry – A European Journal* **2010,** *16* (31), 9350-9365.

56. Allen, A. E.; MacMillan, D. W. C., Synergistic catalysis: A powerful synthetic strategy for new reaction development. *Chemical Science* **2012,** *3* (3), 633-658.

57. Meeuwissen, J.; Reek, J. N. H., Supramolecular catalysis beyond enzyme mimics. *Nat Chem* **2010,** *2* (8), 615-621.

58. Du, Z.; Shao, Z., Combining transition metal catalysis and organocatalysis - an update. *Chemical Society Reviews* **2013,** *42* (3), 1337-1378.

59. Shao, Z.; Zhang, H., Combining transition metal catalysis and organocatalysis: a broad new concept for catalysis. *Chemical Society Reviews* **2009,** *38* (9), 2745-2755.

60. Xu, H.; Zuend, S. J.; Woll, M. G.; Tao, Y.; Jacobsen, E. N., Asymmetric Cooperative Catalysis of Strong Brønsted Acid–Promoted Reactions Using Chiral Ureas. *Science* **2010,** *327* (5968), 986-990.

61. Wieland, J.; Breit, B., A combinatorial approach to the identification of self-assembled ligands for rhodium-catalysed asymmetric hydrogenation. *Nat Chem* **2010,** *2* (10), 832-837.

62. Breit, B.; Seiche, W., Hydrogen Bonding as a Construction Element for Bidentate Donor Ligands in Homogeneous Catalysis: Regioselective Hydroformylation of Terminal Alkenes. *Journal of the American Chemical Society* **2003,** *125* (22), 6608-6609.

63. Diab, L.; Šmejkal, T.; Geier, J.; Breit, B., Supramolecular Catalyst for Aldehyde Hydrogenation and Tandem Hydroformylation–Hydrogenation. *Angewandte Chemie International Edition* **2009,** *48* (43), 8022-8026.

64. Šmejkal, T.; Breit, B., A Supramolecular Catalyst for Regioselective Hydroformylation of Unsaturated Carboxylic Acids. *Angewandte Chemie International Edition* **2008,** *47* (2), 311-315.

65. Gatzenmeier, T.; van Gemmeren, M.; Xie, Y.; Höfler, D.; Leutzsch, M.; List, B., Asymmetric Lewis acid organocatalysis of the Diels–Alder reaction by a silylated C–H acid. *Science* **2016,** *351* (6276), 949-952.

66. Knowles, R. R.; Jacobsen, E. N., Attractive noncovalent interactions in asymmetric catalysis: Links between enzymes and small molecule catalysts. *Proceedings of the National Academy of Sciences* **2010,** *107* (48), 20678-20685.

67. Zhao, Q.; Li, S.; Huang, K.; Wang, R.; Zhang, X., A Novel Chiral Bisphosphine-Thiourea Ligand for Asymmetric Hydrogenation of β,β-Disubstituted Nitroalkenes. *Organic Letters* **2013,** *15* (15), 4014-4017.

Chapter two

Rhodium catalyzed asymmetric hydrogenation of *N*-unprotected iminiums via thiourea-chloride anion binding

2.1 Introduction

Chiral amines are powerful pharmacophores of biologically active molecules for pharmaceuticals and agrochemicals.[1] In 2010, 45 out of the top 200 brand name drugs contained chiral amines.[2] The elastase inhibitor DMP 777, calcimimetic agent Sensipar (Cinacalcet), and type II calcimimetics NPS R-568 are the representatives of bio-active molecules (Scheme 2.1). As one of most efficient approaches to prepare chiral amines, the asymmetric hydrogenation of enamines and imines has received particular attention. To date, although a number catalytic systems has been successfully applied to their industrial production, it is still a largely underdeveloped area in contrast to the great advances in asymmetric hydrogenation of olefins and ketones.[3-5] Compared with enamines and N-protected imines, asymmetric hydrogenation of prochiral iminium salts is a more atom economical and challenging method, which eliminates the extra steps of protection and deprotection of the NH_2 group. The first example of asymmetric hydrogenation of *N*-unprotected imines with high enantioselectivity was reported by our group with well-established Ir-f-BINAPHINE catalysts.[6-8] High catalyst loading (5%), however, still

limits its application for large-scale application. We aimed to develop a novel and efficient catalytic system for this transformation.

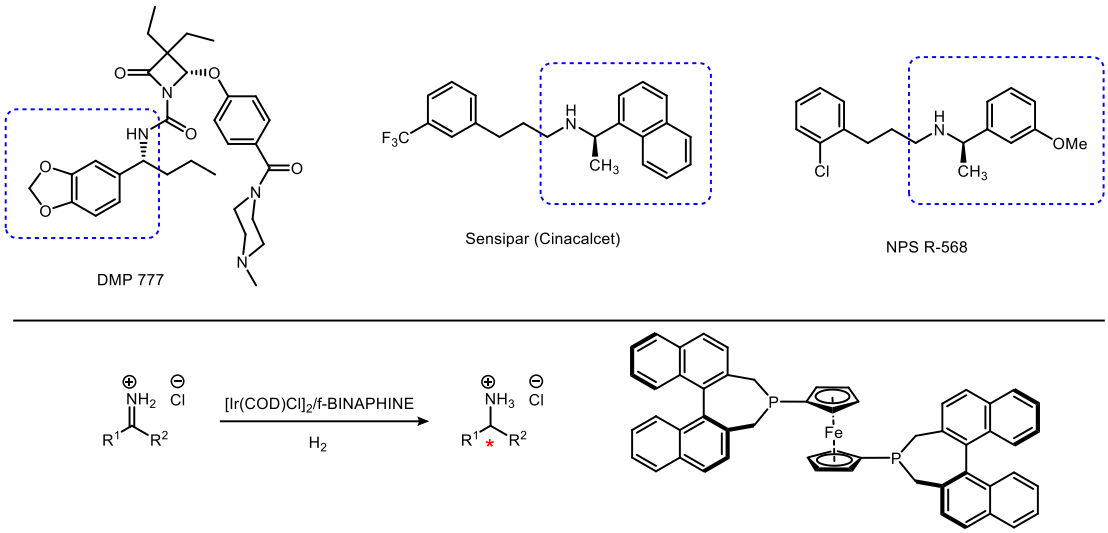

Scheme 2.1 Chiral amine in drugs and asymmetric hydrogenation of umprotected imines with iridium/f-BINAPHINE

Thiourea as have been widely used as a H-bond donor in organocatalysis.[9-11] Most research focuses on the direct activation of neutral substrates by H-bonding while more recent studies take advantage of the anion binding of ion-pairing intermediates.[12-14] Our initial work explored the activation of nitroalkenes by thioureas *via* proposed H-bonding interactions in the enantioselective hydrogenation (Scheme 2.2).[15] Inspired by the powerful strategies developed in ion-pairing catalysis,[16-24] we sought to extend the anion-binding catalysis concept to the field of asymmetric hydrogenation. Based on the reports in anion-binding catalysis, especially the enantioselective reactions of iminium ions[25] and the mechanism study[26], we envisioned that the thiourea could interact with the counteranion in the catalytic pathway (Scheme 2.2). We are looking forward to exploring the application of this Rh/bisphosphine-thiourea catalyst in asymmetric hydrogenation of N-H imines assisted by anion binding.

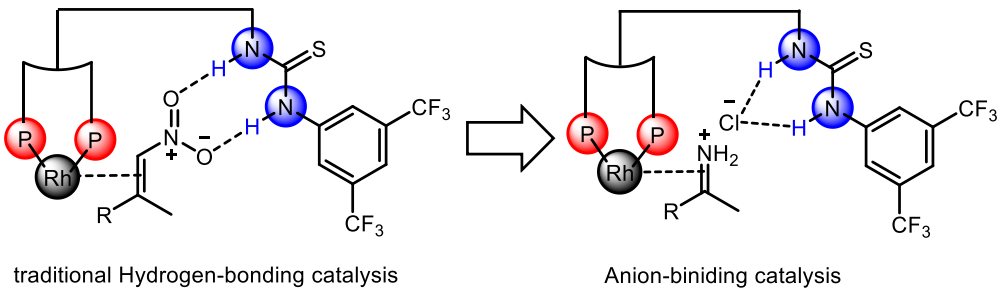

Scheme 2.2 Extension of our Rh/Bisphosphine-Thiourea catalytic system.

2.2 Method development

To evaluate the synthetic protocols, we carried out measurement of *ee*'s by chiral HPLC. In accordance with the hydrogenation of nitroolefins,[15] after careful screening of various of metal precursors, $[Rh(COD)Cl]_2$ afforded the best results and the catalytic system was solvent dependent (Table 1, entries 1-9). Excellent results were observed when the $[Rh(COD)Cl]_2$ and **ZhaoPhos** was used in protic solvents. 99% Conversion and 92% *ee* were obtained in *i*-PrOH (Table 2.1, entries 3).

Table 2.1 Optimization of conditions. [a]

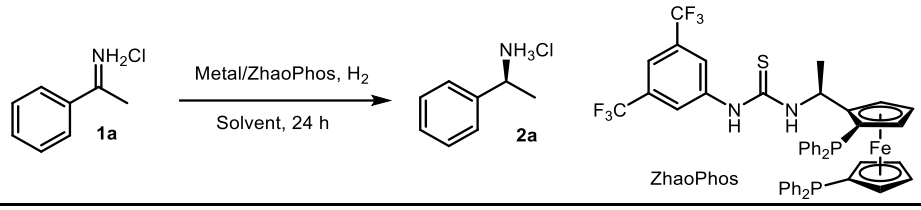

Entry	Solvent	Metal Source	S/C	Conversion [b]	*ee* [c]
1	*i*-PrOH	$[Rh(COD)_2]BF_4$	25	93%	77%
2	*i*-PrOH	$[Rh(NBD)_2]SbF_6$	25	95%	47%
3	*i*-PrOH	$[Rh(COD)Cl]_2$	25	99%	92%
4	*i*-PrOH	$[Ir(COD)Cl]_2$	25	90%	84%
5	*i*-PrOH	$Pd(OAc)_2$	25	0	ND
6	*i*-PrOH	$Pd(TFA)_2$	25	30%	0%
7	*i*-PrOH	$[RuCl_2(p\text{-cymene})]_2$	25	8%	23%

8	CH_2Cl_2	$[Rh(COD)Cl]_2$	25	91%	30%
9	Toluene	$[Rh(COD)Cl]_2$	25	60%	15%
10	THF	$[Rh(COD)Cl]_2$	25	76%	60%
11	MeOH	$[Rh(COD)Cl]_2$	25	99%	73%
12	EtOH	$[Rh(COD)Cl]_2$	25	92%	89%
13	*t*-BuOH	$[Rh(COD)Cl]_2$	25	84%	91%
14 [d]	*i*-PrOH	$[Rh(COD)Cl]_2$	100	99%	93%

[a] Unless otherwise mentioned, reactions were performed with **1a** (0.1 mmol) and a Rh/L/**1a** ratio of 1/1.1/25 in 1.0 mL solvent at 35 °C under 20 atm H_2. [b] Determined by GC and NMR. [c] Determined by GC analysis of the corresponding acetamides. [d] 25 °C, 10 atm H_2.

In addition, pressures, temperatures and additives were examined to optimize the reaction. The best result was observed at 25°C under 10 atm H_2 with 1 mol % catalyst (Table 2.2, entry 4). The substrate/catalyst ratio can be up to 400 with >90 % conversion and a retention of high enantiometic excess. Addition of base (triethylamine) and molecular seive resulted a poor conversion with low enantioselectivity, while acids influence the enantioselectivity in a negive way (Table 2.3). This might be caused by a interference of the anion binding of original chloride ion with thiourea ligand.

Table 2.2 Hydrogen pressure, temperature and catalyst loading. [a]

Entry	Solvent	H_2[atm]	S/C	T [°C]	Conversion[b]	*ee*[c]
1	*i*-PrOH	20	25	35	99%	92%
2	*i*-PrOH	20	50	35	99%	93%
3	*i*-PrOH	20	100	35	99%	93%
4	*i*-PrOH	10	100	25	99%	94%
5	*i*-PrOH	10	200	25	96%	94%
6	*i*-PrOH	10	400	25	86%	93%
7	*i*-PrOH	20	200	25	97%	93%

8	*i*-PrOH	20	200	35	97%	92%
9	*i*-PrOH	20	400	35	90%	93%

[a] Reactions were performed with **1a** (0.1 mmol) and a [Rh(COD)Cl]$_2$/**L6** ratio of 1/1.1. [b] Determined by GC analysis of the corresponding acetamides.

Table 2.3 Influence from additives [a]

Entry	S/C	Addtive	T [°C]	Conversion[b]	*ee*[c]
1	50	4A MS (100mg)	35	67%	53%
2	50	CF_3COOH (10 mmol %)	35	99%	75%
3	50	CH_3COOH (10 mmol %)	35	98%	79%
4	50	Et_3N (10 mmol %)	35	63%	35%

[a] Reactions were performed in i-PrOH with **1a** (0.1 mmol) and a **1a**/[Rh(COD)Cl]$_2$/**L6** ratio of 100/1/2.2. [b] NMR analysis; [c] Determined by GC analysis of the corresponding acetamides.

2.3 Substrate scope of *N*-unprotected imines

Under the optimized conditions, a variety of N-H imines were tested (Table 2.4). Mostly substrates with *meta* and *para* substitutions on the phenyl ring afforded high yields and enantioselectivities (96-99% yield and 90-94% *ee*). However, the chloro group and methoxy group resulted in an obvious decrease of the yields (**2d**, **2e** and **2g**). The *ortho*-methoxy group on the phenyl ring resulted in 34% yield and 84% *ee* (**2h**). 1- and 2-naphthyl products were obtained with 92% *ee* and 93% *ee* respectively. The R_2 group had a significant effect on the outcome. When R_2 was ethyl group, lower conversion and enantioselectivity were observed (**2k**). As the R_2 group changed to butyl, the conversion and enantioselectivity of the product gradually decreased to 70% and 75% (**2l**).

Table 2.4 Substrates Scope Screening. [a]

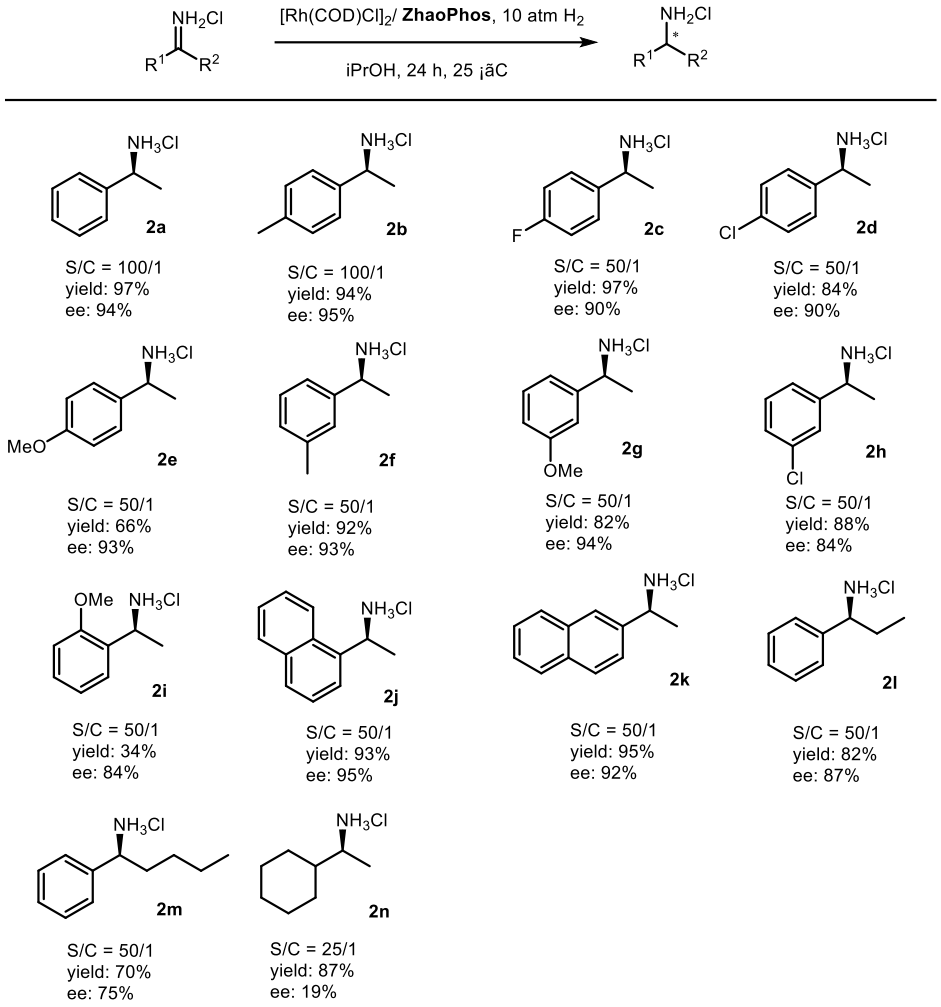

[a] **1** (0.2 mmol) and a Rh/**L**ratio of 1/1.1 in 2.0 mL solvent at 25°C under 10 atm H_2. [b] Isolated yield. [c]*ee* was determined by chiral by GC analysis of the corresponding acetamides.

2.4 Mechanistic study

To obtain insight of this catalytic system, a series of chiral ligands were prepared and some control experiments were undertaken (Table 2.5). The urea L1 provided 22% conversion and 66% *ee* in sharp contrast with the more acidic and less self-assembling thiourea ZhaoPhos (Table 2.5, entry 1 *vs* 2).[27] The CF_3 group on the 3,5-(trifluoromethyl)phenyl moiety remained important in the catalytic system (Table 2.5, entries 3-5).[28] For further research, several

modified ligands were prepared and screened. The methylation of ZhaoPhos led to a dramatic decrease of the conversion and enantioselectivity (Table 2.5, entry 6). This finding suggested that the NH may be involved in the activation of iminium salts and the stereoselectivity of hydrogenation. The low conversion and enantioselectivity obtained with monodentated phosphorus ligand proved that the bisphosphine was essential (Table 2.5, entry 7). Neither the combination of the chiral phosphine with the simple thiourea nor the combination of the simple phosphine with the chiral thiourea improved the activity and enantioselectivity of this reaction (Table 2.5, entry 8 and 9), which pointed to the importance of a covalent linker.

Table 2.5 Ligands study and control experiments. [a]

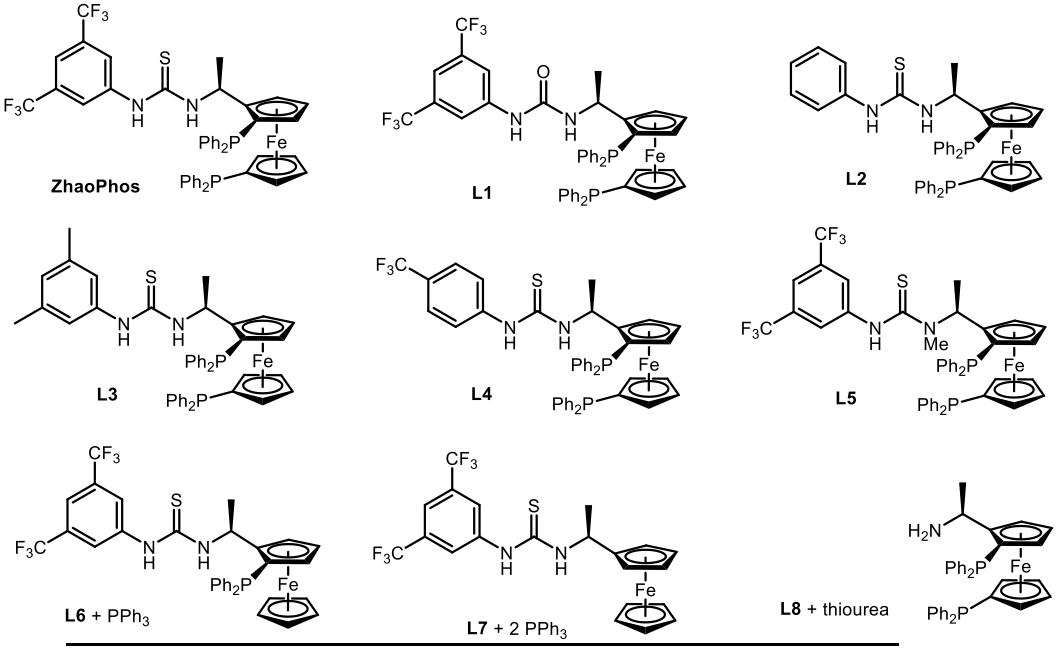

Entry	Ligands	Conversion [b]	*ee*[%][c]
1	ZhaoPhos	99%	94%
2	L1	22%	66%
3	L2	6%	11%
4	L3	76%	90%
5	L4	72%	87%
6	L5	26%	38%

7[d]	L6	9%	84%
8[e]	L7	2%	11%
9[f]	L8	9%	57%

[a] Unless otherwise mentioned, reactions were performed with **1a** (0.1 mmol) and a Rh/**L**/**1a** ratio of 1/1.1/100 in 1.0 mL solvent at 25 °C under 10 atm H_2. [b] Determined by NMR. [c] Determined by GC analysis of the corresponding acetamides. [d] Rh/**L6**/**1a**/Ph_3P ratio of 1/1.1/100/1.1. [e] Rh/**L7**/**1a**/Ph_3P ratio of 1/1.1/100/2.2. [f] Rh/**L8**/**1a**/thiourea ratio of 1/1.1/100/1.1.

Meanwhile, different substrates and additives were investigated. When the chloride counterion in **1a** was replaced with trifluoromethanesulfonate, only 20% conversion and 53% *ee* was observed (Table 2.6, entries 1). Interestingly, the addition of chloride counterion increased the conversions and enantioselectivities (Table 2.6, entries 2 and 3). However, the addition of bromide counterion and iodide counterion decreased the conversions and enantioselectivities (Table 2.6, entries 4-6). This finding implied that the chloride counterion played an important role in this catalytic system. We tried activated imine **1q** and iminium salts **1q•**HCl but no desired product was obtained.

Table 2.6 Substrates study and control experiments.[a]

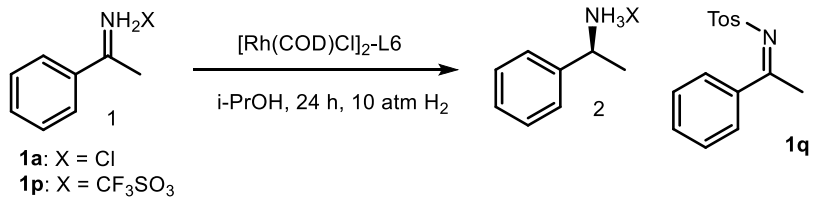

Entry	Substrate	Additive	Conversion[b]	ee[c]
1	1p	--	20	53
2	1p	TBAC	81	93
3	1p	LiCl	75	94
4	1a	--	99	94
5	1a	TBAB	22	66
6	1a	TBAI	32	89
7[d]	1q	--	0	ND

8[d]	1q•HCl	--	0	ND

[a] Unless otherwise mentioned, reactions were performed with **1a** (0.1 mmol) and a Rh/**L**/**1a**/Additive ratio of 1/1.1/100/100 in 1.0 mL solvent at 25 °C under 10 atm H_2. [b] Determined by ^{1}H NMR. [c] Determined by GC analysis of the corresponding acetamides. [d] Rh/**L**/**1a**/TBAC ratio of 1/1.1/100/50. TBAC = tetrabutylammonium chloride, TBAB = tetrabutylammonium bromide, TBAI = tetrabutylammonium iodide.

Further information about the reaction was obtained by ^{1}H NMR studies of mixtures generated from ligands and tetrabutylammonium chloride (TBAC). The addition of varying amounts of tetrabutylammonium chloride (TBAC) to ZhaoPhos in $CDCl_3$ resulted in a downfield shift of the NH proton signals (Figure 2.1). As 1 equivalent of TBAC was added, the signal for NH was at 9.73 ppm. When 3 equivalents of TBAC were added, the NH signal appeared at 10.16 ppm. Analogous experiments employing different ligands and TBAC gave similar result.[29] This finding was consistent with a dual H-bond interaction[19, 22, 30-31] and indicated that the reaction may involve the recognition of chloride ions. Based on well-established anion-binding properties of thiourea, we proposed this catalytic intermediates were responsible for the anion binding.

2.5 Summary

In conclusion, asymmetric hydrogenation of N-H iminiums could be catalyzed by a Rh/bisphosphine-thiourea complex. The chiral amines were obtained in high yields and enantioselectivities. Based on the control experiments and ^{1}H NMR studies, we proposed that the anion binding interaction between thiourea and chloride counterion played an important role in the catalytic system. Further research on the mechanism and application is currently under way.

Figure 2.1 ^{1}H NMR spectra of **ZhaoPhos** with tetrabutylammonium chloride (TBAC). The NH were marked.

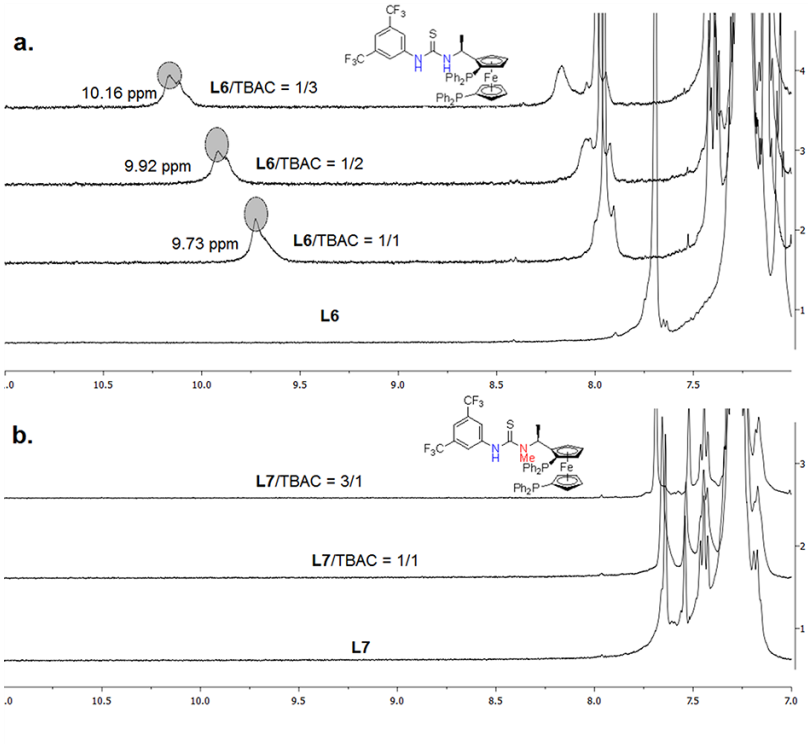

2.6 Experimental section

2.6.1 Synthesis of N-H imines.

All the N-H imines were prepared according the literature.[6]

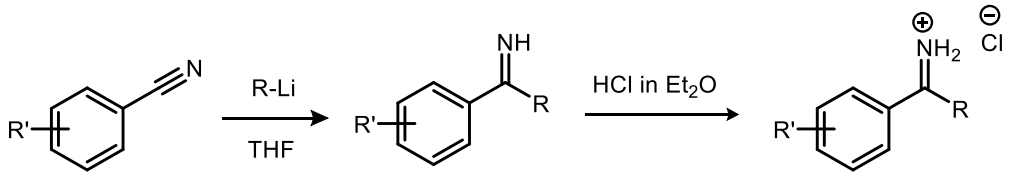

A round-bottom flask was charged with nitrile (50.0 mmol) and THF (50 mL). The mixture was cooled to −78 ºC and MeLi (50.0 mL, 1.6 M in diethyl ether) was added dropwise over 1h. After addition, the resulting mixture was stirred for 2 h and quenched with anhydrous MeOH (12 mL). The mixture was then stirred at rt for 2 h. The suspension was filtered on a Celite pad and the filtrate was concentrated under vacuum. The residue was dissolved in MTBE (50 mL) and treated with HCl/Et_2O (50.0 mL, 1 M). The slurry was stirred for 30 min and filtered to obtain the product as free-flowing white to yellow solids.

All the spectral data are consistent with the literature values.[6]

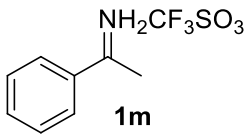

1m

^{1}H NMR (400 MHz, $CDCl_3$) δ 11.46 (s, 2H), 8.20 – 7.91 (m, 2H), 7.78 (t, *J* = 7.5 Hz, 1H), 7.61 (dd, *J* = 17.7, 9.6 Hz, 2H), 2.94 (d, *J* = 5.2 Hz, 3H).

^{13}C NMR (100 MHz, $CDCl_3$) δ 186.36 (s), 136.95 (s), 129.92 (s), 129.35 (s), 129.33 (s), 21.73 (s).

2.6.2 General Procedure for asymmetric hydrogenation of N-H imines:

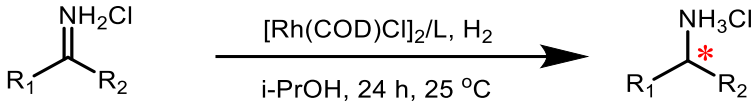

In the nitrogen-filled glovebox. A solution of **L** (2.2 eqv.) and $[Rh(COD)Cl]_2$ (3.0 mg, 0.006 mmol) in 6.0 mL anhydrous *i*-PrOH was stirred at room temperature for 30 min. A specified amount of the resulting solution (1 mL) was transferred to a vial charged with **1a** (0.1 mmol) by syringe. The vials were transferred to an autoclave, which was then charged with 10 atm of H_2 and stirred at 25 °C for 24 h. The resulting mixture was concentrated under vacuum and dissolved in saturated aqueous $NaHCO_3$ (5 mL). After stirring for 10 min, the mixture was extracted with CH_2Cl_2 (3×2 mL) and dried over Na_2SO_4. To the resulting solution was added Ac_2O (300 μL) and stirred for 30 min. The resulting solution was then analyzed for conversion and *ee* directly by GC. The product was purified by chromatography on silica gel column with dichloromethane/methanol (90:10).

All the spectral data are consistent with the literature values.[6]

2.6.3 sCharacterization data for chiral amines.

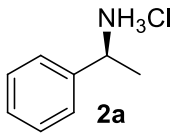

2a

^{1}H NMR (400 MHz, $CDCl_3$) δ 7.53 (s, 3H), 7.45 (d, *J* = 6.9 Hz, 2H), 7.32 (m, 3H), 4.29 (d, *J* = 6.5 Hz, 1H), 1.59 (d, *J* = 6.4 Hz, 3H).

^{13}C NMR (100 MHz, $CDCl_3$) δ 138.79 (s), 128.96 (s), 128.63 (s), 126.91 (s), 51.74 (s), 21.01 (s).

Supelco gama Dex™ 225 column (30 m ×0.25 mm × 0.25 μm), He 1.0 mL/min, column 160 °C, t_R (major) =16.3 min, t_R (minor) =17.9 min. [2, 6]

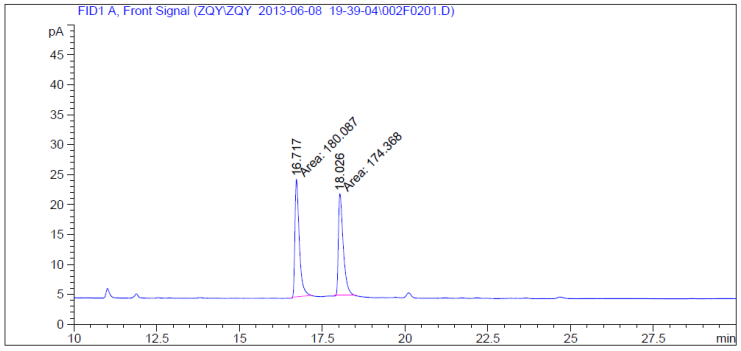

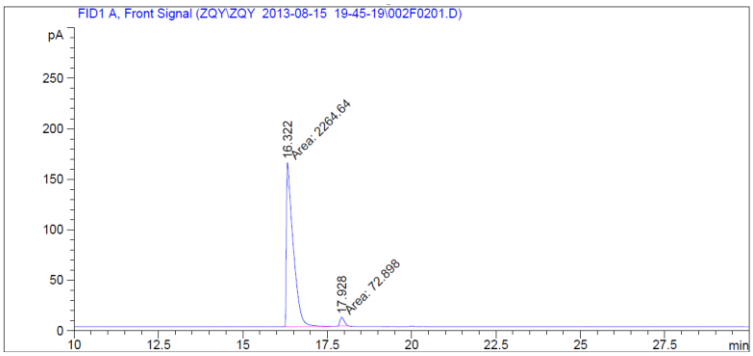

RetTime # [min]	Type	Width [min]	Area [pA*s]	Height [pA]	Area %
1 16.322	MM	0.2321	2264.64111	162.61743	96.88142
2 17.928	MM	0.1444	72.89803	8.41520	3.11858

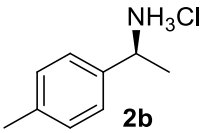

2b

^{1}H NMR (400 MHz, $CDCl_3$) δ 7.32 (d, *J* = 7.5 Hz, 2H), 7.14 (d, *J* = 7.6 Hz, 2H), 6.57 (s, 3H), 4.23 (d, *J* = 6.0 Hz, 1H), 2.32 (s, 3H), 1.55 (d, *J* = 6.3 Hz, 3H).

^{13}C NMR (100 MHz, $CDCl_3$) δ 138.13 (s), 137.05 (s), 129.56 (s), 126.60 (s), 51.38 (s), 21.58 (s), 21.11 (s).

Supelco gama Dex™ 225 column (30 m ×0.25 mm × 0.25 μm), He 1.0 mL/min, column 160 °C, t_R (major) =23.6 min, t_R (minor) =25.6 min. [2, 6]

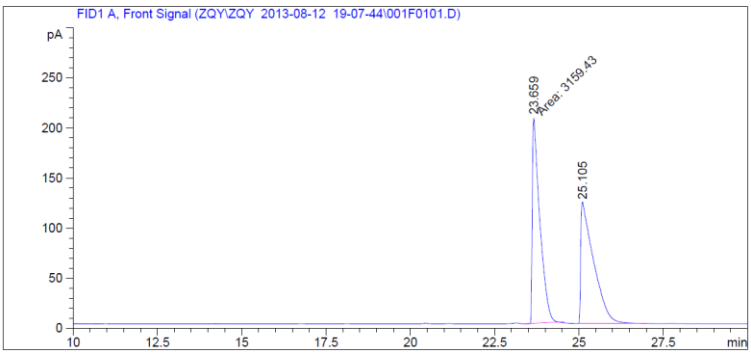

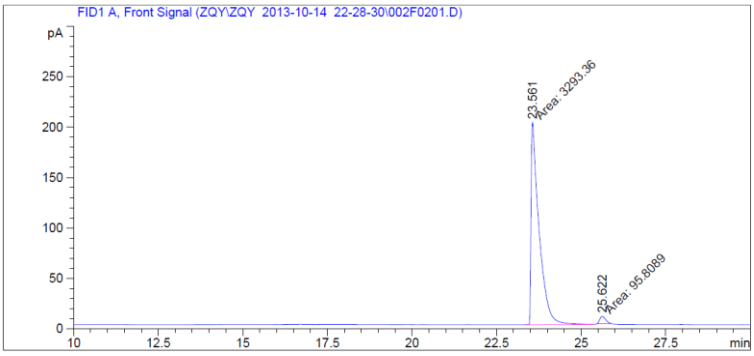

RetTime # [min]	Type	Width [min]	Area [pA*s]	Height [pA]	Area %
1 23.561	MM	0.2738	3293.35986	200.45435	97.17308
2 25.622	MM	0.2119	95.80892	7.53432	2.82692

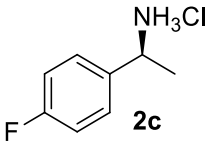

2c

^{1}H NMR (400 MHz, $CDCl_3$) δ 7.50 – 7.36 (m, 2H), 7.13 (s, 3H), 7.06 – 6.94 (m, 2H), 4.30 (d, *J* = 6.0 Hz, 1H), 1.58 (d, *J* = 6.4 Hz, 3H).

^{13}C NMR (100 MHz, $CDCl_3$) δ 162.72 (d, *J* = 246 Hz), 134.86 (s), 128.79 (d, *J* = 8.2 Hz), 115.87 (d, *J* = 21.6 Hz), 51.06 (s), 21.17 (s).

Supelco gama Dex™ 225 column (30 m ×0.25 mm × 0.25 μm), He 1.0 mL/min, column 160 °C, t_R (major) =19.7 min, t_R (minor) =21.9 min. [2, 6]

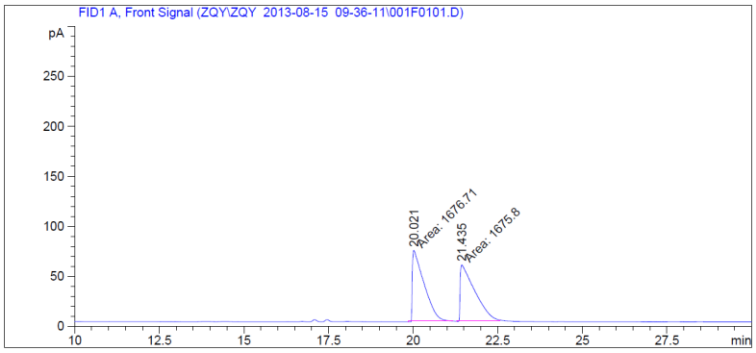

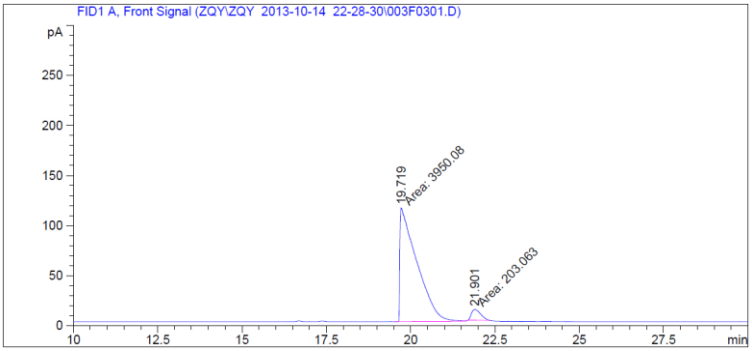

RetTime Type Width Area Height Area

[min] [min] [pA*s] [pA] %

-|-----|----|-------|-------|----------|--------|

1 19.719 MM 0.5803 3950.08472 113.45764 95.11063

2 21.901 MM 0.3178 203.06262 10.64807 4.88937

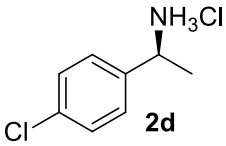

2d

^{1}H NMR (400 MHz, $CDCl_3$) δ 7.30 (d, *J* = 10.0 Hz, 4H), 4.17 (d, *J* = 6.1 Hz, 1H), 3.85 (s, 3H), 1.44 (d, *J* = 6.4 Hz, 3H).

^{13}C NMR (100 MHz, $CDCl_3$) δ 142.90 (s), 133.26 (s), 128.81 (s), 127.60 (s), 50.89 (s), 24.02 (s).

Supelco gama Dex™ 225 column (30 m ×0.25 mm × 0.25 μm), He 1.0 mL/min, column 160 °C, t_R (major) =55.5 min, t_R (minor) =61.8 min. [2, 6]

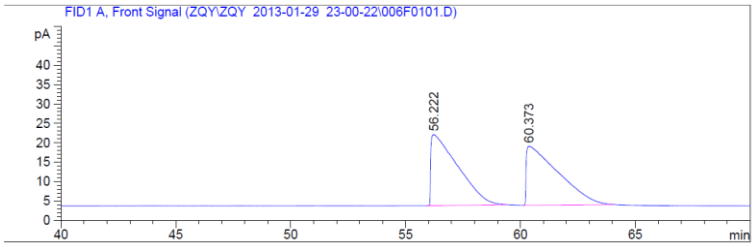

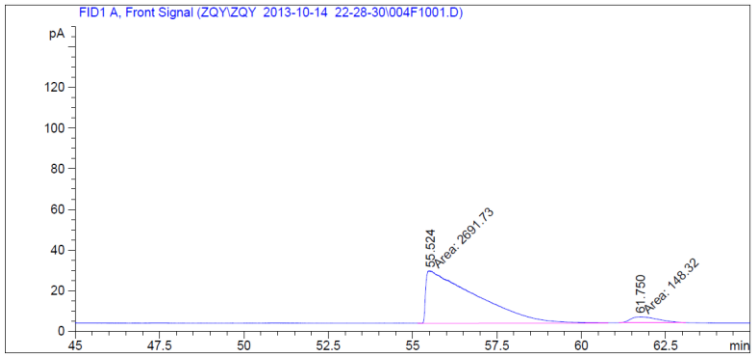

RetTime Type Width Area Height Area

[min] [min] [pA*s] [pA] %

-|-----|----|-------|-------|----------|--------|

1 55.524 MM 1.7378 2691.72803 25.81494 94.77756

2 61.750 MM 0.8877 148.31989 2.78473 5.22244

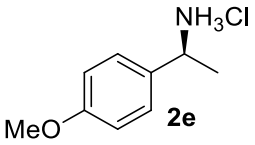

2e

^{1}H NMR (400 MHz, $CDCl_3$) δ 7.37 (d, *J* = 8.5 Hz, 1H), 6.86 (d, *J* = 8.5 Hz, 1H), 6.62 (s, 1H), 4.25 (d, *J* = 6.6 Hz, 1H), 3.78 (s, 3H), 1.57 (d, *J* = 6.6 Hz, 2H).

^{13}C NMR (100 MHz, $CDCl_3$) δ 159.66 (s), 131.65 (s), 128.09 (s), 114.28 (s), 55.26 (s), 51.18 (s), 21.39 (s).

Supelco gama Dex™ 225 column (30 m ×0.25 mm × 0.25 μm), He 1.0 mL/min, column 160 °C, t_R (major) =53.4 min, t_R (minor) =57.5 min. [2, 6]

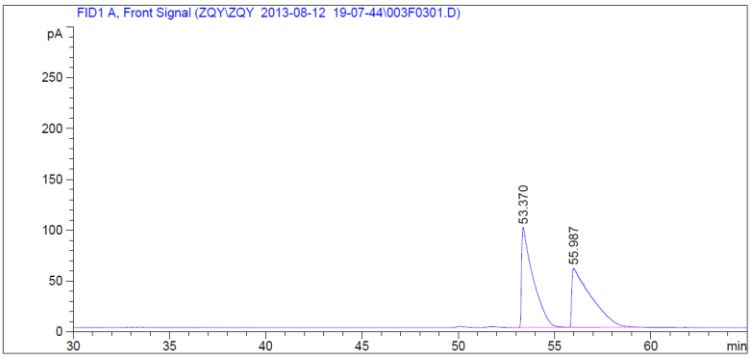

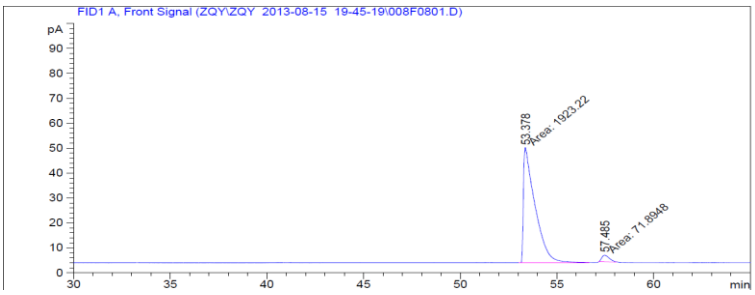

RetTime Type Width Area Height Area

[min] [min] [pA*s] [pA] %

-|-----|----|-------|-------|----------|--------|

1 53.378 MM 0.6950 1923.21802 46.12228 96.39646

2 57.485 MM 0.4483 71.89476 2.67307 3.60354

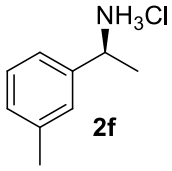

2f

^{1}H NMR (400 MHz, $CDCl_3$) δ 7.28 – 7.15 (m, 3H), 7.09 (dd, *J* = 5.8, 3.8 Hz, 1H), 5.52 (s, 3H), 4.20 (q, *J* = 6.7 Hz, 1H), 2.33 (s, 3H), 1.54 (d, *J* = 6.8 Hz, 3H).

^{13}C NMR (100 MHz, $CDCl_3$) δ 140.90 (s), 138.54 (s), 128.88 (d, *J* = 18.3 Hz), 127.29 (s), 123.52 (s), 51.58 (s), 22.07 (s), 21.39 (s).

Supelco beta Dex™ 390 column (30 m ×0.25 mm × 0.25 μm), He 1.0 mL/min, column programmed from 100 °C to 180 °C at 1.0 °C/min, t_R (major) =59.5 min, t_R (minor) =60.0 min. [2, 6]

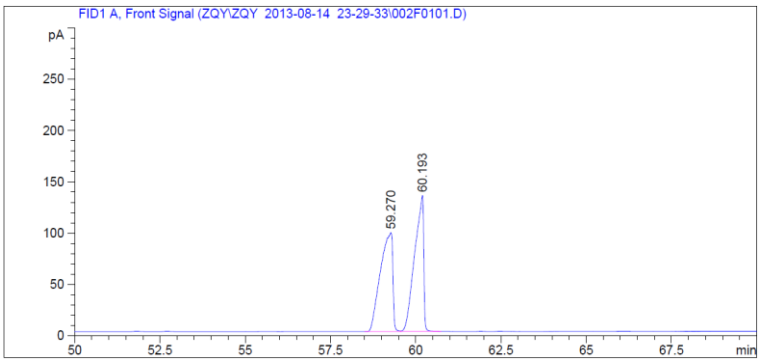

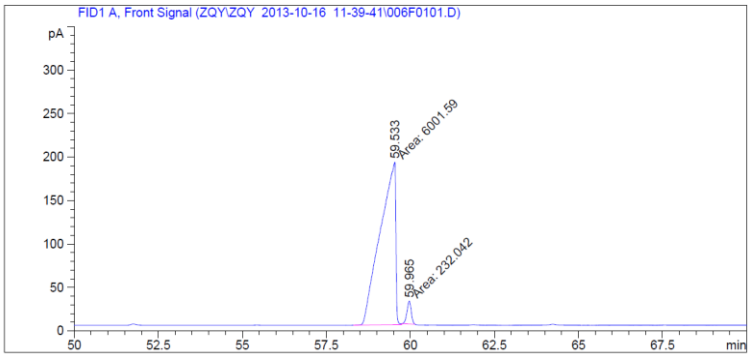

RetTime Type Width Area Height Area

[min] [min] [pA*s] [pA] %

-|-----|----|-------|-------|----------|--------|

1 59.533 MM 0.5347 6001.59375 187.05707 96.27759

2 59.965 MM 0.1460 232.04152 26.49493 3.72241

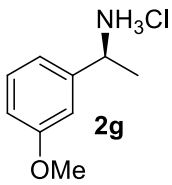

^{1}H NMR (400 MHz, $CDCl_3$) δ 7.25 (dd, *J* = 14.0, 6.2 Hz, 1H), 7.04 (s, 1H), 6.98 (d, *J* = 7.4 Hz, 1H), 6.83 (dd, *J* = 8.2, 2.0 Hz, 1H), 6.57 (s, 3H), 4.25 (dd, *J* = 13.0, 6.4 Hz, 1H), 3.75 (s, 3H), 1.57 (d, *J* = 6.7 Hz, 3H).

^{13}C NMR (100 MHz, $CDCl_3$) δ 159.97 (s), 141.59 (s), 129.96 (s), 118.79 (s), 114.42 (s), 111.80 (s), 55.35 (s), 51.71 (s), 21.68 (s).

Supelco gama Dex™ 225 column (30 m ×0.25 mm × 0.25 μm), He 1.0 mL/min, column 160 °C, t_R (major) =44.9 min, t_R (minor) =48.5 min. [2, 6]

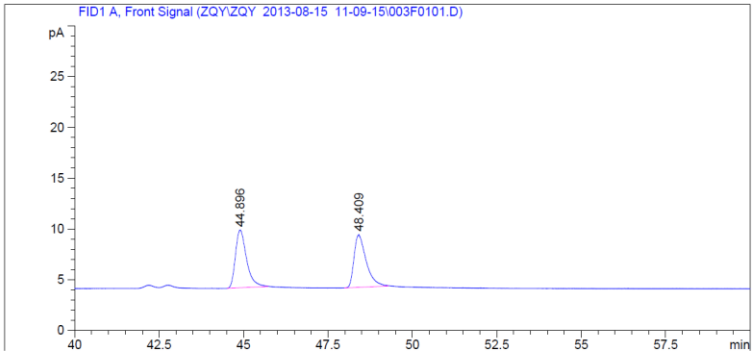

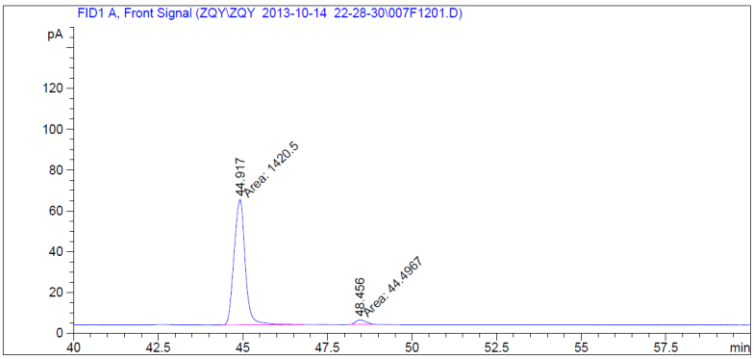

RetTime Type Width Area Height Area

[min] [min] [pA*s] [pA] %

-|-----|----|-------|-------|----------|--------|

1 44.917 MM 0.3856 1420.49768 61.39237 96.96267

2 48.456 MM 0.3390 44.49672 2.18780 3.03733

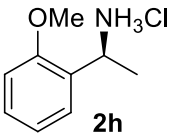

2h

^{1}H NMR (400 MHz, $CDCl_3$) δ 7.39 (d, *J* = 7.5 Hz, 1H), 7.33 – 7.27 (m, 1H), 6.94 (t, *J* = 7.5 Hz, 1H), 6.87 (d, *J* = 8.2 Hz, 1H), 6.15 (s, 3H), 4.64 (d, *J* = 6.5 Hz, 1H), 3.83 (s, 3H), 1.65 (d, *J* = 6.7 Hz, 3H).

^{13}C NMR (100 MHz, $CDCl_3$) δ 156.77 (s), 129.74 (s), 127.50 (s), 126.68 (s), 120.92 (s), 110.67 (s), 55.43 (s), 47.13 (s), 19.02 (s).

Supelco gama Dex™ 225 column (30 m ×0.25 mm × 0.25 μm), He 1.0 mL/min, column 160 °C, t_R (major) =27.9 min, t_R (minor) =28.4 min. [2, 6]

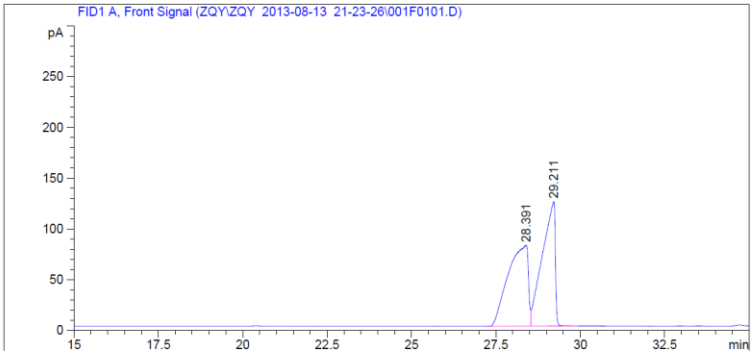

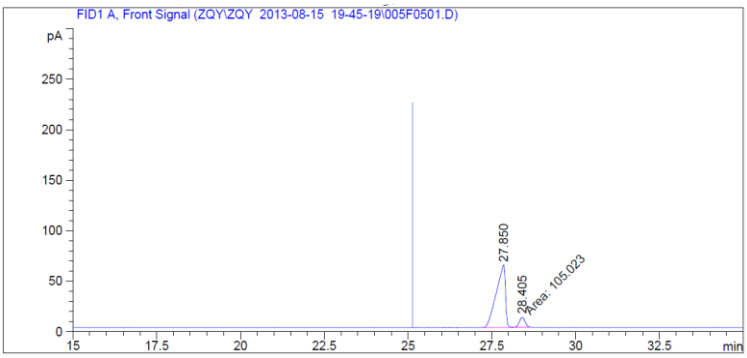

Peak RetTime Type Width Area Height Area

[min] [min] mAU*s [mAU] %

-|-----|----|-------|-------|----------|--------|

1 27.850 BV 0.2535 1188.60608 61.70966 91.88155

2 28.405 MM 0.1863 105.02265 9.39646 8.11845

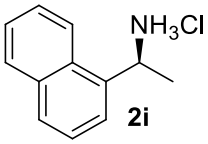

2i

^{1}H NMR (400 MHz, $CDCl_3$) δ 8.08 (d, *J* = 8.2 Hz, 1H), 7.87 (d, *J* = 8.1 Hz, 1H), 7.76 (d, *J* = 8.2 Hz, 1H), 7.68 (s, 1H), 7.60 – 7.40 (m, 3H), 5.94 (s, 3H), 5.03 (s, 1H), 1.61 (d, *J* = 6.4 Hz, 3H).

^{13}C NMR (100 MHz, $CDCl_3$) δ 133.90 (s), 130.54 (s), 129.02 (s), 127.68 (s), 126.19 (s), 125.63 (s), 125.58 (s), 122.70 (s), 121.77 (s), 46.68 (s), 24.04 (s).

Supelco gama Dex™ 225 column (30 m ×0.25 mm × 0.25 μm), He 1.0 mL/min, column 160 °C, t_R (major) =69.2 min, t_R (minor) =76.9 min. [2, 6]

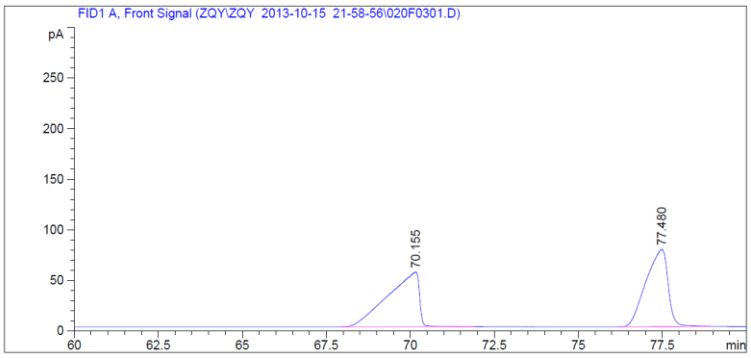

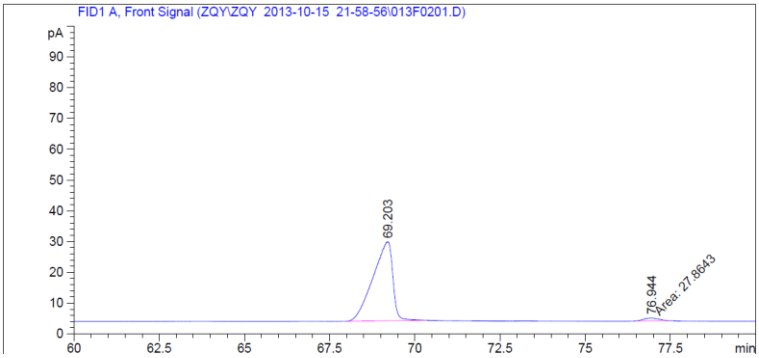

RetTime Type Width Area Height Area

[min] [min] [pA*s] [pA] %

-|-----|----|-------|-------|----------|--------|

1 69.203 BB 0.5190 1042.84412 25.65778 97.39758

2 76.944 MM 0.5035 27.86432 9.22378e-1 2.60242

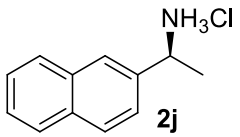

2j

^{1}H NMR (400 MHz, $CDCl_3$) δ 7.85 – 7.60 (m, 4H), 7.47 (dd, *J* = 8.5, 1.6 Hz, 1H), 7.45 – 7.32 (m, 2H), 6.87 (s, 1H), 4.27 (dd, *J* = 13.3, 6.6 Hz, 1H), 1.51 (d, *J* = 6.7 Hz, 3H).

^{13}C NMR (100 MHz, $CDCl_3$) δ 137.68 (s), 133.18 (s), 133.09 (s), 128.69 (s), 128.18 (s), 127.61 (s), 126.29 (s), 126.26 (s), 125.81 (s), 124.40 (s), 51.75 (s), 21.75 (s).

Supelco gama Dex™ 225 column (30 m ×0.25 mm × 0.25 µm), He 1.0 mL/min, column 160 °C, t_R (major) =95.6 min, t_R (minor) =103.8 min. [2, 6]

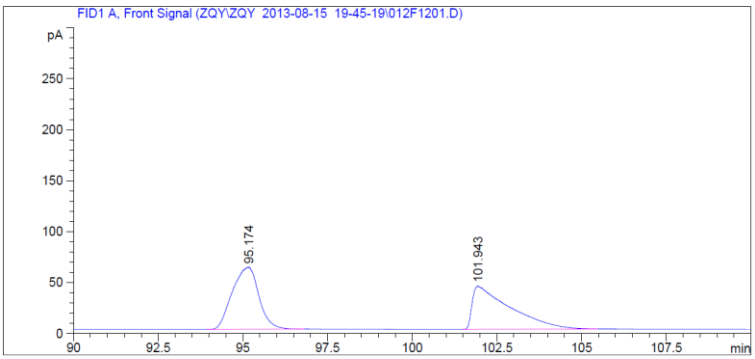

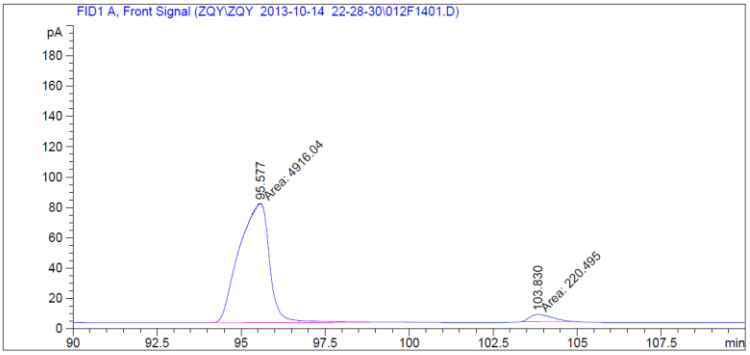

RetTime Type Width Area Height Area

[min] [min] [pA*s] [pA] %

-|-----|----|-------|-------|----------|--------|

1 95.577 MM 1.0421 4916.03711 78.62239 95.70733

2 103.830 MM 0.7545 220.49457 4.87091 4.29267

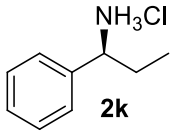

2k

^{1}H NMR (400 MHz, $CDCl_3$) δ 7.56 – 7.35 (m, 2H), 7.35 – 7.20 (m, 3H), 6.48 (s, 1H), 4.05 – 3.89 (m, 1H), 2.12 – 1.75 (m, 2H), 0.82 (t, *J* = 7.3 Hz, 3H).

^{13}C NMR (100 MHz, $CDCl_3$) δ 138.76 (s), 128.87 (s), 128.39 (s), 127.27 (s), 57.82 (s), 28.96 (s), 10.46 (s).

Supelco beta Dex™ 390 column (30 m ×0.25 mm × 0.25 μm), He 1.0 mL/min, column 140 °C, t_R (major) =41.5 min, t_R (minor) =42.7 min. [2, 6]

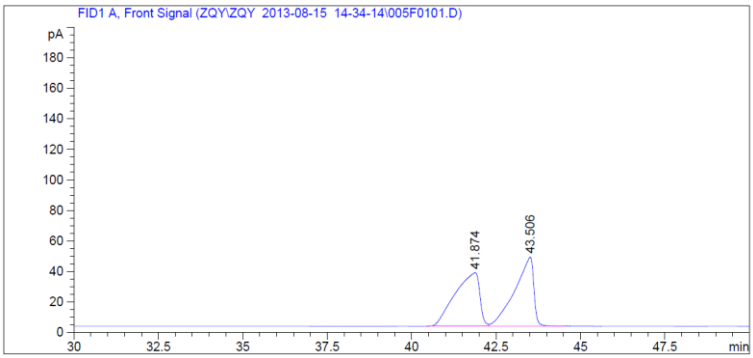

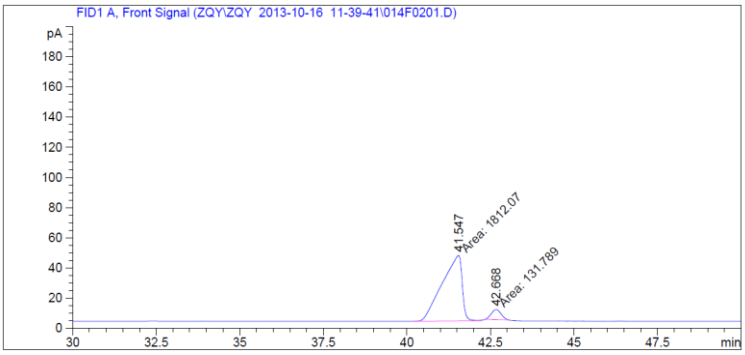

RetTime Type Width Area Height Area

[min] [min] [pA*s] [pA] %

-|-----|----|-------|-------|----------|--------|

1 41.547 MM 0.6948 1812.06750 43.46968 93.22024

2 42.668 MM 0.3346 131.78882 6.56533 6.77976

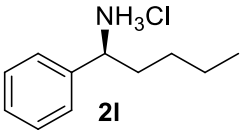

2l

^{1}H NMR (400 MHz, $CDCl_3$) δ 7.47 – 7.38 (m, 2H), 7.37 – 7.29 (m, 3H), 6.87 (s, 1H), 4.06 (dd, *J* = 8.5, 5.8 Hz, 1H), 2.10 – 1.82 (m, 2H), 1.37 – 1.17 (m, 3H), 1.14 – 1.04 (m, 1H), 0.82 (t, *J* = 7.1 Hz, 3H).

^{13}C NMR (100 MHz, $CDCl_3$) δ 136.44 (s), 129.03 (s), 128.87 (s), 127.45 (s), 56.40 (s), 34.23 (s), 27.74 (s), 22.06 (s), 13.77 (s).

Supelco gama Dex™ 225 column (30 m ×0.25 mm × 0.25 μm), He 1.0 mL/min, column programmed from 100 °C to 150 °C at 1.0 °C/min, t_R (major) =87.5 min, t_R (minor) =90.4 min. [2, 6]

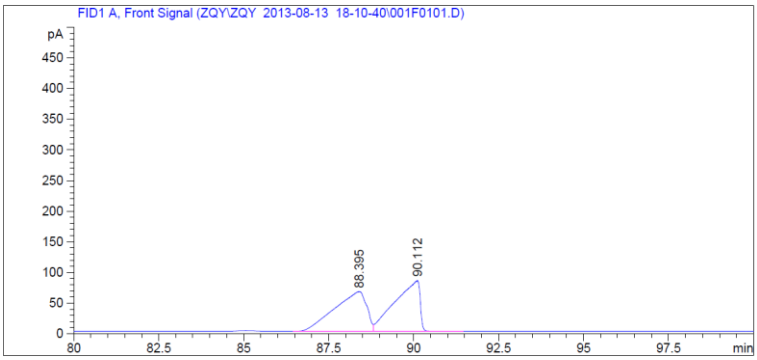

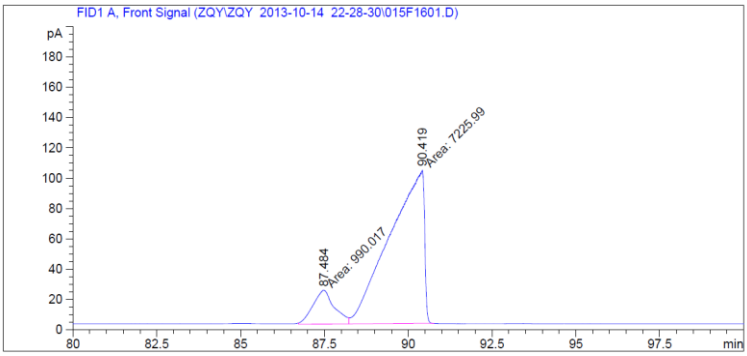

RetTime Type Width Area Height Area

[min] [min] [pA*s] [pA] %

-|-----|----|-------|-------|----------|--------|

1 87.484 MF 0.7369 990.01672 22.39206 12.04985

2 90.419 FM 1.1909 7225.99023 101.12375 87.95015

Reference:

1. Nugent, T. C., *Chiral Amine Synthesis*. Wiley-VCH: Weinheim, 2010.

2. Huang, K.; Li, S.; Chang, M.; Zhang, X., Rhodium-Catalyzed Enantioselective Hydrogenation of Oxime Acetates. *Organic Letters* **2013,** *15* (3), 484-487.

3. Church, T. L.; Andersson, P. G., Chiral Amines from Transition-Metal-Mediated Hydrogenation and Transfer Hydrogenation. In *Chiral Amine Synthesis*, Wiley-VCH Verlag GmbH & Co. KGaA: 2010; pp 179-223.

4. Zhang, W.; Zhang, X., 5.12 Asymmetric Hydrogenation of Prochiral C=N Bonds. In *Comprehensive Chirality*, Editors-in-Chief: Erick, M. C.; Hisashi, Y., Eds. Elsevier: Amsterdam, 2012; pp 301-317.

5. Xie, J.-H.; Zhu, S.-F.; Zhou, Q.-L., Transition Metal-Catalyzed Enantioselective Hydrogenation of Enamines and Imines. *Chemical Reviews* **2010,** *111* (3), 1713-1760.

6. Hou, G.; Gosselin, F.; Li, W.; McWilliams, J. C.; Sun, Y.; Weisel, M.; O'Shea, P. D.; Chen, C.-y.; Davies, I. W.; Zhang, X., Enantioselective Hydrogenation of N−H Imines. *Journal of the American Chemical Society* **2009,** *131* (29), 9882-9883.

7. Hou, G.; Li, W.; Ma, M.; Zhang, X.; Zhang, X., Highly Efficient Iridium-Catalyzed Asymmetric Hydrogenation of Unprotected β-Enamine Esters. *Journal of the American Chemical Society* **2010,** *132* (37), 12844-12846.

8. Hou, G.; Tao, R.; Sun, Y.; Zhang, X.; Gosselin, F., Iridium−Monodentate Phosphoramidite-Catalyzed Asymmetric Hydrogenation of Substituted Benzophenone N−H Imines. *Journal of the American Chemical Society* **2010,** *132* (7), 2124-2125.

9. Knowles, R. R.; Jacobsen, E. N., Attractive noncovalent interactions in asymmetric catalysis: Links between enzymes and small molecule catalysts. *Proceedings of the National Academy of Sciences* **2010,** *107* (48), 20678-20685.

10. Takemoto, Y., Development of Chiral Thiourea Catalysts and Its Application to Asymmetric Catalytic Reactions. *Chem. Pharm. Bull.* **2010,** *58* (5), 593-601.

11. Zhang, Z.; Schreiner, P. R., (Thio)urea organocatalysis-What can be learnt from anion recognition? *Chemical Society Reviews* **2009,** *38* (4), 1187-1198.

12. Phipps, R. J.; Hamilton, G. L.; Toste, F. D., The progression of chiral anions from concepts to applications in asymmetric catalysis. *Nat Chem* **2012,** *4* (8), 603-614.

13. Brak, K.; Jacobsen, E. N., Asymmetric Ion-Pairing Catalysis. *Angewandte Chemie International Edition* **2013,** *52* (2), 534-561.

14. Mahlau, M.; List, B., Asymmetric Counteranion-Directed Catalysis: Concept, Definition, and Applications. *Angewandte Chemie International Edition* **2013,** *52* (2), 518-533.

15. Zhao, Q.; Li, S.; Huang, K.; Wang, R.; Zhang, X., A Novel Chiral Bisphosphine-Thiourea Ligand for Asymmetric Hydrogenation of β,β-Disubstituted Nitroalkenes. *Organic Letters* **2013,** *15* (15), 4014-4017.

16. Taylor, M. S.; Jacobsen, E. N., Highly Enantioselective Catalytic Acyl-Pictet−Spengler Reactions. *Journal of the American Chemical Society* **2004,** *126* (34), 10558-10559.

17. Taylor, M. S.; Tokunaga, N.; Jacobsen, E. N., Enantioselective Thiourea-Catalyzed Acyl-Mannich Reactions of Isoquinolines. *Angewandte Chemie International Edition* **2005,** *44* (41), 6700-6704.

18. Knowles, R. R.; Lin, S.; Jacobsen, E. N., Enantioselective Thiourea-Catalyzed Cationic Polycyclizations. *Journal of the American Chemical Society* **2010,** *132* (14), 5030-5032.

19. Xu, H.; Zuend, S. J.; Woll, M. G.; Tao, Y.; Jacobsen, E. N., Asymmetric Cooperative Catalysis of Strong Brønsted Acid–Promoted Reactions Using Chiral Ureas. *Science* **2010,** *327* (5968), 986-990.

20. Birrell, J. A.; Desrosiers, J.-N.; Jacobsen, E. N., Enantioselective Acylation of Silyl Ketene Acetals through Fluoride Anion-Binding Catalysis. *Journal of the American Chemical Society* **2011,** *133* (35), 13872-13875.

21. Burns, N. Z.; Witten, M. R.; Jacobsen, E. N., Dual Catalysis in Enantioselective Oxidopyrylium-Based [5 + 2] Cycloadditions. *Journal of the American Chemical Society* **2011,** *133* (37), 14578-14581.

22. Lin, S.; Jacobsen, E. N., Thiourea-catalysed ring opening of episulfonium ions with indole derivatives by means of stabilizing non-covalent interactions. *Nat Chem* **2012,** *4* (10), 817-824.

23. Lalonde, M. P.; McGowan, M. A.; Rajapaksa, N. S.; Jacobsen, E. N., Enantioselective Formal Aza-Diels–Alder Reactions of Enones with Cyclic Imines Catalyzed by Primary Aminothioureas. *Journal of the American Chemical Society* **2013**.

24. De, C. K.; Klauber, E. G.; Seidel, D., Merging Nucleophilic and Hydrogen Bonding Catalysis: An Anion Binding Approach to the Kinetic Resolution of Amines. *Journal of the American Chemical Society* **2009,** *131* (47), 17060-17061.

25. Lee, Y. S.; Alam, M. M.; Keri, R. S., Enantioselective Reactions of N-Acyliminium Ions Using Chiral Organocatalysts. *Chemistry – An Asian Journal* **2013**, n/a-n/a.

26. Zuend, S. J.; Jacobsen, E. N., Mechanism of Amido-Thiourea Catalyzed Enantioselective Imine Hydrocyanation: Transition State Stabilization via Multiple Non-Covalent Interactions. *Journal of the American Chemical Society* **2009,** *131* (42), 15358-15374.

27. Pihko, P. M., *Hydrogen Bonding in Organic Synthesis*. Wiley-VCH: Weinheim,Germany, 2009.

28. Lippert, K. M.; Hof, K.; Gerbig, D.; Ley, D.; Hausmann, H.; Guenther, S.; Schreiner, P. R., Hydrogen-Bonding Thiourea Organocatalysts: The Privileged 3,5-Bis(trifluoromethyl)phenyl Group. *European Journal of Organic Chemistry* **2012,** *2012* (30), 5919-5927.

29. , For more details, see supplementary information.

30. Raheem, I. T.; Thiara, P. S.; Peterson, E. A.; Jacobsen, E. N., Enantioselective Pictet−Spengler-Type Cyclizations of Hydroxylactams: H-Bond Donor Catalysis by Anion Binding. *Journal of the American Chemical Society* **2007,** *129* (44), 13404-13405.

31. Schafer, A. G.; Wieting, J. M.; Fisher, T. J.; Mattson, A. E., Chiral Silanediols in Anion-Binding Catalysis. *Angew. Chem. Int. Ed.* **2013**, n/a-n/a.

Chapter three

Strong Brønsted acid promoted asymmetric hydrogenation of isoquinolines and quinolines catalyzed by a Rh-thiourea chiral phosphine complex via anion binding

3.1 introduction

As continuing research on the ferrocene-based thiourea chiral phosphine system, we sought to expand the success of asymmetric hydrogenation of unprotected iminium to a broad field in organic synthesis methodology. *N*-heterocycles would be a good target since they are a class of very important organic compounds both in nature and in pharma.

Tetrahydroquinolines (THQs) and tetrahydroisoquinolines (THIQs) are an important family of biologically active molecules, including natural alkaloids and important pharmaceutical products. [1-3] Among various synthetic approaches to synthesizing chiral THQs and THIQs, direct hydrogenation, with high atom economy, relatively simple procedure and easy work-up, deserves special attention. To our best knowledge, however, asymmetric hydrogenation of *N*-heteroaromatics, especially isoquinolines, remains a challenging task. [4-5] Although quinolines have been successfully hydrogenated in several cases (Scheme 3.1), [6-13] there were only few examples of isoquinolines. Zhou's

group used iridium-bisphosphine catalyst to obtain high enantioselectivity, but this transformation needs activation by chloroformate or addition of BCDMH. [8, 14] By introducing chiral phosphoric acid, transfer hydrogenation of isoquinoline was achieved by Zhou in 2014 and *N*-protected 1,2-dihydroisoquinolines were synthesized with moderate enantioselectivities.[15] In 2013, Mashima's group synthesized chiral THIQ using a dinuclear iridium(III)-bisphosphine complex, but the substrate scope is still limited to aromatic or bulky substituents (schemie 3.1). [16] Isoquinolines with less hindered alkyl substituents on the prochiral carbons are still challenging. Most of these catalysis cases for *N*-heteroaromatics are performed with ruthenium, iridium and palladium complexes. Rhodium was rarely reported in direct asymmetric hydrogenation of *N*-heteroaromatics with high turnovers and ee's. This is in sharp contrast to the broad application of Rh complex in asymmetric hydrogenation of olefins, enamides and imines. [17-19]

After introducing strong Brønsted acid such HCl, we were looking forward to developing a highly reactive and enantioselective example of rhodium/bisphosphine-catalyzed asymmetric hydrogenation of *N*-heteroaromatics. In this catalysis system, a secondary interaction between the catalyst and the substrates was believed to occur via anion binding of ion-pair intermediates. We envision that the strong Brønsted acid such as HCl, brings dual benefits: (1) activating the aromatic ring, [2013] (2) establishing a salt bridge between the catalyst and the substrates.

Scheme 3.1 Asymmetric hydrogenation of quinolines and isoquinolines

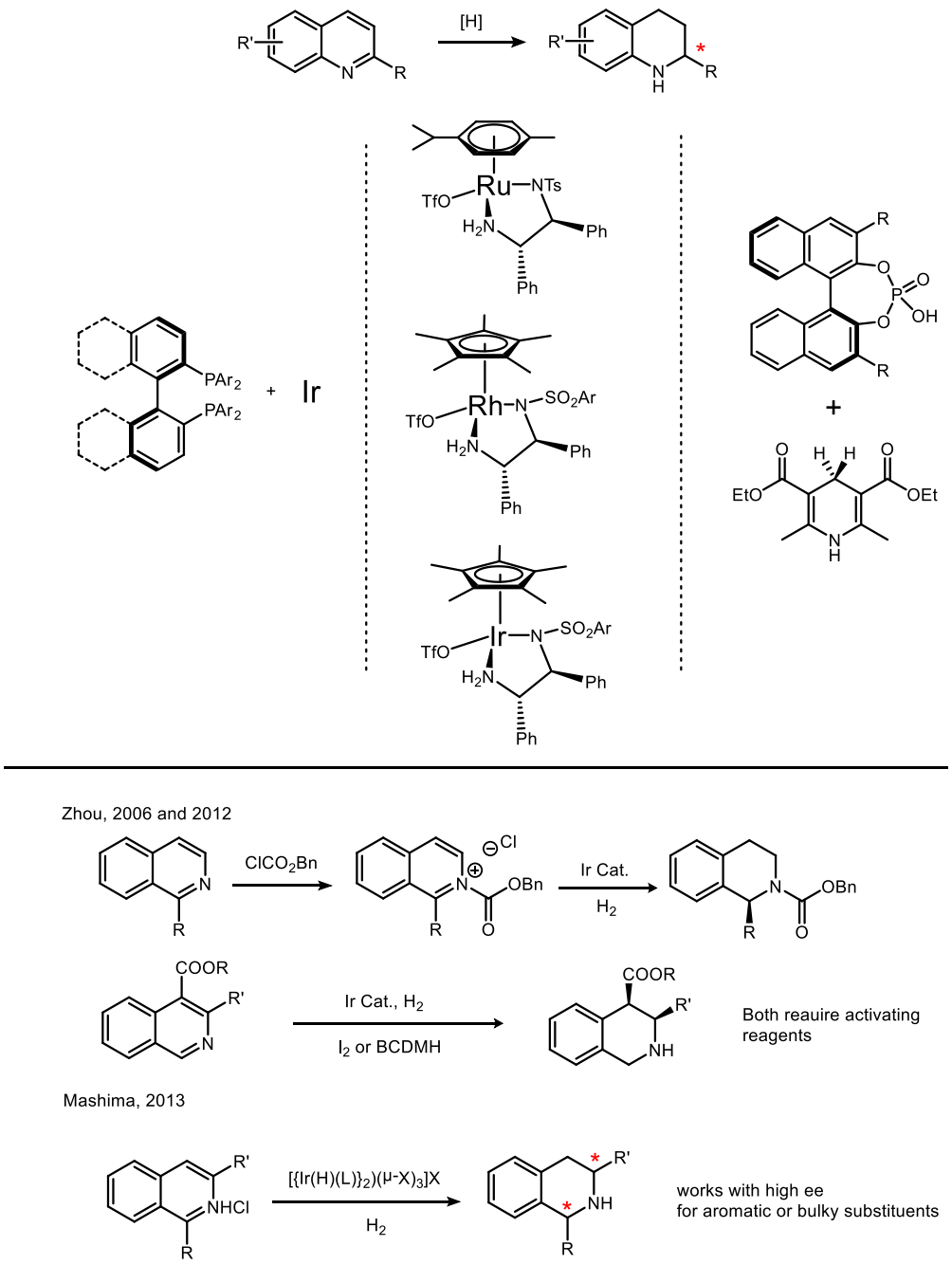

3.2 Method development

Our study was initiated with 3-methylisoquinoline hydrochloride as a model substrate. The Rh catalyst was prepared *in situ* by mixing the metal precursor $[Rh(COD)Cl]_2$ with (S,R)-ZhaoPhos. In accordance with our previous reports, [21-22] this catalysis system is solvent-dependent. After screening of alkyl halide, alcohols and ethers, we found that

under 40 atm H_2 pressure at 40 °C, dichloromethane gives the best result (>99% conversion and 92% ee were observed with 1% catalyst loading). In addition to using single solvents, solvent pairs were also tested. The mixture of dichloromethane and isopropanol (2:1, v/v) at 25 °C gives the optimal condition with 99% ee and full conversion. Iridium complex $[Ir(COD)Cl]_2$/ZhaoPhos also shows high activity with, but lower enantioselectivity than its Rh counterpart (table 3.1, entry 5 vs entry 8). Halide effect, which causes considerable difference in some cases,[23] was evaluated as well. Using $[Rh(COD)I]_2$ as a metal precursor resulted in small changes in conversion and enantioselectivity (table 3.1, entry 6 vs entry 7).

Table 3.1, Optimization of condition. [a]

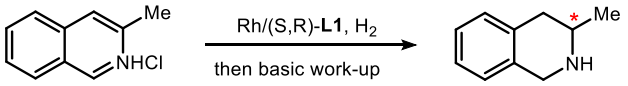

3a **4a**

Entry	Metal	Solvent	conversion[b]	ee[c]
1	[Rh(COD)Cl]2	i-PrOH	>99%	70%
2	[Rh(COD)Cl]2	MeOH	85%	30%
3	[Rh(COD)Cl]2	DCM	>99%	92%
4	[Rh(COD)Cl]2	Dioxane	95%	90%
5	[Rh(COD)Cl]2	Dioxane/i-PrOH=2:1	>99%	90%
6[d]	[Rh(COD)Cl]2	DCM/i-PrOH=2:1	>99%	99%
7[d]	[Rh(COD)I]2	DCM/i-PrOH=2:1	99%	93%
8	[Ir(COD)Cl]2	Dioxane/i-PrOH=2:1	>99%	83%

[a] Reaction condition: 3a (0.1 mmol) in 1.0 ml solvent, 3/$[Rh(COD)Cl]_2$/L ratio=100/0.5/1, 40 atm H2, 40 °C, 24 h; [b]conversion was determined by ^{1}H NMR analysis, no by product was observed; [c]ee was determined by GC with a chiral stationary phase; [d]performed at 25 °C.

Counterion effects were also investigated. When tetrabutylammonium chloride (TBAC) was added, no significant changes in conversion and enantioselectivity was observed (Table 3.2, entry 2 vs 1). This suggests the spectator role of tetrabutylammonium cation. The introduction of bromide anion from TBAB does not influence this catalytic reaction (entry 3 vs 2). The presence of Iodide anion decreases the conversion, but it shows trace influence on the enantioselectivity (entry 4 vs 2). Fluoride anion, however, inhibits this catalytic reaction dramatically: no product was observed after adding TBAF (entry 5). To gain plausible explanation of these observations, further study will be needed in the future.

Table 3.2 Counterion effect. [a]

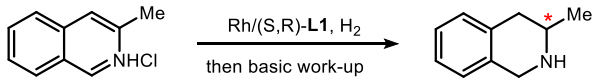

3a **4a**

Entry	additive	conversion[b]	ee[c]
1	none	99%	99%
2	TBAC (1.0 eq.)	98%	99%
3	TBAB (1.0 eq.)	99%	99%
4	TBAI (1.0 eq.)	90%	98%
5	TBAF (1.0 eq.)	0	-

[a]Reaction condition: 3a (0.1 mmol) in 0.6 ml solvent, 1/[Rh(COD)Cl]$_2$/L1 ratio=100/0.5/1, 40 atm H2, 25 oC, 48 h; bconversion was determined by 1H NMR analysis, no by product was observed; cee was determined by GC with a chiral stationary phase.

3.3 Substrate scope

Then we applied this method to synthesize various chiral THIQs. Different alkyl substituents at 3-position or benzo ring do not show obvious changes in yields and

enantioselectivities. Aryl substituent, such as phenyl group, on 3- position leads to full conversion and moderate enantioselectivity (76% ee). In addition to 3-alkyl isoquinolines, 1-methylisouinoline was also hydrogenated with high enantioselectivity (Table 3.3).

Table 3.3 Substrate scope for isoquinolines. [a]

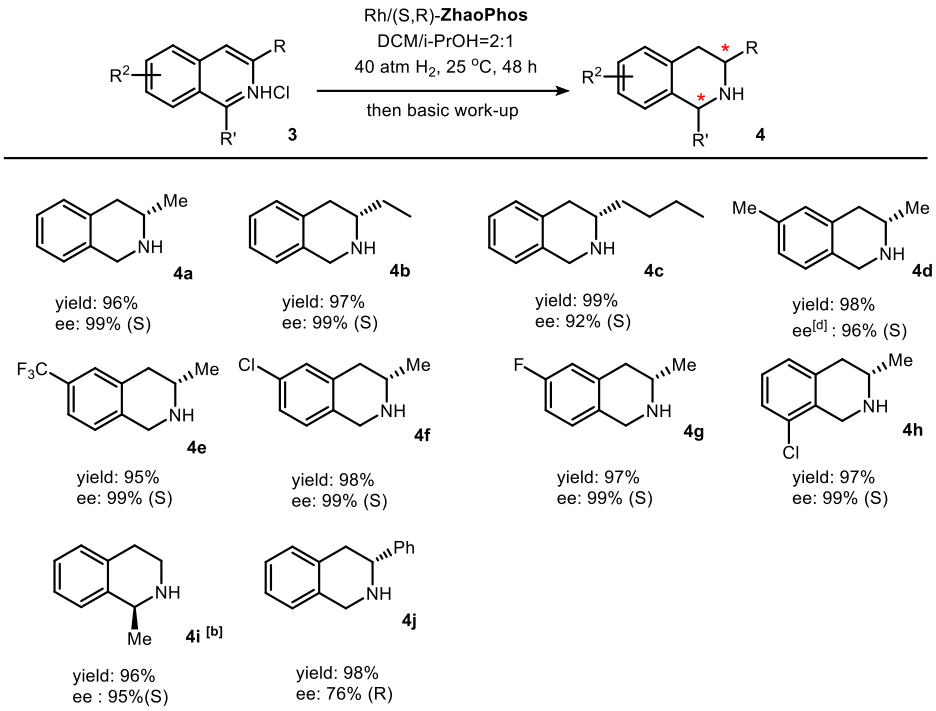

[a] reaction condition: 1 (0.2 mmol) in 1.2 ml solvent, 1/[Rh(COD)Cl]$_2$/L ratio = 100/0.5/1; yield was determined with isolated THIQ products; ee was determined by GC or HPLC with a chiral stationary phase; [b] performed in Dioxane/iPrOH = 2:1(v/v) at 60 °C under 60 atm H_2 with 2% catalyst.

As far as we know, few catalysis systems can be applied in asymmetric hydrogenation of both isoquinolines and quinolines with both high turn-overs and excellent enantioselectivities. [6-13] Then a question merged to us: can this synthetic protocol be used to synthesize chiral THQs with high ee? By employing the optimized condition (DCM/iPrOH=2:1, v/v) in the case asymmetric hydrogenation of isoquinolines, we found that the enantioselectivity was dramatically increased to 99% ee. This observation,

in return, suggests that this thiourea-Rh-bisphosphine catalysis system is highly solvent-dependent. Substrate scope of asymmetric hydrogenation of quinolines is broad. High enantioselectivities have been obtained with various substituents (Table 3.4).

Table 3.4 Substrate scope for quinolines. [a]

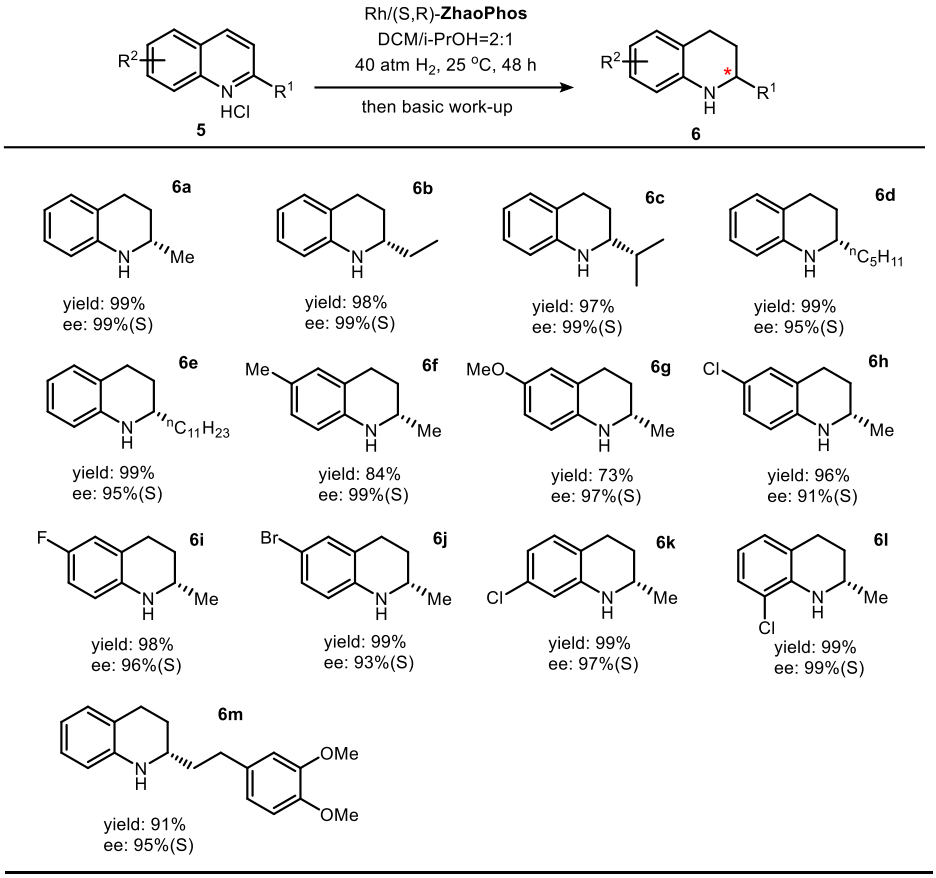

[a] reaction condition: 5 (0.2 mmol) in 1.2 ml solvent, 5/[Rh(COD)Cl]$_2$/L ratio = 100/0.5/1; yield was determined with isolated THQ products; ee was determined by GC or HPLC with a chiral stationary phase.

The potential application of this synthetic protocol was estimated: we have scaled up this asymmetric hydrogenation reaction into gram scale. No significant sign of changes in conversion or enantioselectivity was observed with 0.5% catalyst loading. 99% Yield and 98% ee was obtain in asymmetric hydrogenation of 5 mmol 2-methylisoquinolinium chloride with 0.5% catalyst. In addition, the role of strong Brønsted acid HCl is essential

in this chemical transformation. Without HCl, no hydrogenation product was observed. [16]

3.4 NMR study for evidence of interaction between ligand and substrate

To gain evidence of a secondary interaction of ZhaoPhos with chloride anion of substrates, we mixed ZhaoPhos and 3a (3 eq.) in $CDCl_3$. The ^{1}HNMR showed similar obvious changes of chemical shifts (Figure 3.1). The original thiourea N-H peaks (hidden in the aromatic peaks within 7.3~7.0 ppm) shift downfield to 9.10 and 7.62 (marked with red circles in Figure 3.1). In addition, the three protons on the 3,5-bis(trifluoromethyl)phenyl group also shift downfield a little by 0.19 ppm (marked by arrow). These changes of chemical shifts, consistent with the case of ZhaoPhos with Cl^- from TBAC, [22] suggest the anion binding between the ligand and the substrate.

Figure 3.1 NMR study for the interaction of ZhaoPhos and 3a.

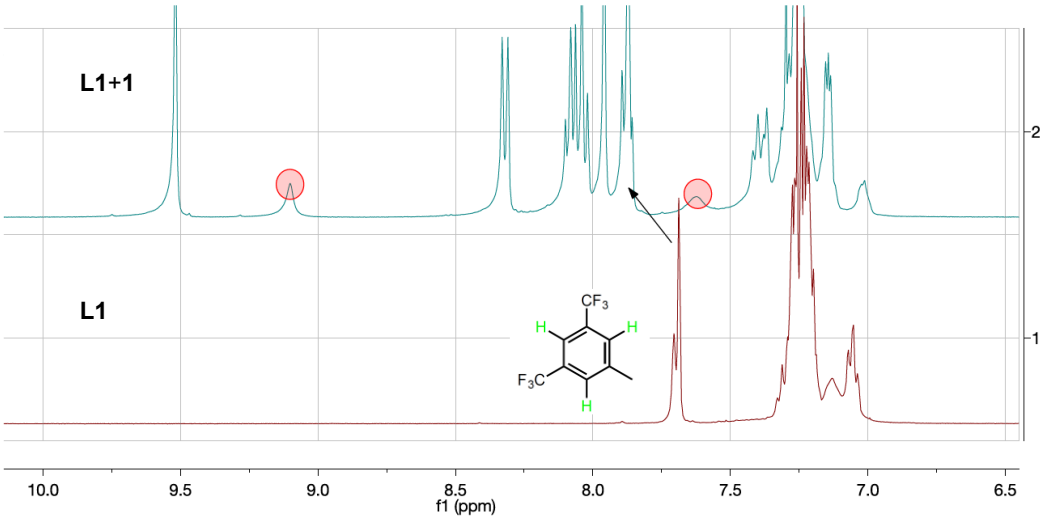

3.5 Control experiments to evaluate each unit in ZhaoPhos

We conducted control experiments to evaluate the collaboration manner of each unit of ZhaoPhos in asymmetric hydrogenation of 3-methylisoquinolines (Table 3.5). Urea bisphosphine ligand L1 only gives trace product, and this sharp contrast suggests the crucial role of thiourea moiety. Compared to H (L2) and methyl (L3), more electron-withdrawing trifluoromethyl group at 3- and 5- position on the phenyl ring increases the enantioselectivity, which is probably due to the stronger acidity of N-H proton on the thiourea. After *N*-methylation of the less acidic thiourea N-H proton, enantioselectivity results in a minor decrease. This observation reveals that the more acidic thiourea N-H proton contributes mostly in anion binding with chloride. Furthermore, monophosphine ligand L6 and the mixture of ferrocene-thiourea compound L7 with triphenylphosphine can hardly catalyzed the hydrogenation reaction. On the other hand, the mixture of thiourea molecule and bisphosphine-Ugi's amine L8 failed to show catalytic activity. These results (ZhaoPhos vs L7/PPh_3 and L8/thiourea) demonstrate the importance of a covalent incorporation of bisphosphine moiety and thiourea. The idea of secondary offers an alternative strategy for asymmetric hydrogenation.

Table 3.5. Ligand evaluation and control experiment.

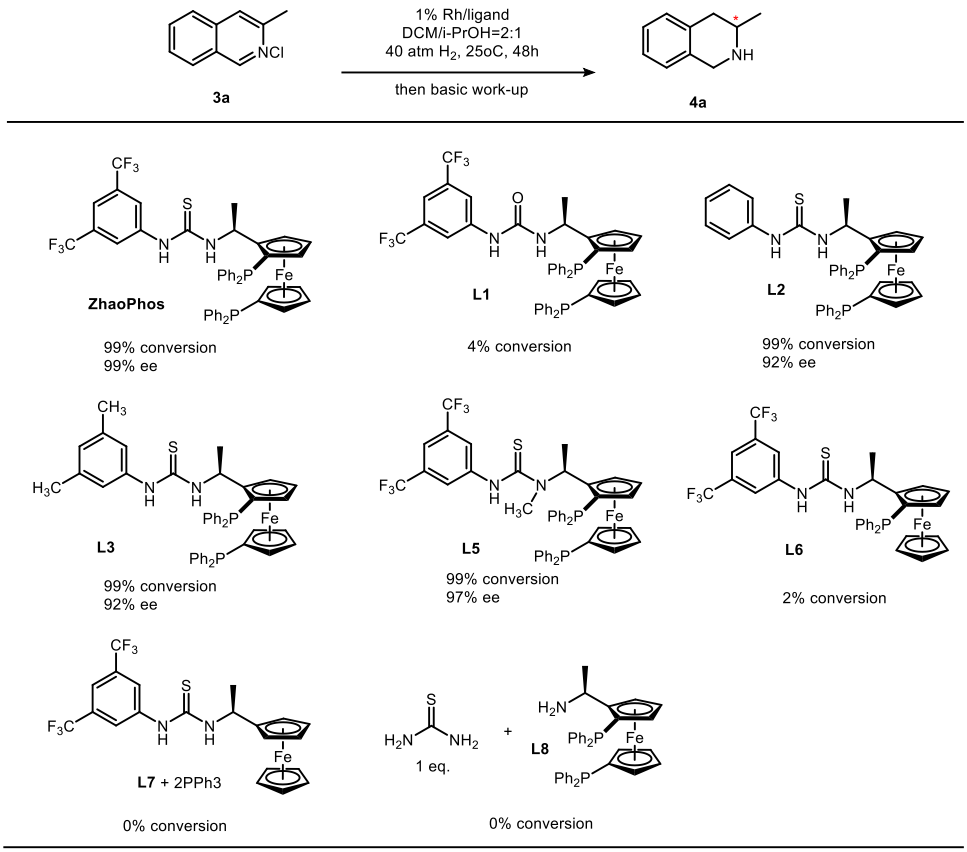

[a] reaction condition: **1** (0.1 mmol) in 0.6 ml solvent, **1**/[Rh(COD)Cl]$_2$/ligand ratio = 100/0.5/1; conversion was determined by ^{1}H NMR analysis; ee was determined by GC with a chiral stationary phase.

3.6 Deuterium labelling experiments and proposed mechanism

In order to obtain insight of this transformation, deuterium labeling experiments was conducted. First, 3-methylisoquinoline hydrochloride was reduced by deuterium gas in methanol (Scheme 3.2, Eq. 1). D atoms are added only at 1- and 3- position respectively. This indicates that the hydrogen atom at 4- position of the product comes from the methanol solvent. Second, 3-methylisoquinoline deuterochloride was reduced with hydrogen gas in deuterated methanol (Scheme 3.2, Eq. 2). Hydrogen atoms are added at 1- and 3- position. The original H at 4- position, however, was exchanged with D, resulting two D atoms at 4- position. This indicates that D atoms at 4- position come

from the Methanol-d_4 solvent. A tautomerization is probably responsible for this H-D exchange. Interestingly, H-D exchange also occurs on the methyl group (53% original H was replaced by D). This observation, in return, proves the existence of tautomerization. Based on this results, we proposed a possible path in this transformation (Scheme 3.2). After addition of a hydrogen at 1- position, the substrate is partially reduced, leading to conjugate enamine, which could not be further reduced in this rhodium-thiourea-bisphosphine catalytic system. After a tautomerization follows, giving an iminiums intermediate, which could be easily hydrogenated. [5] Another tautomer, a terminal enamine is less preferred than its conjugate counterpart, because the latter is more stable. This explains why H atoms on methyl group was partially replaced by D (but H at 4- position is almost replaced by D). (For details, please see supporting information.)

Scheme 3.2 Deuterium labeling experiment and proposed transformation path.

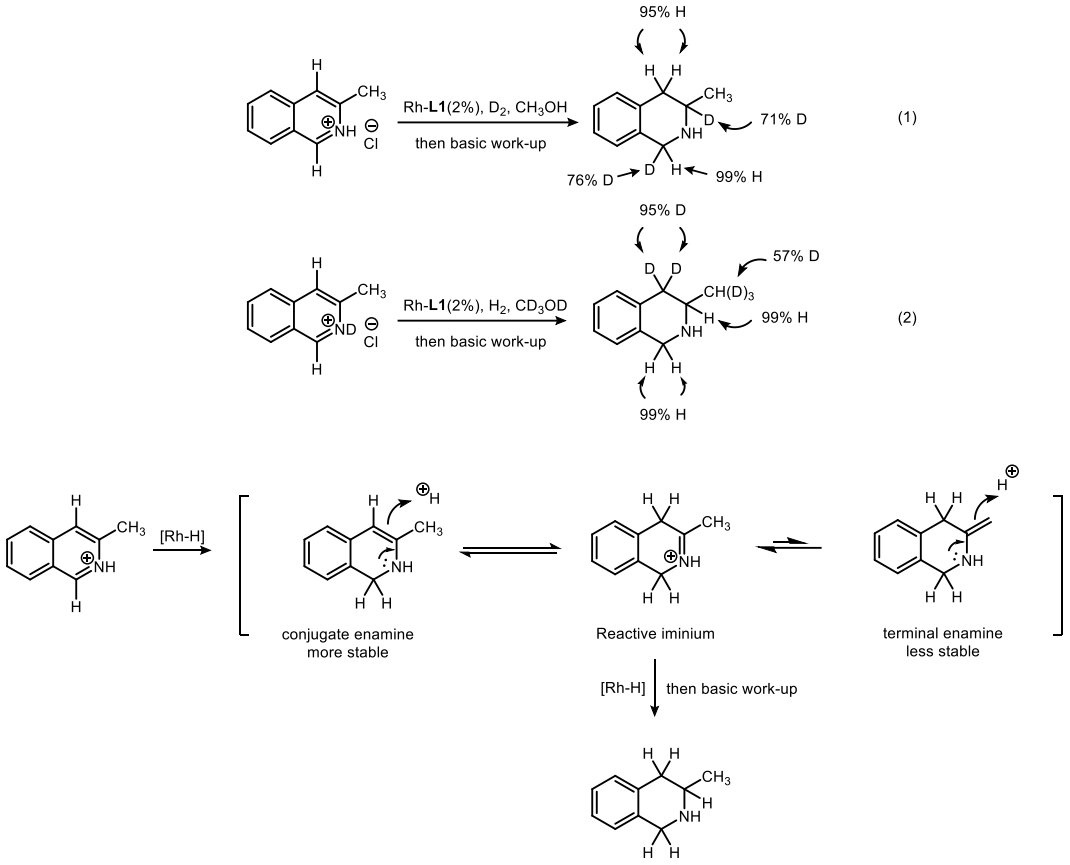

Recent reports revealed an outer-sphere mechanism for bisphosphine-transition metal catalyzed hydrogenation. In 2014, Zhou reported a series of detailed studies on palladium catalyzed asymmetric hydrogenation of protonated indoles. After careful evaluation, hydride transfer from a Pd-H complex to an iminium intermediate was proposed. (Scheme 3.3, Eq. 1) [24] In 2015, Mashima's group proposed a mechanism on iridium-catalyzed asymmetric hydrogenation of isoquinoline hydrogen halide salts. Strong experimental evidence was presented to favor an outer-sphere mechanism, in which hydrogen bonding between Ir-Cl complex and N-H proton was proposed. (Scheme 3.3, Eq. 2) [25] Both of these mechanism studies above were focused on hydrogenation of the halide salts of aromatic compounds.

Similarly, the nature of protonated (iso)quinolines suggests that it seems not possible for the substrates to coordinate to the rhodium complex in this case, no matter in a σ-bonding or a π-bonding manner. A hydride transfer mechanism is more possible in this catalytic case, instead of the traditional inner-sphere mechanism that involves the direct coordination of unsaturated bonds to the metal. Based on previous reports and our deuterium labeling experiments, we propose a catalytic cycle to explain a plausible outer-sphere mechanism (scheme 3). After oxidative addition of H_2, a dihydride rhodium (III) complex is formed. The chloride anion of the isoquinolinium salt will bind with the hydrogen of thiourea, forming a Rh dichloro-dihydride anionic complex. The equatorial hydride of the active rhodium complex will be transferred to the isoquinolinium due to strong trans effect of a phosphine. After this 1,2- addition, a tautomerization step will follow, giving an iminium intermediate. The iminium, instead of an enamine, will undergo the insertion of hydride from a rhodium dihydride complex. The chirality of the product is originated in this step. Another molecule of hydrogen will react and form the active rhodium dihydride species, finishing the catalytic cycle. In order to approve the mechanism of this rhodium catalyzed asymmetric hydrogenation of (iso)quinolinium salts, further study is needed in the future.

Scheme 3.3 Outer-sphere mechanism for hydrogenation of *N*-heteroaromatics.

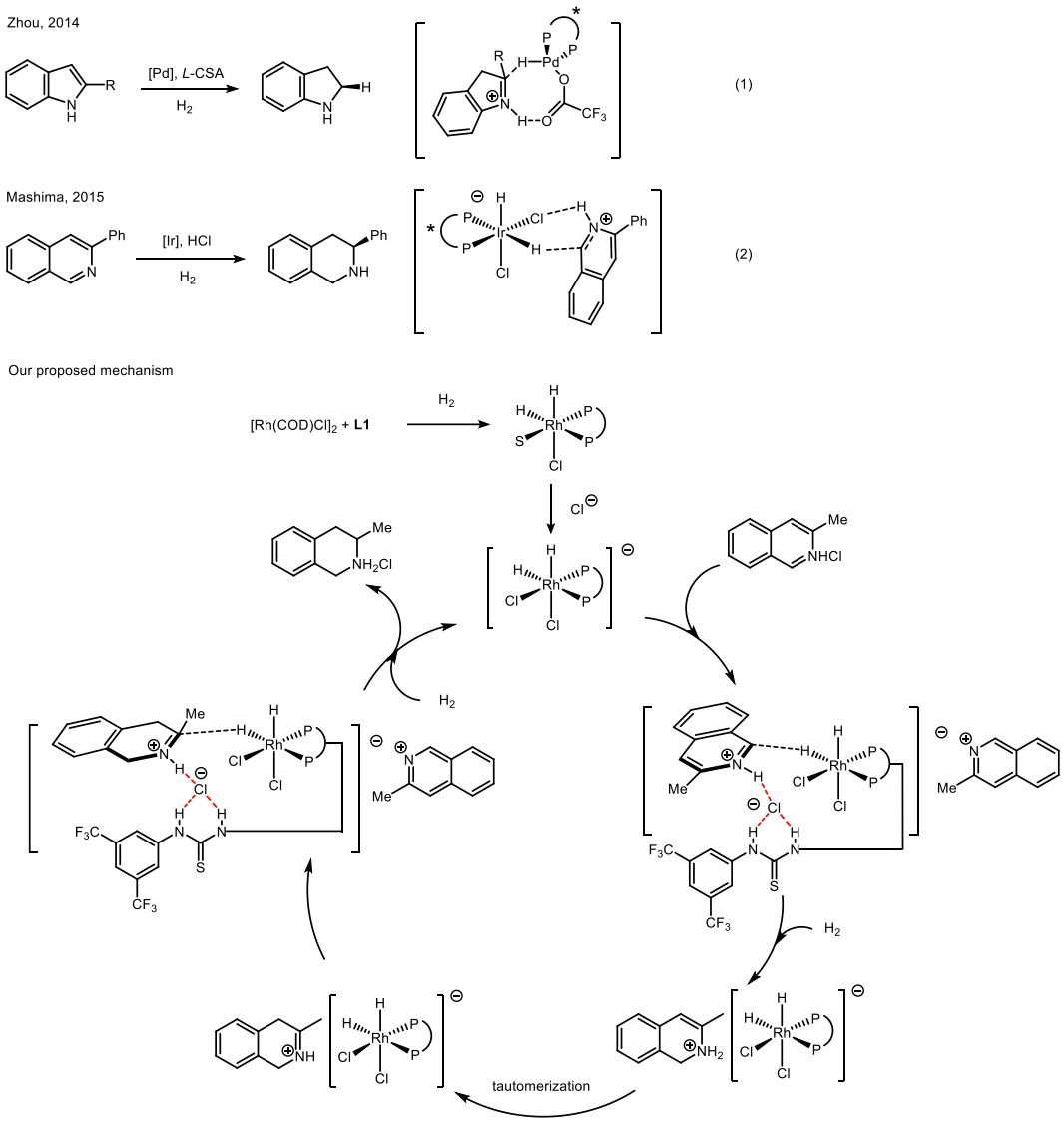

3.7 Conclusions

In summary, we report a successful example of Rh-catalyzed asymmetric hydrogenation of both isoquinolines and quinolines. Compared with previous catalysis systems, this method has broader substrates scope. The strong Brønsted acid HCl activates the *N*-heteroaromatic substrates and introduces anion binding into the catalysis system, which played an important role in this transformation. Deuterium labeling

experiments revealed an enamine-iminium tautomerization equilibrium after the first hydride transfer step.

3.8 Experimental Section

3.8.1 Synthesis of isoquinolines and quinolines

3-substituted isoquinolines were synthesized according to literature with modification:[26]

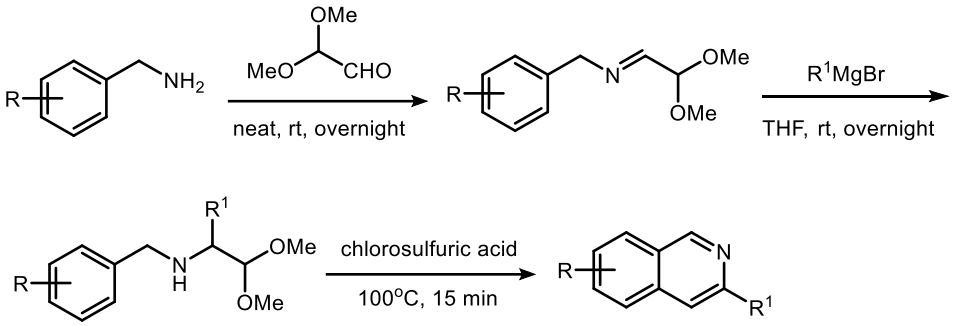

A round-bottom flask was charged with benzylamine (10 mmol) and glyoxal 1,1-dimethyl acetal (1.1 eq., 60% soluition in water) was added dropwise. The mixture was stirred at room temperature overnight and two layers were separated. After removal of the aqueous layer, trace water was removed by azeotropic distillation with toluene. The crude imine was used for next step without purification.

To the solution of this imine in dry THF was added Grignard reagent dropwise at 0oC. The mixture was then stirred at room temperature. Once TLC showed the completion of the reaction (usually overnight), saturated aqueous NH4Cl was added at 0oC. The mixture was extracted with ether and the organic layer was dried with anhydrous sodium sulfate. After removal of solvent, the crude product was obtained as yellow or orange oil. After ^{1}H NMR shows the majority of the desired amine in the crude product, it is used for next step without purification.

A round-bottom flask was filled with nitrogen and charged with chlorosulfuric acid (5 ml). The mixture was cooled at 0 ^{o}C and the crude amine was added dropwise. The mixture was heated at 100 ^{o}C for 15 min and then cooled to 0 ^{o}C. The resulting mixture

was poured on ice and the neutralized carefully with 40% NaOH solution. After the mixture turned to alkaline, ether was added to extract. The organic phase was dried with sodium sulfate and the solvent was removed under reduced pressure. The residue was purified by flash chromatography (on silica gel, eluent: hexane/ethyl acetate). 3-alkylisoquinoline was obtained as yellow oils.

3-ethylisoquinoline

Yellow oil. 43% yield for 3 steps. ^{1}H NMR (400 MHz, CDCl3): δ 9.06 (s, 1H), 7.75 (d, J = 8.1 Hz, 1H), 7.58 (d, J = 8.2 Hz, 1H), 7.47 (t, J = 6.8 Hz, 1H), 7.35 (t, J = 6.8 Hz, 1H), 7.31 (s, 1H), 2.84 (q, J = 7.5 Hz, 2H), 1.27 (t, J = 7.5 Hz, H). ^{13}C NMR (400 MHz, CDCl3): δ 155.92, 150.95, 135.55, 129.08, 126.37, 126.02, 125.16, 125.02, 115.98, 30.06, 13.02. m/z (ESI–MS) 158.04 $[M + H]^{+}$.

3-butylisoquinoline

Yellow oil. 38% yield for 3 steps. ^{1}H NMR (400 MHz, CDCl3): δ 9.19 (s, 1H), 7.90 (d, J = 8.1 Hz, 1H), 7.72 (d, J = 8.2 Hz, 1H), 7.62 (t, J = 7.5 Hz, 1H), 7.50 (t, J = 7.5 Hz, 1H), 7.45 (s, 1H), 2.94 (d, J = 8.1 Hz, 2H), 1.80 (m, 2H), 1.43 (m, 2H), 0.96 (t, J = 7.3 Hz, 3H). ^{13}C NMR (400 MHz, CDCl3): δ 155.88, 152.04, 136.54, 130.14, 127.46, 127.07, 126.22, 126.06, 117.87, 37.84, 32.14, 22.50, 13.97. m/z (ESI–MS) 186.06 $[M + H]^{+}$.

3,6-dimethylisoquinoline

White solid. 38% yield for 3 steps. ^{1}H NMR (400 MHz, CDCl3): δ 9.10 (s, 1H), 7.81 (d, J = 8.4 Hz, 1H), 7.48 (s, 1H), 7.38 (s, 1H), 7.34 (dd, J = 8.4, 1.4 Hz, 1H), 2.38 (s, 3H), 2.52 (s, 3H). ^{13}C NMR (400 MHz, CDCl3): δ 151.67, 151.51, 140.56, 136.92, 128.56, 127.28, 125.37, 124.80, 117.93, 24.18, 22.05.

MP: m/z (ESI–MS) 158.14 $[M + H]^{+}$.

6-chloro-3-methylisoquinoline

Yellow oil. 56% yield for 3 steps. ^{1}H NMR (400 MHz, CDCl3): δ 9.14 (s, 1H), 7.85 (d, J = 8.7 Hz, 1H), 7.69 (d, J = 1.8 Hz, 1H), 7.45 (dd, J = 8.7, 2.0 Hz, 1H), 7.38 (s, 1H),

2.69 (s, 3H). ^{13}C NMR (400 MHz, CDCl3): δ 152.99, 151.72, 137.26, 129.15, 127.41, 125.04, 124.80, 117.53, 24.25. m/z (ESI–MS) 178.14 [M + H]$^+$.

6-fluoro-3-methylisoquinoline

Yellow oil. 34% yield for 3 steps. ^{1}H NMR (400 MHz, CDCl3): δ 9.12 (s, 1H), 7.91 (dd, J = 8.9, 5.6 Hz, 1H), 7.41 (s, 1H), 7.30 (dd, J = 10.1, 2.0 Hz, 1H), 7.25 (dd, J = 8.7, 2.5 Hz, 1H), 2.68 (s, 3H). ^{13}C NMR (400 MHz, CDCl3): δ 163.28 (d, J = 251.9 Hz), 152.66, 151.52, 137.94 (d, J = 10.5 Hz), 130.43 (d, J = 9.9 Hz), 124.04, 118.01 (d, J = 5.3 Hz), 116.81 (d, J = 25.8 Hz), 109.14 (d, J = 20.9 Hz). m/z (ESI–MS) 162.04 [M + H]$^+$.

6-trifluoromethyl-3-methylisoquinoline

Yellow oil. 27% yield for 3 steps. ^{1}H NMR (400 MHz, CDCl3): δ 9.26 (s, 1H), 8.05 (s, 1H), 8.03 (s, 2H), 7.68 (dd, J = 8.4, 1.6 Hz, 1H), 7.56 (s, 1H), 2.74 (s, 3H). ^{13}C NMR (400 MHz, CDCl3): δ 153.40, 151.92, 144.38, 135.56, 131.90 (q, J = 128.4 Hz), 128.69, 127.47, 123.79 (q, J = 18.1 Hz), 121.96 (q, J = 12.1 Hz), 118.98, 24.20. m/z (ESI–MS) 211.97 [M + H]$^+$.

8-chloro-3-methylisoquinoline

Yellow oil. 41% yield for 3 steps. ^{1}H NMR (400 MHz, CDCl3) δ 9.56 (s, 1H), 7.64 (dd, J = 5.5, 3.7 Hz, 1H), 7.54 (s, 1H), 7.53 (d, J = 2.3 Hz, 1H), 7.47 (s, 1H), 2.72 (s, 3H). ^{13}C NMR (400 MHz, CDCl3): δ 152.79, 148.94, 137.89, 132.52, 130.19, 126.52, 125.14, 124.01, 118.15, 24.08. m/z (ESI–MS) 178.16 [M + H]$^+$.

2-substituted quinolines were synthesized according to literature:

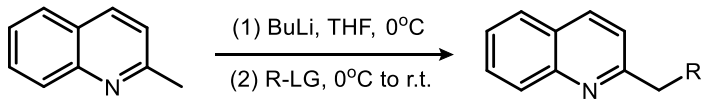

To a solution of 1-methylquinoline (10 mmol) in dry THF (20 ml) at 0°C was added n-butyllithium in THF solution (2.5M) dropwise. The mixture was stirred at room temperature for 1.5h and was cooled back to 0°C. Iodomethane was added dropwise. The mixture was stirred overnight. Water was added carefully to quench the reaction and the mixture was extracted by ethyl acetate (20 ml*3). Organic phases were combined and dried with sodium sulfate. After

removing solvent, the crude product was purified by flash chromatography (on silica gel, eluent: hexanes/ethyl acetate). 2-methylquinoline was obtained as yellow oil with 95% yield.

All characterization data are consistent with literature. [12, 27]

2-ethylquinoline

Known compound. ^{1}H NMR (400 MHz, $CDCl_3$) δ 8.04 (dd, *J* = 11.8, 8.5 Hz, 1H), 7.74 (d, *J* = 8.1 Hz, 1H), 7.65 (ddd, *J* = 8.3, 6.9, 1.4 Hz, 1H), 7.45 (dd, *J* = 11.0, 4.0 Hz, 1H), 7.28 – 7.25 (d, *J* = 8.5 Hz, 1H), 2.99 (q, *J* = 7.6 Hz, 2H), 1.39 (dd, *J* = 7.6 Hz, 3H).

^{13}C NMR (400 MHz, $CDCl_3$): δ 163.97, 147.87, 136.31, 129.30, 128.79, 127.46, 126.37, 125.63, 120.81, 32.28, 13.97

2-isopropylquinoline

Followed the standard procedure above, using 2-ethylquinoline and iodomethane, 2-isopropylquinoline was abotained as yellow oil with 76% yield. ^{1}H NMR (400 MHz, $CDCl_3$) δ 8.05 (dd, *J* = 8.2, 6.0 Hz, 2H), 7.74 (dd, *J* = 8.1, 1.1 Hz, 1H), 7.65 (ddd, *J* = 8.4, 6.9, 1.4 Hz, 1H), 7.45 (ddd, *J* = 8.1, 7.0, 1.1 Hz, 1H), 7.30 (t, *J* = 8.6 Hz, 1H), 3.26 (hept, *J* = 6.9 Hz, 1H), 1.38 (d, *J* = 6.9 Hz, 3H). ^{13}C NMR (400 MHz, CDCl3): δ 167.63, 147.79, 136.36, 129.21, 129.04, 127.42, 126.95, 125.62, 119.16, 37.29, 22.52.

2-pentylquinoline

Yellow oil. ^{1}H NMR (400 MHz, $CDCl_3$) δ 8.04 (t, *J* = 8.4 Hz, 2H), 7.75 (d, *J* = 8.1 Hz, 1H), 7.66 (t, *J* = 7.7 Hz, 1H), 7.45 (t, *J* = 7.5 Hz, 1H), 7.27 (d, *J* = 8.4 Hz, 1H), 2.99 – 2.94 (m, 2H), 1.86 – 1.77 (m, 2H), 1.37 (m, 2H), 0.90 (t, *J* = 6.7 Hz, 3H). ^{13}C NMR (400 MHz, CDCl3): δ 163.10, 147.97, 136.10, 129.25, 128.88, 127.45, 126.72, 125.59, 121.34, 39.35, 31.76, 29.71, 22.56, 14.00.

2-undecylquinoline

Yellow oil. ^{1}H NMR (400 MHz, $CDCl_3$) δ 7.76 (dd, *J* = 8.1, 1.4 Hz, 1H), 7.67 (ddd, *J* = 8.3, 6.9, 1.4 Hz, 1H), 7.46 (ddd, *J* = 8.0, 7.0, 1.0 Hz, 1H), 7.28 (d, *J* = 8.4 Hz, 1H), 2.96 (t, *J* = 8.0 Hz, 2H), 1.86 – 1.76 (m, 2H), 1.46 – 1.19 (m, 16H), 0.90 – 0.85 (m, 3H). ^{13}C NMR (400 MHz, CDCl3): δ 163.12, 147.97, 136.09, 129.25, 128.88, 127.44, 126.72, 125.58, 121.34, 39.40, 31.68, 30.03, 29.58, 29.56, 29.52, 29.30, 22.66, 14.09.

2-(3,4-dimethoxyphenethyl)quinoline

Yellow oil. ^{1}H NMR (400 MHz, $CDCl_3$) δ 8.07 (d, *J* = 8.4, 1H), 8.03 (d, *J* = 8.4 Hz, 1H), 7.77 (dd, *J* = 8.1, 0.8 Hz, 1H), 7.69 (ddd, *J* = 8.4, 6.9, 1.4 Hz, 1H), 7.49 (d, *J* = 8.4, 6.9, 1.4 Hz, 1H), 7.22 (d, *J* = 8.4 Hz, 1H), 6.78 (d, *J* = 1.0 Hz, 1H), 6.75 (s, 1H), 3.84 (s, 1H), 3.79 (s, 1H), 3.27 (dd, *J* = 9.6, 6.2 Hz, 1H), 3.10 (dd, *J* = 9.5, 6.4 Hz, 1H). ^{13}C NMR (400 MHz, CDCl3): δ 161.84, 148.83, 148.01, 147.34, 136.16, 134.17, 129.40, 128.86, 127.52, 126.60, 125.79, 121.62, 120.34, 112.01, 111.34, 55.92, 55.77, 41.23, 35.54.

3.8.2 General procedure for asymmetric hydrogenation of isoquinolines and quinolines

In the nitrogen-filled glovebox, solution of [Rh(COD)Cl]2 (4.9 mg, 0.01 mmol) and ligand (2.1 eq.) in 5.0 ml anhydrous solvent was stirred at room temperature for 30 min. A specified volume of the resulting solution (0.5 ml, 1% Rh catalyst) was transferred) by syringe to a Score-Break ampule charged with substrate solution (0.2 mmol in 0.5 ml). The ampule was placed into an autoclave, which was then charged with 40 atm H2. The autoclave was stirred at desired temperature for the indicated period of time. After release of H2, the resulting mixture was concentrated under vacuum. Saturated potassium carbonate solution and dichloromethane was added and the mixture was stirred for 30 min. The organic layer was dried with anhydrous sodium sulfate. After removal of solvent, the crude product was analysed by 1H NMR to determine the conversion. The enantiomeric excess was determined by GC or HPLC analysis of the crude product or its corresponding trifluoroacetamides. The absolute configurations were assigned according to literature [11, 28-30] and their analogues.

3.8.3 Result of deuterium labeling experiments

Following standard hydrogenation procedure, deuterium labeling experiments were conducted with specific modification.

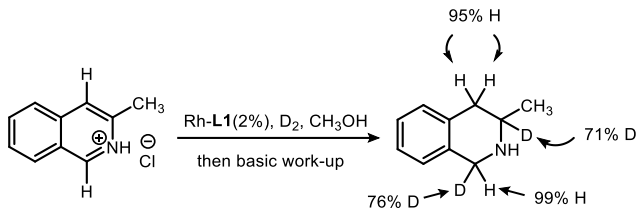
95% H
H H
CH3
D
71% D
NH
76% D
D H
99% H
H
CH3
NH
Cl
H
Rh-L1(2%), D2, CH3OH
then basic work-up

(1)

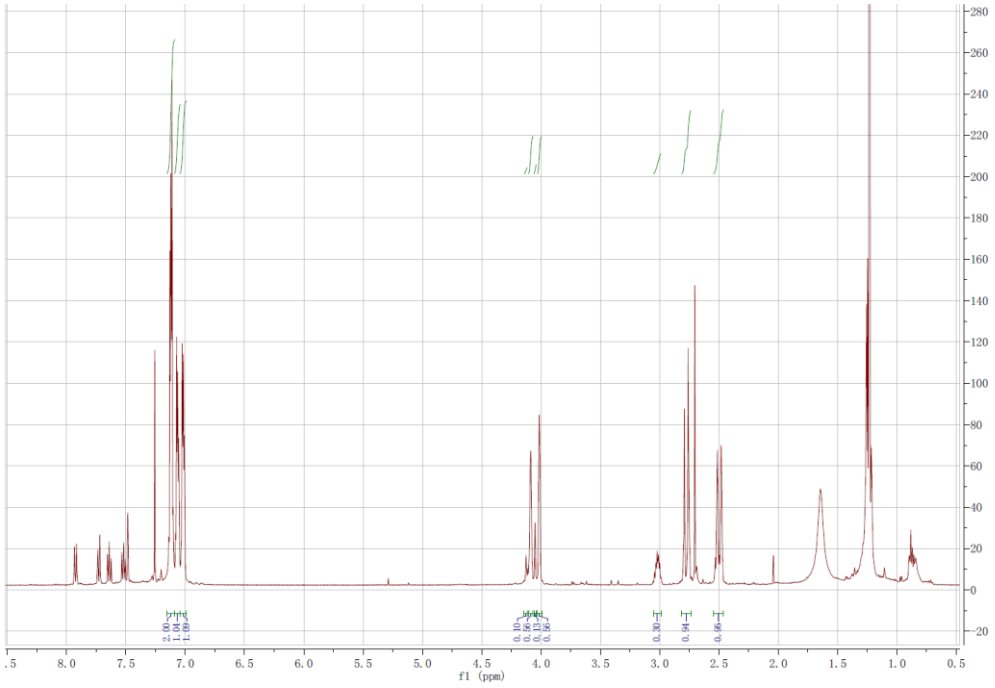
f1 (ppm)

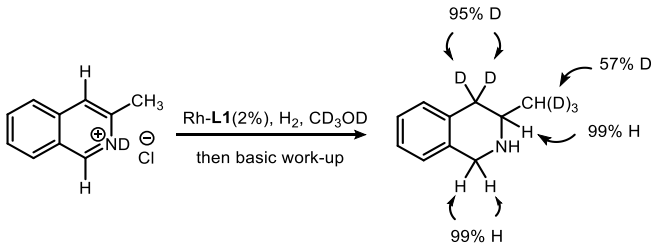
95% D
D D
57% D
CH(D)3
H
99% H
NH
H H
99% H
H
CH3
ND
Cl
H
Rh-L1(2%), H2, CD3OD
then basic work-up

(2)

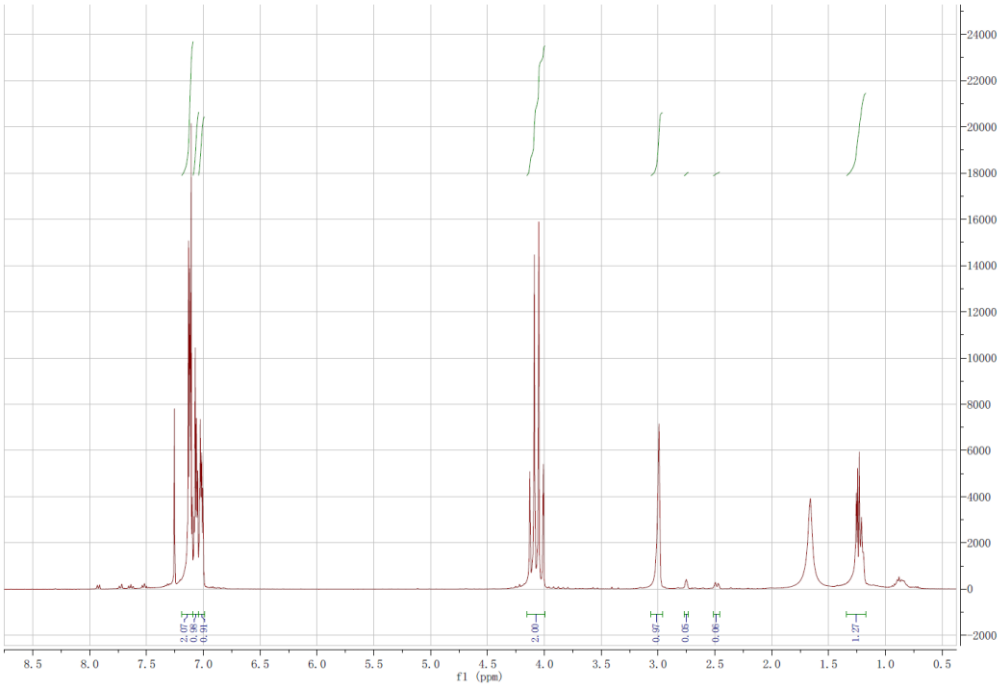

For clarity, combined spectrum for the original 2a and the two deuterated 2a were shown as below:

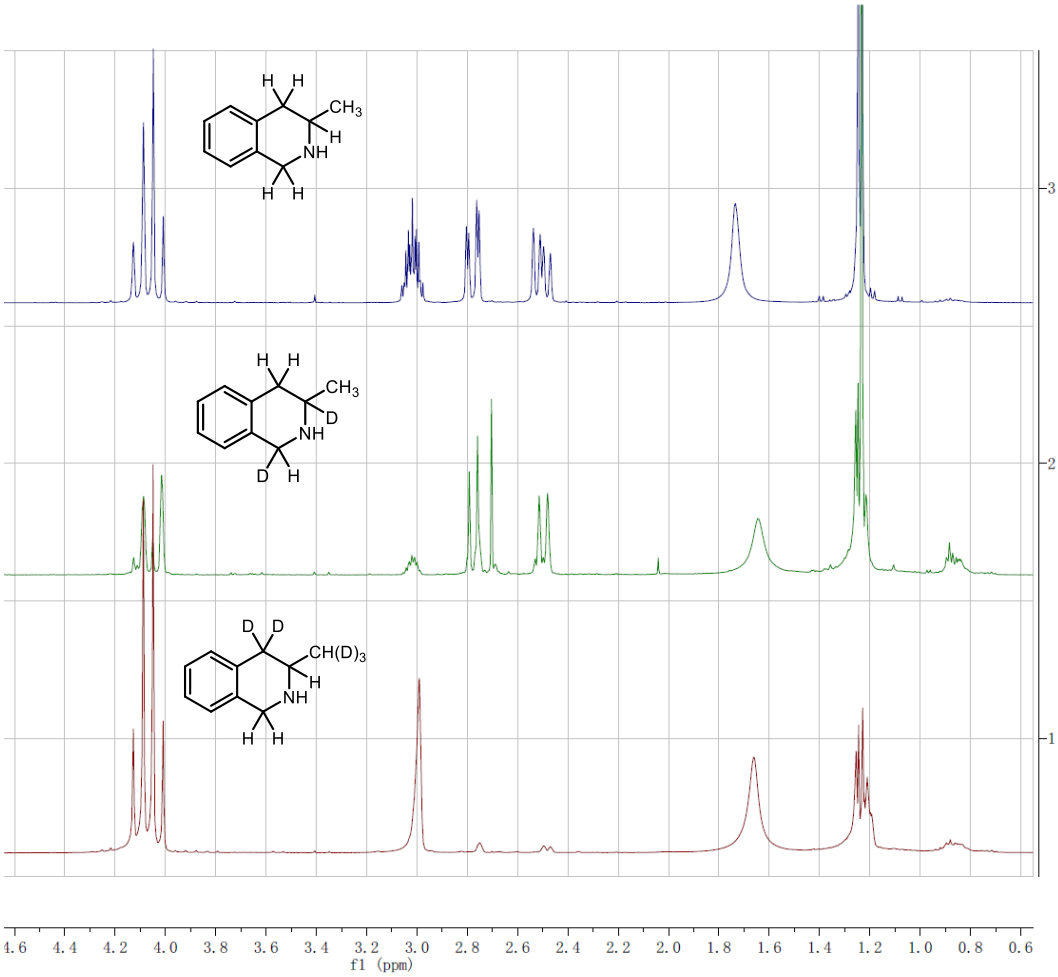

3.8.4 Characterization data of chiral THQs and THIQs

3-methyl-1,2,3,4-tetrahydroisoquinoline (4a)

Yellow oil. 1H NMR (400 MHz, CDCl3): δ 7.11 (m, 2H), 7.06 (m, 1H), 7.01 (t, 1H), 4.11 (d, J =16.0 Hz, 1H), 4.02 (d, J =16.0 Hz, 1H), 3.02 (dqd, J = 10.3, 6.3, 4.0 Hz, 1H), 2.78 (dd, J = 16.4, 3.8 Hz, 1H), 2.51 (dd, J = 16.3, 10.7 Hz, 1H), 1.73 (br, 1H), 1.24 (d, J = 6.3 Hz, 3H).

13C NMR (400 MHz, CDCl3): δ 135.39, 134.92, 129.11, 126.01, 126.00, 125.70, 49.25, 48.59, 37.26, 22.50.

$[\alpha]^{22}_{D}$ +103.6 (*c* 0.5, $CHCl_3$).

m/z (ESI–MS) 148.22 $[M + H]^+$.

Supelco gama Dex 225 column (30 m ×0.25 mm × 0.25 μm), He 1.0 mL/min, column 100 °C, t_1 =46.3 min, t_2 =47.7 min.

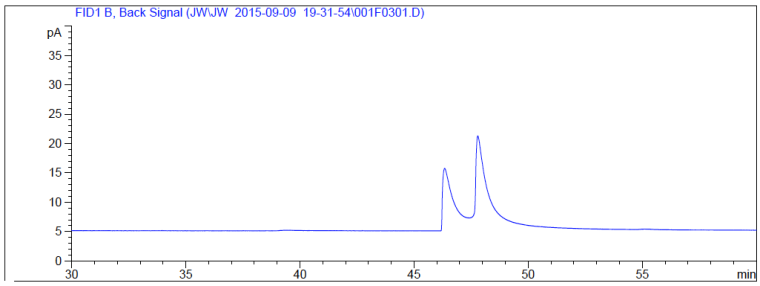

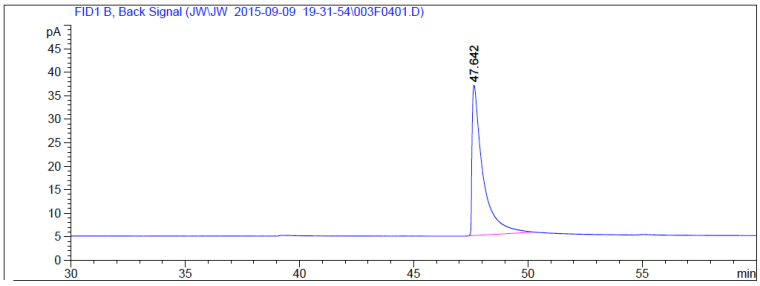


```
Signal 1: FID1 B, Back Signal

Peak RetTime Type  Width     Area      Height     Area
  #   [min]        [min]   [pA*s]      [pA]        %
----|-------|----|-------|----------|----------|--------|
   1  47.642 BB    0.4541 1052.56445   32.00426 1.000e2

Totals :                  1052.56445   32.00426

===================================================================
                          *** End of Report ***
```

3-ethyl-1,2,3,4-tetrahydroisoquinoline (4b)

Yellow oil. ^{1}H NMR (400 MHz, CDCl3): δ 7.12 (m, 3H), 7.02 (m, 1H), 4.09 (d, *J* = 12.0 Hz, 1H), 4.03 (d, *J* = 12.0 Hz, 2H), 2.79 (tdd, *J* = 10.4, 6.8, 3.8 Hz, 1H), 2.50 (dd, *J* = 17.0, 11.5 Hz, 1H), 1.74 (br, 1H), 1.64-1.47 (m, 2H), 1.02 (t, 3H).

^{13}C NMR (400 MHz, CDCl3): δ 135.76, 134.92, 129.46, 126.01, 125.99, 125.65, 55.25, 48.62,

35.11, 29.61, 10.39.

$[\alpha]^{22}_{D}$ +97.3 (*c* 0.5, $CHCl_3$).

m/z (ESI–MS) 162.09 $[M + H]^+$.

Supelco gama Dex 225 column (30 m ×0.25 mm × 0.25 µm), He 1.0 mL/min, column 100 °C, t_1 =83.2 min, t_2 =85.3 min.

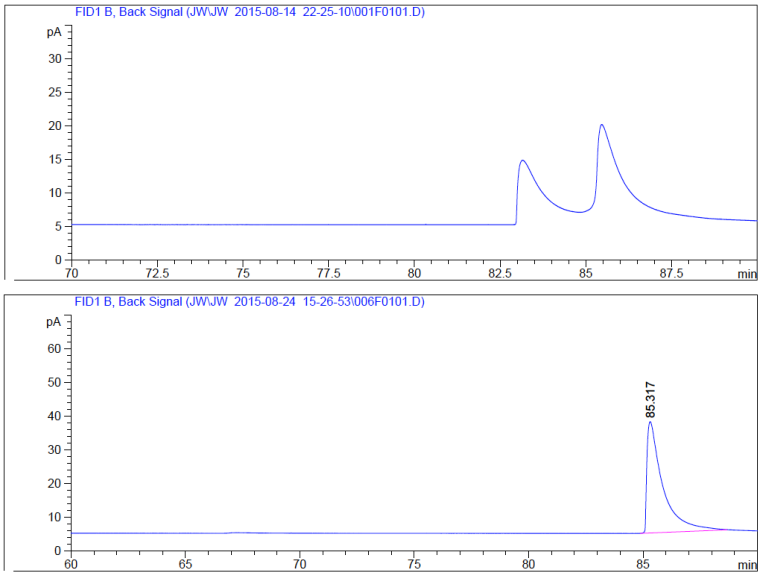


```
Signal 1: FID1 B, Back Signal

Peak RetTime Type  Width     Area      Height     Area
  #   [min]        [min]   [pA*s]      [pA]        %
----|-------|----|-------|----------|----------|--------|
   1  85.317 BB    0.6529 1595.54932   33.04603 1.000e2

Totals :                  1595.54932   33.04603

===================================================================
                         *** End of Report ***
```

3-butyl-1,2,3,4-tetrahydroisoquinoline (4c)

Yellow oil. ^{1}H NMR (400 MHz, CDCl3): δ 7.11 (m, 3H), 7.02 (m, 1H), 4.08 (d, *J* =16.0 Hz, 2H), 4.03 (d, *J* =16.0 Hz, 2H), 2.82 (comp., 2H), 2.50 (dd, *J* = 16.1, 10.4 Hz, 1H), 1.50 (br, 1H), 1.30-1.60 (m, 6H), 1.02 (t, *J* = 3.2 Hz, 3H).

^{13}C NMR (400 MHz, CDCl3): δ 135.78, 134.97, 129.22, 125.99, 125.66, 57.72, 48.60, 36.60, 35.58, 28.19, 22.86, 14.06.

$[\alpha]^{22}_{D}$ +81.8 (*c* 0.5, $CHCl_3$).

m/z (ESI–MS) 190.17 $[M + H]^+$.

Supelco gama Dex 225 column (30 m ×0.25 mm × 0.25 µm), He 1.0 mL/min, column 100 °C, t_1 =278.3 min, t_2 =285.0 min.

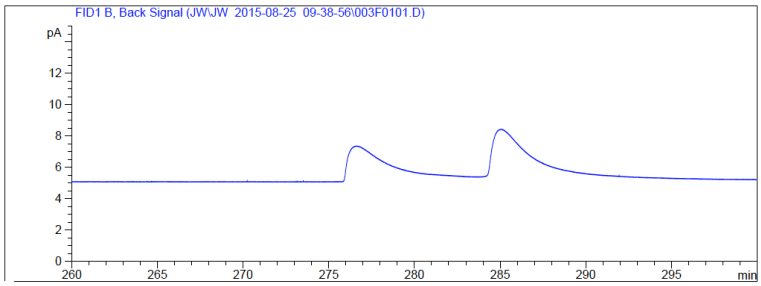

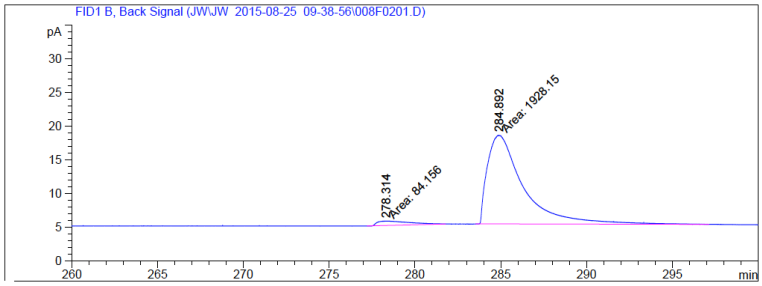


```
Signal 1: FID1 B, Back Signal

Peak RetTime Type  Width     Area      Height     Area
  #   [min]        [min]   [pA*s]      [pA]         %
----|-------|----|-------|----------|----------|--------|
   1 278.314 MM    2.1398   84.15600 6.55473e-1  4.18207
   2 284.892 MM    2.4380 1928.14819   13.18125 95.81793

Totals :                  2012.30419   13.83672


=====================================================================
                          *** End of Report ***
```

3,6-dimethyl-1,2,3,4-tetrahydroisoquinoline (4d)

Yellow oil. ^{1}H NMR (400 MHz, CDCl3): δ 7.00 – 6.77 (m, 3H), 4.06 (d, *J* = 15.7 Hz, 1H), 3.99 (d, *J* = 15.8 Hz, 1H), 3.05–2.94 (m, 1H), 2.73 (dd, *J* = 16.3, 3.4 Hz, 1H), 2.46 (dd, *J* = 16.0, 10.8 Hz, 1H), 2.29 (s, 3H), 1.69 (s, 1H), 1.23 (d, *J* = 6.3 Hz, 3H).

^{13}C NMR (400 MHz, CDCl3): δ 135.45, 134.76, 132.38, 129.60, 126.65, 125.88, 49.28, 48.33, 37.27, 22.49, 20.98.

$[\alpha]^{22}_{D}$ +87.4 (*c* 0.5, $CHCl_3$).

m/z (ESI–MS) 162.08 $[M + H]^+$.

Supelco Chiral Select 1000 column (30 m ×0.25 mm × 0.25 μm) for its corresponding trifluoroacetamide, He 1.0 mL/min, column 120 °C, t_1 =91.4 min, t_2 =93.0 min.

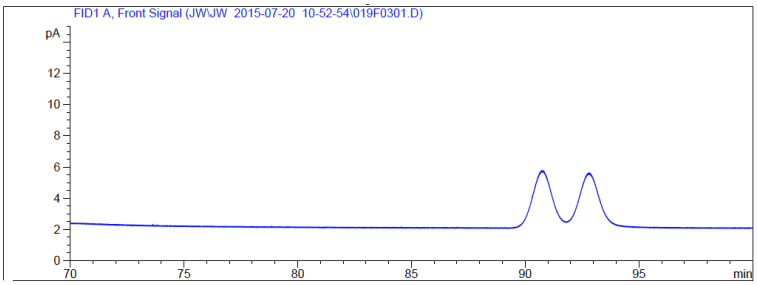

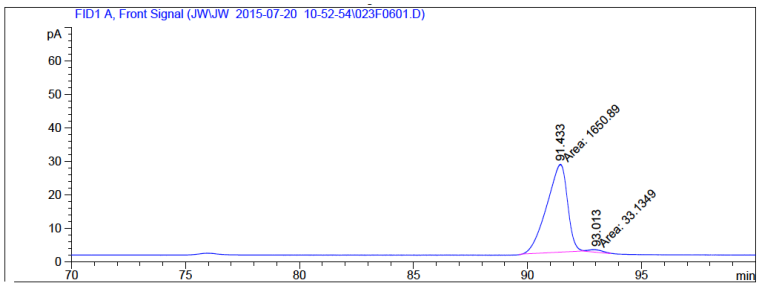


```
Signal 1: FID1 A, Front Signal

Peak RetTime Type  Width     Area      Height     Area
  #   [min]        [min]   [pA*s]      [pA]         %
----|-------|----|-------|----------|----------|--------|
   1  91.433 MM    1.0499 1650.89038   26.20647 98.03240
   2  93.013 MM    0.7184   33.13491 7.68718e-1  1.96760

Totals :                  1684.02529   26.97519


=====================================================================
                         *** End of Report ***
```

6-trifluoromethyl-3-methyl-1,2,3,4-tetrahydroisoquinoline (4e)

Yellow oil. ^{1}H NMR (400 MHz, CDCl3): δ 7.36 (d, *J* = 8.1 Hz, 1H), 7.32 (s, 1H), 7.12 (d, *J* = 8.0 Hz, 1H), 3.14 (d, *J* = 16.4 Hz, 1H), 3.09 (d, *J* = 16.4 Hz, 1H), 2.83 (dd, *J* = 16.5, 3.7 Hz, 1H), 2.54 (dd, *J* = 16.4, 10.6 Hz, 1H), 1.26 (d, *J* = 6.3 Hz, 3H).

^{13}C NMR (400 MHz, CDCl3): δ 139.32, 135.72, 128.46 (q, *J* = 127.6 Hz), 126.46, 125.96 (q, *J* = 15.2 Hz), 122.97, 122.48 (q, *J* = 7.0 Hz), 49.03, 48.44, 37.13, 22.27.

$[\alpha]^{22}_{D}$ +80.2 (*c* 0.5, $CHCl_3$).

m/z (ESI–MS) 216.01 $[M + H]^+$.

Supelco gama Dex 225 column (30 m ×0.25 mm × 0.25 μm), He 1.0 mL/min, column 100 °C, t_1 =60.8 min, t_2 =64.7 min.

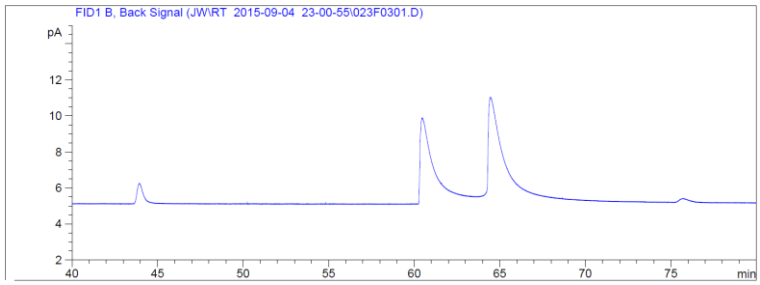

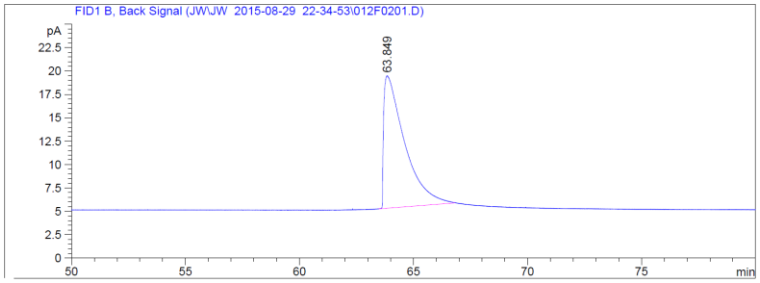

```
Signal 1: FID1 B, Back Signal

Peak RetTime Type  Width     Area      Height     Area
  #   [min]        [min]   [pA*s]      [pA]         %
----|-------|----|-------|----------|----------|--------|
   1  63.849 BB    0.8115  897.82019   14.13314 1.000e2

Totals :                   897.82019   14.13314

=====================================================================
                          *** End of Report ***
```

6-chloro-3-methyl-1,2,3,4-tetrahydroisoquinoline (4f)

Yellow oil. ^{1}H NMR (400 MHz, CDCl3): δ 7.07 (t, 2H), 6.94 (d, *J* = 8.1 Hz, 1H), 4.05 (d, *J* = 16.0 Hz, 1H), 3.99 (d, *J* = 16.0 Hz, 1H), 2.99 (dqd, *J* = 12.6, 6.3, 4.0 Hz, 1H), 2.74 (dd, *J* = 16.5, 3.7 Hz, 1H), 2.48 (dd, *J* = 16.5, 10.6 Hz, 1H), 1.71 (br, 1H), 1.24 (d, *J* = 6.3 Hz, 3H).

^{13}C NMR (400 MHz, CDCl3): δ 136.86, 133.77, 131.48, 128.83, 127.33, 125.87, 48.92, 48.09, 37.04, 29.29.

$[\alpha]^{22}_{D}$ +72.1 (*c* 0.5, $CHCl_3$).

m/z (ESI–MS) 182.15, 184.02 $[M + H]^+$.

Supelco gama Dex 225 column (30 m ×0.25 mm × 0.25 μm), He 1.0 mL/min, column 120 °C, t_1 =67.5 min, t_2 =69.4 min.

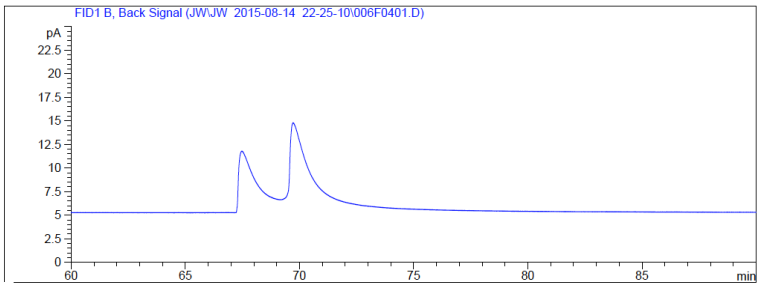

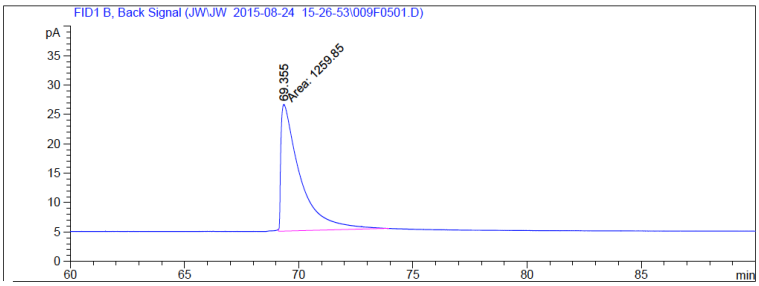


```
Signal 1: FID1 B, Back Signal

Peak RetTime Type  Width     Area      Height     Area
  #   [min]        [min]   [pA*s]      [pA]         %
----|-------|----|-------|----------|----------|--------|
   1  69.355 MM    0.9725 1259.84631   21.59215 1.000e2

Totals :                  1259.84631   21.59215

=====================================================================
                          *** End of Report ***
```

6-fluoro-3-methyl-1,2,3,4-tetrahydroisoquinoline (4g)

Yellow oil. ^{1}H NMR (400 MHz, CDCl3): δ 6.96 (dd, *J* = 8.3, 5.8 Hz, 1H), 6.81 (td, *J* = 8.5, 2.6 Hz, 1H), 6.76 (dd, *J* = 9.6, 2.5 Hz, 1H), 4.05 (d, *J* = 15.6 Hz, 2H), 4.00 (d, *J* = 15.6 Hz, 2H), 2.99 (dqd, *J* = 10.3, 6.3, 4.0 Hz, 1H), 2.75 (dd, *J* = 16.5, 3.8 Hz, 1H), 2.49 (dd, *J* = 16.5, 10.7 Hz, 1H), 1.24 (d, *J* = 6.3 Hz, 3H).

^{13}C NMR (400 MHz, CDCl3): δ 161.18 (d, *J* = 964.4 Hz), 137.00 (d *J* = 29.4 Hz), 130.90 (d, *J* = 11.6 Hz), 127.35 (d, *J* = 32.4 Hz), 115.34 (d, *J* = 81.2 Hz), 112.79 (d, *J* = 86.0 Hz), 48.93, 48.05, 37.32, 22.30.

$[\alpha]^{22}_{D}$ +82.1 (*c* 0.5, $CHCl_3$).

m/z (ESI–MS) 166.24 $[M + H]^+$.

Supelco gama Dex 225 column (30 m ×0.25 mm × 0.25 µm), He 1.0 mL/min, column 100 °C, t_1 =58.0 min, t_2 =60.0 min.

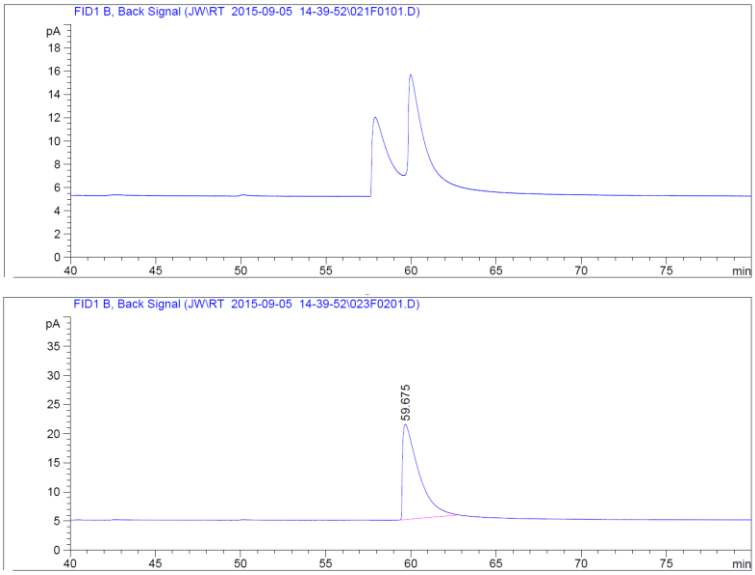

Signal 1: FID1 B, Back Signal

Peak #	RetTime [min]	Type	Width [min]	Area [pA*s]	Height [pA]	Area %
1	59.675	BB	0.8510	1079.47339	16.33518	1.000e2
Totals :				1079.47339	16.33518	

*** End of Report ***

8-chloro-3-methyl-1,2,3,4-tetrahydroisoquinoline (4h)

Yellow oil. ^{1}H NMR (400 MHz, CDCl3): δ 7.16 (d, *J* = 7.8 Hz, 1H), 7.06 (t, *J* = 7.7 Hz, 1H),

6.97 (d, *J* = 7.5 Hz, 1H), 4.20 (d, *J* = 16.9 Hz, 1H), 3.94 (d, *J* = 16.9 Hz, 1H), 2.97 (dqd, *J* = 10.1, 6.3, 3.8 Hz, 1H), 2.77 (dd, *J* = 16.3, 3.5 Hz, 1H), 2.50 (dd, *J* = 16.3, 10.6 Hz, 1H), 1.67 (s, 1H), 1.24 (d, *J* = 6.3 Hz, 3H).

^{13}C NMR (400 MHz, CDCl3): δ 137.42, 133.23, 132.21, 127.52, 126.84, 126.52, 48.57, 46.79, 37.36, 22.19.

$[\alpha]^{22}_{D}$ +117.7 (*c* 0.5, $CHCl_3$).

m/z (ESI–MS) 182.09, 184.01 $[M + H]^+$.

Supelco gama Dex 225 column (30 m ×0.25 mm × 0.25 μm), He 1.0 mL/min, column 100 °C, t_1 =158.2 min, t_2 =160.4 min.

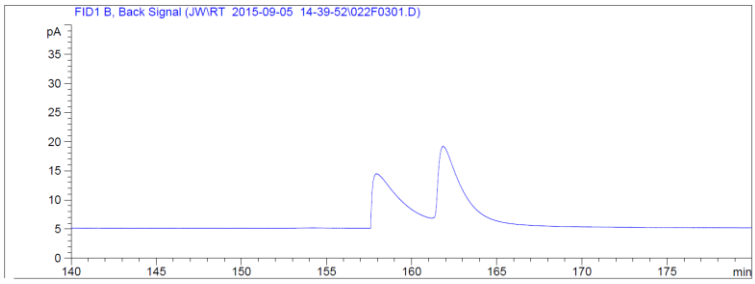

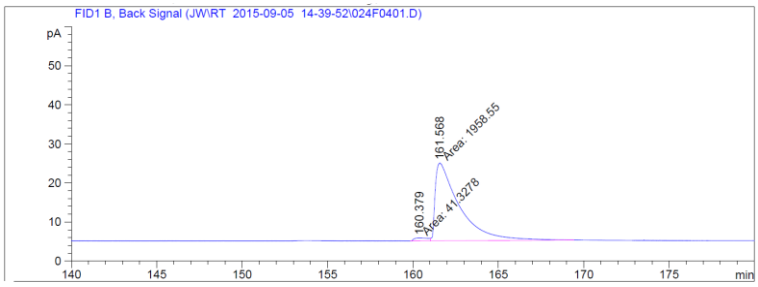

Signal 1: FID1 B, Back Signal

Peak #	RetTime [min]	Type	Width [min]	Area [pA*s]	Height [pA]	Area %
1	160.379	MF	0.9163	41.32780	7.51749e-1	2.06652
2	161.568	FM	1.6383	1958.54700	19.92477	97.93348

Totals : 1999.87479 20.67652

*** End of Report ***

1-methyl-1,2,3,4-tetrahydroisoquinoline (4i)

Yellow oil. ^{1}H NMR (400 MHz, $CDCl_3$) δ7.22 – 7.03 (m, 4H), 4.14 (d, *J* = 6.8 Hz, 1H), 3.31 (M, 1H), 3.03 (m, 1H), 2.92 (m, 1H), 2.82 – 2.60 (m, 1H), 2.25 (br, 1H), 1.47 (d, *J* = 5.6 Hz, 3H).

^{13}C NMR (400 MHz, CDCl3): δ 140.32, 134.68, 129.20, 125.99, 129.90 (overlap), 51.57, 41.71, 29.91, 22.63.

$[\alpha]^{22}_{D}$ -77.0 (*c* 0.5, $CHCl_3$).

Supelco Chiral Select 1000 column (30 m ×0.25 mm × 0.25 μm) for its corresponding trifluoroacetamide, He 1.0 mL/min, column 120 °C, t_1 =56.8 min, t_2 =58.3 min.

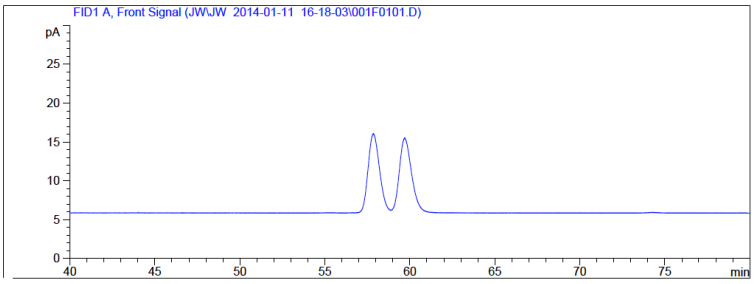

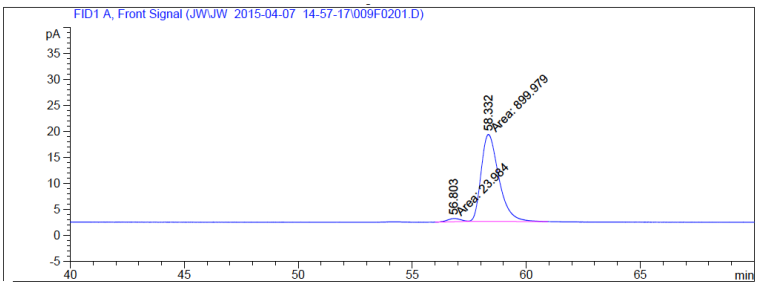


```
Signal 1: FID1 A, Front Signal

Peak RetTime Type  Width     Area      Height     Area
  #   [min]        [min]   [pA*s]      [pA]         %
----|-------|----|-------|----------|----------|--------|
   1  56.803 MM    0.6386   23.98396 6.25927e-1  2.59577
   2  58.332 MM    0.8972  899.97919   16.71776 97.40423

Totals :                   923.96314   17.34369


=====================================================================
                          *** End of Report ***
```

3-phenyl-1,2,3,4-tetrahydroisoquinoline (4j)

Yellow oil. ^{1}H NMR (400 MHz, $CDCl_3$) δ 7.43 (d, *J* = 7.9 Hz, 2H), 7.36 (dd, *J* = 8.0, 6.5 Hz, 2H), 7.28 (t, *J* = 7.2 Hz, 1H), 7.18-7.05 (m, 4H), 4.26 (d, *J* = 15.6 Hz, 1H), 4.16 (d, *J* = 15.6 Hz, 1H), 4.00 (t, *J* = 7.5 Hz, 1H), 2.97 (d, *J* = 7.3 Hz, 2H), 1.93 (br, 1H).

^{13}C NMR (400 MHz, CDCl3): δ 144.33, 135.04, 134.92, 129.10, 128.63, 127.39, 126.55, 126.26, 126.18, 125.90, 58.61, 49.27, 37.73.

Daicel Chiralpak OD-H for its corresponding trifluoroacetamide, hexanes/i-PrOH = 98/2, Flow rate = 1.0 ml/min, UV = 220 nm, t_1 = 10.4 min, t_2 = 13.1 min.

$[\alpha]^{22}_{D}$ -77.0 (*c* 0.5, $CHCl_3$).

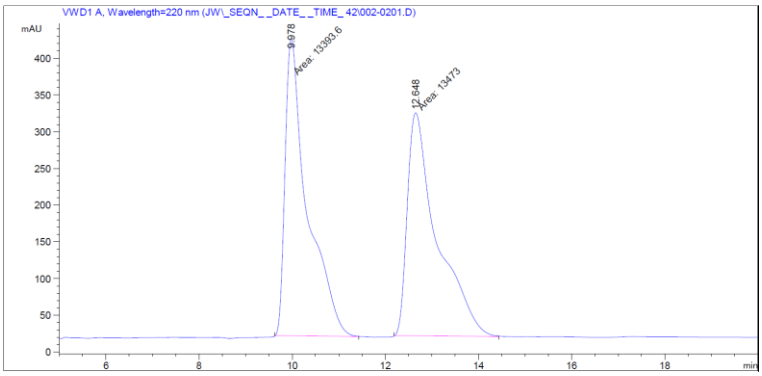

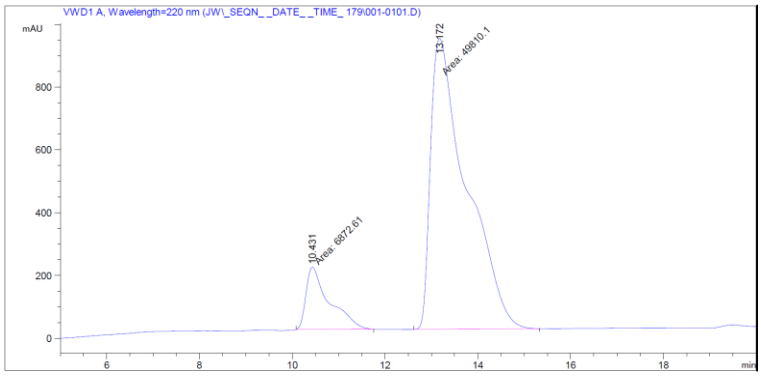

Signal 1: VWD1 A, Wavelength=220 nm

Peak #	RetTime [min]	Type	Width [min]	Area mAU *s	Height [mAU]	Area %
1	10.431	MM	0.5781	6872.61035	198.15254	12.1247
2	13.172	MM	0.8965	4.98101e4	925.97284	87.8753
Totals :				5.66827e4	1124.12538	

2-methyl-1,2,3,4-tetrahydroquinoline (6a)

Yellow oil. ^{1}H NMR (400 MHz, CDCl3): δ 6.98 – 6.92 (m, 2H), 6.59 (td, *J* = 7.4, 1.1 Hz, 1H), 6.45 (dd, *J* = 5.2, 3.2 Hz, 1H), 3.67 (b, 1H), 3.43 – 3.35 (m, 1H), 2.83 (ddd, *J* = 16.9, 11.5, 5.6 Hz, 1H), 2.75 – 2.68 (m, 1H), 1.95 – 1.88 (m, 1H), 1.58 (dddd, *J* = 12.8, 11.6, 10.0, 5.4 Hz, 1H), 1.20 (d, *J* = 6.3 Hz, 3H).

^{13}C NMR (400 MHz, CDCl3): δ 143.73, 128.22, 125.65, 120.09, 115.97, 112.98, 46.15, 29.12, 25.55, 21.56.

$[\alpha]^{22}_{D}$ -44.3 (*c* 0.5, $CHCl_3$).

Supelco gama Dex 225 column (30 m ×0.25 mm × 0.25 µm), He 1.0 mL/min, column 120 °C, t_1 =30.5 min, t_2 =31.3 min.

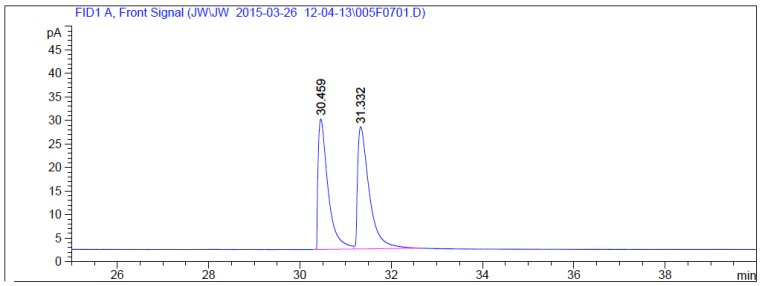

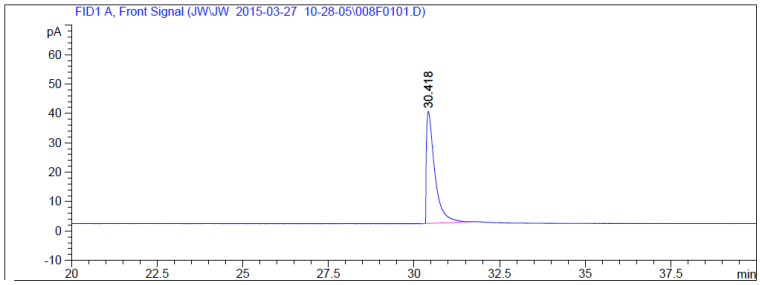


```
Signal 1: FID1 A, Front Signal

Peak RetTime Type  Width     Area      Height     Area
  #   [min]        [min]   [pA*s]      [pA]        %
----|-------|----|-------|----------|----------|--------|
   1  30.418 BB    0.2479  643.22015   38.15113 1.000e2

Totals :                   643.22015   38.15113

===================================================================
                        *** End of Report ***
```

2-ethyl-1,2,3,4-tetrahydroquinoline (6b)

Yellow oil. ^{1}H NMR (400 MHz, CDCl3): δ 6.95 (t, *J* = 7.2 Hz, 2H), 6.59 (t, *J* = 7.3 Hz, 1H), 6.47 (d, *J* = 8.1 Hz, 1H), 3.76 (br, 1H), 3.20 – 3.12 (m, 1H), 2.81 (ddd, *J* = 16.4, 11.0, 5.5 Hz, 1H), 2.76 – 2.68 (m, 1H), 2.00 – 1.92 (m, 1H), 1.65 – 1.55 (m, 1H), 1.51 (dd, *J* = 14.3, 7.2 Hz, 2H), 0.98 (t, *J* = 7.5 Hz, 3H).

^{13}C NMR (400 MHz, CDCl3): δ 143.72, 128.18, 125.66, 120.36, 115.84, 112.96, 52.03, 28.73, 26.57, 25.38, 8.98.

$[\alpha]^{22}_{D}$ -74.4 (*c* 0.5, $CHCl_3$).

Supelco gama Dex 225 column (30 m ×0.25 mm × 0.25 µm), He 1.0 mL/min, column 120 °C, t_1 =51.3 min, t_2 =53.7 min.

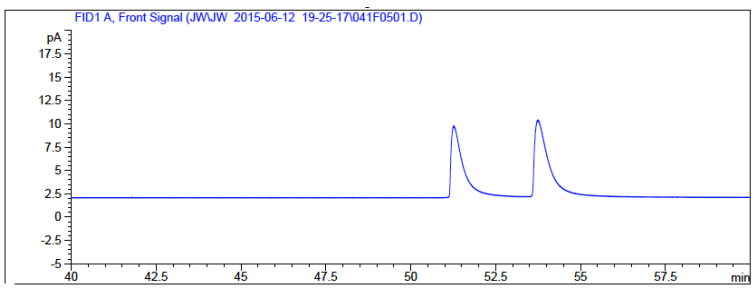

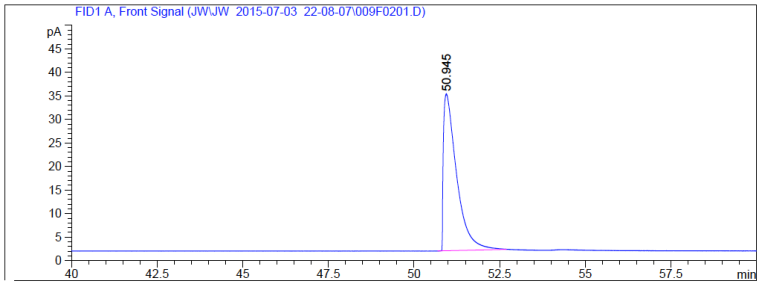


```
Signal 1: FID1 A, Front Signal

Peak RetTime Type  Width     Area      Height     Area
  #   [min]        [min]   [pA*s]      [pA]        %
----|-------|----|-------|----------|----------|--------|
   1  50.945 BB    0.3928  892.10315   33.27738 1.000e2

Totals :                  892.10315   33.27738

===================================================================
                        *** End of Report ***
```

2-isopropyl-1,2,3,4-tetrahydroquinoline (6c)

Yellow oil. ^{1}H NMR (400 MHz, CDCl3): δ 6.95 (t, *J* = 7.7 Hz, 2H), 6.58 (t, *J* = 7.3 Hz, 1H), 6.47 (d, *J* = 8.0 Hz, 1H), 3.75 (s, 1H), 3.05 – 3.00 (m, 1H), 2.80 (ddd, *J* = 14.0, 9.9, 4.2 Hz, 1H), 2.76 – 2.68 (m, 1H), 1.91 (ddt, *J* = 5.9, 4.5, 3.2 Hz, 1H), 1.76 – 1.58 (m, 2iH), 0.98 (dd, *J* = 10.2, 6.8 Hz, 6H).δ 6.95 (t, 2H), 6.58 (t, 1H), 6.47 (d, 1H), 3.03 (m, 1H), 2.75 (m, 2H), 1.91 (m, 1H), 1.69 (m, 2H), 0.98 (dd, 6H).

^{13}C NMR (400 MHz, CDCl3): δ 144.00, 128.08, 125.66, 120.40, 115.70, 112.93, 56.29, 31.51, 25.61, 23.53, 17.38 (d).

$[\alpha]^{22}_{D}$ -44.0 (*c* 0.5, $CHCl_3$).

Supelco gama Dex 225 column (30 m ×0.25 mm × 0.25 µm), He 1.0 mL/min, column 140 °C, t_1 =27.9 min, t_2 =29.4 min.

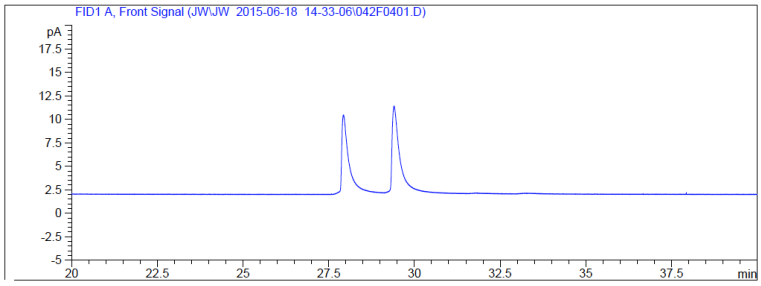

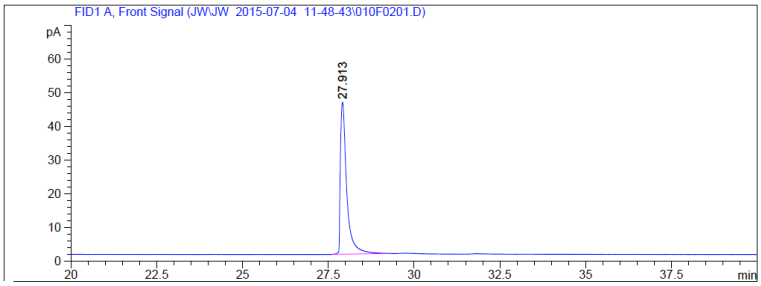


```
Signal 1: FID1 A, Front Signal

Peak RetTime Type  Width     Area      Height     Area
  #   [min]        [min]   [pA*s]      [pA]         %
----|-------|----|-------|----------|----------|--------|
   1  27.913 BB    0.1944  578.82666   45.13346 1.000e2

Totals :                   578.82666   45.13346


=====================================================================
                         *** End of Report ***
```

2-pentyl-1,2,3,4-tetrahydroquinoline (6d)

Yellow oil. ^{1}H NMR (400 MHz, CDCl3): δ 6.95 (t, *J* = 7.2 Hz, 2H), 6.58 (t, *J* = 7.4, 1H), 6.46 (d, *J* = 7.5 Hz, 1H), 3.75 (br, 1H), 3.22 (dtd, *J* = 9.4, 6.3, 2.9 Hz, 1H), 2.86 – 2.75 (m, 1H), 2.71 (dt, *J* = 16.3, 4.8 Hz, 1H), 1.99 – 1.91 (m, 1H), 1.64 – 1.53 (m, 1H), 1.47 (t, *J* = 6.7 Hz, 2H), 1.42 – 1.27 (m, 6H), 0.90 (t, *J* = 6.9 Hz, 3H).

^{13}C NMR (400 MHz, CDCl3): δ 143.71, 128.19, 125.65, 120.36, 115.84, 112.99, 50.58, 35.66, 30.93, 27.11, 25.40, 24.36, 21.59, 12.98 (d).

$[\alpha]^{22}_{D}$ -78.2 (*c* 0.5, $CHCl_3$).

Daicel Chiralpak OD-H, hexanes/i-PrOH = 99/1, Flow rate = 1.0 ml/min, UV = 254 nm, t_1 = 6.9 min, t_2 = 8.0 min.

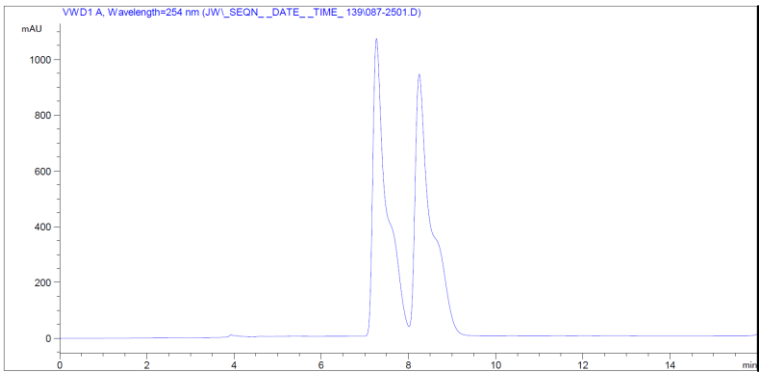

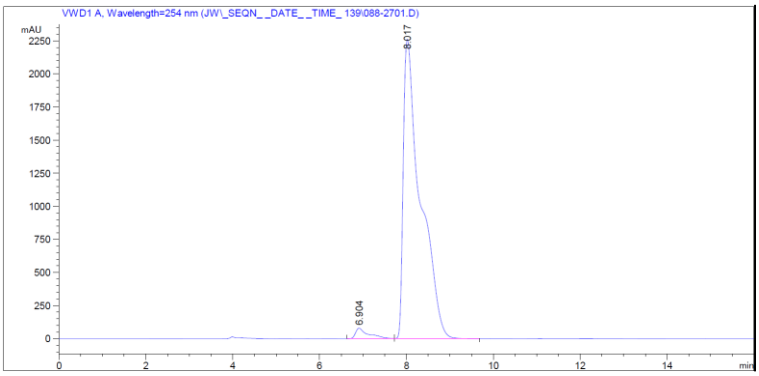

Signal 1: VWD1 A, Wavelength=254 nm

Peak #	RetTime [min]	Type	Width [min]	Area mAU *s	Height [mAU]	Area %
1	6.904	VV	0.2857	1660.45337	79.54791	2.6200
2	8.017	VB	0.3809	6.17146e4	2262.38330	97.3800
Totals :				6.33750e4	2341.93121	

2-undecyl-1,2,3,4-tetrahydroquinoline (6e)

Yellow oil. ^{1}H NMR (400 MHz, CDCl3): δ 6.95 (t, *J* = 7.5 Hz, 2H), 6.58 (td, *J* = 7.4, 1.1 Hz, 1H), 6.47 (dd, *J* = 9.0, 8.2 Hz, 1H), 3.74 (br, 1H), 3.27 – 3.18 (m, 1H), 2.80 (ddd, *J* = 16.4, 10.9, 5.5 Hz, 1H), 2.71 (dt, *J* = 16.3, 4.7 Hz, 1H), 1.95 (ddt, *J* = 6.9, 5.5, 4.0 Hz, 1H), 1.65 – 1.53 (m, 1H), 1.43 – 1.51 (m, 2H), 1.34 (dd, *J* = 45.4, 7.5 Hz, 18H), 0.88 (t, *J* = 7.2 Hz, 3H).

^{13}C NMR (400 MHz, CDCl3): δ 143.71, 128.19, 125.65, 120.35, 115.84, 112.99, 50.59, 35.71, 30.88, 28.74, 28.59, 28.30, 27.12, 25.41, 24.70, 21.65, 13.05 (d).

Daicel Chiralpak OD-H, hexanes/i-PrOH = 98/2, Flow rate = 1.0 ml/min, UV = 254 nm, t_1 = 5.2 min, t_2 = 6.2 min.

$[\alpha]^{22}_{D}$ -55.1 (*c* 0.5, $CHCl_3$).

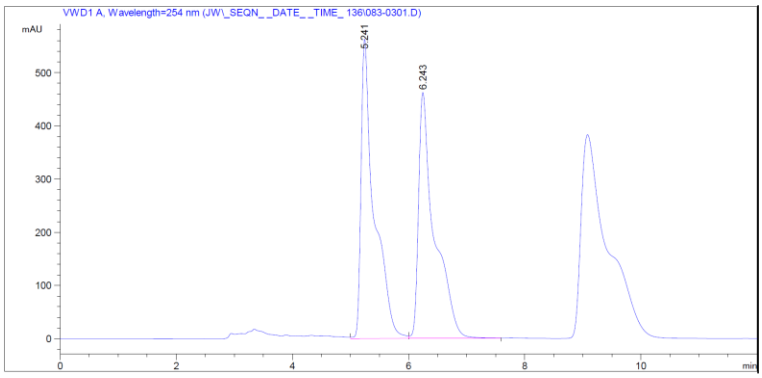

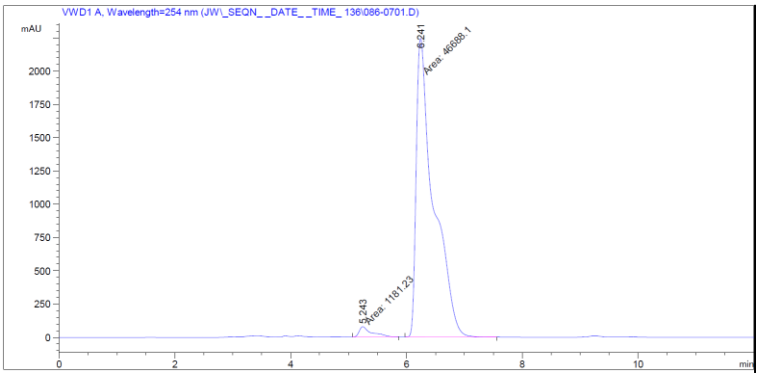

Signal 1: VWD1 A, Wavelength=254 nm

Peak #	RetTime [min]	Type	Width [min]	Area mAU *s	Height [mAU]	Area %
1	5.243	MM	0.2518	1181.22571	78.17448	2.4676
2	6.241	MM	0.3466	4.66881e4	2244.74536	97.5324
Totals :				4.78693e4	2322.91985	

2,6-dimethyl-1,2,3,4-tetrahydroquinoline (6f)

Yellow oil. ^{1}H NMR (400 MHz, CDCl3): 6.77 (d, *J* = 8.4 Hz, 2H), 6.39 (d, *J* = 8.4 Hz, 1H), 3.35 (dqd, *J* = 12.5, 6.3, 2.8 Hz, 1H), 2.80 (ddd, *J* = 17.1, 11.5, 5.8 Hz, 1H), 2.68 (ddd, *J* = 16.4, 5.3, 3.5 Hz, 1H), 2.19 (s, 3H), 1.94 – 1.86 (m, 1H), 1.56 (dddd, *J* = 12.8, 11.5, 10.0, 5.4 Hz, 1H), 1.18 (d, *J* = 6.3 Hz, 3H).

^{13}C NMR (400 MHz, CDCl3): δ 142.46, 129.83, 127.23, 126.26, 121.24, 114.27, 47.35, 30.39, 26.59, 22.59, 20.40.

$[\alpha]^{22}_{D}$ -44.8 (*c* 0.5, $CHCl_3$).

Supelco gama Dex 225 column (30 m ×0.25 mm × 0.25 μm), He 1.0 mL/min, column 120 °C, t_1 =47.8 min, t_2 =48.8 min.

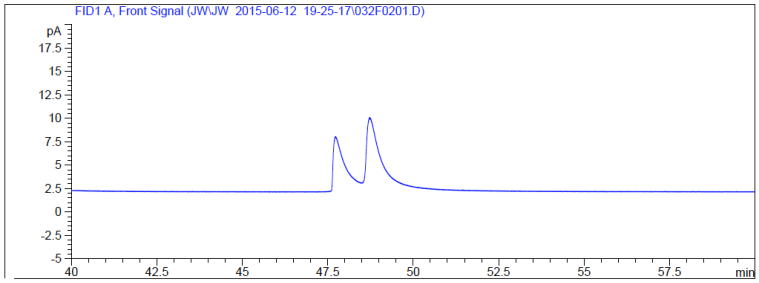

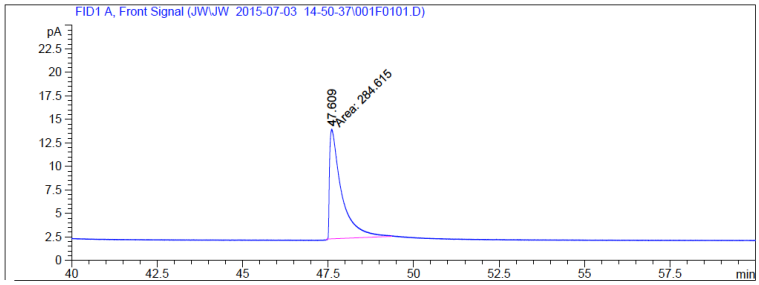


```
Signal 1: FID1 A, Front Signal

Peak RetTime Type  Width     Area      Height     Area
  #   [min]        [min]   [pA*s]      [pA]         %
----|-------|----|-------|----------|----------|--------|
   1  47.609 MM    0.4073  284.61505   11.64730 1.000e2

Totals :                   284.61505   11.64730


=====================================================================
                         *** End of Report ***
```

6-methoxy-2-methyl-1,2,3,4-tetrahydroquinoline (6g)

Yellow oil. ^{1}H NMR (400 MHz, CDCl3): δ 6.58 (m, 2H), 6.44 (d, *J* = 8.3 Hz, 1H), 3.72 (s, 3H), 3.37 – 3.27 (m, 1H), 3.17 (br, 1H), 2.83 (ddd, *J* = 17.3, 11.6, 5.9 Hz, 1H), 2.70 (ddd, *J* = 16.6, 5.4, 3.2 Hz, 1H), 1.90 (ddt, *J* = 12.6, 5.9, 2.9 Hz, 1H), 1.56 (dddd, *J* = 12.8, 11.6, 10.2, 5.5 Hz, 1H), 1.19 (d, *J* = 6.3 Hz, 3H).

^{13}C NMR (400 MHz, CDCl3): δ 151.92, 138.93, 122.53, 115.33, 114.72, 112.91, 55.83, 47.50, 30.34, 26.91, 22.54.

$[\alpha]^{22}_{D}$ -34.7 (*c* 0.5, $CHCl_3$).

Supelco gama Dex 225 column (30 m ×0.25 mm × 0.25 μm), He 1.0 mL/min, column 120 °C, t_1 =121.3 min, t_2 =124.5 min.

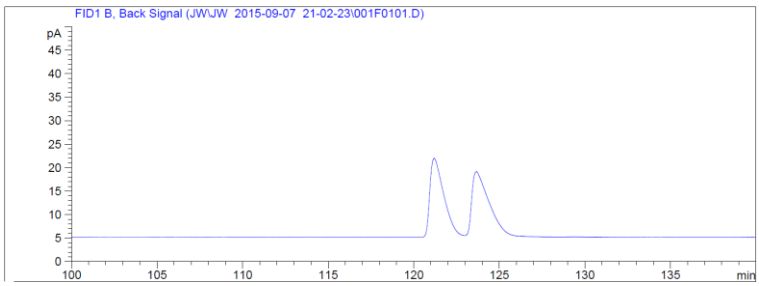

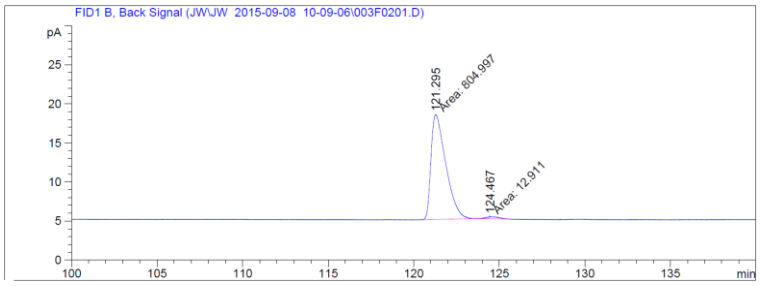

Signal 1: FID1 B, Back Signal

Peak #	RetTime [min]	Type	Width [min]	Area [pA*s]	Height [pA]	Area %
1	121.295	MM	0.9984	804.99701	13.43821	98.42146
2	124.467	MM	0.7978	12.91097	2.69705e-1	1.57854
Totals :				817.90798	13.70791	

==========

*** End of Report ***

6-chloro-2-methyl-1,2,3,4-tetrahydroquinoline (6h)

Yellow oil. ^{1}H NMR (400 MHz, CDCl3): δ 6.93 – 6.86 (m, 2H), 6.37 (d, *J* = 8.4 Hz, 1H), 3.68 (br, 1H), 3.41 – 3.32 (m, 1H), 2.84 – 2.72 (m, 1H), 2.72 – 2.63 (m, 1H), 1.95 – 1.87 (m, 1H), 1.54 (dddd, *J* = 12.9, 11.4, 9.9, 5.4 Hz, 1H), 1.20 (t, *J* = 5.2 Hz, 3H).

^{13}C NMR (400 MHz, CDCl3): δ 142.29, 127.78, 125.45, 121.56, 120.25, 113.90, 46.12, 28.67, 25.41, 21.41.

$[\alpha]^{22}_{D}$ -81.4 (*c* 0.5, $CHCl_3$).

Supelco gama Dex 225 column (30 m ×0.25 mm × 0.25 μm), He 1.0 mL/min, column 140 °C, t_1 =55.9 min, t_2 =58.0 min.

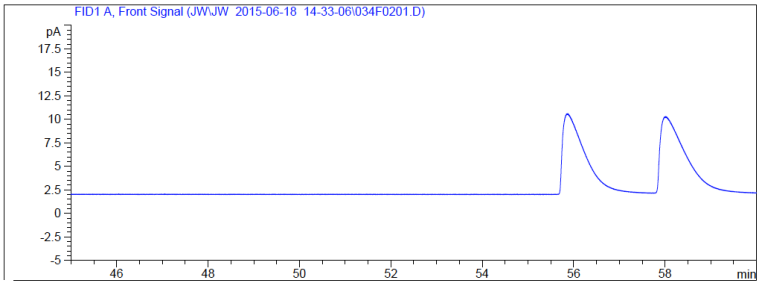

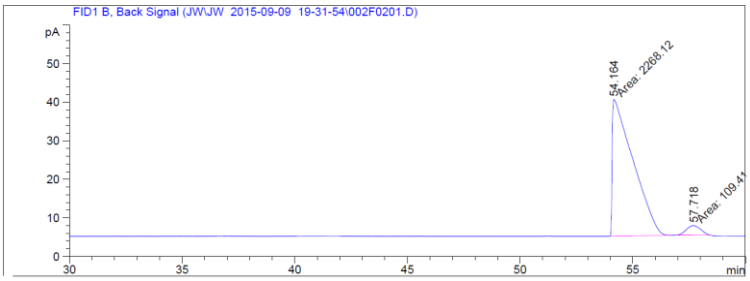

```
Signal 1: FID1 B, Back Signal

Peak RetTime Type  Width     Area      Height     Area
  #   [min]        [min]   [pA*s]      [pA]        %
----|-------|----|-------|----------|----------|--------|
   1  54.164 MM    1.0692 2268.11865   35.35589 95.39800
   2  57.718 MM    0.7403  109.41407    2.46312  4.60200

Totals :                  2377.53272   37.81902


=====================================================================
                         *** End of Report ***
```

6-fluoro-2-methyl-1,2,3,4-tetrahydroquinoline (6i)

Yellow oil. ^{1}H NMR (400 MHz, CDCl3): δ 6.64 – 6.70 (m, 5.8 Hz, 2H), 6.42 – 6.35 (m, 1H), 3.57 (br, 1H), 3.34 (dqd, *J* = 12.6, 6.2, 2.7 Hz, 1H), 2.81 (ddd, *J* = 11.6, 8.7, 5.6 Hz, 1H), 2.69 (ddd, *J* = 16.6, 5.3, 3.4 Hz, 1H), 1.91 (dtd, *J* = 8.8, 5.9, 3.0 Hz, 1H), 1.55 (dddd, *J* = 12.9, 11.6, 10.1, 5.5 Hz, 1H), 1.20 (d, *J* = 6.3 Hz, 3H).

^{13}C NMR (400 MHz, CDCl3): δ 154.51 (d, *J* = 938.4 Hz), 139.95, 121.44 (d, *J* = 26.4 Hz), 114.34 (d, *J* = 86.4 Hz), 113.68 (d, *J* = 30.4 Hz), 112.12 (d, *J* = 89.6 Hz), 46.29, 28.87, 25.67, 21.44.

$[\alpha]^{22}_{D}$ –63.84 (*c* 0.5, $CHCl_3$).

Supelco gama Dex 225 column (30 m ×0.25 mm × 0.25 μm), He 1.0 mL/min, column 120 °C, t_1 =39.0 min, t_2 =40.7 min.

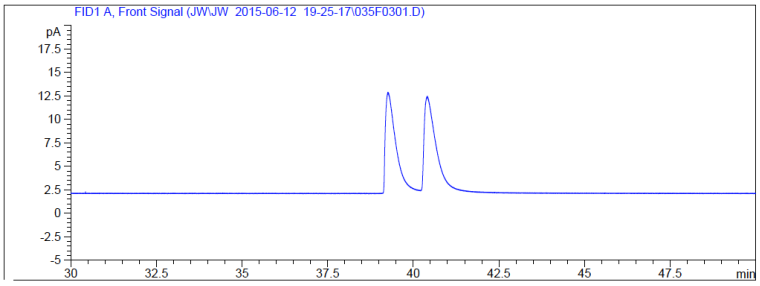

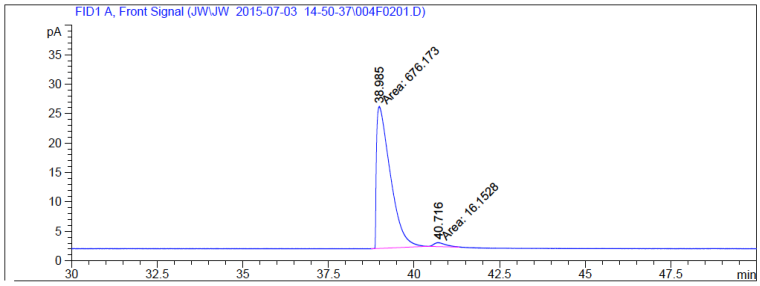

```
Signal 1: FID1 A, Front Signal

Peak RetTime Type  Width     Area      Height     Area
  #   [min]        [min]   [pA*s]      [pA]        %
----|-------|----|-------|----------|----------|--------|
   1  38.985 MM    0.4684  676.17346   24.05771 97.66689
   2  40.716 MM    0.4012   16.15275 6.71097e-1  2.33311

Totals :                   692.32621   24.72881

=====================================================================
                          *** End of Report ***
```

6-bromo-2-methyl-1,2,3,4-tetrahydroquinoline (6j)

Yellow oil. ^{1}H NMR (400 MHz, CDCl3): δ 7.05 (d, *J* = 1.0 Hz, 1H), 7.02 (d, *J* = 8.4 Hz, 1H), 6.32 (d, *J* = 8.4 Hz, 1H), 3.69 (s, 1H), 3.41 – 3.31 (m, 1H), 2.84 – 2.73 (m, 1H), 2.72 – 2.64 (m, 1H), 1.90 (dtd, *J* = 8.4, 5.6, 2.8 Hz, 1H), 1.53 (dtd, *J* = 11.8, 10.7, 5.3 Hz, 2H), 1.19 (d, *J* = 6.4 Hz, 3H).

^{13}C NMR (400 MHz, CDCl3): δ 142.73, 130.62, 128.30, 122.08, 114.33, 107.25, 46.06, 28.60, 25.35, 21.40.

$[\alpha]^{22}_{D}$ –66.7 (*c* 0.5, $CHCl_3$).

Supelco gama Dex 225 column (30 m ×0.25 mm × 0.25 μm), He 1.0 mL/min, column 160 °C, t_1 =36.6 min, t_2 =37.6 min.

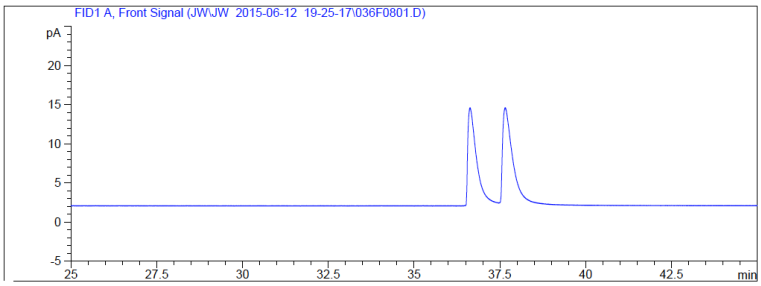

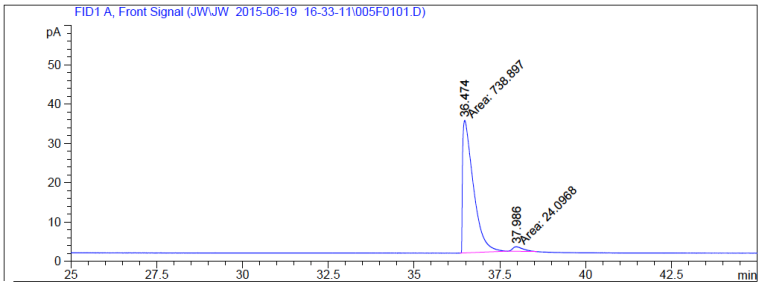


```
Signal 1: FID1 A, Front Signal

Peak RetTime Type  Width     Area      Height     Area
  #   [min]        [min]   [pA*s]      [pA]        %
----|-------|----|-------|----------|----------|--------|
   1  36.474 MM    0.3649  738.89734   33.75223 96.84181
   2  37.986 MM    0.3442   24.09677    1.16684  3.15819

Totals :                   762.99411   34.91906

=====================================================================
                          *** End of Report ***
```

7-chloro-2-methyl-1,2,3,4-tetrahydroquinoline (6k)

Yellow oil. ^{1}H NMR (400 MHz, CDCl3): δ 6.84 (d, *J* = 8.0 Hz, 1H), 6.53 (dd, *J* = 8.0, 2.0 Hz, 1H), 6.42 (d, *J* = 2.0 Hz, 1H), 3.72 (br, 1H), 3.38 (dqd, *J* = 9.3, 6.3, 3.0 Hz, 1H), 2.81 – 2.61 (m, 1H), 1.97 – 1.82 (m, 1H), 1.54 (dddd, *J* = 12.9, 11.1, 9.8, 5.5 Hz, 1H), 1.18 (t, *J* = 10.1 Hz, 3H).

^{13}C NMR (400 MHz, CDCl3): δ 144.89, 130.89, 129.11, 118.28, 115.55, 112.24, 45.96, 28.75, 25.01, 21.41.

$[\alpha]^{22}_{D}$ -73.3 (*c* 0.5, $CHCl_3$).

Supelco gama Dex 225 column (30 m ×0.25 mm × 0.25 μm), He 1.0 mL/min, column 140 °C, t_1 =49.8 min, t_2 =50.7 min.

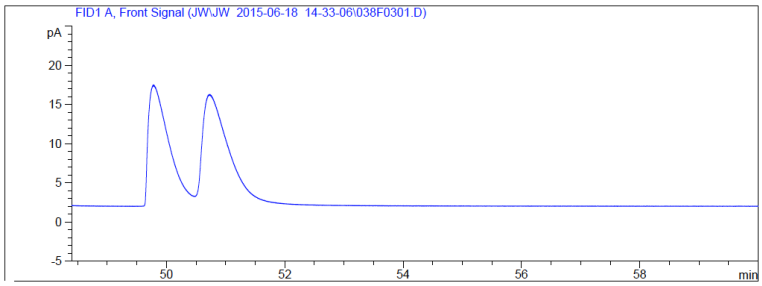

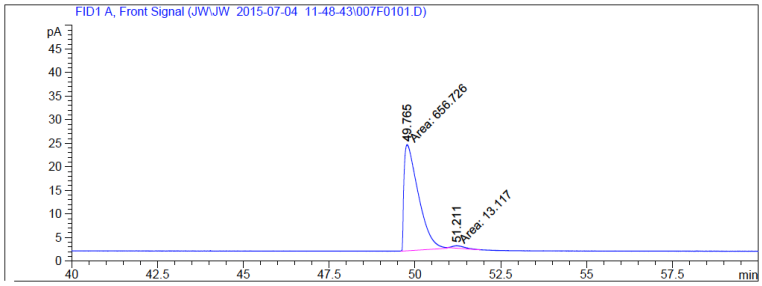


```
Signal 1: FID1 A, Front Signal

Peak RetTime Type  Width     Area      Height     Area
  #   [min]        [min]   [pA*s]      [pA]        %
----|-------|----|-------|----------|----------|--------|
   1  49.765 MM    0.4851  656.72589   22.56477 98.04178
   2  51.211 MM    0.4062   13.11703 5.38164e-1  1.95822

Totals :                   669.84292   23.10293

=====================================================================
                         *** End of Report ***
```

8-chloro-2-methyl-1,2,3,4-tetrahydroquinoline (6l)

Yellow oil. ^{1}H NMR (400 MHz, CDCl3): δ 7.05 (d, *J* = 7.9 Hz, 1H), 6.86 (dd, *J* = 7.4, 0.9 Hz, 1H), 6.50 (t, *J* = 7.7 Hz, 1H), 4.25 (br, 1H), 3.46 (dqd, *J* = 9.4, 6.3, 3.1 Hz, 1H), 2.83 (ddd, *J* = 16.6, 11.2, 5.4 Hz, 1H), 2.78 – 2.70 (m, 1H), 1.98 – 1.90 (m, 1H), 1.58 (dddd, *J* = 12.9, 11.2,

9.8, 5.3 Hz, 1H), 1.27 (d, J = 6.3 Hz, 3H).

^{13}C NMR (400 MHz, CDCl3): δ 140.74, 127.43, 126.74, 122.39, 117.84, 116.35, 47.18, 29.64, 26.74, 22.52.

$[\alpha]^{22}_{D}$ -68.7 (c 0.5, $CHCl_3$).

Supelco gama Dex 225 column (30 m ×0.25 mm × 0.25 μm), He 1.0 mL/min, column 120 °C, t_1 =52.9 min, t_2 =54.0 min.

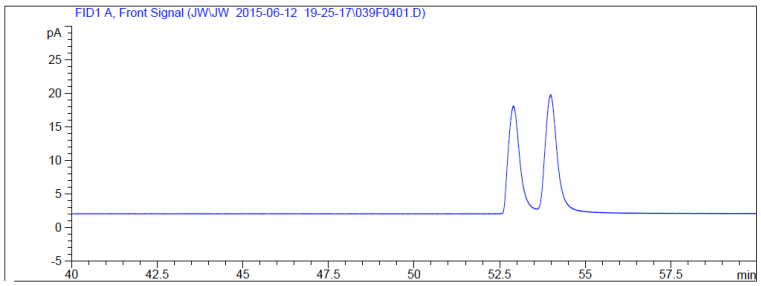

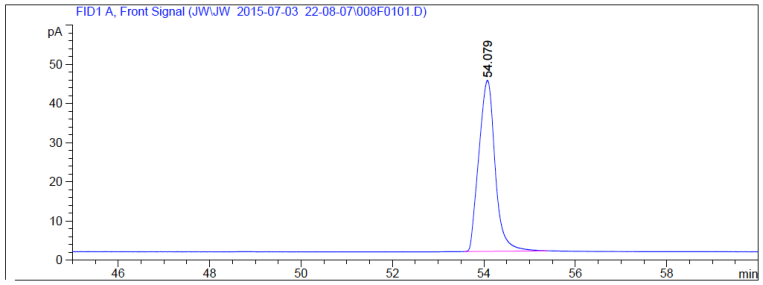


```
Signal 1: FID1 A, Front Signal

Peak RetTime Type  Width     Area      Height     Area
  #   [min]        [min]   [pA*s]      [pA]        %
----|-------|----|-------|----------|----------|--------|
   1  54.079 BB    0.3756 1081.64124   43.63175 1.000e2

Totals :                  1081.64124   43.63175

===================================================================
                          *** End of Report ***
```

2-(3,4-dimethoxyphenethyl)-1,2,3,4-tetrahydroquinoline (6m)

Yellow oil. ^{1}H NMR (400 MHz, $CDCl_3$) δ 6.95 (t, J = 7.1 Hz, 2H), 6.83–6.77 (m, 1H), 6.77–6.71 (m, 2H), 6.60 (td, J = 7.4, 0.9 Hz, 1H), 6.44 (dd, J = 8.4, 0.9 Hz, 1H), 3.87 (s, 3H), 3.85 (s, 3H), 3.77 (br, 1H), 3.30 (dtd, J = 9.3, 6.3, 3.0 Hz, 1H), 2.81 (ddd, J = 13.1, 9.0, 4.1 Hz, 1H), 2.73–2.64 (m, 2H), 2.03 – 1.95 (m, 1H), 1.81 (ddd, J = 10.2, 7.2, 1.2 Hz, 2H), 1.72–1.61 (m, 1H).

^{13}C NMR (400 MHz, CDCl3): δ 149.02, 147.37, 144.54, 134.52, 129.27, 126.76, 121.30, 120.17, 117.05, 114.16, 111.74, 111.43, 56.00, 55.90, 51.25, 38.44, 31.86, 28.05, 26.23.

$[\alpha]^{22}_{D}$ -60.8 (c 0.5, $CHCl_3$).

Daicel Chiralpak AS-H, hexanes/i-PrOH = 95/5, Flow rate = 0.5 ml/min, UV = 254 nm, t_1 = 24.4 min, t_2 = 27.0 min.

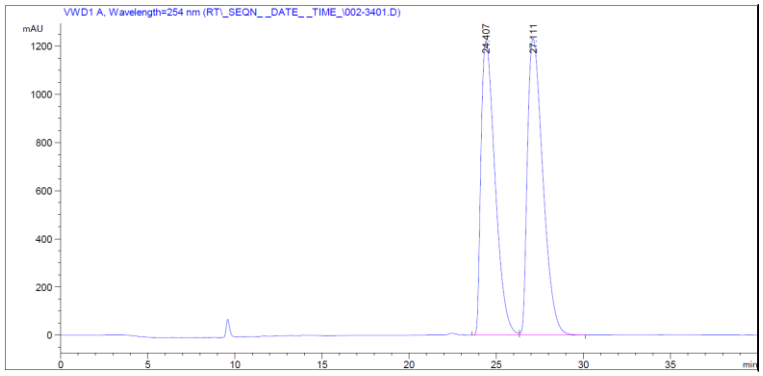

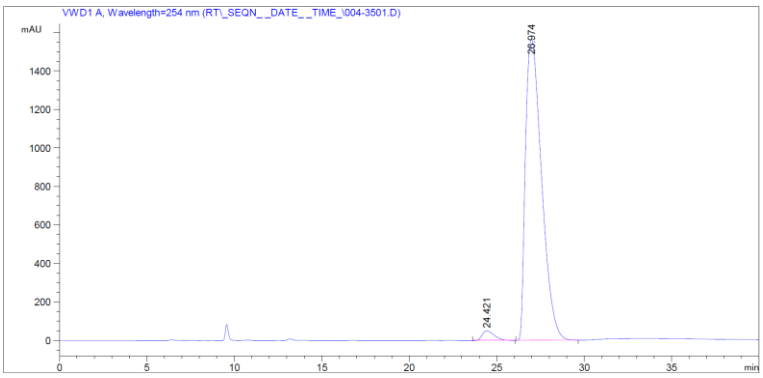

Signal 1: VWD1 A, Wavelength=254 nm

Peak #	RetTime [min]	Type	Width [min]	Area mAU *s	Height [mAU]	Area %
1	24.421	BB	0.7352	2461.57397	51.10365	2.3987
2	26.974	BB	1.0158	1.00159e5	1565.46924	97.6013
Totals :				1.02621e5	1616.57289	

1. Sridharan, V.; Suryavanshi, P. A.; Menendez, J. C., Advances in the Chemistry of Tetrahydroquinolines. *Chem. Rev. (Washington, DC, U. S.)* **2011,** *111* (11), 7157-7259.

2. Scott, J. D.; Williams, R. M., Chemistry and Biology of the Tetrahydroisoquinoline Antitumor Antibiotics. *Chem. Rev. (Washington, D. C.)* **2002,** *102* (5), 1669-1730.

3. Bentley, K. W., β-Phenylethylamines and the isoquinoline alkaloids. *Nat. Prod. Rep.* **2006,** *23* (3), 444-463.

4. Wang, D.-S.; Chen, Q.-A.; Lu, S.-M.; Zhou, Y.-G., Asymmetric Hydrogenation of Heteroarenes and Arenes. *Chemical Reviews* **2012,** *112* (4), 2557-2590.

5. Zhou, Y.-G., Asymmetric Hydrogenation of Heteroaromatic Compounds. *Accounts of Chemical Research* **2007,** *40* (12), 1357-1366.

6. Lu, S.-M.; Han, X.-W.; Zhou, Y.-G., Asymmetric hydrogenation of quinolines catalyzed by iridium with chiral ferrocenyloxazoline derived N,P ligands. *Adv. Synth. Catal.* **2004,** *346* (8), 909-912.

7. Lam, K. H.; Xu, L.; Feng, L.; Fan, Q.-H.; Lam, F. L.; Lo, W.-h.; Chan, A. S. C., Highly enantioselective iridium-catalyzed hydrogenation of quinoline derivatives using chiral phosphinite H8-BINAPO. *Adv. Synth. Catal.* **2005,** *347* (14), 1755-1758.

8. Lu, S.-M.; Wang, Y.-Q.; Han, X.-W.; Zhou, Y.-G., Asymmetric hydrogenation of quinolines and isoquinolines activated by chloroformates. *Angew. Chem., Int. Ed.* **2006,** *45* (14), 2260-2263.

9. Zhou, H.; Li, Z.; Wang, Z.; Wang, T.; Xu, L.; He, Y.; Fan, Q.-H.; Pan, J.; Gu, L.; Chan, A. S. C., Hydrogenation of quinolines using a recyclable phosphine-free chiral cationic ruthenium catalyst: enhancement of catalyst stability and selectivity in an ionic liquid. *Angew. Chem., Int. Ed.* **2008,** *47* (44), 8464-8467.

10. Tang, W.-J.; Tan, J.; Xu, L.-J.; Lam, K.-H.; Fan, Q.-H.; Chan, A. S. C., Highly Enantioselective Hydrogenation of Quinoline and Pyridine Derivatives with Iridium-(P-Phos) Catalyst. *Adv. Synth. Catal.* **2010,** *352* (6), 1055-1062.

11. Gou, F.-R.; Li, W.; Zhang, X.; Liang, Y.-M., Iridium-Catalyzed Asymmetric Hydrogenation of Quinoline Derivatives with C3*-TunePhos. *Advanced Synthesis & Catalysis* **2010,** *352* (14-15), 2441-2444.

12. Wang, T.; Zhuo, L.-G.; Li, Z.; Chen, F.; Ding, Z.; He, Y.; Fan, Q.-H.; Xiang, J.; Yu, Z.-X.; Chan, A. S. C., Highly Enantioselective Hydrogenation of Quinolines Using Phosphine-Free Chiral Cationic Ruthenium Catalysts: Scope, Mechanism, and Origin of Enantioselectivity. *J. Am. Chem. Soc.* **2011,** *133* (25), 9878-9891.

13. Deport, C.; Buchotte, M.; Abecassis, K.; Tadaoka, H.; Ayad, T.; Ohshima, T.; Genet, J.-P.; Mashima, K.; Ratovelomanana-Vidal, V., Novel Ir-SYNPHOS® and Ir-DIFLUORPHOS® Catalysts for Asymmetric Hydrogenation of Quinolines. *Synlett* **2007,** *2007* (17), 2743-2747.

14. Shi, L.; Ye, Z.-S.; Cao, L.-L.; Guo, R.-N.; Hu, Y.; Zhou, Y.-G., Enantioselective Iridium-Catalyzed Hydrogenation of 3,4-Disubstituted Isoquinolines. *Angew. Chem., Int. Ed.* **2012,** *51* (33), 8286-8289, S8286/1-S8286/57.

15. Shi, L.; Ji, Y.; Huang, W.; Zhou, Y., Application of chiral anion metathesis strategy in asymmetric transfer hydrogenation of isoquinolines. *Huaxue Xuebao* **2014,** *72* (7), 820-824.

16. Iimuro, A.; Yamaji, K.; Kandula, S.; Nagano, T.; Kita, Y.; Mashima, K., Asymmetric Hydrogenation of Isoquinolinium Salts Catalyzed by Chiral Iridium Complexes: Direct Synthesis for Optically Active 1,2,3,4-Tetrahydroisoquinolines. *Angew. Chem., Int. Ed.* **2013,** *52* (7), 2046-2050.

17. Xie, J.-H.; Zhu, S.-F.; Zhou, Q.-L., Transition Metal-Catalyzed Enantioselective Hydrogenation of

Enamines and Imines. *Chem. Rev. (Washington, DC, U. S.)* **2011,** *111* (3), 1713-1760.

18. Tang, W.; Zhang, X., New Chiral Phosphorus Ligands for Enantioselective Hydrogenation. *Chem. Rev. (Washington, DC, U. S.)* **2003,** *103* (8), 3029-3069.

19. Zhang, W.; Chi, Y.; Zhang, X., Developing Chiral Ligands for Asymmetric Hydrogenation. *Acc. Chem. Res.* **2007,** *40* (12), 1278-1290.

20. Yu, Z.; Jin, W.; Jiang, Q., Bronsted Acid Activation Strategy in Transition-Metal Catalyzed Asymmetric Hydrogenation of N-Unprotected Imines, Enamines, and N-Heteroaromatic Compounds. *Angew. Chem., Int. Ed.* **2012,** *51* (25), 6060-6072.

21. Zhao, Q.; Li, S.; Huang, K.; Wang, R.; Zhang, X., A Novel Chiral Bisphosphine-Thiourea Ligand for Asymmetric Hydrogenation of β,β-Disubstituted Nitroalkenes. *Organic Letters* **2013,** *15* (15), 4014-4017.

22. Zhao, Q.; Wen, J.; Tan, R.; Huang, K.; Metola, P.; Wang, R.; Anslyn, E. V.; Zhang, X., Rhodium-Catalyzed Asymmetric Hydrogenation of Unprotected NH Imines Assisted by a Thiourea. *Angewandte Chemie International Edition* **2014,** *53* (32), 8467-8470.

23. Fagnou, K.; Lautens, M., Reviews: Halide effects in transition metal catalysis. *Angew. Chem., Int. Ed.* **2002,** *41* (1), 26-47.

24. Duan, Y.; Li, L.; Chen, M.-W.; Yu, C.-B.; Fan, H.-J.; Zhou, Y.-G., Homogenous Pd-Catalyzed Asymmetric Hydrogenation of Unprotected Indoles: Scope and Mechanistic Studies. *Journal of the American Chemical Society* **2014,** *136* (21), 7688-7700.

25. Kita, Y.; Yamaji, K.; Higashida, K.; Sataiah, K.; Iimuro, A.; Mashima, K., Enhancing Effects of Salt Formation on Catalytic Activity and Enantioselectivity for Asymmetric Hydrogenation of Isoquinolinium Salts by Dinuclear Halide-Bridged Iridium Complexes Bearing Chiral Diphosphine Ligands. *Chem. - Eur. J.* **2015,** *21* (5), 1915-1927.

26. Kido, K.; Watainabe, Y., A one-pot isoquinoline synthesis by cyclodehydrogenation of N-benzyl-.ALPHA.-alkylaminoacetals with chlorosulfonic acid. Formation of 3-alkylisoquinolines. *Chemical and Pharmaceutical Bulletin* **1987,** *35* (12), 4964-4966.

27. Qian, B.; Guo, S.; Shao, J.; Zhu, Q.; Yang, L.; Xia, C.; Huang, H., Palladium-Catalyzed Benzylic Addition of 2-Methyl Azaarenes to N-Sulfonyl Aldimines via C−H Bond Activation. *Journal of the American Chemical Society* **2010,** *132* (11), 3650-3651.

28. Fakhfakh, M. A.; Franck, X.; Fournet, A.; Hocquemiller, R.; Figadère, B., Expeditious preparation of 2-substituted quinolines. *Tetrahedron Letters* **2001,** *42* (23), 3847-3850.

29. Mangas-Sanchez, J.; Busto, E.; Gotor-Fernandez, V.; Gotor, V., Enantiopure 3-methyl-3,4-dihydroisocoumarins and 3-methyl-1,2,3,4-tetrahydroisoquinolines via chemoenzymatic asymmetric transformations. *Catalysis Science & Technology* **2012,** *2* (8), 1590-1595.

30. Xie, J.-H.; Yan, P.-C.; Zhang, Q.-Q.; Yuan, K.-X.; Zhou, Q.-L., Asymmetric Hydrogenation of Cyclic Imines Catalyzed by Chiral Spiro Iridium Phosphoramidite Complexes for Enantioselective Synthesis of Tetrahydroisoquinolines. *ACS Catalysis* **2012,** *2* (4), 561-564.

Chapter Four

Rhodium catalyzed asymmetric synthesis of chiral indolines: the cooperation of transition metal, Brønsted acid and thiourea anion binding

4.1 Introduction

Proton is the simplest and most efficient catalyst. Recent two decades have witnessed the prosperous development of chiral Brønsted acid catalysis.[1-2] Chiral Brønsted acid catalysis has been demonstrated as a powerful tool in organic synthetic methodologies.[3-5] Anion binding, on the other hand, commonly exists in bio-system and enzyme catalysis. As a non-covalent interaction, hydrogen bonding has some unique characteristics, such as moderate bond energy and directionality.[6-11] However, each of these kinds of catalysis systems has some limitations: the pKa's of phosphoric acids are in a certain range of 1~3, which can hardly catalyze reactions that require more potent activating reagents; chiral thiourea catalysts with anion binding usually require a high catalyst loading (5%~20%). These drawbacks limit their application in large-scale synthesis.

Figure 4.1. Chiral Brønsted acid catalysis versus thiourea anion binding with simple Brønsted acid.

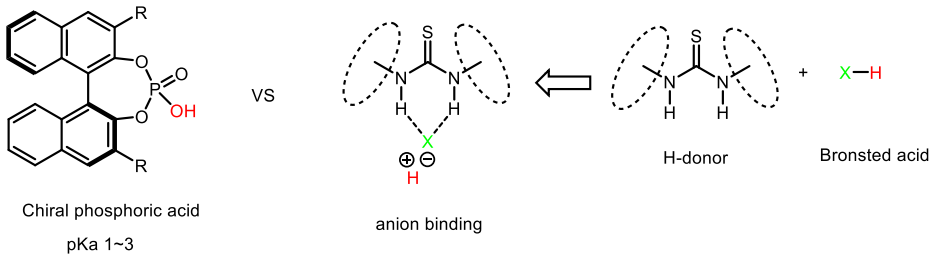

The strategy of cooperative catalysis emerged in recent years, aiming to combine two or more catalytic centers to achieve a single reaction.[12-16] Recently, several breakthroughs were made with the application of this strategy in several kinds of reactions, such as Pararov reaction[17], hydrogenation[18], hydroformylation[19-21] and Diels-Alder reaction[22]. The combination of thiourea/urea derivatives and simple Brønsted acids offers a similar effect to chiral phosphoric acids, but it can render a broader acidity range. Moreover, tunable substituents on bifunctional thiourea/urea catalysts can introduce many kinds of secondary interactions, such as charge-charge electrostatics, cation-π interaction, π-π stacking, etc.[8-9, 23-25] By establishing a bridge between the thiourea and the conjugate base anion of the Brønsted acid, anion binding makes the chiral catalyst associate with a protonated substrate. This strategy combines the essences of both approaches (Figure 4.1). Transition metal catalysis, with high turnover numbers and potent reactivity, plays a crucial role in synthetic chemistry. It shows a very broad application in pharmaceutical and fine chemical industries. The integration of transition metal catalysis and small molecule organocatalysis has shown its potential in the synthetic chemistry communities.[15-16] We envision that certain kinds of reactions could

be catalyzed by the cooperative catalysis of transition metal, Brønsted acid and thiourea anion binding.

Scheme 4.1 Asymmetric hydrogenation of unprotected indole

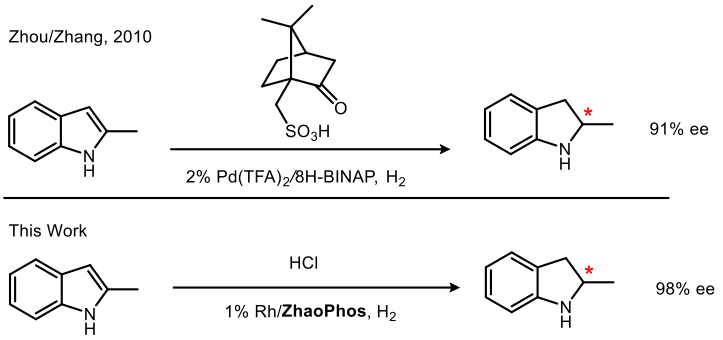

Chiral indolines are ubiquitous N-heterocycles. This structural motif could be found in natural alkaloids and drugs.[26-28] Comparing with other synthetic approaches, hydrogenation is the most straight forward method to obtain chiral indolines because of its 100% atom efficiency. N-protected indoles have been successfully reduced with Ru, Ir or Rh complexes.[29-30] The protecting groups lower the aromaticity of indoles, and therefore enable the asymmetric reduction on enamide C=C bonds. However, the removal of protecting groups requires extra steps and leads to loss of yields, thus increasing the cost for synthetic chemistry. The only successful example of asymmetric hydrogenation of unprotected indoles was reported by Zhang and Zhou group with a palladium/H8-BINAP complex.[31-32] In this case, good enantioselectivity (91% ee) was achieved in hydrogenation of 2-methylindole, but it requires the addition of a chiral auxiliary, camphorsulfonic acid. Moreover, the use of expensive trifluoroethanol increases the cost in its industrial application. So we were looking forward to developing a new synthetic method to approach chiral indoles with excellent enantioselectivity\ies and lower cost.

We aimed to utilize the strategy of cooperative catalysis to achieve this goal. Strong Brønsted acid such as HCl was introduced to activate the aromatic substrates, while the thiourea (linked to the bisphosphine ligand) formed a secondary interaction with the substrates. Rhodium/bisphosphine complex delivers a potent hydride to reduce the C=N bond after a tautomerization. Based on these theoretical reasoning, we initiated our research with asymmetric hydrogenation of 2-methylindole.

Figure 4.2 ZhaoPhos and cooperative catalysis of transition metal, Brønsted acid and thiourea anion binding.

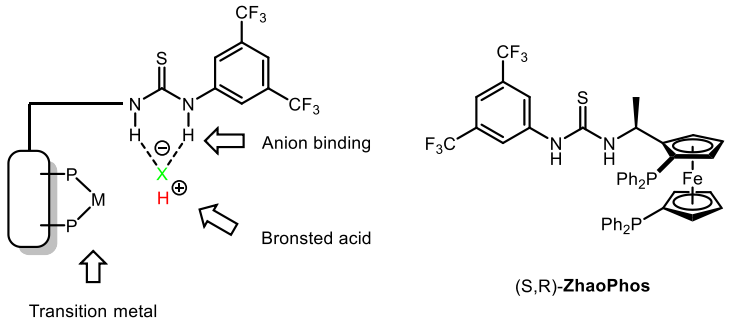

4.2 Method development

We conducted hydrogenation reactions with (S,R)-ZhaoPhos and used [Rh(COD)Cl]2 as the metal precursor since this rhodium(I) dimer gave excellent results in the previous examples. We introduced strong Brønsted HCl by adding its diethyl ether solution. After screening solvents from alcohols, alkyl chlorides, ethers and toluene, we found that dichloromethane and 1,2-dichloroethane gave the highest conversion with the highest enantiomeric excess (Table 4.1, entry 7 and 8). 1H NMR study showed no dimer or other byproducts which could be usually found in acidic conditions. Application of HCl ether solution leads to mixed solvents. Diethyl ether is extraordinarily volatile and therefore its HCl solution is difficult to handle and measure, especially in a sealed container like

a glovebox. The concentration of HCl in reaction mixture can hardly maintain since it is a gas-liquid bi-phase system. Isopropanol, with much higher boiling point and better solubility with HCl, might be a desirable alternative. Another reason for isopropanol is that this solvent gives very good results in hydrogenation of nitroolefins and iminium with Rh/ZhaoPhos.[33-34] When we applied HCl (5M) in isopropanol, the conversion was driven to nearly 100% with the retention of high enantioselectivity (Table 4.1, entry 9).

Table 4.1 Condition optimization for 2-methylindole. [a]

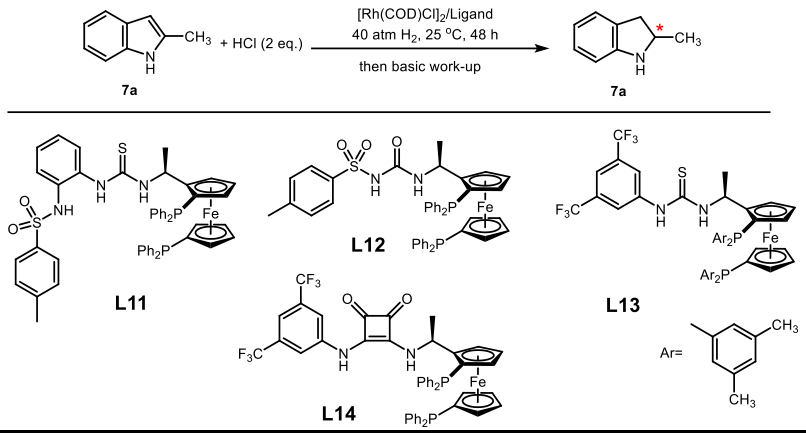

entry	Ligand	solvent	conversion[b]	ee[c]
1	(S,R)-ZhaoPhos	MeOH	56%	27%
2	(S,R)-ZhaoPhos	i-PrOH	>99%	60%
3	(S,R)-ZhaoPhos	CF3CH2OH	21%	84%
4	(S,R)-ZhaoPhos	Toluene	26%	91%
5	(S,R)-ZhaoPhos	THF	14%	84%
6	(S,R)-ZhaoPhos	1,4-dioxane	trace	N.D.
7	(S,R)-ZhaoPhos	DCM	76%	94%
8	(S,R)-ZhaoPhos	1,2-DCE	71%	95%
9[d]	(S,R)-ZhaoPhos	DCM	>99%	95%
10[d]	(S,R)-L11	DCM	6%	80%
11[d]	(S,R)-L12	DCM	0	N.D.
12[d]	(S,R)-L13	DCM	68%	89%

13[d]	(S,R)-L14	DCM	0	N.D.
13[e]	(S,R)-ZhaoPhos	DCM	99%	98%

[a] reaction condition: 7a (0.1 mmol) in 1.0 ml solvent, 1/[Rh(COD)Cl]$_2$/ligand ratio=100/0.50/1.0, 0.1 ml of HCl (2 M) in Et2O solution was added; [b] conversion was determined by 1H NMR analysis, no side product was observed; [c] ee was determined by GC with a chiral stationary phase; [d] 0.04 ml of HCl (5 M) in i-PrOH solution was added; [e] 0.1 ml of HCl (1 M) in AcOH solution was applied.

A series of analogues of ZhaoPhos were prepared. Multi-hydrogen-donor ligand L11 could not catalyze this hydrogenation efficiently under the optimized condition (Table 4.1, entry 10). Sulfonyl urea catalyst L12 does not give hydrogenation product at all (entry 11). A more bulky substituent on the phosphorus atom failed to improve neither reactivity nor enantioselectivity (entry 12). Compared to thiourea, a squaramide analogue L4 does not show any catalytic activity (entry 13).

Table 4.2 Brønsted acid screening for 2,3-disustituted indole. [a]

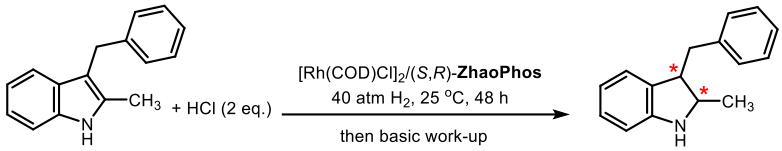

7m **8m**

entry	Brønsted acid	actual solvent	conversion[b]	ee[c]
1	HCl (2 eq.)	DCM/i-PrOH = 10:1	41%	94%
2	TfOH (1 eq.)	DCM	trace	N.D.
3	*p*-TsOH•H2O (1 eq.)	DCM	80%	90%
4	CF3COOH (1 eq.)	DCM	7%	92%
5	2 HCl + 1 TfOH	DCM/i-PrOH = 10:1	70%	90%
6	2 HCl + 1 *p*-TsOH•H2O	DCM/i-PrOH = 10:1	67%	90%
7	2 HCl + 1 CF3COOH	DCM/i-PrOH = 10:1	49%	94%
8	HCl (2 eq.)	DCM/AcOH = 10:1	60%	98%
9	HCl (2 eq.)	DCM/AcOH = 5:1	74%	97%
10	HCl (2 eq.)	DCM/AcOH = 2:1	88%	96%
11	HCl (2 eq.)	DCM/AcOH = 1:1	90%	95%

12	HCl (2 eq.)	DCM/AcOH = 1:2	93%	93%
13	HCl (2 eq.)	DCM/AcOH = 1:5	94%	92%

[a] reaction condition: 7m (0.1 mmol) in 1.0 ml solvent, 1/[Rh(COD)Cl]$_2$/ligand ratio=100/0.50/1.0; [b] conversion was determined by 1H NMR analysis, no side product was observed; [c] ee was determined by HPLC with a chiral stationary phase.

We applied the optimized condition to hydrogenate 2,3-disubstituted indole (2-methyl-3-benzyl indole), moderate conversion was observed while high enantioselectivity was obtained (Table 4.2, entry 1). Only one diastereomer was observed. Lower conversion was probably caused by the difficulty in protonation. In order to achieve higher yield, altering the acidity of the protonation reagent would be a plausible solution. A series of strong Brønsted acids was applied in this reaction since the anion binding between the thiourea/urea and sulfonate anions was well studied.[35] Triflic acid gave no hydrogenation product and lead to full recovery of starting material. This might be due to its extraordinarily strong acidity (pKa = -12[36]), which would probably protonate the catalyst and therefore inhibits the reaction.[37] *p*-Toluenesulfonic acid also works for this catalysis, giving higher conversion and moderate enantioselectivity. Trifluoroacetic acid, on the other hand, gives higher ee but low conversion. When combined with HCl in isopropanol, these strong Brønsted acids improved the performance of HCl (entry 5, 6, 7).

Scheme 4.2. Leveling effect of HCl in solutions.

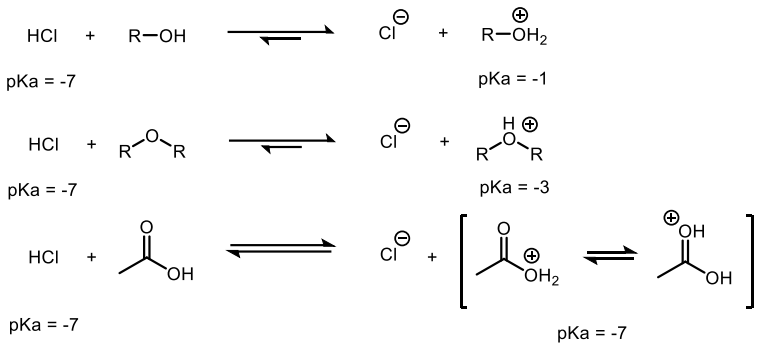

Another factor that influences the acidity of Brønsted acid is the solvation effect. In water or alcohols, the strongest species in acidity is protonated hydroxyl group, whose pKa's are around -1. Protonated ethers offer similar pKa (~ -3). Due to leveling effect, HCl in such solutions as alcohols or ethers cannot provide stronger acidity. If the solvent media is altered to acetic acid, we believed the protonation step would be more efficient. Guided by this qualitative reasoning, we use HCl in acetic acid solution. It turned out that both of the conversion and ee were increased. The ratio of acetic acid and dichloromethane is tricky: higher proportion of acetic acid leads to higher conversion but lower ee's (Table 4.2, entry 8~13). Then we apply this Brønsted acid source in the hydrogenation of the standard substrate 2-methylindole, the ee increased up to 98% with full conversion (Table 4.1, entry 14). Again, no significant sign of by-products was observed by 1H NMR study on the crude products. These results suggest that Rh/ZhaoPhos complex could tolerate highly acidic reaction condition.

Stereoselectivity in hydrogenation of 2,3-disubstituted indoles could be explained as a result of a dynamic kinetic resolution. After a protonation, two enantiomers both exist in the solution. Due to the chirality of the ligand, only one isomer could be reduced efficiently ($k_1 >> k_3 >> k_2$). In the hydride transfer step, Due to the steric effect, addition

of hydride could only be conducted at one side, resulting in trans- addition and a cis-product.

The ligand/metal ratio could be wide-ranging for both high conversion and high enantioselectivity. Good performance (>95% conv. and 97% ee for chiral 2-methylindoline) was retained with a ligand/Rh ratio from 0.5 to 2.0. In addition, the equivalent of hydrogen chloride to indole substrate is also wide-ranging.[38] This advantage makes the ZhaoPhos/Rh catalytic system an ease in organic synthesis communities. However, without Brønsted acid HCl, no product was observed, leading to almost 100% recovery of starting material.

Scheme 4.2. Origin of stereoselectivity in the hydrogenation of disubstituted indoles.

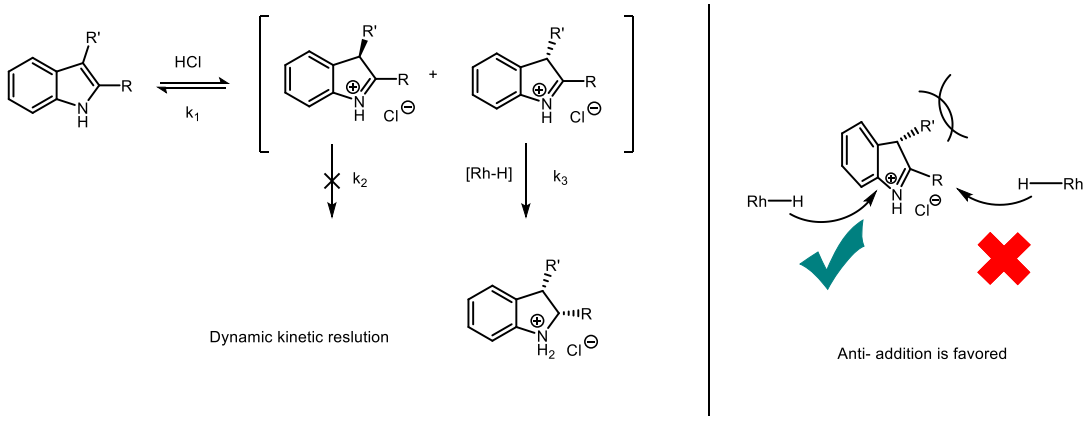

4.3 Substrate scope

The substrate scope with this optimal condition was examined (Table 3). By adding hydrogen chloride in acetic acid solution as the Brønsted acid source, 2-monosubstituted indoles and 2,3-disubstituted indoles were hydrogenated with high enantioselectivities (94%~99% ee). Various substituents on 2- position or on the benzo ring bring no significant influence on the enantioselectivity while the yields vary from case to case.

Phenyl substituent on the 2-position remains a challenge and this might be caused by a more stable conjugate enamine C=C bond, which is more difficult for protonation. 2,3-Disubstituted indoles were also hydrogenated successfully with both high diastereoselectivities (>25:1) and high enantioselectivities.

Table 4.3 Substrate scope for asymmetric hydrogenation of indoles. [a]

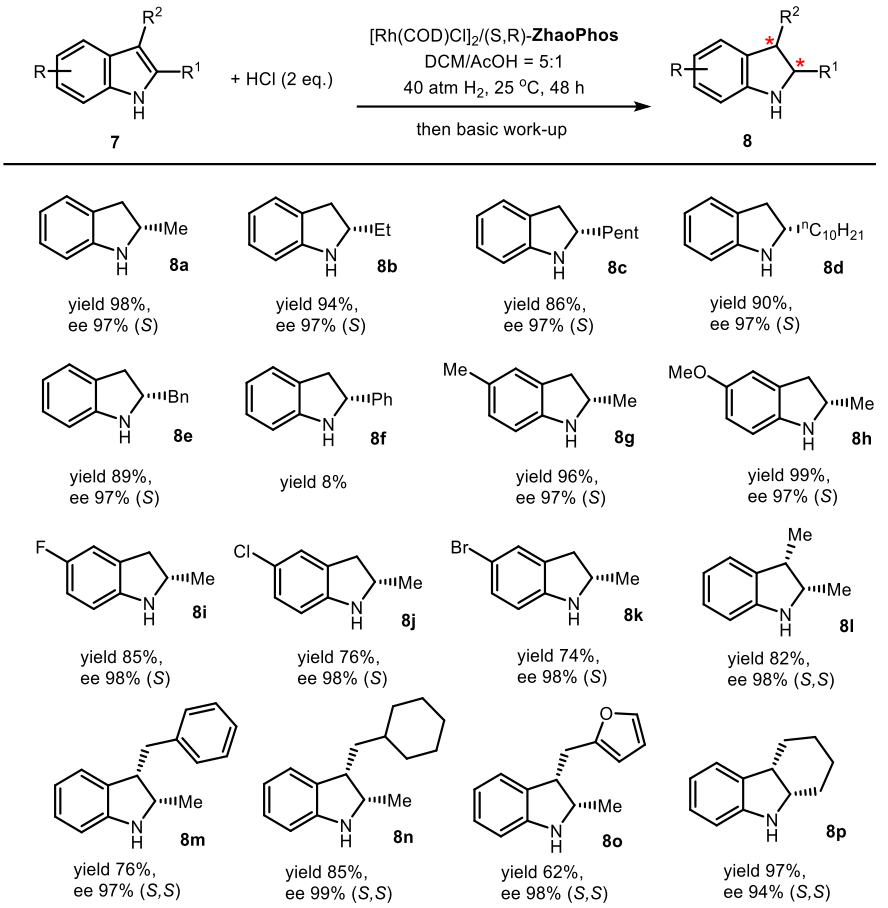

[a] reaction condition: 7 (0.2 mmol) in 2.0 ml solvent, 7/[Rh(COD)Cl]$_2$/ligand ratio=100/0.50/1.0, 0.4 ml of HCl (1.0 M) in AcOH solution was added; isolation yield, no significant sign of side product was observed; ee was determined by HPLC or GC with a chiral stationary phase

4.4 Mechanistic study

The anion binding effect of ZhaoPhos with chloride ion was already observed in previous studies. [34, 39] Control experiments were conducted to proof the cooperation of

thiourea moiety and the bisphosphine scaffold. Each unit within ZhaoPhos was demonstrated to be necessary for an efficient asymmetric hydrogenation of 2-methylindole. We synthesized a series of analogues of ZhaoPhos and conducted control experiments to evaluate the collaboration manner of each unit of ZhaoPhos. Urea bisphosphine ligand L2 only gives no product, and this sharp contrast suggests the crucial role of thiourea moiety. Compared to H (L2) and methyl (L3), more electron-withdrawing trifluoromethyl group at 3- and 5- position on the phenyl ring increases the enantioselectivity, which is probably due to the stronger acidity of N-H proton on the thiourea. After *N*-methylation of the less acidic thiourea N-H proton, enantioselectivity results in a minor decrease. This observation reveals that the more acidic thiourea N-H proton contributes mostly in anion binding with chloride. Furthermore, monophosphine ligand L6 and the mixture of ferrocene-thiourea compound L7 with triphenylphosphine can hardly catalyzed the hydrogenation reaction. On the other hand, the mixture of thiourea molecule and bisphosphine-Ugi's amine L8 failed to show catalytic activity. These results (ZhaoPhos vs L6 or L7 with PPh_3 and L8/thiourea) demonstrate the importance of a covalent incorporation of bisphosphine moiety and thiourea. The idea of secondary offers an alternative strategy for asymmetric hydrogenation.

Table 4.4 Control experiments and ligand evaluation. [a]

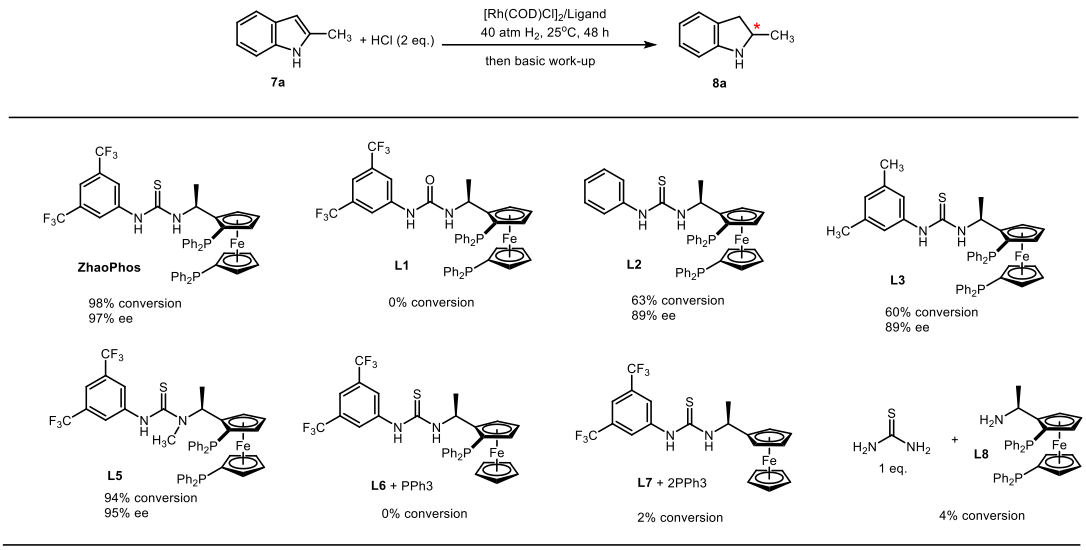

[a] reaction condition: 7a (0.2 mmol) in 2.0 ml solvent,7/[Rh(COD)Cl]$_2$/ligand ratio=100/0.50/1.0, 0.4 ml of HCl (1.0 M) in AcOH solution was added; conversion was determined by ^{1}H NMR analysis, no side product was observed; ee was determined by HPLC or GC with a chiral stationary phase.

Counterion effect was also examined. When tetrabutylammonium chloride (TBAC) was added, no significant changes in conversion and enantioselectivity was observed (Table 4.5, entry 2 vs 1). This suggests the spectator role of tetrabutylammonium cation. The introduction of fluoride anion from TBAF does not influence this catalytic reaction (entry 3 vs 2). The presence of bromide anion decreases the conversion, but it shows trace influence on the enantioselectivity (entry 4 vs 2). Iodide, however, lowers the both of the conversion and enantioselectivity dramatically (entry 5 vs 2).

Table 4.5 Counterion effects. [a]

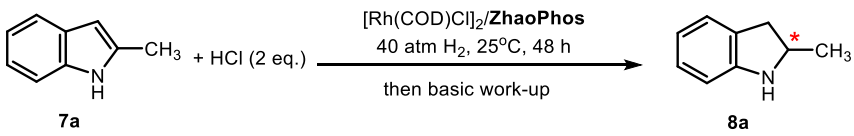

Entry	additive	conversion[b]	ee[c]
1	none	98%	97%
2	TBAC (1.0 eq.)	92%	94%
3	TBAF (1.0 eq.)	93%	93%

4	TBAB (1.0 eq.)	61%	92%
5	TBAI (1.0 eq.)	13%	76%

[a] reaction condition: 7a (0.2 mmol) in 2.0 ml solvent, 7/[Rh(COD)Cl]$_2$/ligand ratio=100/0.50/1.0, 0.4 ml of HCl (1.0 M) in AcOH solution was added; [b] conversion was determined by ^{1}H NMR analysis, no side product was observed; [c] ee was determined by HPLC or GC with a chiral stationary phase.

In order to get insight of this reaction progress, isotope labeling experiments (scheme 3) were conducted. When the reaction was performed in deuterated solvent (CD3OD/CD2Cl2) with hydrogen gas, D atoms were added only at 3-position while H atom is added at 2-position. When regular solvent and deuterium gas were applied, D atom was added exclusively at 2-position, no significant sign of D atom was observed at 3-position. This result suggests that it is C=N bond, rather than C=C, to be hydrogenated. A protonation and the following enamine-imine tautomerization probably occurs prior to the hydrogenation. The low abundance (32%) of deuterium at 2-position in experiment 2 seems to suggest an H-D exchange before the hydrogenation step. In order to gain a plausible explanation, systematic kinetic studies are in need in the future.

Scheme 4.3. Deuterium labeling experiments.

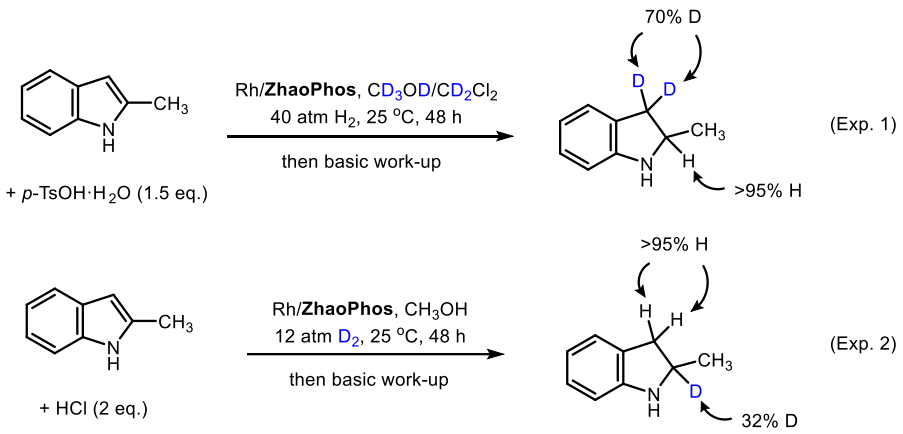

4.5 Nonlinear effect

The hydrogen bonding between (thio)urea molecules in supramolecular chemistry promoted us to investigate the potential dimerization or high-order aggregation of this thiourea-containing catalyst. Quantitative nonlinear effect (NLE) was carried out and we observed an obvious positive NLE in hydrogenation of 2-methylindole with ZhaoPhos/Rh complex (Table 4.6).

Table 4.6. Nonlinear effects for asymmetric hydrogenation of indole. [a]

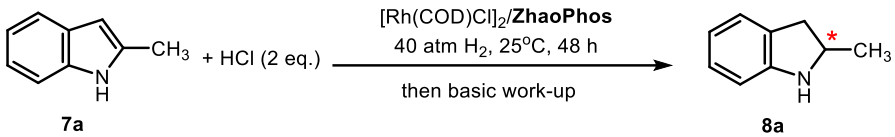

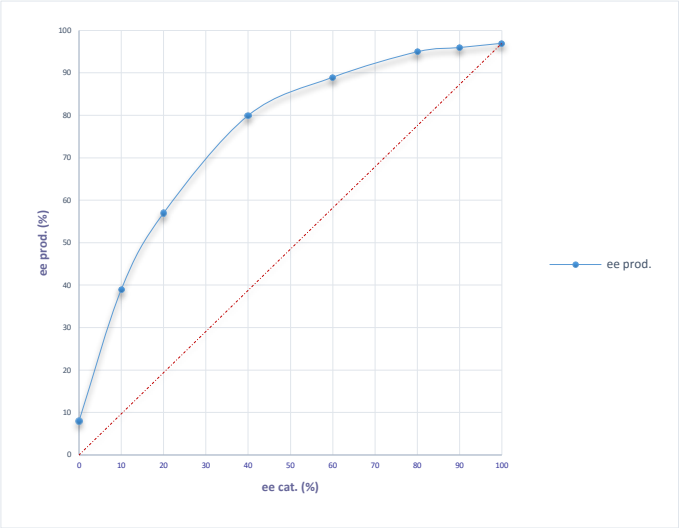

Entry	ee fo ZhaoPhos	conversion[b]	ee[c]
1	0	98%	8%
2	10%	98%	39%
3	20%	98%	57%
4	40%	98%	80%
5	60%	98%	89%
6	80%	98%	95%
7	90%	98%	96%

8	100%	98%	97%

[a] reaction condition: 7a (0.2 mmol) in 2.0 ml solvent, **7a**/[Rh(COD)Cl]$_2$/ligand ratio=100/0.50/1.0, 0.4 ml of HCl (1.0 M) in AcOH solution was added; [b] conversion was determined by ^{1}H NMR analysis, no side product was observed; [c] ee was determined by HPLC or GC with a chiral stationary phase.

A non-covalent interaction between thiourea ligands might be responsible for this phenomenon. This bisphosphine/rhodium complex, categorized in bidentate L-L/M system, is not suitable for Kagan's classic ML_1L_2 model or "Reservoir Model". [40] So another mechanism may explain this phenomenon. When the Hayashi group studied the rhodium catalyzed 1,4-addition of phenylboronic acid to enones,[41] they observed an negative NLE. With kinetic and NMR studies, they proposed that a dimeric rhodium complex serves as the precursor of the catalytically active Rh complex. Only homochiral dimer was observed. Similarly, in Wilkinson's Rh-catalyzed hydrogenation system, a μ-chloro-bridged dimeric complex is in a great population prior to the hydrogenation catalytic cycle (Scheme 4). Based on Hayashi's studies, we proposed that this dimer is responsible for this NLE. After treating the metal precursor [Rh(COD)Cl]$_2$ with enantiopure ZhaoPhos, a homochiral dimer is formed, which will sequentially dissociate to form a monomer. Once reacting with hydrogen gas, an oxidative addition will change this square planar monomer into a reactive octahedral complex. On the other hand, if the precursor is treated with mixed ZhaoPhos, both homochiral and heterochiral dimers are formed. The heterochiral dimer is possibly more stable than the homochiral ones, resulting in an enantiomeric enrichment for the reactive dihydro-rhodium complexes. A positive NLE will be therefore observed in hydrogenation of 2-methylindole.

Scheme 4.4 Equilibrium scheme for nonlinear effect.

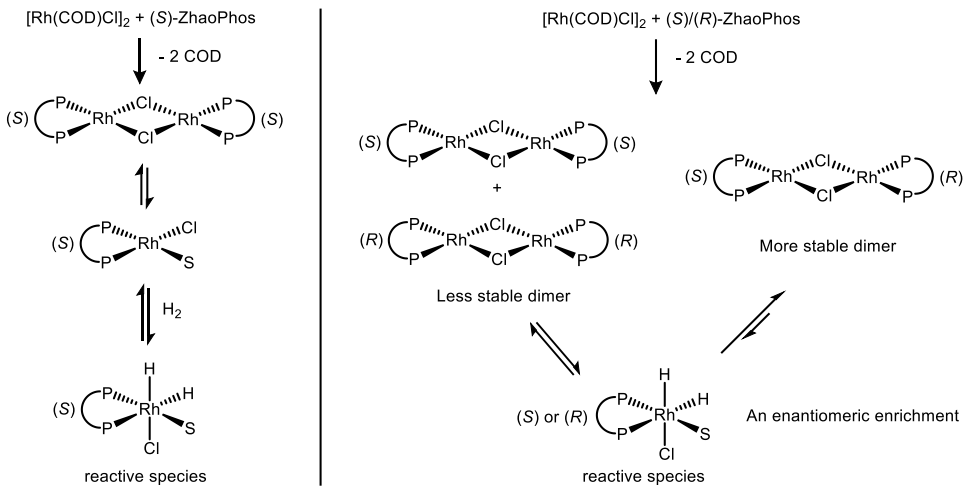

4.5 Summary

In summary, we developed an efficient method to synthesize chiral indolines. By employing a cooperative catalysis of transition metal, Brønsted acid and anion binding, prochiral indoles are successfully hydrogenated with high enantioselectivities. After introducing strong Brønsted acid HCl, protonation of indole leads to an enamine-imine tautomerization equilibrium. This resulting iminium was reduced by a rhodium-ZhaoPhos complex. Isotope labeling experiments supported this chemical process. Nonlinear effect was observed in this catalysis.

4.6 Experimental Section

4.6.1 Synthesis of indole substrates.

Method A[42]

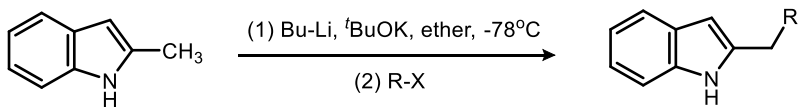

2-methylindole (10 mmol, 1.31 g) was dissolved in ether at room temperature, the mixture was

under nitrogen protection. Butyllithium in hexane solution was added dropwise to the stirring mixture. Then potassium tert-butoxide was added in one portion. The color of the mixture became bright yellow. After stirring for 30 min, the mixture was cooled to -78°C, methyl iodide was added dropwise. After stirring for another 2 hours at -78°C, several drops of water was added to quench the reaction. Ammonium chloride solution was added to adjust the pH to neutral. After separation, the aqueous layer was washed with ether and the organic layer was combine. The ether solution was dried over anhydrous sodium sulfate and then the volatile was evaporated under reduced pressure. The crude product was purified by flash chromatography (hexanes/ethyl acetate).

Method B[43]

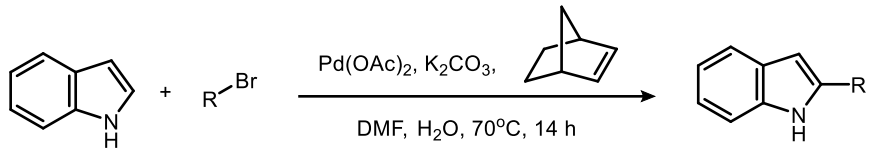

A Schlenk flask was charged with indole (5 mmol, 0.65 g), alkyl bromide, norbornene, potassium carbonate and palladium(II) acetate. Water (0.1 M) in DMF was added. The mixture was frozen at -78 °C and the flask was evacuated and backfilled with nitrogen for 3 times. The stoppered mixture was stirred at 70°C for 14 hours. After cooled to room temperature, the mixture was diluted with ether and washed with water. The organic layer was dried over anhydrous sodium sulfate and the volatile was evaporated under reduced pressure. The crude product was purified by flash chromatography (hexanes/ethyl acetate).

Method C[32]

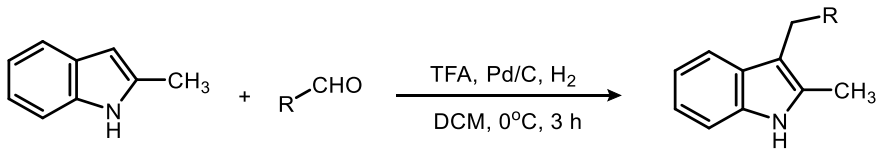

In a round bottom flask, a solution of 2-methylindole (5 mmol, 0.65 g) and aldehyde in dichloromethane was added to a stirring ice-cold mixture of trifluoroacetice acid and palladium on carbon in DCM. This flask was filled with hydrogen and the mixture was stirred at 0°C. After TCL monitoring showed the consumption of indole (approximately 3 h), the Pd/C was

filtered and the solvent was concentrated under reduced pressure. The crude product was purified by chromatography (hexane/ethyl acetate).

Method D[44]

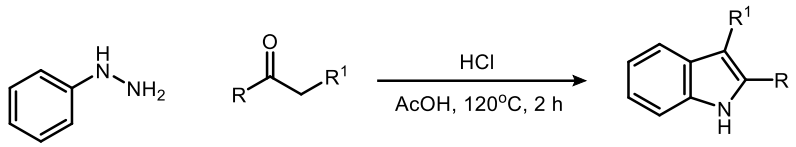

A round bottom flask was charged with 0.5 ml phenyl hydrazine, 0.78 ml cyclohexanone, 1ml of concentrate HCl and 20 ml of acetic acid. The mixture was heated at 120°C for 2 hours and cooled back to room temperature. 2M of NaOH solution was added. After the pH became 6-7, the mixture was cooled in ice. The aqueous layer was extracted with ether 3 times and the combined mixture was dried over anhydrous sodium sulfate and concentrated under reduced pressure. The crude product was purified by chromatography (hexane/ethyl acetate).

Method A	Method B	Method C	Method D
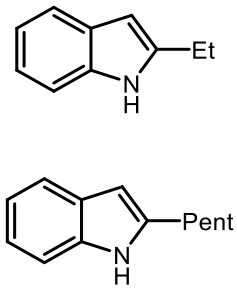	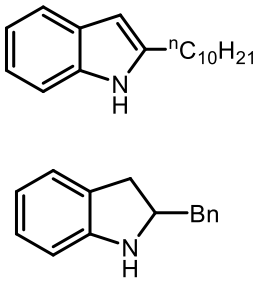	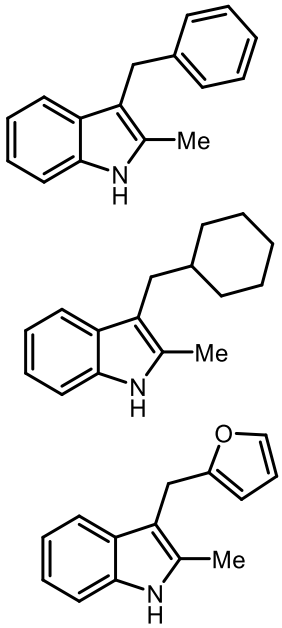	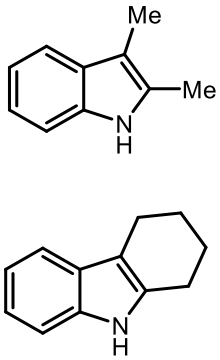

4.6.2 General procedure for asymmetric hydrogenation of indoles.

In the nitrogen-filled glovebox, solution of $[Rh(COD)Cl]_2$ (2.46 mg, 0.005 mmol) and ZhaoPhos (2.1 eq.) in 5.0 ml anhydrous solvent was stirred at room temperature for 20

min. A specified volume of the resulting solution (0.50 ml, 1% Rh catalyst) was transferred to a Score-Break ampule charged with substrate solution (0.1 mmol in 0.5 ml) by syringe. 0.2 ml of hydrogen chloride in acetic acid solution (1.0 M) was added by syringe. The ampule was placed into an autoclave, which was then charged with 40 atm H2. The autoclave was stirred at desired temperature for the indicated period of time. After release of H2, saturated potassium carbonate solution and dichloromethane was added and the mixture was stirred for 30 min. The organic layer was dried with Na2SO4. After removal of solvent, the crude product was analyzed by 1H NMR to determine the conversion. The enantiomeric excess was determined by GC or HPLC analysis.

The absolute configurations were assigned according to literature. [32]

4.6.3 Deuterium labeling experiments.

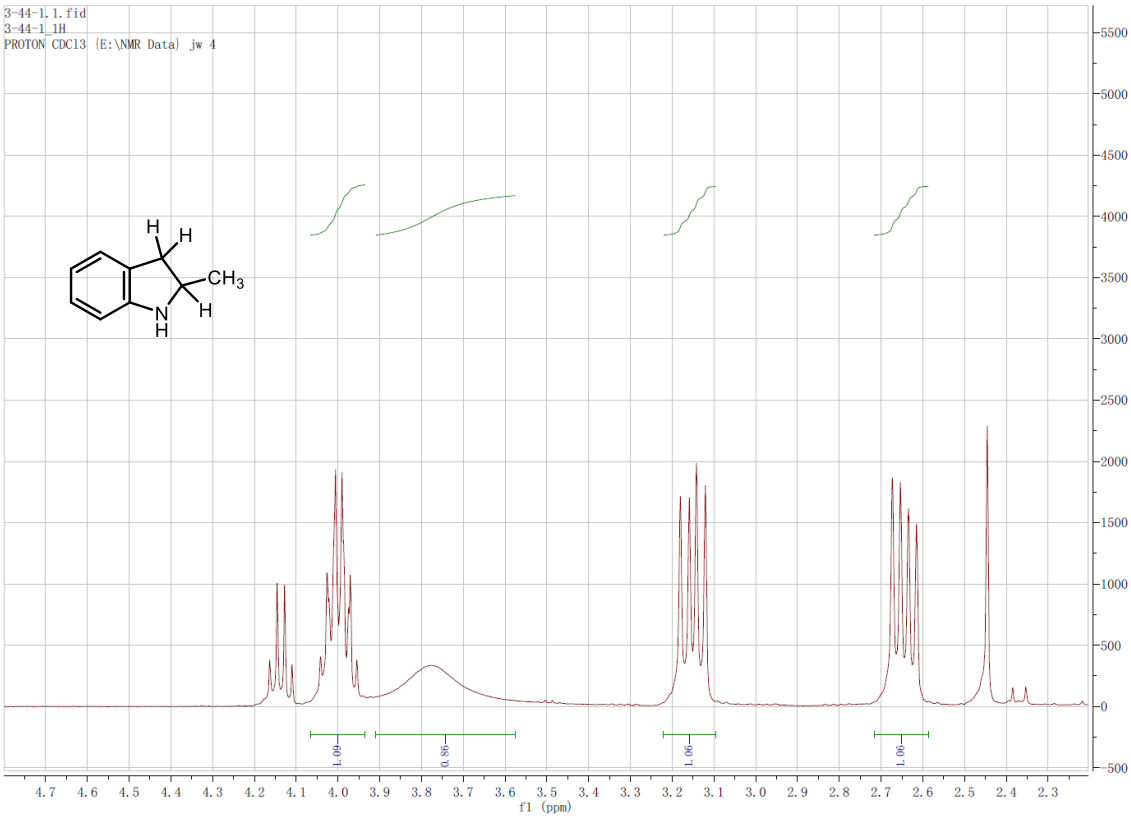

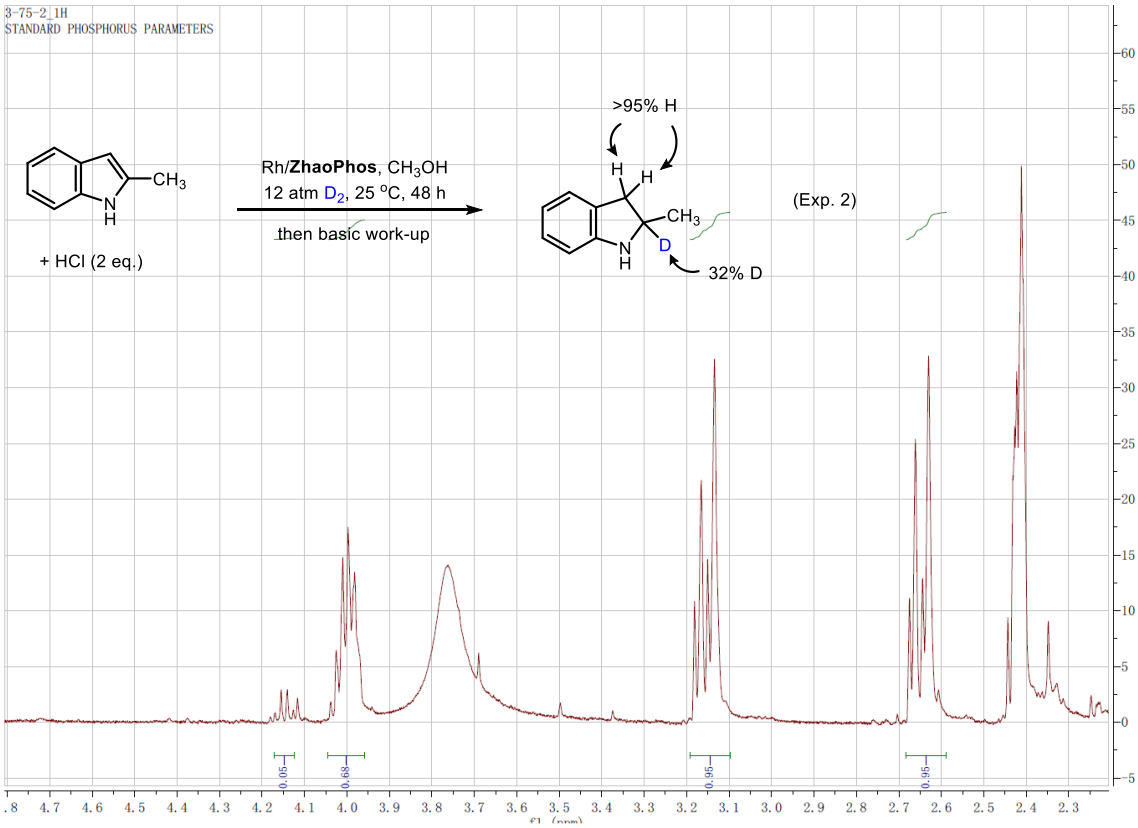

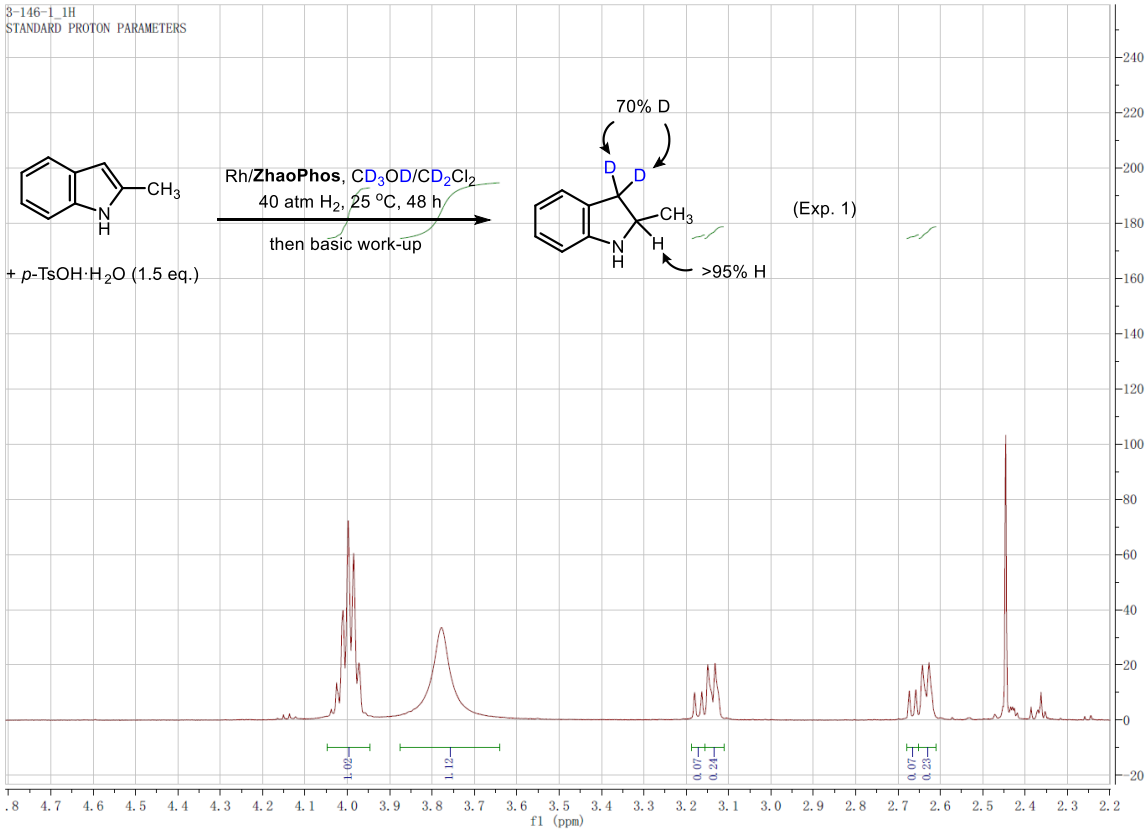

4.6.4 Characterization data for chiral indolines.

(S)-2-methylindoline (8a) [32]

Colorless oil. ^{1}H NMR (400 MHz, $CDCl_3$) δ 7.09 (d, *J* = 7.3 Hz, 1H), 7.02 (t, *J* = 7.6 Hz, 1H), 6.70 (t, *J* = 7.4 Hz, 1H), 6.62 (d, *J* = 7.7 Hz, 1H), 4.00 (tq, *J* = 8.1, 6.2 Hz, 1H), 3.79 (br, 1H), 3.16 (dd, *J* = 15.4, 8.5 Hz, 1H), 2.65 (dd, *J* = 15.4, 7.8 Hz, 1H), 1.30 (d, *J* = 6.2 Hz, 3H). ^{13}C NMR (400 MHz, $CDCl_3$): δ 150.96, 128.89, 127.23, 124.72, 118.52, 109.16, 55.23, 37.78, 22.30. HPLC (Daicel Chiralpak OD-H, hexanes/i-PrOH = 97/3, Flow rate = 0.8 ml/min, UV = 254 nm): t_1 = 12.1 min, t_2 = 13.8 min.

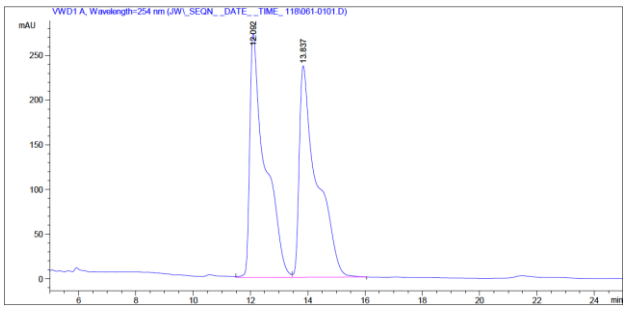

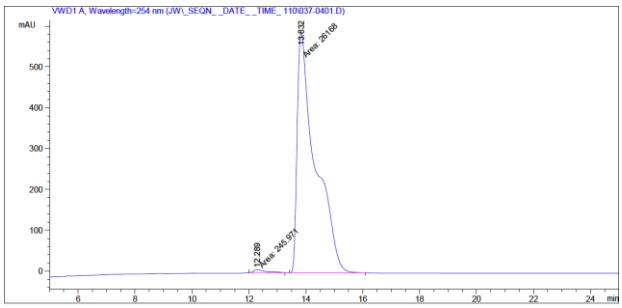

Peak #	RetTime [min]	Type	Width [min]	Area mAU *s	Height [mAU]	Area %
1	12.289	MM	0.5220	245.97058	7.85383	0.9312
2	13.832	MM	0.7410	2.61680e4	588.53992	99.0688
Totals :				2.64140e4	596.39375	

(S)-2-ethylindoline (8b) [32]

Colorless oil. ^{1}H NMR (400 MHz, CDCl3) δ 7.07 (d, J = 7.2 Hz, 1H), 7.01 (t, J = 7.6 Hz, 1H), 6.68 (td, J = 7.4, 0.9 Hz, 1H), 6.60 (d, J = 7.7 Hz, 1H), 3.88 (br, 1H), 3.78 (tt, J = 8.5, 6.6 Hz, 1H), 3.13 (dd, J = 15.5, 8.6 Hz, 1H), 2.69 (dd, J = 15.5, 8.4 Hz, 1H), 1.64 (qd, J = 7.5, 4.0 Hz, 2H), 0.98 (t, J = 7.4 Hz, 3H). ^{13}C NMR (400 MHz, $CDCl_3$) δ 151.00, 128.86, 127.17, 124.62,

118.37, 108.99, 61.49, 35.72, 29.55, 10.69. HPLC (Daicel Chiralpak OD-H, hexanes/i-PrOH = 97/3, Flow rate = 0.8 ml/min, UV = 254 nm): t_1 = 9.5 min, t_2 = 11.3 min.

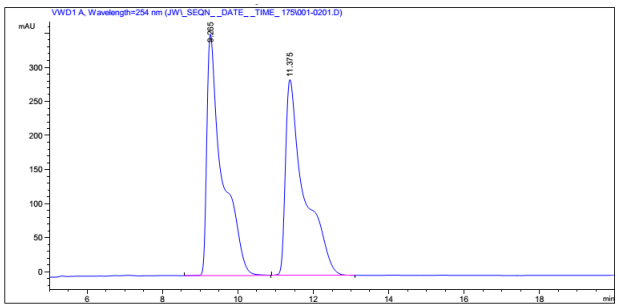

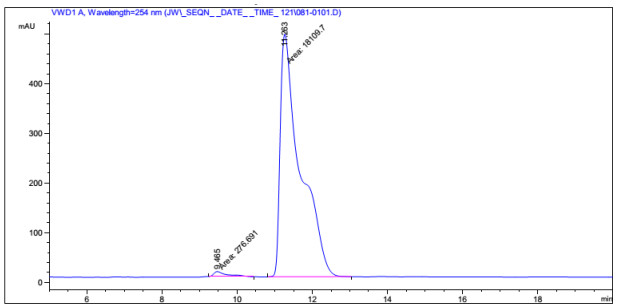

Peak #	RetTime [min]	Type	Width [min]	Area mAU *s	Height [mAU]	Area %
1	9.465	MM	0.4431	276.69092	10.40781	1.5049
2	11.263	MM	0.6176	1.81097e4	488.70456	98.4951
Totals :				1.83864e4	499.11237	

(S)-2-pentylindoline (8c) [32]

Colorless oil. ^{1}H NMR (400 MHz, $CDCl_3$) δ 7.07 (d, *J* = 7.2 Hz, 1H), 7.00 (t, *J* = 7.6 Hz, 1H), 6.68 (td, *J* = 7.4, 0.7 Hz, 1H), 6.60 (d, *J* = 7.7 Hz, 1H), 3.84 (dq, *J* = 8.5, 6.7 Hz, 1H), 3.35 (br, 1H), 3.12 (dd, *J* = 15.5, 8.6 Hz, 1H), 2.68 (dd, *J* = 15.4, 8.4 Hz, 1H), 1.68 – 1.53 (m, 2H), 1.47 – 1.17 (m, 6H), 0.91 (dd, *J* = 8.9, 4.8 Hz, 3H). ^{13}C NMR (400 MHz, $CDCl_3$) δ 150.98, 128.91, 127.19, 124.63, 118.45, 109.08, 60.08, 36.81, 36.18, 31.87, 26.23, 22.62, 13.99. HPLC (Daicel Chiralpak OD-H, hexanes/i-PrOH = 97/3, Flow rate = 0.8 ml/min, UV = 254 nm): t_1 = 6.7 min, t_2 = 8.8 min.

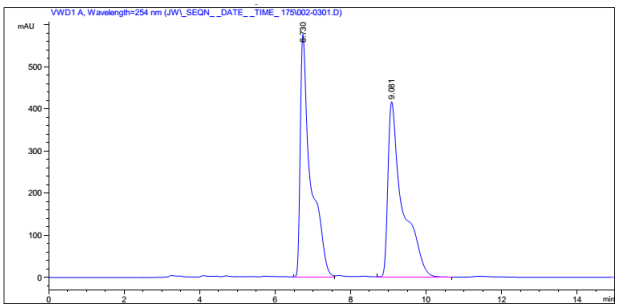

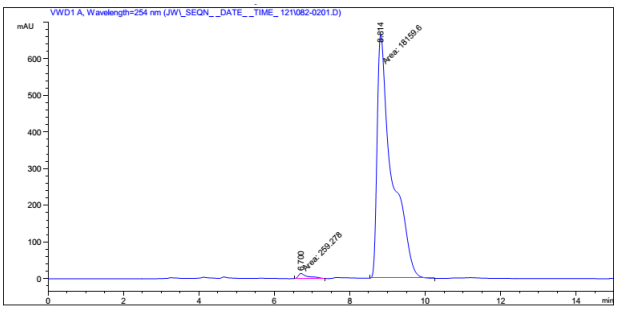

Peak #	RetTime [min]	Type	Width [min]	Area mAU *s	Height [mAU]	Area %
1	6.700	MM	0.3064	259.27817	14.10447	1.4077
2	8.814	MM	0.4549	1.81596e4	665.32605	98.5923
Totals :				1.84189e4	679.43052	

(S)-2-decylindoline (8d)

Colorless oil. ^{1}H NMR (400 MHz, $CDCl_3$) δ 7.07 (d, *J* = 7.2 Hz, 1H), 7.00 (t, *J* = 7.6 Hz, 1H), 6.68 (t, *J* = 7.4 Hz, 1H), 6.60 (d, *J* = 7.7 Hz, 1H), 3.83 (ddd, *J* = 15.2, 8.5, 6.7 Hz, 2H), 3.12 (dd, *J* = 15.4, 8.6 Hz, 1H), 2.67 (dd, *J* = 15.4, 8.5 Hz, 1H), 1.71 – 1.55 (m, 4H), 1.30 (d, *J* = 21.9 Hz, 14H), 0.89 (t, *J* = 6.8 Hz, 3H). ^{13}C NMR (400 MHz, $CDCl_3$) δ 150.99, 128.90, 127.17, 124.63, 118.40, 109.04, 60.09, 36.84, 36.16, 31.90, 29.63, 29.33, 26.58, 22.68, 14.10. HPLC (Daicel Chiralpak OD-H, hexanes/i-PrOH = 97/3, Flow rate = 0.8 ml/min, UV = 254 nm): t_1 = 6.0 min, t_2 = 8.2 min.

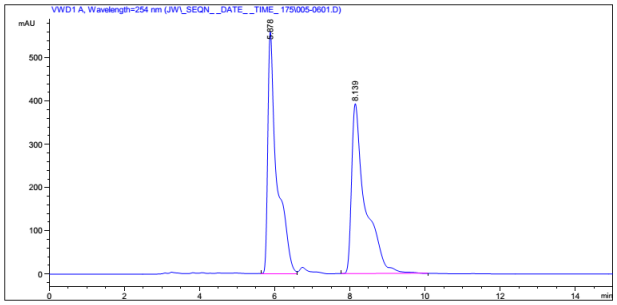

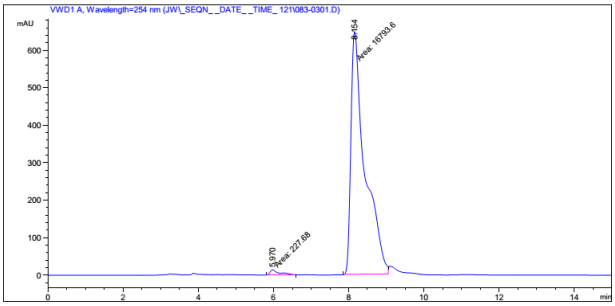

Peak #	RetTime [min]	Type	Width [min]	Area mAU *s	Height [mAU]	Area %
1	5.970	MM	0.2832	227.68025	13.40041	1.3376
2	8.154	MM	0.4317	1.67936e4	648.28119	98.6624
Totals :				1.70213e4	661.68159	

(S)-2-benzylindoline (8e) [32]

Colorless oil. ^{1}H NMR (400 MHz, $CDCl_3$) δ 7.34 (t, *J* = 7.3 Hz, 3H), 7.25 (dd, *J* = 10.7, 7.6 Hz, 2H), 7.09 (d, *J* = 7.3 Hz, 1H), 7.02 (t, *J* = 7.6 Hz, 1H), 6.70 (t, *J* = 7.4 Hz, 1H), 6.58 (d, *J* = 7.7 Hz, 1H), 4.09 (ddd, *J* = 15.8, 8.4, 5.6 Hz, 1H), 3.81 (br, 1H), 3.15 (dd, *J* = 15.5, 8.5 Hz, 1H), 3.00 – 2.74 (m, 3H). ^{13}C NMR (400 MHz, $CDCl_3$) δ 150.53, 139.08, 129.11, 128.62, 128.35, 127.33, 126.43, 124.79, 118.51, 109.07, 60.96, 42.72, 35.94. HPLC (Daicel Chiralpak OD-H, hexanes/i-PrOH = 97/3, Flow rate = 0.8 ml/min, UV = 254 nm): t_1 = 9.8 min, t_2 = 11.1 min.

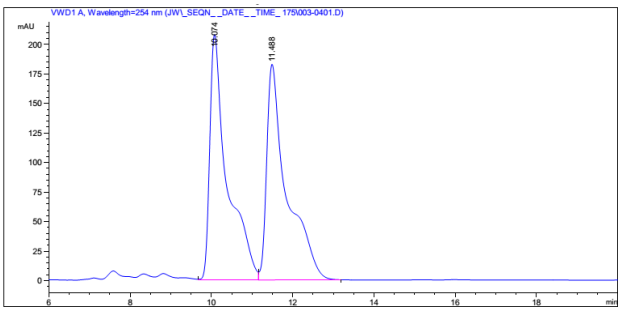

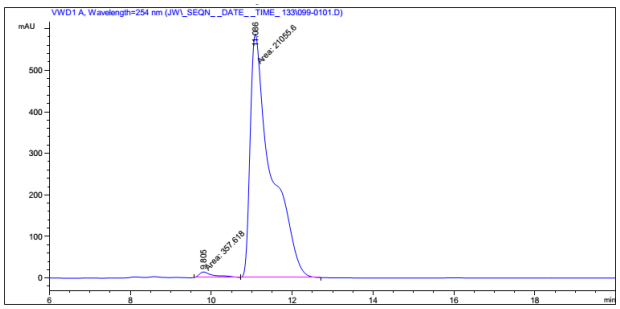

Peak #	RetTime [min]	Type	Width [min]	Area mAU *s	Height [mAU]	Area %
1	9.805	MM	0.4497	357.61798	13.25354	1.6701
2	11.086	MM	0.5992	2.10556e4	585.62494	98.3299

Totals : 2.14132e4 598.87847

(S)-2,5-dimethylindoline (8g) [32]

Colorless oil. ^{1}H NMR (400 MHz, $CDCl_3$) δ 6.91 (s, 1H), 6.82 (d, *J* = 7.7 Hz, 1H), 6.52 (d, *J* = 7.8 Hz, 1H), 4.09 – 3.77 (m, 1H), 3.44 (br, 1H), 3.10 (dd, *J* = 15.4, 8.4 Hz, 1H), 2.60 (dd, *J* = 15.4, 7.7 Hz, 1H), 2.25 (s, 3H), 1.28 (d, *J* = 6.2 Hz, 3H). ^{13}C NMR (400 MHz, $CDCl_3$) δ 148.56, 129.23, 127.89, 127.48, 125.49, 109.14, 55.37, 37.85, 22.22, 20.74. HPLC (Daicel Chiralpak OD-H, hexanes/i-PrOH = 97/3, Flow rate = 0.8 ml/min, UV = 254 nm): t_1 = 7.2 min, t_2 = 9.1 min.

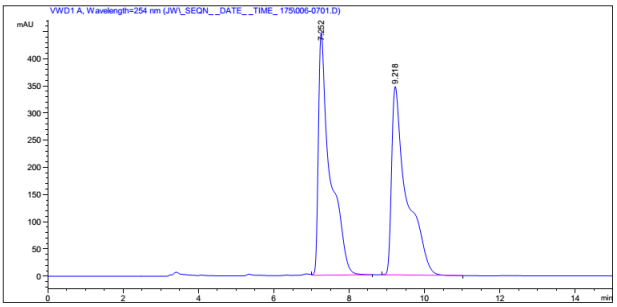

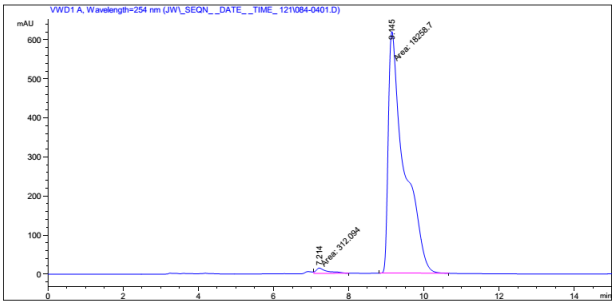

Peak #	RetTime [min]	Type	Width [min]	Area mAU *s	Height [mAU]	Area %
1	7.214	MM	0.3670	312.09412	14.17488	1.6806
2	9.145	MM	0.4916	1.82587e4	619.00964	98.3194
Totals :				1.85708e4	633.18452	

(S)-5-methoxy-2-methylindoline (8h) [45]

Colorless oil. ^{1}H NMR (400 MHz, $CDCl_3$) δ 6.74 (dd, J = 5.5, 4.3 Hz, 1H), 6.60 (dd, J = 8.3, 2.4 Hz, 1H), 6.55 (d, J = 8.4 Hz, 1H), 4.04 – 3.94 (m, 1H), 3.75 (s, 3H), 3.40 (br, 1H), 3.12 (dd, J = 15.5, 8.3 Hz, 1H), 2.63 (dd, J = 15.5, 7.9 Hz, 1H), 1.30 (d, J = 6.2 Hz, 3H). ^{13}C NMR (400 MHz, $CDCl_3$) δ 153.47, 144.77, 130.66, 112.13, 111.71, 109.79, 55.95, 55.65, 38.29, 22.17. HPLC (Daicel Chiralpak OD-H, hexanes/i-PrOH = 97/3, Flow rate = 0.8 ml/min, UV = 254 nm): t_1 = 12.1 min, t_2 = 25.1 min.

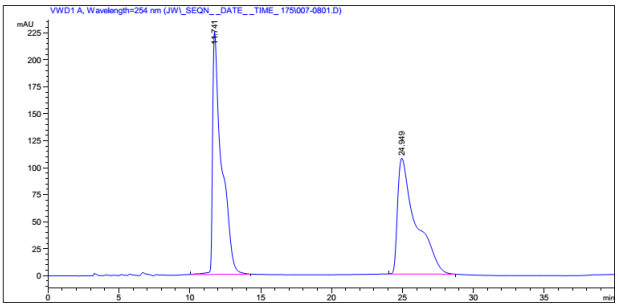

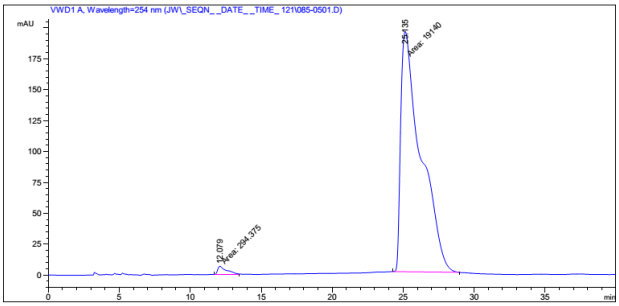

Peak #	RetTime [min]	Type	Width [min]	Area mAU *s	Height [mAU]	Area %
1	12.079	MM	0.7445	294.37491	6.58973	1.5147
2	25.135	MM	1.6384	1.91400e4	194.70343	98.4853
Totals :				1.94343e4	201.29316	

(S)-5-fluoro-2-methylindoline (8i) [32]

Colorless oil. ^{1}H NMR (400 MHz, $CDCl_3$) δ 6.87 – 6.77 (m, 1H), 6.74 – 6.66 (m, 1H), 6.50 (dd, *J* = 8.4, 4.4 Hz, 1H), 4.06 – 3.96 (m, 1H), 3.33 (br, 1H), 3.12 (dd, *J* = 15.7, 8.5 Hz, 1H), 2.62 (ddd, *J* = 15.7, 7.8, 0.7 Hz, 1H), 1.29 (d, *J* = 6.2 Hz, 3H). ^{13}C NMR (400 MHz, $CDCl_3$) δ 156.97 (d, *J* = 234.7 Hz), 146.92 (s), 130.64 (d, *J* = 8.2 Hz), 113.09 (d, *J* = 23.2 Hz), 112.11 (d, *J* = 23.7 Hz), 109.28 (d, *J* = 8.2 Hz), 55.89, 38.02, 22.16. HPLC (Daicel Chiralpak OD-H, hexanes/i-PrOH = 97/3, Flow rate = 0.8 ml/min, UV = 254 nm): t_1 = 7.3 min, t_2 = 10.7 min.

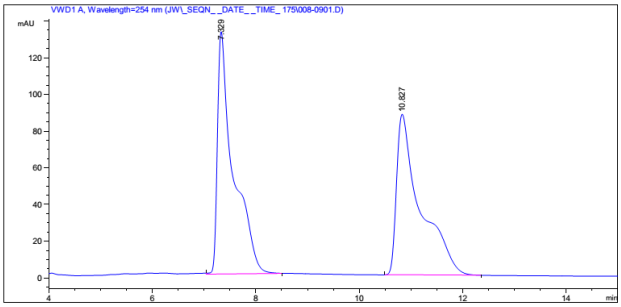

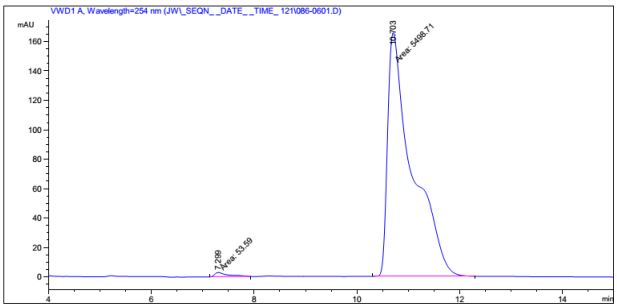

Peak #	RetTime [min]	Type	Width [min]	Area mAU *s	Height [mAU]	Area %
1	7.299	MM	0.3069	53.58995	2.91006	0.9652
2	10.703	MM	0.5535	5498.71191	165.58165	99.0348
Totals :				5552.30187	168.49171	

(S)-5-chloro-2-methylindoline (8j) [46]

Colorless oil. ^{1}H NMR (400 MHz, $CDCl_3$) δ 7.02 (s, 1H), 6.95 (dd, *J* = 8.2, 1.8 Hz, 1H), 6.49 (d, *J* = 8.2 Hz, 1H), 4.01 (tt, *J* = 14.4, 6.2 Hz, 1H), 3.76 (br, 1H), 3.12 (dd, *J* = 15.7, 8.6 Hz, 1H), 2.61 (dd, *J* = 15.7, 7.6 Hz, 1H), 1.28 (d, *J* = 6.2 Hz, 3H). ^{13}C NMR (400 MHz, $CDCl_3$) δ 149.50, 130.75, 126.94, 124.86, 122.93, 109.69, 55.61, 37.60, 22.16. HPLC (Daicel Chiralpak OD-H, hexanes/i-PrOH = 97/3, Flow rate = 0.8 ml/min, UV = 254 nm): t_1 = 8.1 min, t_2 = 14.5 min.

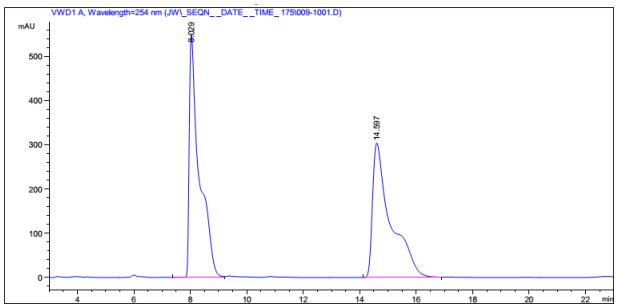

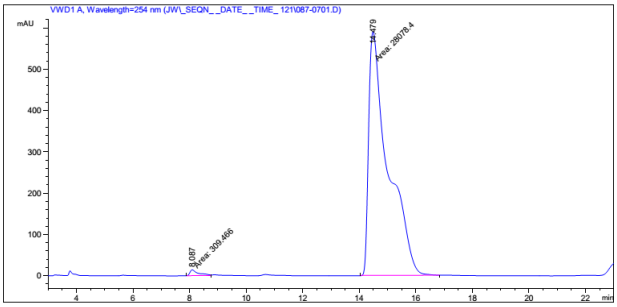

Peak #	RetTime [min]	Type	Width [min]	Area mAU *s	Height [mAU]	Area %
1	8.087	MM	0.3608	309.46597	14.29349	1.0901
2	14.479	MM	0.7926	2.80784e4	590.45758	98.9099
Totals :				2.83879e4	604.75107	

(S)-5-bromo-2-methylindoline (8k) [46]

Colorless oil. ^{1}H NMR (400 MHz, $CDCl_3$) δ 7.17 – 7.14 (m, 1H), 7.09 (dd, *J* = 8.2, 2.0 Hz, 1H), 6.45 (d, *J* = 8.2 Hz, 1H), 4.10 – 3.91 (m, 1H), 3.76 (br, 1H), 3.12 (dd, *J* = 15.7, 8.5 Hz, 1H), 2.62 (dd, *J* = 15.7, 7.6 Hz, 1H), 1.27 (d, *J* = 6.2 Hz, 3H). ^{13}C NMR (400 MHz, $CDCl_3$) δ 149.95, 131.23, 129.82, 127.65, 110.25, 109.90, 55.53, 37.51, 22.15. HPLC (Daicel Chiralpak OD-H, hexanes/i-PrOH = 97/3, Flow rate = 0.8 ml/min, UV = 254 nm): t_1 = 8.6 min, t_2 = 15.4 min.

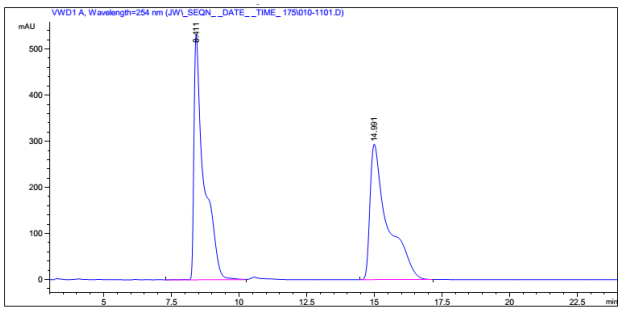

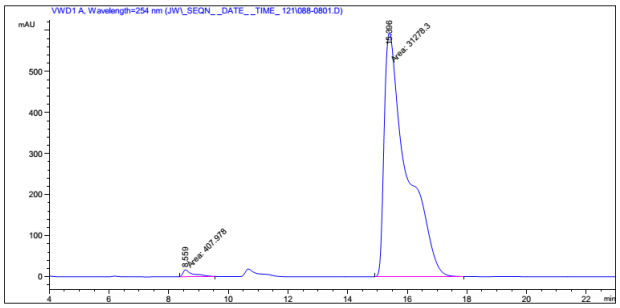

Peak #	RetTime [min]	Type	Width [min]	Area mAU *s	Height [mAU]	Area %
1	8.559	MM	0.4066	407.97836	16.72300	1.2876
2	15.396	MM	0.8760	3.12783e4	595.09326	98.7124

Totals : 3.16862e4 611.81626

(S,S)-2,3-dimethylindoline (8l) [32]

Colorless oil. ^{1}H NMR (400 MHz, $CDCl_3$) δ 7.12 – 6.98 (m, 2H), 6.73 (t, *J* = 7.4 Hz, 1H), 6.62 (d, *J* = 7.7 Hz, 1H), 4.01 – 3.89 (m, 1H), 3.64 (br, 1H), 3.33 – 3.22 (m, 1H), 1.18 (d, *J* = 7.2 Hz, 3H), 1.14 (d, *J* = 6.5 Hz, 3H). ^{13}C NMR (400 MHz, $CDCl_3$) δ 150.09, 134.24, 127.21, 123.75, 118.67, 109.28, 58.34, 39.43, 16.28, 13.60. HPLC (Daicel Chiralpak OD-H, hexanes/i-PrOH = 97/3, Flow rate = 0.8 ml/min, UV = 254 nm): t_1 = 31.1 min, t_2 = 36.0 min.

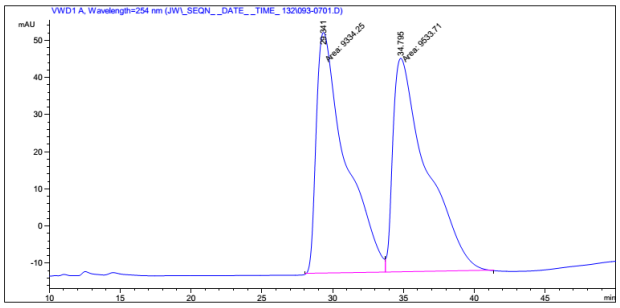

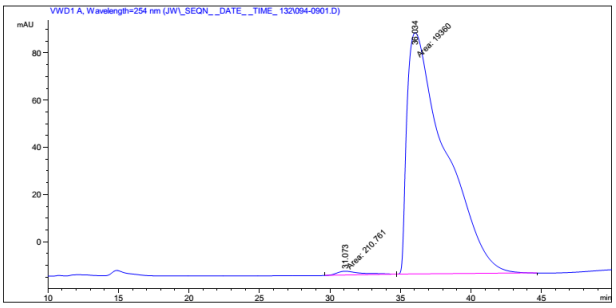

Peak #	RetTime [min]	Type	Width [min]	Area mAU *s	Height [mAU]	Area %
1	31.073	MM	1.4677	210.76115	1.69098	1.0769
2	36.034	MM	3.1541	1.93600e4	102.29957	98.9231
Totals :				1.95708e4	103.99055	

(S,S)-3-benzyl-2-methylindoline (8m) [32]

Colorless oil. ^{1}H NMR (400 MHz, $CDCl_3$) δ 7.31 (t, J = 7.2 Hz, 2H), 7.27 – 7.22 (m, 1H), 7.20 (t, J = 6.8 Hz, 2H), 7.07 – 6.97 (m, 1H), 6.65 (d, J = 7.7 Hz, 1H), 6.59 (q, J = 7.5 Hz, 2H), 4.06 – 3.97 (m, 1H), 3.69 (br, 1H), 3.54 (dd, J = 15.9, 7.8 Hz, 1H), 2.93 (ddd, J = 22.8, 13.9, 8.1 Hz, 2H), 1.24 (d, J = 6.5 Hz, 3H).

^{13}C NMR (400 MHz, $CDCl_3$) δ 150.37, 140.32, 131.90, 129.13, 128.23, 127.42, 125.96, 124.82, 118.23, 109.36, 58.43, 45.94, 34.23, 16.46. HPLC (Daicel Chiralpak OD-H, hexanes/i-PrOH = 97/3, Flow rate = 0.8 ml/min, UV = 254 nm): t_1 = 14.6 min, t_2 = 21.3 min.

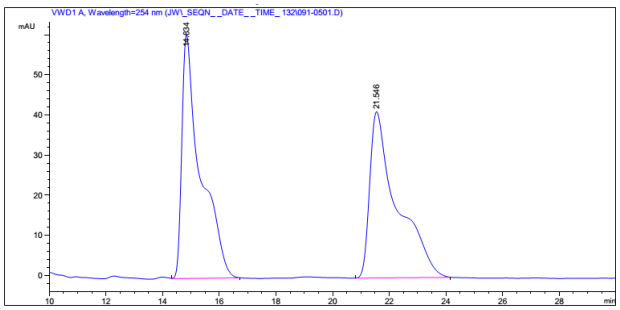

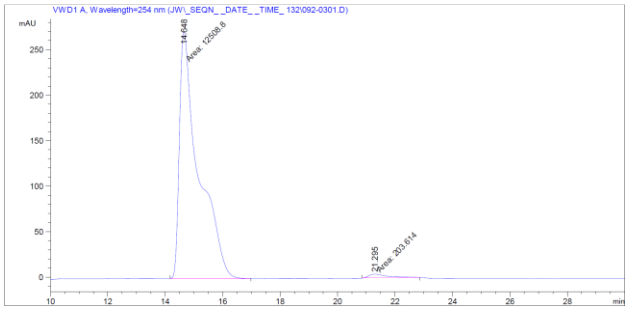

Peak #	RetTime [min]	Type	Width [min]	Area mAU *s	Height [mAU]	Area %
1	14.648	MM	0.7682	1.25088e4	271.38623	98.3983
2	21.295	MM	0.8002	203.61430	4.24083	1.6017
Totals :				1.27124e4	275.62706	

(S,S)-3-(cyclohexylmethyl)-2-methylindoline (8n) [32]

Colorless oil. ^{1}H NMR (400 MHz, $CDCl_3$) δ 7.09 – 6.95 (m, 2H), 6.72 (td, *J* = 7.4, 0.9 Hz, 1H), 6.62 (d, *J* = 7.7 Hz, 1H), 3.94 (dq, *J* = 13.1, 6.5 Hz, 1H), 3.59 (br, 1H), 3.26 (dd, *J* = 15.1, 7.5 Hz, 1H), 1.94 – 1.82 (m, 1H), 1.82 – 1.61 (m, 4H), 1.61 – 1.48 (m, 1H), 1.50 – 1.32 (m, 2H), 1.34 – 1.15 (m, 3H), 1.13 (dd, *J* = 13.7, 4.8 Hz, 3H), 0.96 (ddd, *J* = 19.8, 9.7, 3.6 Hz, 2H). ^{13}C NMR (400 MHz, $CDCl_3$) δ 150.40, 132.91, 127.12, 124.16, 118.43, 109.41, 58.57, 41.55, 35.28, 33.59, 26.71, 26.35, 16.27. HPLC (Daicel Chiralpak OD-H, hexanes/i-PrOH = 97/3, Flow rate = 0.8 ml/min, UV = 254 nm): t_1 = 8.4 min, t_2 = 9.6 min.

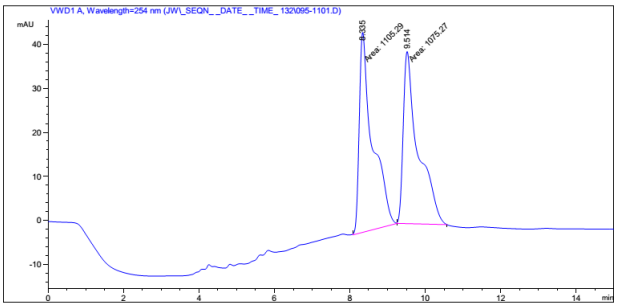

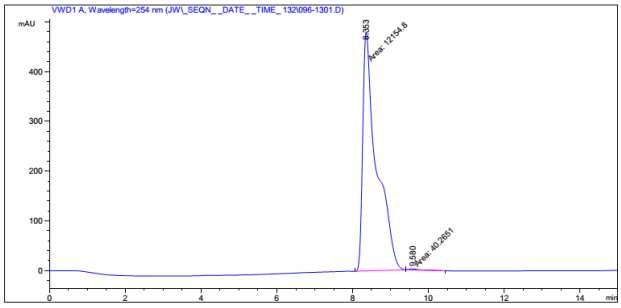

Peak #	RetTime [min]	Type	Width [min]	Area mAU *s	Height [mAU]	Area %
1	8.353	MM	0.4212	1.21548e4	480.94183	99.6698
2	9.580	MM	0.3124	40.26510	2.14804	0.3302
Totals :				1.21950e4	483.08987	

(S,S)-3-(furan-2-ylmethyl)-2-methylindoline (8o)

Colorless oil. ^{1}H NMR (400 MHz, $CDCl_3$) δ 7.38 – 7.36 (m, 1H), 7.03 (t, *J* = 7.6 Hz, 1H), 6.74 (d, *J* = 7.2 Hz, 1H), 6.69 – 6.61 (m, 2H), 6.32 (dd, *J* = 2.9, 2.0 Hz, 1H), 6.01 (d, *J* = 3.1 Hz, 1H), 4.10 – 3.99 (m, 1H), 3.68 (br, 1H), 3.60 (dd, *J* = 15.7, 7.8 Hz, 1H), 3.03 – 2.83 (m, 2H), 1.21 (d, *J* = 6.5 Hz, 3H). ^{13}C NMR (400 MHz, $CDCl_3$) δ 154.33, 150.27, 140.89, 131.49, 127.58, 124.48, 118.49, 110.22, 109.36, 106.32, 58.12, 43.55, 27.04, 16.30. HPLC (Daicel Chiralpak OD-H, hexanes/i-PrOH = 97/3, Flow rate = 0.8 ml/min, UV = 254 nm): t_1 = 17.1 min, t_2 = 21.8 min.

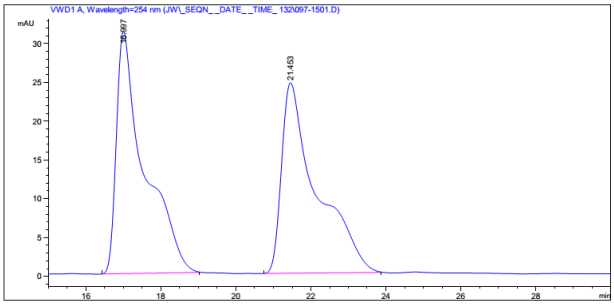

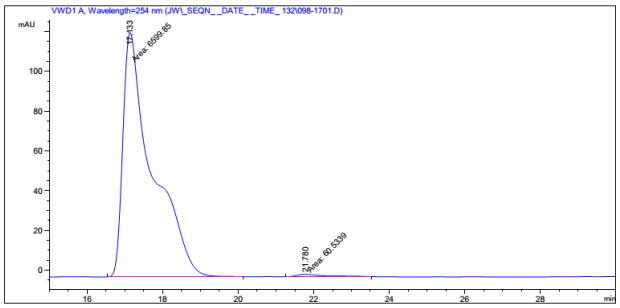

Peak #	RetTime [min]	Type	Width [min]	Area mAU *s	Height [mAU]	Area %
1	17.133	MM	0.8961	6599.84961	122.75162	99.0911
2	21.780	MM	0.8642	60.53390	1.16744	0.9089
Totals :				6660.38351	123.91906	

(S,S)-2,3,4,4a,9,9a-hexahydro-1H-carbazole (2p) [32]

White solid. ^{1}H NMR (400 MHz, $CDCl_3$) δ 7.09 (d, *J* = 7.2 Hz, 1H), 7.03 (t, *J* = 7.6 Hz, 1H), 6.75 (t, *J* = 7.4 Hz, 1H), 6.68 (d, *J* = 7.7 Hz, 1H), 3.74 (dd, *J* = 11.7, 6.6 Hz, 1H), 3.65 (br, 1H),

3.11 (q, J = 6.6 Hz, 1H), 1.78 (dd, J = 12.1, 6.2 Hz, 2H), 1.70 – 1.63 (m, 1H), 1.57 (tt, J = 6.7, 4.4 Hz, 2H), 1.48 – 1.29 (m, 3H). ^{13}C NMR (400 MHz, $CDCl_3$) δ 150.73, 133.50, 126.96, 123.11, 118.75, 110.12, 59.61, 40.91, 29.17, 26.95, 22.50, 21.65. Chiral GC (Supelco γ-Dex225, 140°C, Flow rate = 1.0 ml/min): t_1 = 37.7 min, t_2 = 38.9 min.

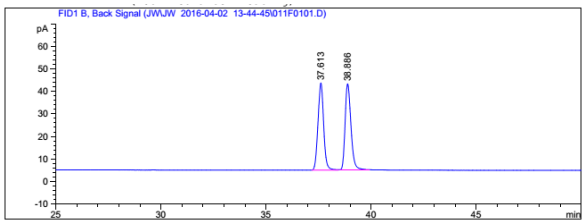

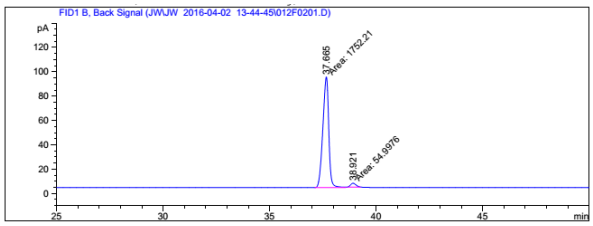

Peak #	RetTime [min]	Type	Width [min]	Area [pA*s]	Height [pA]	Area %
1	37.665	MM	0.3213	1752.20508	90.89358	96.95675
2	38.921	MM	0.2880	54.99761	3.18315	3.04325
Totals :				1807.20269	94.07672	

1. Akiyama, T., Stronger Brønsted Acids. *Chemical Reviews* **2007,** *107* (12), 5744-5758.

2. Akiyama, T.; Mori, K., Stronger Brønsted Acids: Recent Progress. *Chemical Reviews* **2015,** *115* (17), 9277-9306.

3. Parmar, D.; Sugiono, E.; Raja, S.; Rueping, M., Complete Field Guide to Asymmetric BINOL-Phosphate Derived Brønsted Acid and Metal Catalysis: History and Classification by Mode of Activation; Brønsted Acidity, Hydrogen Bonding, Ion Pairing, and Metal Phosphates. *Chemical Reviews* **2014,** *114* (18), 9047-9153.

4. Rueping, M.; Nachtsheim, B. J.; Ieawsuwan, W.; Atodiresei, I., Modulating the Acidity: Highly Acidic Brønsted Acids in Asymmetric Catalysis. *Angewandte Chemie International Edition* **2011,** *50* (30), 6706-6720.

5. James, T.; van Gemmeren, M.; List, B., Development and Applications of Disulfonimides in Enantioselective Organocatalysis. *Chemical Reviews* **2015,** *115* (17), 9388-9409.

6. Pihko, P. M., *Hydrogen Bonding in Organic Synthesis*. Wiley: 2009.

7. Pihko, P. M., Activation of Carbonyl Compounds by Double Hydrogen Bonding: An Emerging Tool in Asymmetric Catalysis. *Angewandte Chemie International Edition* **2004,** *43* (16), 2062-2064.

8. Taylor, M. S.; Jacobsen, E. N., Asymmetric Catalysis by Chiral Hydrogen-Bond Donors. *Angewandte Chemie International Edition* **2006,** *45* (10), 1520-1543.

9. Doyle, A. G.; Jacobsen, E. N., Small-Molecule H-Bond Donors in Asymmetric Catalysis. *Chemical Reviews* **2007,** *107* (12), 5713-5743.

10. Phipps, R. J.; Hamilton, G. L.; Toste, F. D., The progression of chiral anions from concepts to applications in asymmetric catalysis. *Nat Chem* **2012,** *4* (8), 603-614.

11. Mahlau, M.; List, B., Asymmetric Counteranion-Directed Catalysis: Concept, Definition, and Applications. *Angewandte Chemie International Edition* **2013,** *52* (2), 518-533.

12. Rueping, M.; Koenigs, R. M.; Atodiresei, I., Unifying Metal and Brønsted Acid Catalysis—Concepts, Mechanisms, and Classifications. *Chemistry – A European Journal* **2010,** *16* (31), 9350-9365.

13. Allen, A. E.; MacMillan, D. W. C., Synergistic catalysis: A powerful synthetic strategy for new reaction development. *Chemical Science* **2012,** *3* (3), 633-658.

14. Meeuwissen, J.; Reek, J. N. H., Supramolecular catalysis beyond enzyme mimics. *Nat Chem* **2010,** *2* (8), 615-621.

15. Du, Z.; Shao, Z., Combining transition metal catalysis and organocatalysis - an update. *Chemical Society Reviews* **2013,** *42* (3), 1337-1378.

16. Shao, Z.; Zhang, H., Combining transition metal catalysis and organocatalysis: a broad new concept for catalysis. *Chemical Society Reviews* **2009,** *38* (9), 2745-2755.

17. Xu, H.; Zuend, S. J.; Woll, M. G.; Tao, Y.; Jacobsen, E. N., Asymmetric Cooperative Catalysis of Strong Brønsted Acid–Promoted Reactions Using Chiral Ureas. *Science* **2010,** *327* (5968), 986-990.

18. Wieland, J.; Breit, B., A combinatorial approach to the identification of self-assembled ligands for rhodium-catalysed asymmetric hydrogenation. *Nat Chem* **2010,** *2* (10), 832-837.

19. Breit, B.; Seiche, W., Hydrogen Bonding as a Construction Element for Bidentate Donor Ligands in Homogeneous Catalysis: Regioselective Hydroformylation of Terminal Alkenes. *Journal of the American Chemical Society* **2003,** *125* (22), 6608-6609.

20. Diab, L.; Šmejkal, T.; Geier, J.; Breit, B., Supramolecular Catalyst for Aldehyde Hydrogenation and Tandem Hydroformylation–Hydrogenation. *Angewandte Chemie International Edition* **2009,** *48* (43), 8022-8026.

21. Šmejkal, T.; Breit, B., A Supramolecular Catalyst for Regioselective Hydroformylation of

Unsaturated Carboxylic Acids. *Angewandte Chemie International Edition* **2008,** *47* (2), 311-315.

22. Gatzenmeier, T.; van Gemmeren, M.; Xie, Y.; Höfler, D.; Leutzsch, M.; List, B., Asymmetric Lewis acid organocatalysis of the Diels–Alder reaction by a silylated C–H acid. *Science* **2016,** *351* (6276), 949-952.

23. Zhang, Z.; Schreiner, P. R., (Thio)urea organocatalysis-What can be learnt from anion recognition? *Chemical Society Reviews* **2009,** *38* (4), 1187-1198.

24. Takemoto, Y., Development of Chiral Thiourea Catalysts and Its Application to Asymmetric Catalytic Reactions. *Chemical and Pharmaceutical Bulletin* **2010,** *58* (5), 593-601.

25. Brak, K.; Jacobsen, E. N., Asymmetric Ion-Pairing Catalysis. *Angewandte Chemie International Edition* **2013,** *52* (2), 534-561.

26. Fattorusso, E.; Taglialatela-Scafati, O., *Modern Alkaloids: Structure, Isolation, Synthesis, and Biology*. Wiley: 2008.

27. Kochanowska-Karamyan, A. J.; Hamann, M. T., Marine Indole Alkaloids: Potential New Drug Leads for the Control of Depression and Anxiety. *Chemical Reviews* **2010,** *110* (8), 4489-4497.

28. Ishikura, M.; Abe, T.; Choshi, T.; Hibino, S., Simple indole alkaloids and those with a non-rearranged monoterpenoid unit. *Natural Product Reports* **2013,** *30* (5), 694-752.

29. Wang, D.-S.; Chen, Q.-A.; Lu, S.-M.; Zhou, Y.-G., Asymmetric Hydrogenation of Heteroarenes and Arenes. *Chemical Reviews* **2012,** *112* (4), 2557-2590.

30. Zhou, Y.-G., Asymmetric Hydrogenation of Heteroaromatic Compounds. *Accounts of Chemical Research* **2007,** *40* (12), 1357-1366.

31. Wang, D.-S.; Chen, Q.-A.; Li, W.; Yu, C.-B.; Zhou, Y.-G.; Zhang, X., Pd-Catalyzed Asymmetric Hydrogenation of Unprotected Indoles Activated by Brønsted Acids. *Journal of the American Chemical Society* **2010,** *132* (26), 8909-8911.

32. Duan, Y.; Li, L.; Chen, M.-W.; Yu, C.-B.; Fan, H.-J.; Zhou, Y.-G., Homogenous Pd-Catalyzed Asymmetric Hydrogenation of Unprotected Indoles: Scope and Mechanistic Studies. *Journal of the American Chemical Society* **2014,** *136* (21), 7688-7700.

33. Zhao, Q.; Li, S.; Huang, K.; Wang, R.; Zhang, X., A Novel Chiral Bisphosphine-Thiourea Ligand for Asymmetric Hydrogenation of β,β-Disubstituted Nitroalkenes. *Organic Letters* **2013,** *15* (15), 4014-4017.

34. Zhao, Q.; Wen, J.; Tan, R.; Huang, K.; Metola, P.; Wang, R.; Anslyn, E. V.; Zhang, X., Rhodium-Catalyzed Asymmetric Hydrogenation of Unprotected NH Imines Assisted by a Thiourea. *Angewandte Chemie International Edition* **2014,** *53* (32), 8467-8470.

35. Kelly, T. R.; Kim, M. H., Relative Binding Affinity of Carboxylate and Its Isosteres: Nitro, Phosphate, Phosphonate, Sulfonate, and .delta.-Lactone. *Journal of the American Chemical Society* **1994,** *116* (16), 7072-7080.

36. All pka's are data measured in water, for qualitative analysis.

37. 31P NMR study of ligand shows a significant change in chemical shift (from -25.1 and -17.9 ppm to +1.9 and +7.6 ppm). This change suggests protonation on phosphorus.

38. 1.0 eq. of HCl gives 95% conversion and 5.0 eq. HCl give 98% conversion, 97% ee was observed for both cases.

39. Wen, J.; Tan, R.; Liu, S.; Zhao, Q.; Zhang, X., Strong Bronsted acid promoted asymmetric hydrogenation of isoquinolines and quinolines catalyzed by a Rh-thiourea chiral phosphine complex via anion binding. *Chemical Science* **2016**.

40. Guillaneux, D.; Zhao, S.-H.; Samuel, O.; Rainford, D.; Kagan, H. B., Nonlinear Effects in

Asymmetric Catalysis. *Journal of the American Chemical Society* **1994,** *116* (21), 9430-9439.

41. Kina, A.; Iwamura, H.; Hayashi, T., A Kinetic Study on Rh/Binap-Catalyzed 1,4-Addition of Phenylboronic Acid to Enones: Negative Nonlinear Effect Caused by Predominant Homochiral Dimer Contribution. *Journal of the American Chemical Society* **2006,** *128* (12), 3904-3905.

42. Olsen, H. B.; Kaarsholm, N. C.; Madsen, P.; Balschmidt, P., Phamaceutical preparations comprising insulin. Google Patents: 2006.

43. Jiao, L.; Bach, T., Palladium-Catalyzed Direct 2-Alkylation of Indoles by Norbornene-Mediated Regioselective Cascade C–H Activation. *Journal of the American Chemical Society* **2011,** *133* (33), 12990-12993.

44. Li, C.; Chen, J.; Fu, G.; Liu, D.; Liu, Y.; Zhang, W., Highly enantioselective hydrogenation of N-unprotected indoles using (S)-C10–BridgePHOS as the chiral ligand. *Tetrahedron* **2013,** *69* (33), 6839-6844.

45. Arp, F. O.; Fu, G. C., Kinetic Resolutions of Indolines by a Nonenzymatic Acylation Catalyst. *Journal of the American Chemical Society* **2006,** *128* (44), 14264-14265.

46. Talwar, D.; Li, H. Y.; Durham, E.; Xiao, J., A Simple Iridicycle Catalyst for Efficient Transfer Hydrogenation of N-Heterocycles in Water. *Chemistry – A European Journal* **2015,** *21* (14), 5370-5379.

Chapter Five

Rhodium catalyzed asymmetric hydrogenation of α, β-unsaturated carbonyl compounds via a thiourea hydrogen bonding

5.1 Introduction

As an important non-covalent interaction, hydrogen bonding plays a crucial role in bio-system and enzyme catalysis[1]. From the inspiration of enzyme catalysis to the prosperity of small-molecule catalysis, many studies have been elaborated in the past two decades. This strategy of hydrogen bonding has been successfully applied in numerous cases of organocatalysis, which provide the synthetic community with many solutions for enantioselective synthesis[2-3]. As a double hydrogen donor, thiourea could activate carbonyl compounds by lowering their LUMO energy[4-7]. Effective bonding with neutral functional groups, potent binding affinity and high tunability make thiourea catalysts versatile for many kinds of organic reactions[8-11]. Originated in serine protease (Figure 1) catalyzed hydrolysis of amides[1], the interaction of a double hydrogen donor with an amide substrate became as an important paradigm for carbonyl activation in small molecule catalysis. The hydrogen bonding of (thio)urea with ketones, aldehydes and carboxylic acid derivatives enables enantioselective chemical transformations, and

therefore emerged as an effective strategy in asymmetric catalysis.

Figure 5.1. Double H-bonding with carbonyl.

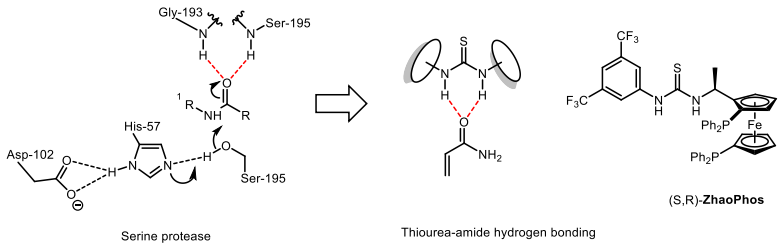

Asymmetric hydrogenation of unsaturated carboxylic acids and esters has been developed with several systems[12]: Crabtree's catalyst (iridium/P-N ligand) and Wilkinson-Osborn system (rhodium/bisphosphine ligand) are successful representatives. To our best knowledge, hydrogenation of unsaturated carboxamides, however, is still a less explored field yet. Successful cases of asymmetric reduction of α,β-unsaturated amides mainly engaged with transition metal catalyzed conjugate addition of hydrides[13-14] and iridium-catalyzed direct hydrogenation by Ding[15]. We were seeking for an efficient catalytic system to synthesize different types of chiral carboxylic acid derivatives with high enantioselectivity.

Figure 5.2 Hydrogen bonding between ZhaoPhos and amide

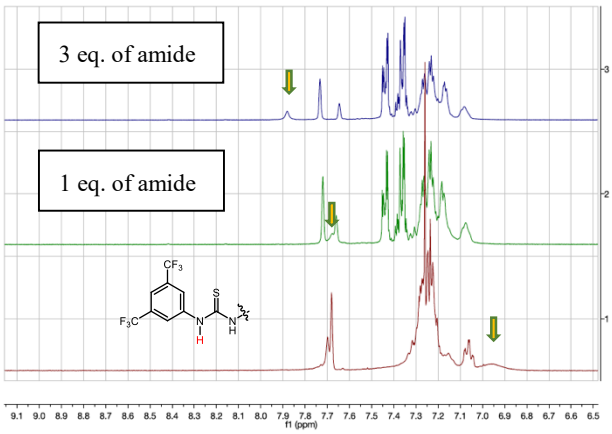

The binding affinity of (thio)urea with carboxylic acid derivatives is in a similar range to that with nitro groups or sulfonates[16], which inspires us to explore the application of ZhaoPhos in homogeneous hydrogenation of unsaturated carbonyl compounds. ^{1}H NMR study suggests hydrogen bonding between thiourea of ZhaoPhos and an unsaturated amide (Figure 2, one of the thiourea protons is marked with arrow). We envision that the secondary interaction of hydrogen bonding between thiourea and carbonyl substrates could play a dual role: (1) H-bond activates the substrate by decreasing the LOMO; (2) the binding between the ligand and substrate enhances the enantiomeric control. We report herein a successful example of rhodium/ZhaoPhos catalyzed asymmetric hydrogenation of α, β-unsaturated carbonyl compounds.

5.2 Method development

Table 5.1 Condition optimization[a]

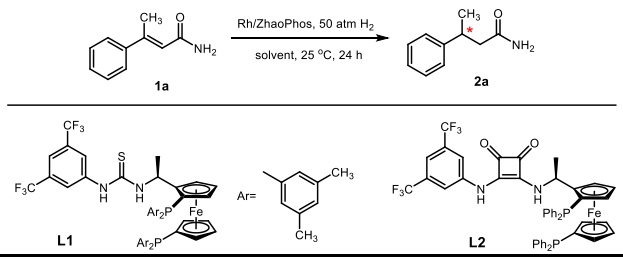

entry	solvent	ligand	conversion[b]	ee[c]
1	MeOH	**ZhaoPhos**	24%	65%
2	i-PrOH	**ZhaoPhos**	50%	86%
3	DCM	**ZhaoPhos**	42%	94%
4	DCE	**ZhaoPhos**	18%	90%
5	dioxane	**ZhaoPhos**	<5%	74%
6	acetone	**ZhaoPhos**	trace	-
7	ethyl acetate	**ZhaoPhos**	36%	91%

8	DCM/Tol=3:1	**ZhaoPhos**	69%	91%
9	DCM/i-PrOH=3:1	**ZhaoPhos**	58%	95%
10[d]	DCM/i-PrOH=3:1	**ZhaoPhos**	99%	95%
11[d]	DCM/i-PrOH=3:1	**L1**	63%	90%
12[d]	DCM/i-PrOH=3:1	**L2**	38%	36%

[a] Reaction condition: **1a** (0.1 mmol) in 1.0 ml solvent, **1**/[Rh(COD)Cl]$_2$/**L** =100/0.50/1.0. [b] Conversion was determined by ^{1}H NMR analysis, no side product was observed; [c] Enantiomeric excess was determined by HPLC with a chiral stationary phase. [d] Conducted at 35 ^{o}C for 48 h

Initially we chose *trans*-β-methylcinnamide as the target and [Rh(COD)Cl]$_2$ as the metal precursor, since this rhodium (I) dimer showed excellent performance in hydrogenation of nitroolefins and (iso)quinolines with ZhaoPhos in our previous studies. After screening of various types of solvent, we found that dichloromethane gave the best enantioselectivity. Solvent pairs were also tested. Solvent pairs were also tested, and we finally selected a mixture of dichloromethane and isopropanol with a volume ratio 3:1 as the solvent (Table 1, entry9). When we increased the temperature and elongated the reaction time, desired conversion (99%) and high enantioselectivity (95%) were obtained under 50 atm hydrogen gas pressure (entry 10). Similar to the previous hydrogenation cases with Rh/ZhaoPhos system[17-20], this reaction is solvent-dependent. More bulky substituents on phosphine dose not bring higher enantioselectivity, but lowers conversion (entry 11). Squaramide, which usually plays a role of an alternative for (thio)urea in hydrogen bonding catalysis, fails to show any advantages over thiourea (entry 12).

5.3 Substrate scope

The substrate scope of Rh/ZhaoPhos catalyzed hydrogenation of α,β-unsaturated amides was shown in Table 2. β,β-Disubstituted acrylamides were reduced with high enantioselectivities. Various substituents with different electronic effects do not bring significant changes in enantioselectivities. Steric effects, however, shows influence on the reactivity of this chemical transformation: compared to *meta*- or *para*- position, methyl group at *ortho*- position on the phenyl slows down the reaction rate significantly. Thienyl group, a representative of heteroaryl, also works smoothly in this homogeneous hydrogenation reaction.

Table 5.2 Substrate scope of rhodium catalyzed asymmetric hydrogenation of α,β-unsaturated amides[a]

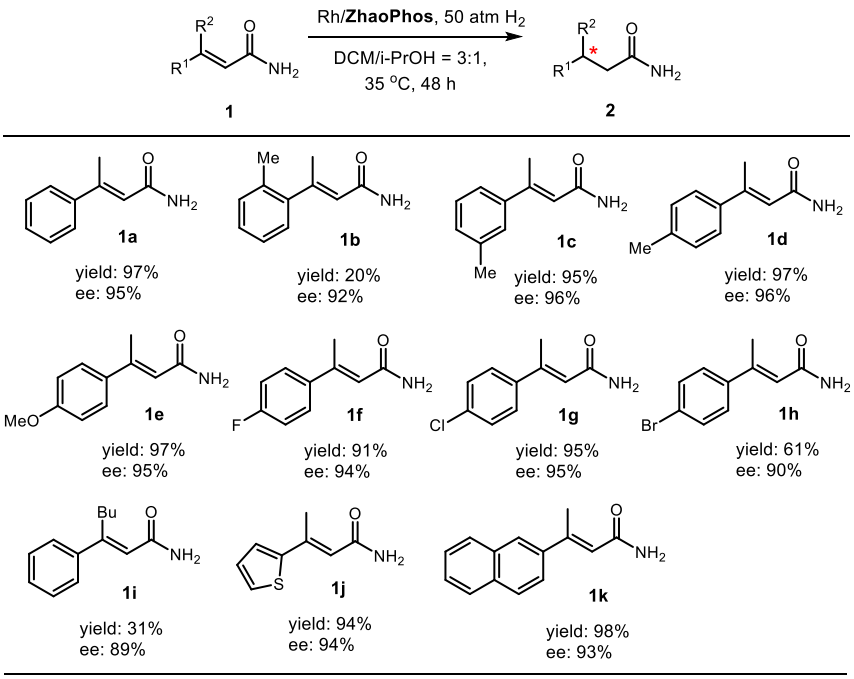

[a] Reaction condition: **1** (0.2 mmol) in 1.0 ml solvent, **1**/[Rh(COD)Cl]$_2$/**L** =100/0.50/1.0; yields were obtained after isolation; ee's were determined by HPLC with a chiral stationary phase.

With the success of hydrogenation of unsaturated amides in hand, we were seeking an expansion of substrate scope into other unsaturated carbonyl compounds. When applying the optimized condition in the reaction of esters, high conversions with high enatioselectivities were obtained. Scope of β,β-disubstituted ester substrates include various substituents on the β-phenyl ring with different electronic and steric effects, which is in accordance with hydrogenation of unsaturated amides. A broad substrate scope of this Rh/ZhaoPhos catalytic system suggests its potential application in synthetic chemistry.

Table 5.3 Substrate scope of rhodium catalyzed asymmetric hydrogenation of α,β-unsaturated esters and ketone[a]

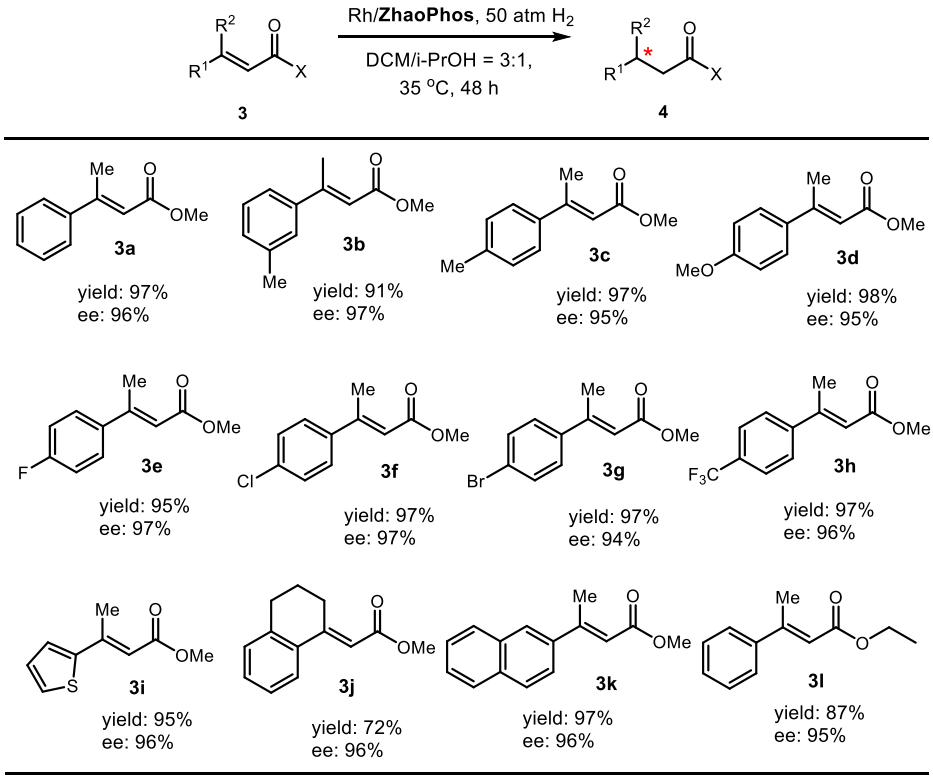

[a] Reaction condition: **3** (0.2 mmol) in 1.0 ml solvent, **3**/[Rh(COD)Cl]$_2$/**L** =100/0.50/1.0; yields were obtained after isolation; ee's were determined by HPLC with a chiral stationary phase.

5.3 Mechanistic sduties

Table 5.4 Ligand evaluation and control experiment.

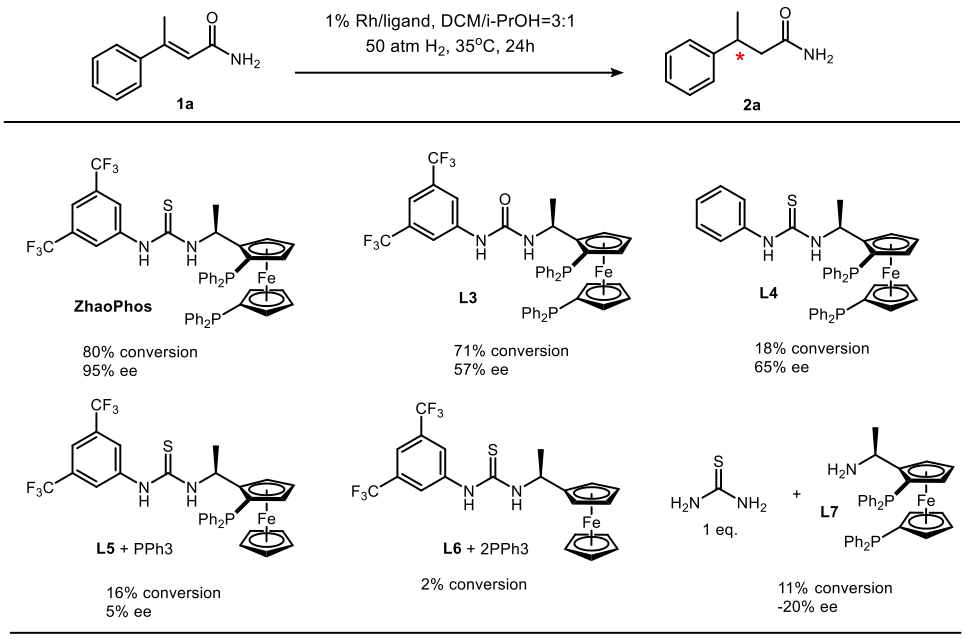

To investigate the cooperation of thiourea moiety and ferrocene-based bisphosphine skeleton, we synthesized a series of analogues of **ZhaoPhos** and conducted control experiments to evaluate the collaboration manner of each unit of **ZhaoPhos**. Urea bisphosphine ligand **L3** only gives both lower conversion and ee. Compared to H (**L6**), more electron-withdrawing trifluoromethyl group at 3- and 5- position on the phenyl ring increases the enantioselectivity, which is probably due to the stronger acidity of N-H proton on the thiourea. Furthermore, monophosphine ligand **L5** and the mixture of ferrocene-thiourea compound **L6** with triphenylphosphine can hardly catalyzed the hydrogenation reaction. On the other hand, the mixture of thiourea molecule and bisphosphine-Ugi's amine **L7** failed to show catalytic activity. These results (**ZhaoPhos** vs **L5 or L6** with PPh_3 and **L7**/thiourea) demonstrate the importance of a covalent incorporation of bisphosphine moiety and thiourea. The stragety of secondary offers an

alternative strategy for asymmetric hydrogenation.In accordance with previous studies on hydrogenation of nitroolefins[19], unprotected inmines[20] and (iso)quinolines[18], control experiments revealed that (1) each unit within ZhaoPhos is irreplaceable for high conversion and high enantioselectivity in catalytic chemical transformation; (2) a covalent linker enables the incorporation.

Scheme 5.2 Deuterium labeling experiment

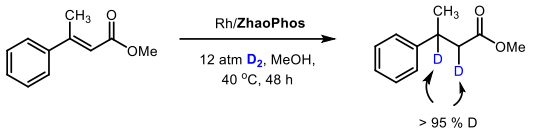

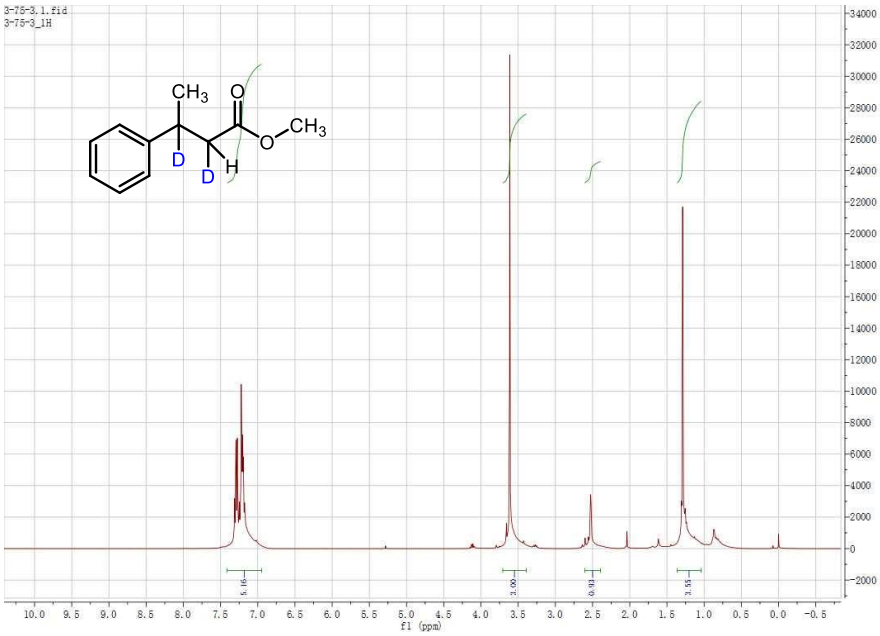

We previously proposed a hydride transfer mechanism for asymmetric hydrogenation of (iso)quinolines with rodium/ ZhaoPhos complex[18], which involving an outer-sphere model[21-22] rather than the traditional inner-sphere mechanism[23]. In order to gain insight of hydrogenation of α,β-unsaturated carbonyl compounds, isotope labeling experiment was conducted. When applying deuterium gas to conduct this hydrogenation, D atoms

are added at α- and β- position. No obvious H atoms are observed to be added to the C=C bond. This result supports a traditional inner-sphere mechanism, which was well studies and widely accepted in rhodium-catalyzed hydrogenation. Based on these results, we proposed a ligand-substrate coordinating complex involving a secondary interaction between the thiourea and the carbonyl substrate (Figure 3).

Figure 5.3 Nonlinear effect and proposed transition state

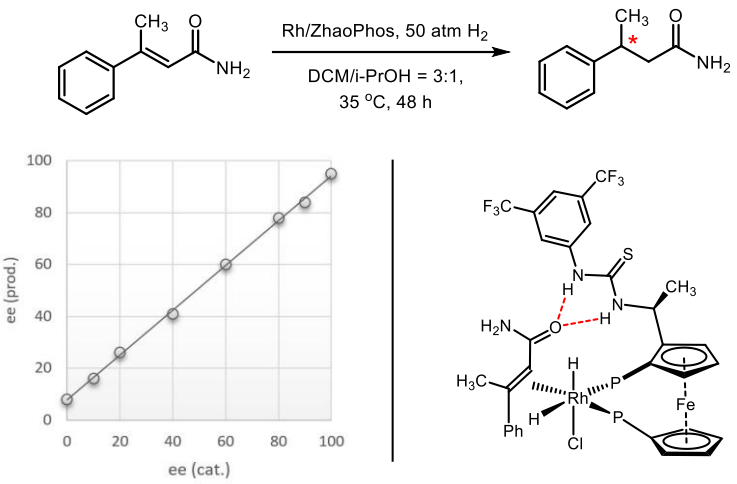

Entry	ee of ZhaoPhos	conversion	ee
1	0		8%
2	10%		16%
3	20%		26%
4	40%	> 95 %	41%
5	60%		60%
6	80%		78%
7	90%		84%
8	100%		95%

Nonlinear effect, which is could be observed in catalytic asymmetric reactions, suggests potential dimerization or high-order aggregation of catalysts[24]. In order to gain insight into this Rh/ZhaoPhos catalyzed hydrogenation of unsaturated carbonyl

compounds, we prepared a series of chiral ligands with different enantiomeric excess and applied them into hydrogenation of *trans*-β-methylcinnamide. However, no non-linear effect was observed (Figure 3). It supports an assumption that no catalyst self-aggregation or ligand-substrate agglomeration occur prior to the catalytic cycle.

5.4 Conclusion

In summary, we developed a synthetic method to approach β-chiral carbonyl compounds. Catalyzed by a Rh/ZhaoPhos complex, α,β-unsaturated carbonyl substrates were hydrogenated with high enantioselectivities. A secondary interaction between thiourea ligand and carbonyl of the substrates is believed to be crucial for the success. In addition, we did not observe nonlinear effect in this catalytic chemical transformation.

5.5 Experimental section

5.5.1 Typical procedure for the synthesis of α,β-unsaturated esters[25] and amides.

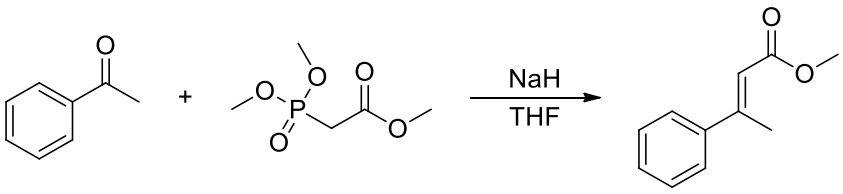

3

To a suspension of sodium hydride (60% dispersion in mineral oil, 10 mmol) in dry THF (20 mL) trimethyl phosphonoacetate (10 mmol) was added dropwise at 0 ºC under argon atmosphere. After 30 min, the appropriate ketones (8 mmol) was added dropwise at the same temperature. The reaction mixture was then allowed to warm to room temperature and stirred under reflux for 24 h. After the mixture cooling in an ice bath, saturated aqueous ammonium chloride solution (20 mL) was then added dropwise. The aqueous phase was extracted with diethyl ether (2 x 50mL) and the combined organic

phase was washed with brine (50mL), dried over sodium sulfate, and concentrated *in vacuo*. Flash chromatography (hexanes/ethyl acetate, 95:5) yielded ester as a clear oil with 60-80% yields.

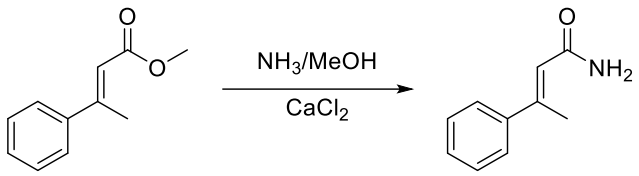

3a **1a**

A schlenk tube was charged with α,β-unsaturated ester (10 mmol), anhydrous calcium chloride (2 eq.). The tube was protected under nitrogen and ammonia in methanol solution (7N, 10 eq.) was added. The tube was sealed and heated at 100 ºC. After stirring for 24h, the mixture was cooled to room temperature. Solvent was evaporated *in vacuo*. The residue was dissolved in 30ml water and extracted with dichloromethane (50ml×2). The combined organic layer was dried over sodium sulfate and concentrated. After purification by flash chromatography, α,β-unsaturated amide was obtain.

(*E*)-3-phenylbut-2-enamide **1a**

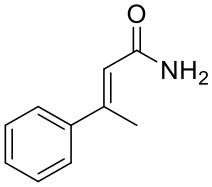

White soild; 66 % yield; m.p. = 116-117 ºC; ^{1}H NMR (400 MHz, $CDCl_3$) δ 7.49 – 7.41 (m, 2H), 7.37-7.35 (m, 3H), 6.08 (d, *J* = 1.1 Hz, 1H), 5.81 (br, 1H), 5.62 (br, 1H), 2.56 (d, *J* = 1.2 Hz, 3H); ^{13}C NMR (101 MHz, $CDCl_3$) δ 168.92, 152.52, 142.52, 128.70, 128.50, 126.20, 118.74, 17.74; *m*/*z* (ESI–MS) 163.21 $[M + H]^+$.

(E)-3-(o-tolyl)but-2-enamide **1b**

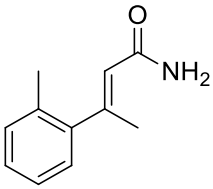

White soild; 42 % yield; m.p. = 92-94 ºC; ^{1}H NMR (400 MHz, $CDCl_3$) δ 7.25 – 7.12 (m, 3H), 7.07-7.06 (m, 1H), 5.70 (d, *J* = 1.3 Hz, 1H), 5.63 (br, 1H), 5.46 (br, 1H), 2.44 (d, *J* = 1.3 Hz, 3H), 2.29 (s, 3H); ^{13}C NMR (101 MHz, $CDCl_3$) δ 168.47, 155.46, 144.08, 133.95, 130.38, 127.57, 127.14, 125.74, 120.50, 20.38, 19.65; *m*/*z* (ESI–MS) 176.72 $[M + H]^+$.

(*E*)-3-(m-tolyl)but-2-enamide **1c**

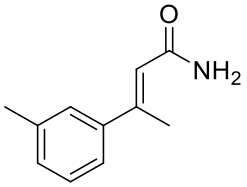

White solid; 63 % yield; m.p. = 79-83 ºC; ^{1}H NMR (400 MHz, $CDCl_3$) δ 7.49 – 6.97 (m, 4H), 6.06 (s, 1H), 5.85 (br, 1H), 5.62 (br, 1H), 2.54 (s, 3H), 2.37 (s, 3H); ^{13}C NMR (101 MHz, $CDCl_3$) δ 169.03, 152.64, 142.57, 138.09, 129.43, 128.38, 126.92, 123.33, 118.59, 21.45, 17.76; *m*/*z* (ESI–MS) 176.73 $[M + H]^+$.

(*E*)-3-(p-tolyl)but-2-enamide **1d**

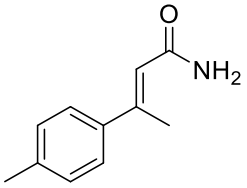

White solid; 70 % yield; m.p. = 123-126 ºC; ^{1}H NMR (400 MHz, $CDCl_3$) δ 7.35 (d, J = 8.1 Hz, 2H), 7.17 (d, J = 7.9 Hz, 2H), 6.06 (d, J = 1.2 Hz, 1H), 5.61 (br, 2H), 2.55 (s, 3H), 2.36 (s, 3H); ^{13}C NMR (101 MHz, $CDCl_3$) δ 168.87, 152.51, 139.56, 138.80, 129.19, 126.10, 117.81, 21.16, 17.63; (ESI–MS) 176.83 $[M + H]^+$.

(*E*)-3-(4-methoxyphenyl)but-2-enamide **1e**

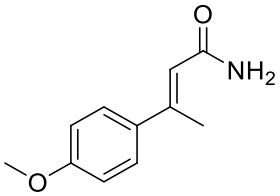

White soild; 64 % yield; m.p. = 134-136 ºC; ^{1}H NMR (400 MHz, $CDCl_3$) δ 7.41 (t, *J* = 5.7 Hz, 2H), 6.89 (d, *J* = 8.6 Hz, 2H), 6.04 (d, *J* = 1.0 Hz, 1H), 5.48 (br, 2H), 3.83 (s, 3H), 2.55 (s, 3H); ^{13}C NMR (101 MHz, $CDCl_3$) δ 168.86, 160.20, 152.05, 134.68, 127.48, 116.89, 113.85, 55.34, 17.50; *m*/*z* (ESI–MS) 192.71 $[M + H]^+$.

(*E*)-3-(4-fluorophenyl)but-2-enamide **1f**

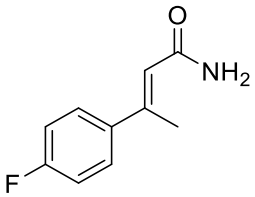

White soild; 51 % yield; m.p. = 145-155 ºC; ^{1}H NMR (400 MHz, $CDCl_3$) δ 7.42 (dd, *J* = 7.8, 5.6 Hz, 2H), 7.05 (t, *J* = 8.4 Hz, 2H), 6.03 (s, 1H), 5.56 (br, 2H), 2.54 (s, 3H); ^{13}C NMR (101 MHz, $CDCl_3$) δ 168.53, 164.28, 161.81, 151.41, 138.53, 127.95 (d, *J* = 8.2 Hz), 118.58, 115.41 (d, *J* = 21.5 Hz), 17.78; *m*/*z* (ESI–MS) 180.45 $[M + H]^+$.

(*E*)-3-(4-chlorophenyl)but-2-enamide **1g**

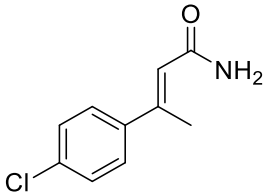

White soild; 61 % yield; m.p. = 146-156 ºC; ^{1}H NMR (400 MHz, $CDCl_3$) δ 7.57 – 7.29 (m, 4H), 6.05 (d, *J* = 1.2 Hz, 1H), 5.52 (br, 2H), 2.53 (s, 3H); ^{13}C NMR (101 MHz, $CDCl_3$) δ 168.31, 151.23, 140.88, 134.69, 128.68, 127.50, 118.95, 17.64; *m*/*z* (ESI–MS) 196.55, 198.30 $[M + H]^+$.

(*E*)-3-(4-bromophenyl)but-2-enamide **1h**

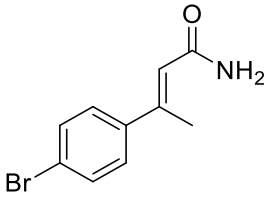

White soild; 65 % yield; m.p. = 151-159 ºC; ^{1}H NMR (400 MHz, $CDCl_3$) δ 7.58 – 7.44 (m, 2H), 7.38 – 7.27 (m, 2H), 6.06 (d, *J* = 1.2 Hz, 1H), 5.61 (br, 2H), 2.53 (d, *J* = 1.2 Hz, 3H); ^{13}C NMR (101 MHz, $CDCl_3$) δ 168.44, 151.25, 141.34, 131.65, 127.81, 122.88, 119.03, 17.59; *m*/*z* (ESI–MS) 240.92, 242.81 $[M + H]^+$.

(*E*)-3-phenylhept-2-enamide **1i**

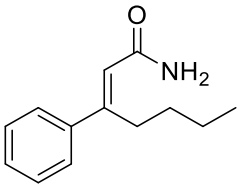

White soild; 33 % yield; m.p. = 56-58 ºC; ^{1}H NMR (400 MHz, $CDCl_3$) δ 7.45 – 7.16 (m, 5H), 5.87 (s, 1H), 5.44 (br, 1H), 4.92 (br, 1H), 2.41 (t, *J* = 6.6 Hz, 2H), 1.34 (m, 4H), 0.87 (t, *J* = 6.6 Hz, 3H); ^{13}C NMR (101 MHz, $CDCl_3$) δ 168.64, 153.45, 139.45, 128.85, 128.28, 127.37, 121.62, 40.02, 29.37, 22.16, 13.79; *m*/*z* (ESI–MS) 205.41 $[M + H]^+$.

(*E*)-3-(thiophen-2-yl)but-2-enamide **1j**

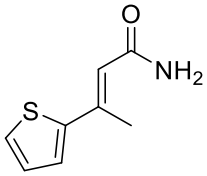

White soild; 47 % yield; m.p. = 125-126 ºC; ^{1}H NMR (400 MHz, $CDCl_3$) δ 7.28 (t, *J* = 4.0 Hz, 2H), 7.04 (dd, *J* = 5.0, 3.8 Hz, 1H), 6.20 (d, *J* = 1.2 Hz, 1H), 5.43 (br, 2H), 2.61 (d, *J* = 1.1 Hz, 3H); ^{13}C NMR (101 MHz, $CDCl_3$) δ 168.25, 145.79, 145.34, 127.90, 126.36 , 126.28, 115.67, 17.08; *m*/*z* (ESI–MS) 168.78 $[M + H]^+$.

(*E*)-3-(naphthalen-2-yl)but-2-enamide **1k**

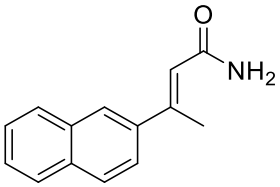

White soild; 55 % yield; m.p. = 147-156 ºC; ^{1}H NMR (400 MHz, $CDCl_3$) δ 7.91 (d, *J* = 1.4 Hz, 1H), 7.89 – 7.81 (m, 3H), 7.57 (dd, *J* = 8.6, 1.9 Hz, 1H), 7.55 – 7.46 (m, 2H), 6.22 (d, *J* = 1.3 Hz, 1H), 5.56 (br, 2H), 2.68 (d, *J* = 1.2 Hz, 3H); ^{13}C NMR (101 MHz, $CDCl_3$) δ 168.69, 152.40, 139.67, 133.37, 133.20, 128.41, 128.15, 127.60, 126.57, 126.51, 125.68, 123.96, 118.99, 17.75; *m*/*z* (ESI–MS) 213.26 $[M + H]^+$.

5.5.2 General procedure for asymmetric hydrogenation.

In the nitrogen-filled glovebox, solution of $[Rh(COD)Cl]_2$ (4.9 mg, 0.01 mmol) and ligand (2.1 eq.) in 5.0 ml anhydrous solvent was stirred at room temperature for 30 min. A specified volume of the resulting solution (0.5 ml, 1% Rh catalyst) was transferred by syringe to a Score-Break ampule charged with substrate solution (0.2 mmol in 0.5 ml). The ampule was placed into an autoclave, which was then charged with 50 atm H_2. The autoclave was stirred at desired temperature for the indicated period of time. After release of hydrogen gas, the resulting mixture was concentrated under vacuum. The residue passed through a silica plug to remove metal complex and then was concentrated under reduced pressure. The crude product was analysed by ^{1}H NMR to determine the conversion. The enantiomeric excess was determined by GC or HPLC analysis. Absolute configuration was assigned according to literatures[26-27].

5.5.3 Characterization data for chiral carbonyl compounds.

(*R*)-3-phenylbutanamide **2a**

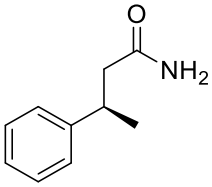

White solid; m.p. = 69-71 ºC; Yield: 97%, 95% ee; $[\alpha]_D^{22}$ = -29.0 (c = 0.2, $CHCl_3$); The enantiomeric excess was determined by HPLC on Chiralpak AD-H column, hexane: isopropanol = 95:5; flow rate = 1 mL/min; UV detection at 220 nm; t_R = 11.0 min (minor), 13.3 min (major); ^{1}H NMR (400 MHz, $CDCl_3$) δ 7.33-7.29 (m, 2H), 7.26 – 7.18 (m, 3H), 5.67 (br, 1H), 5.39 (br, 1H), 3.27 (dd, *J* = 14.4, 7.2 Hz, 1H), 2.47 (m, 2H), 1.32 (d, *J* = 7.0 Hz, 3H); ^{13}C NMR (101 MHz, $CDCl_3$) δ 174.31, 145.77, 128.65, 126.76, 126.51, 44.80, 36.78, 21.77; *m*/*z* (ESI–MS) 164.0 [M + H]+.

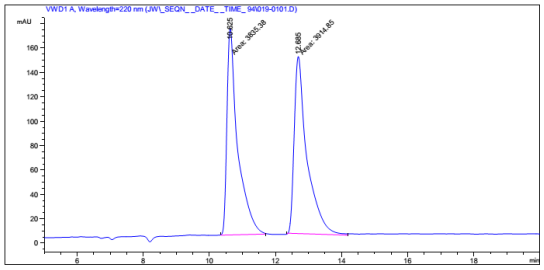

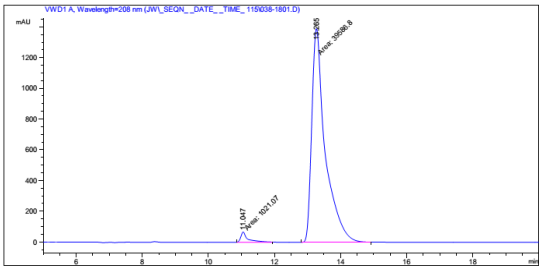

Signal 1: VWD1 A, Wavelength=208 nm

Peak #	RetTime [min]	Type	Width [min]	Area mAU *s	Height [mAU]	Area %
1	11.047	MM	0.2554	1021.06512	66.63529	2.5145
2	13.265	MM	0.4733	3.95868e4	1394.06787	97.4855

Totals : 4.06078e4 1460.70316

(*R*)-3-(o-tolyl)butanamide **2b**

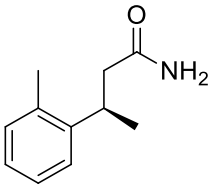

White solid; m.p. = 104-105 ºC; Yield: 20%, 92% ee; $[\alpha]_D^{22}$ = -29.5 (c = 0.2, $CHCl_3$); The enantiomeric excess was determined by HPLC on Chiralpak AD-H column, hexane: isopropanol = 95:5; flow rate = 1 mL/min; UV detection at 208 nm; t_R = 10.8 min (minor), 11.8 min (major); ^{1}H NMR (400 MHz, $CDCl_3$) δ 7.19-7.10 (m, 4H), 5.58 (br, 1H), 5.31 (br, 1H), 3.55 (d, *J* = 7.4 Hz, 1H), 2.52 (m, 1H), 2.48 – 2.30 (m, 4H), 1.28 (d, *J* = 6.9 Hz, 3H); ^{13}C NMR (101 MHz, $CDCl_3$) δ 174.29, 143.97, 135.54, 130.63, 126.36, 126.17, 124.95, 43.98, 31.72, 21.37, 19.51; *m*/*z* (ESI–MS) 179.27 $[M + H]^+$.

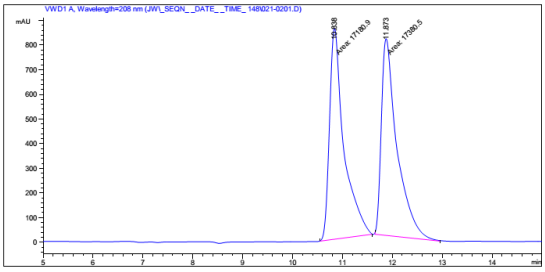

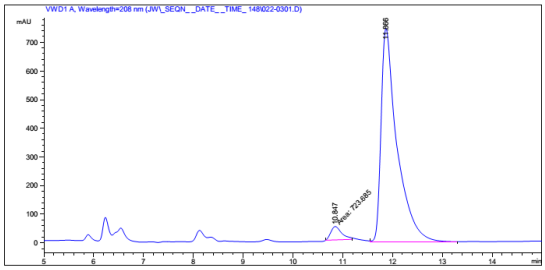

Signal 1: VWD1 A, Wavelength=208 nm

Peak #	RetTime [min]	Type	Width [min]	Area mAU *s	Height [mAU]	Area %
1	10.847	MM	0.2567	723.68524	46.98661	4.1734
2	11.866	VV	0.3183	1.66168e4	745.33368	95.8266

Totals : 1.73405e4 792.32029

(*R*)-3-(m-tolyl)butanamide **2c**

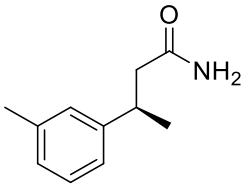

White solid; m.p. = 61-64 ºC; Yield: 95%, 96% ee; $[\alpha]_D^{22}$ = -30.0 (c = 0.2, $CHCl_3$); The enantiomeric excess was determined by HPLC on Chiralpak AD-H column, hexane: isopropanol = 95:5; flow rate = 1 mL/min; UV detection at 208 nm; t_R = 10.4 min (minor), 12.1 min (major); ^{1}H NMR (400 MHz, $CDCl_3$) δ 7.19 (m, 1H), 7.03 (m, 3H), 5.64 (br, 1H), 5.34 (br, 1H), 3.23 (d, *J* = 7.2 Hz, 1H), 2.45 (m, 2H), 2.33 (s, 3H), 1.31 (d, *J* = 7.0 Hz, 3H); ^{13}C NMR (101 MHz, $CDCl_3$) δ 174.23, 145.74, 138.23, 128.55, 127.61, 127.28, 123.68, 44.82, 36.75, 21.86, 21.48; *m/z* (ESI–MS) 179.27 $[M + H]^+$.

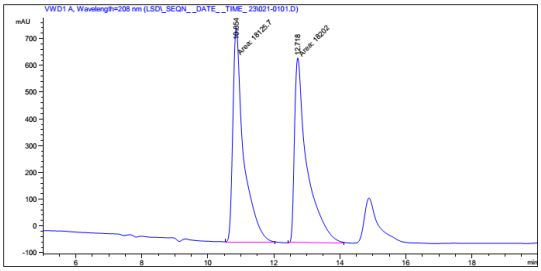

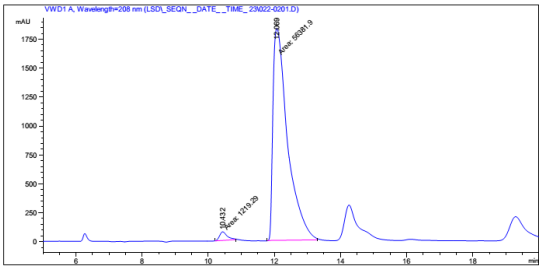

Signal 1: VWD1 A, Wavelength=208 nm

Peak #	RetTime [min]	Type	Width [min]	Area mAU *s	Height [mAU]	Area %
1	10.432	MM	0.2711	1219.29370	74.94867	2.1168
2	12.069	MM	0.5128	5.63819e4	1832.54810	97.8832
Totals :				5.76012e4	1907.49677	

(*R*)-3-(p-tolyl)butanamide **2d**

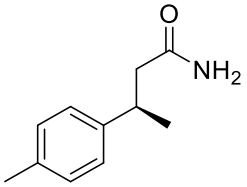

White solid; m.p. = 113-114 ºC; Yield: 97%, 96% ee; $[\alpha]_D^{22}$ = -30.7 (c = 0.2, $CHCl_3$); The enantiomeric excess was determined by HPLC on Chiralpak AD-H column, hexane: isopropanol = 97:3; flow rate = 1 mL/min; UV detection at 208 nm; t_R = 18.5 min (minor), 24.6 min (major); ^{1}H NMR (400 MHz, $CDCl_3$) δ 7.24 – 7.07 (m, 4H), 5.54 (br, 1H), 5.30 (br, 1H), 3.23 (dd, *J* = 14.3, 7.2 Hz, 1H), 2.57 – 2.37 (m, 2H), 2.32 (d, *J* = 6.8 Hz, 3H), 1.31 (d, *J* = 7.0 Hz, 3H); ^{13}C NMR (101 MHz, $CDCl_3$) δ 174.21, 142.72, 136.03, 129.33, 126.62, 44.91, 36.41, 21.92, 20.99; *m/z* (ESI–MS) 179.37 $[M + H]^+$.

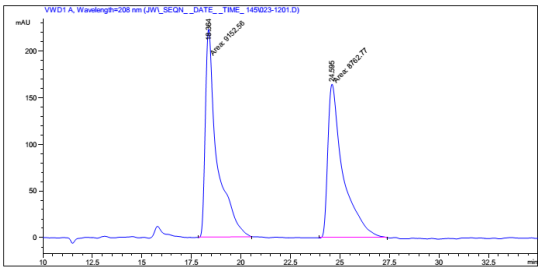

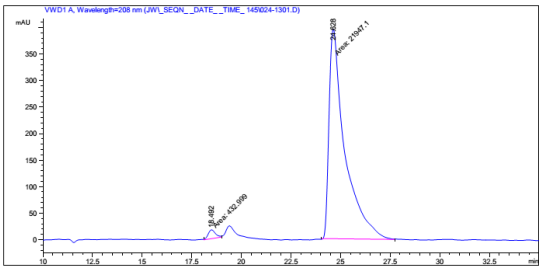

Signal 1: VWD1 A, Wavelength=208 nm

Peak #	RetTime [min]	Type	Width [min]	Area mAU *s	Height [mAU]	Area %
1	18.492	MM	0.4319	432.99863	16.70848	1.9347
2	24.628	MM	0.9252	2.19471e4	395.35178	98.0653

Totals : 2.23801e4 412.06025

(*R*)-3-(4-methoxyphenyl)butanamide **2e**

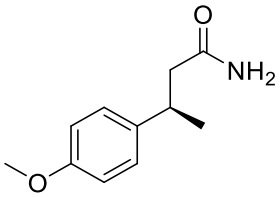

White solid; m.p. = 106-108 ºC; Yield: 96%, 96% ee; $[\alpha]_D^{22}$ = -26.1 (c = 0.2, $CHCl_3$); The enantiomeric excess was determined by HPLC on Chiralpak AD-H column, hexane: isopropanol = 95:5; flow rate = 1 mL/min; UV detection at 208 nm; t_R = 18.3 min (minor), 23.9 min (major); ^{1}H NMR (400 MHz, $CDCl_3$) δ 7.23 – 7.04 (m, 2H), 6.96 – 6.76 (m, 2H), 5.57 (br, 1H), 5.31 (br, 1H), 3.78 (s, 3H), 3.23 (dd, *J* = 14.3, 7.2 Hz, 1H), 2.44 (m, 2H), 1.30 (d, *J* = 7.0 Hz, 3H); ^{13}C NMR (101 MHz, $CDCl_3$) δ 174.24, 158.15, 137.81, 127.68, 114.01, 55.25, 45.09, 36.02, 21.99; *m*/*z* (ESI–MS) 194.77 $[M + H]^+$.

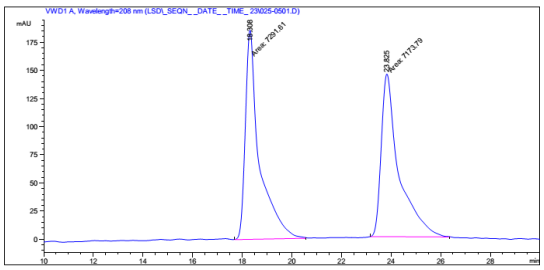

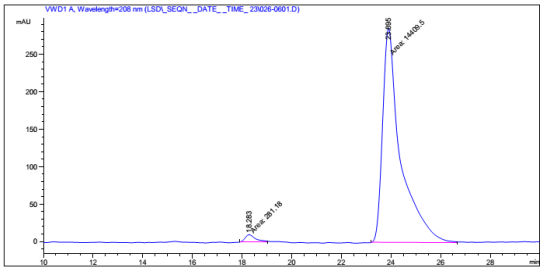

Signal 1: VWD1 A, Wavelength=208 nm

Peak #	RetTime [min]	Type	Width [min]	Area mAU *s	Height [mAU]	Area %
1	18.283	MM	0.4871	281.18048	9.61995	1.9140
2	23.895	MM	0.8411	1.44095e4	285.51715	98.0860

Totals : 1.46907e4 295.13710

(*R*)-3-(4-fluorophenyl)butanamide **2f**

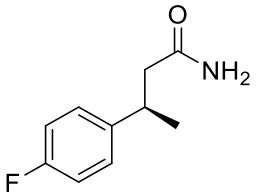

White solid; m.p. = 73-75 ºC; Yield: 91%, 94% ee; $[\alpha]_D^{22}$ = -30.5 (c = 0.2, $CHCl_3$); The enantiomeric excess was determined by HPLC on Chiralpak AD-H column, hexane: isopropanol = 95:5; flow rate = 1 mL/min; UV detection at 208 nm; t_R = 13.2 min (minor), 15.0 min (major); ^{1}H NMR (400 MHz, $CDCl_3$) δ 7.24 – 7.11 (m, 2H), 7.07 – 6.87 (m, 2H), 5.79 (br, 1H), 5.42 (br, 1H), 3.28 (dd, *J* = 14.3, 7.2 Hz, 1H), 2.63 – 2.29 (m, 2H), 1.30 (d, *J* = 7.0 Hz, 3H); ^{13}C NMR (101 MHz, $CDCl_3$) δ 174.01, 161.45 (d, *J* = 244.2 Hz), 141.43 (d, *J* = 3.2 Hz), 128.17 (d, *J* = 7.8 Hz), 115.34 (d, *J* = 21.1 Hz), 44.89, 36.02, 21.85; *m/z* (ESI–MS) 182.62 $[M + H]^+$.

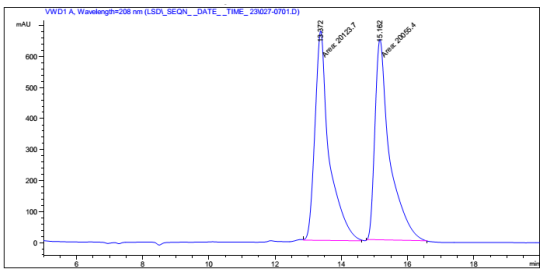

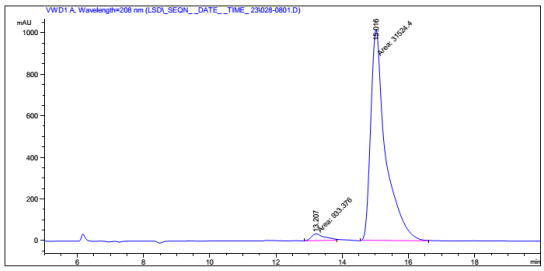

Signal 1: VWD1 A, Wavelength=208 nm

Peak #	RetTime [min]	Type	Width [min]	Area mAU *s	Height [mAU]	Area %
1	13.207	MM	0.4721	933.37561	32.95427	2.8757
2	15.016	MM	0.5176	3.15244e4	1015.01727	97.1243
Totals :				3.24578e4	1047.97154	

(*R*)-3-(4-chlorophenyl)butanamide **2g**

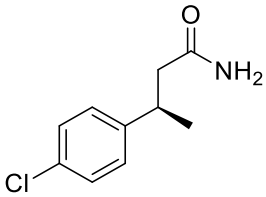

White solid; m.p. = 96-97 ºC; Yield: 95%, 95% ee; $[\alpha]_D^{22}$ = -31.6 (c = 0.2, $CHCl_3$); The enantiomeric excess was determined by HPLC on Chiralpak AD-H column, hexane: isopropanol = 95:5; flow rate = 1 mL/min; UV detection at 208 nm; t_R = 12.3 min (minor), 14.3 min (major); ^{1}H NMR (400 MHz, $CDCl_3$) δ 7.33 – 7.07 (m, 4H), 5.38 (d, *J* = 74.5 Hz, 2H), 3.29 (dd, *J* = 14.3, 7.1 Hz, 1H), 2.43 (m, 2H), 1.31 (d, *J* = 6.9 Hz, 3H); ^{13}C NMR (101 MHz, $CDCl_3$) δ 173.56, 144.23, 132.13, 128.72, 128.17, 44.65, 36.14, 21.66; *m/z* (ESI–MS) 199.45, 201.76 $[M + H]^+$.

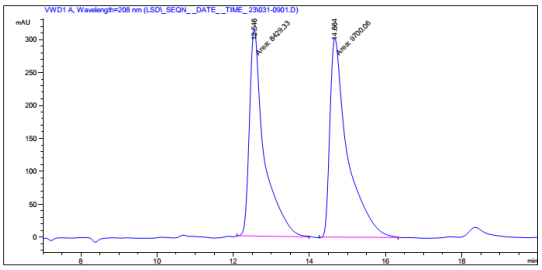

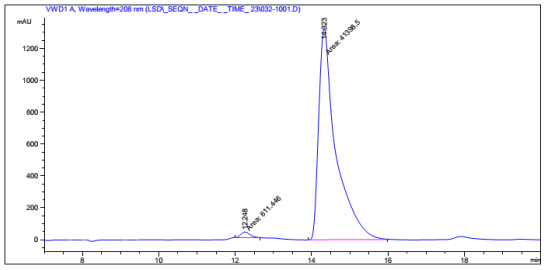

Signal 1: VWD1 A, Wavelength=208 nm

Peak #	RetTime [min]	Type	Width [min]	Area mAU *s	Height [mAU]	Area %
1	12.248	MM	0.2833	611.44568	35.96681	1.4555
2	14.323	MM	0.5203	4.13985e4	1326.08508	98.5445

Totals : 4.20100e4 1362.05190

(*R*)-3-(4-bromophenyl)butanamide **2h**

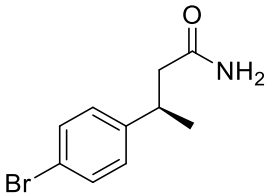

White solid; m.p. = 93-94 ºC; Yield: 61%, 90% ee; $[\alpha]_D^{22}$ = -28.0 (c = 0.2, $CHCl_3$); The enantiomeric excess was determined by HPLC on Chiralpak AD-H column, hexane: isopropanol = 95:5; flow rate = 1 mL/min; UV detection at 208 nm; t_R = 12.8 min (minor), 15.1 min (major); ^{1}H NMR (400 MHz, $CDCl_3$) δ 7.42 (m, 2H), 7.11 (m, 2H), 5.49 (br, 2H), 3.26 (dd, *J* = 14.1, 7.0 Hz, 1H), 2.50 – 2.36 (m, 2H), 1.30 (d, *J* = 6.9 Hz, 3H); ^{13}C NMR (101 MHz, $CDCl_3$) δ 173.68, 144.78, 131.67, 128.58, 120.15, 44.56, 36.19, 21.61; *m/z* (ESI–MS) 243.08, 244.56 $[M + H]^+$.

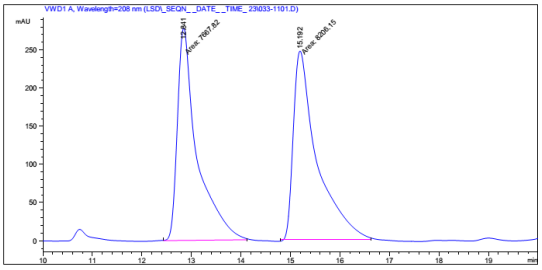

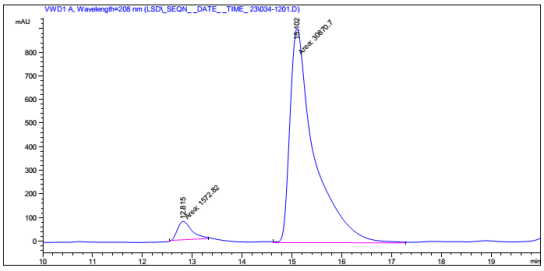

Signal 1: VWD1 A, Wavelength=208 nm

Peak #	RetTime [min]	Type	Width [min]	Area mAU *s	Height [mAU]	Area %
1	12.815	MM	0.3324	1572.82239	78.86093	4.8479
2	15.102	MM	0.5667	3.08707e4	907.83868	95.1521

Totals : 3.24435e4 986.69962

(*S*)-3-phenylheptanamide **2i**

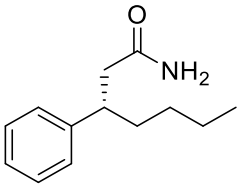

White solid; m.p. = 65-68 ºC; Yield: 31%, 89% ee; $[\alpha]_D^{22}$ = 12.1 (c = 0.1, $CHCl_3$); The enantiomeric excess was determined by HPLC on Chiralpak AD-H column, hexane: isopropanol = 95:5; flow rate = 1 mL/min; UV detection at 208 nm; t_R = 8.8 min (major), 10.9 min (minor); ^{1}H NMR (400 MHz, $CDCl_3$) δ 7.30 (m, 2H), 7.25 – 7.13 (m, 3H), 5.33 (br, *J* = 95.1 Hz, 2H), 3.06 (m, 1H), 2.48 (m, 2H), 1.76 – 1.55 (m, 2H), 1.34 – 1.03 (m, 4H), 0.82 (t, *J* = 7.2 Hz, 3H); ^{13}C NMR (101 MHz, $CDCl_3$) δ 174.19, 144.30, 128.58, 127.45, 126.50, 43.83, 42.64, 35.97, 29.54, 22.57, 13.90; *m*/*z* (ESI–MS) 205.19 $[M + H]^+$.

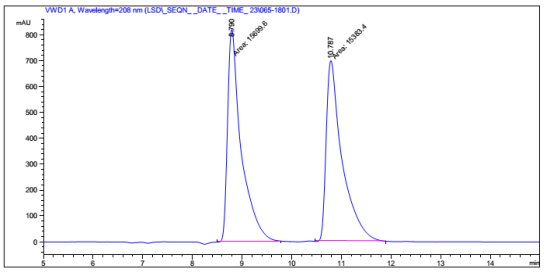

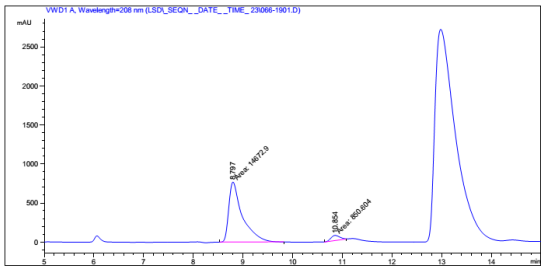

Signal 1: VWD1 A, Wavelength=208 nm

Peak #	RetTime [min]	Type	Width [min]	Area mAU *s	Height [mAU]	Area %
1	8.797	MM	0.3178	1.46729e4	769.49799	94.5205
2	10.854	MM	0.2111	850.60370	67.15005	5.4795
Totals :				1.55235e4	836.64803	

(*R*)-3-(thiophen-2-yl)butanamide **2j**

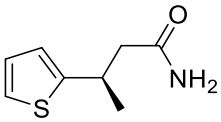

White solid; m.p. = 79-82 ºC; Yield: 94%, 94% ee; $[\alpha]_D^{22}$ = -27.1 (c = 0.2, $CHCl_3$); The enantiomeric excess was determined by HPLC on Chiralpak AD-H column, hexane: isopropanol = 95:5; flow rate = 1 mL/min; UV detection at 208 nm; t_R = 12.1 min (minor), 13.7 min (major); ^{1}H NMR (400 MHz, $CDCl_3$) δ 7.14 (m, 1H), 7.00 – 6.80 (m, 2H), 5.47 (br, 2H), 3.62 (dd, *J* = 14.0, 7.0 Hz, 1H), 2.65 – 2.54 (m, 1H), 2.46 (m, 1H), 1.41 (d, *J* = 6.9 Hz, 3H); ^{13}C NMR (101 MHz, $CDCl_3$) δ 173.50 (s), 149.81 (s), 126.72 (s), 123.19, 123.04, 45.67, 32.32, 22.68; *m*/*z* (ESI–MS) 170.81 $[M + H]^+$.

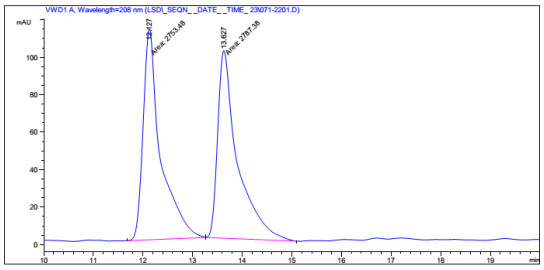

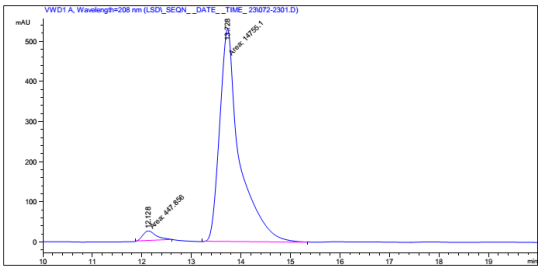

Signal 1: VWD1 A, Wavelength=208 nm

Peak #	RetTime [min]	Type	Width [min]	Area mAU *s	Height [mAU]	Area %
1	12.128	MM	0.3104	447.85587	24.04399	2.9458
2	13.728	MM	0.4641	1.47551e4	529.89001	97.0542

Totals : 1.52030e4 553.93401

(*R*)-3-(naphthalen-2-yl)butanamide **2k**

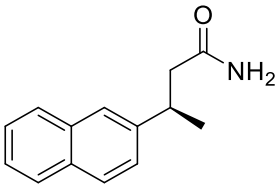

White solid; m.p. = 104-105 ºC; Yield: 98%, 93% ee; $[\alpha]_D^{22}$ = -24.1 (c = 0.2, $CHCl_3$); The enantiomeric excess was determined by HPLC on Chiralpak AD-H column, hexane: isopropanol = 97:3; flow rate = 1 mL/min; UV detection at 208 nm; t_R = 26.9 min (minor), 42.9 min (major); ^{1}H NMR (400 MHz, $CDCl_3$) δ 7.92 – 7.74 (m, 3H), 7.66 (s, 1H), 7.54 – 7.34 (m, 3H), 5.48 (br, 2H), 3.44 (dd, *J* = 14.2, 7.1 Hz, 1H), 2.54 (m, 2H), 1.40 (d, *J* = 6.9 Hz, 3H); ^{13}C NMR (101 MHz, $CDCl_3$) δ 174.20, 143.15, 133.57, 132.34, 128.33, 127.65, 127.60, 126.09 , 125.50, 125.35, 125.06, 44.78, 36.90, 21.76; *m/z* (ESI–MS) 213.29 $[M + H]^+$.

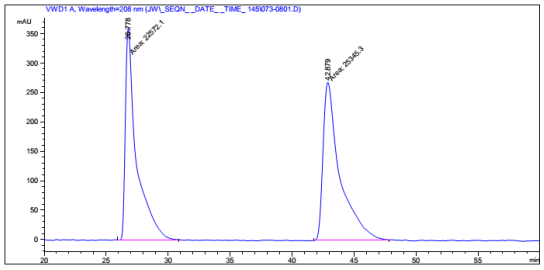

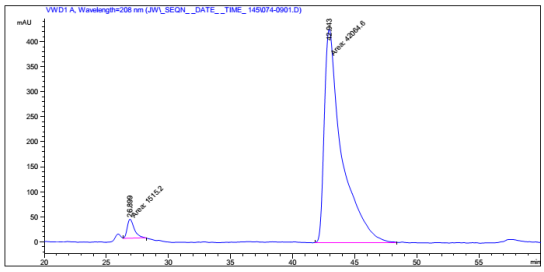

Signal 1: VWD1 A, Wavelength=208 nm

Peak #	RetTime [min]	Type	Width [min]	Area mAU *s	Height [mAU]	Area %
1	26.899	MM	0.6631	1515.20068	38.08642	3.4768
2	42.943	MM	1.6392	4.20646e4	427.68735	96.5232

Totals : 4.35798e4 465.77377

(*R*)-methyl 3-phenylbutanoate **4a**

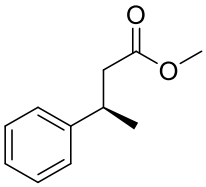

Colorless liquid; Yield: 97%, 96% ee; $[\alpha]_D^{22}$ = -27.3 (c = 0.2, $CHCl_3$); The enantiomeric excess was determined by HPLC on Chiralpak OJ-H column, hexane: isopropanol = 98:2; flow rate = 1.0 mL/min; UV detection at 208 nm; t_R = 14.0 min (major), 17.3 min (minor); ^{1}H NMR (400 MHz, $CDCl_3$) δ 7.33 – 7.27 (m, 2H), 7.24 – 7.17 (m, 3H), 3.62 (s, 3H), 3.28 (dd, *J* = 14.9, 7.1 Hz, 1H), 2.59 (qd, *J* = 15.2, 7.6 Hz, 2H), 1.30 (d, *J* = 7.0 Hz, 3H); ^{13}C NMR (101 MHz, $CDCl_3$) δ 172.85, 145.72, 128.52, 126.72, 126.42, 51.50, 42.75, 36.44, 21.78.

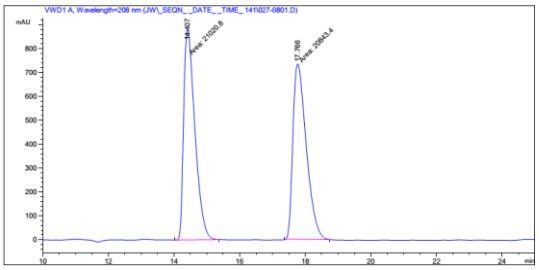

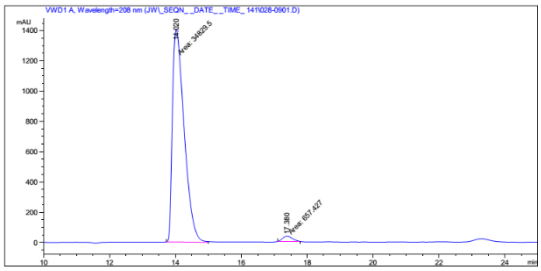

Signal 1: VWD1 A, Wavelength=208 nm

Peak #	RetTime [min]	Type	Width [min]	Area mAU *s	Height [mAU]	Area %
1	14.020	MM	0.4127	3.48295e4	1406.67395	98.1474
2	17.380	MM	0.3325	657.42725	32.95865	1.8526
Totals :				3.54869e4	1439.63260	

(*R*)-methyl 3-(m-tolyl)butanoate **4b**

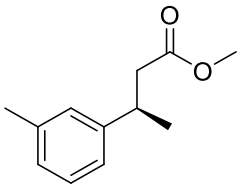

Colorless liquid; Yield: 91%, 97% ee; $[\alpha]_D^{22}$ = -16.1 (c = 0.2, $CHCl_3$); The enantiomeric excess was determined by HPLC on Chiralpak OJ-H column, hexane: isopropanol = 98:2; flow rate = 1.0 mL/min; UV detection at 208 nm; t_R = 9.6 min (major), 11.4 min (minor); ^{1}H NMR (400 MHz, $CDCl_3$) δ 7.18 (m, 1H), 7.02 (m, 3H), 3.63 (s, 3H), 3.24 (dd, *J* = 15.1, 7.0 Hz, 1H), 2.57 (m, 2H), 2.33 (s, 3H), 1.28 (d, *J* = 7.0 Hz, 3H); ^{13}C NMR (101 MHz, $CDCl_3$) δ 172.94, 145.72, 138.05, 128.42, 127.55, 127.18, 123.68, 51.51, 42.75, 36.36, 21.79, 21.49.

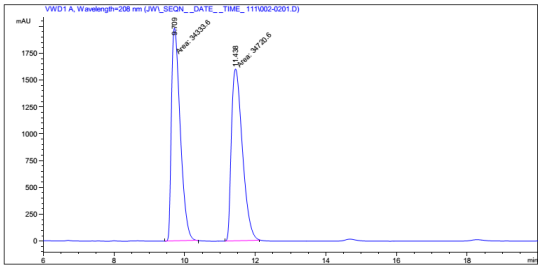

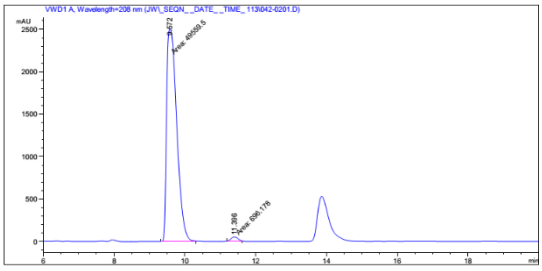

Signal 1: VWD1 A, Wavelength=208 nm

Peak #	RetTime [min]	Type	Width [min]	Area mAU *s	Height [mAU]	Area %
1	9.572	MM	0.3292	4.95595e4	2508.79517	98.6147
2	11.396	MM	0.2350	696.17810	49.37650	1.3853
Totals :				5.02556e4	2558.17166	

(*R*)-methyl 3-(p-tolyl)butanoate **4c**

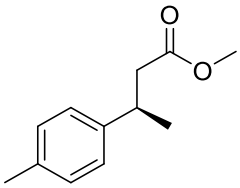

Colorless liquid; Yield: 97%, 95% ee; $[\alpha]_D^{22}$ = -16.8 (c = 0.2, $CHCl_3$); The enantiomeric excess was determined by HPLC on Chiralpak OJ-H column, hexane: isopropanol = 98:2; flow rate = 1.0 mL/min; UV detection at 208 nm; t_R = 14.5 min (major), 16.4 min (minor); ^{1}H NMR (400 MHz, $CDCl_3$) δ 7.11 (s, 4H), 3.62 (s, 3H), 3.25 (m, 1H), 2.57 (m, 2H), 2.31 (s, 3H), 1.28 (d, *J* = 7.0 Hz, 3H); ^{13}C NMR (101 MHz, $CDCl_3$) δ 172.94, 142.72, 135.90, 129.20, 126.58, 51.50, 42.84, 36.03, 21.88, 21.01.

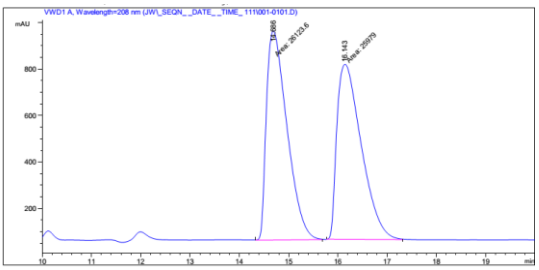

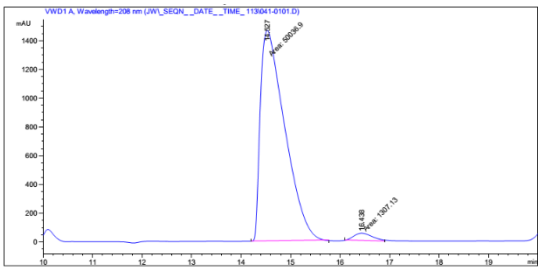

Signal 1: VWD1 A, Wavelength=208 nm

Peak #	RetTime [min]	Type	Width [min]	Area mAU *s	Height [mAU]	Area %
1	14.527	MM	0.5704	5.00369e4	1462.16687	97.4542
2	16.438	MM	0.4320	1307.13208	50.42678	2.5458
Totals :				5.13440e4	1512.59365	

(*R*)-methyl 3-(4-methoxyphenyl)butanoate **4d**

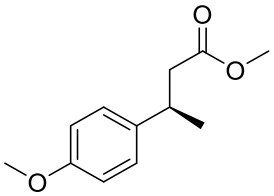

Colorless liquid; Yield: 98%, 95% ee; $[\alpha]_D^{22}$ = -12.4 (c = 0.2, $CHCl_3$); The enantiomeric excess was determined by HPLC on Chiralpak OJ-H column, hexane: isopropanol = 98:2; flow rate = 1.0 mL/min; UV detection at 208 nm; t_R = 23.7 min (major), 31.4 min (minor); ^{1}H NMR (400 MHz, $CDCl_3$) δ 7.21 – 7.08 (m, 2H), 6.91 – 6.79 (m, 2H), 3.78 (s, 3H), 3.62 (s, 3H), 3.23 (m, 1H), 2.55 (m, 2H), 1.27 (d, *J* = 7.0 Hz, 3H); ^{13}C NMR (101 MHz, $CDCl_3$) δ 172.93, 158.08, 137.81, 127.63, 113.86, 77.36, 77.04, 76.72, 55.24, 51.49, 43.01, 35.66, 21.96.

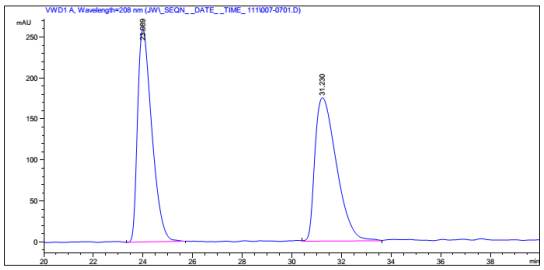

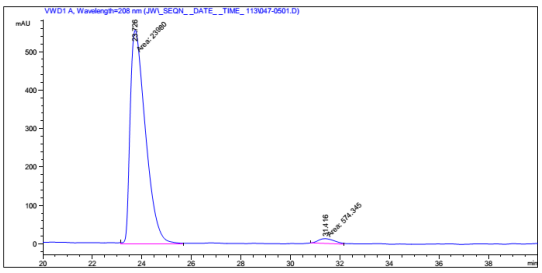

Signal 1: VWD1 A, Wavelength=208 nm

Peak #	RetTime [min]	Type	Width [min]	Area mAU *s	Height [mAU]	Area %
1	23.726	MM	0.7174	2.39800e4	557.07166	97.6609
2	31.416	MM	0.7644	574.34534	12.52320	2.3391
Totals :				2.45544e4	569.59486	

(*R*)-methyl 3-(4-fluorophenyl)butanoate **4e**

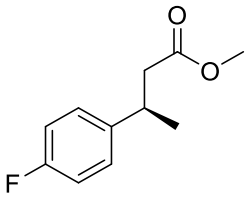

Colorless liquid; Yield: 95%, 97% ee; $[\alpha]_D^{22}$ = -10.9 (c = 0.2, $CHCl_3$); The enantiomeric excess was determined by HPLC on Chiralpak OJ-H column, hexane: isopropanol = 99:1; flow rate = 0.6 mL/min; UV detection at 208 nm; t_R = 19.2 min (major), 20.7 min (minor); ^{1}H NMR (400 MHz, $CDCl_3$) δ 7.23 – 7.14 (m, 2H), 7.03 – 6.93 (m, 2H), 3.62 (d, *J* = 6.9 Hz, 3H), 3.27 (dd, *J* = 14.5, 7.2 Hz, 1H), 2.66 – 2.48 (m, 2H), 1.28 (d, *J* = 7.0 Hz, 3H); ^{13}C NMR (101 MHz, $CDCl_3$) δ 172.65, 161.45 (d, *J* = 244.1 Hz), 141.32, 128.12 (d, *J* = 7.8 Hz), 115.25 (d, *J* = 21.1 Hz), 51.53, 42.85, 35.78, 21.96.

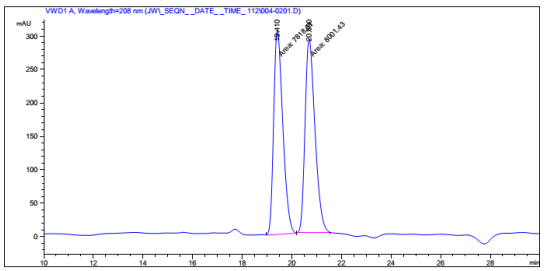

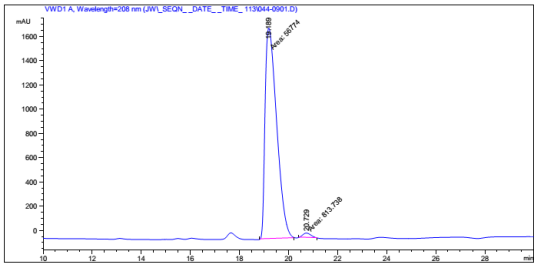

Signal 1: VWD1 A, Wavelength=208 nm

Peak #	RetTime [min]	Type	Width [min]	Area mAU *s	Height [mAU]	Area %
1	19.189	MM	0.5451	5.67740e4	1736.04346	98.5870
2	20.729	MM	0.3745	813.73761	36.21154	1.4130
Totals :				5.75878e4	1772.25499	

(*R*)-methyl 3-(4-chlorophenyl)butanoate **4f**

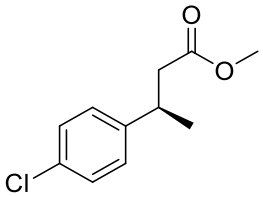

Colorless liquid; Yield: 97%, 97% ee; $[\alpha]_D^{22}$ = -12.7 (c = 0.2, $CHCl_3$); The enantiomeric excess was determined by HPLC on Chiralpak OJ-H column, hexane: isopropanol = 99:1; flow rate = 0.6 mL/min; UV detection at 208 nm; t_R = 19.1 min (major), 20.4 min (minor); ^{1}H NMR (400 MHz, $CDCl_3$) δ 7.34 – 7.27 (m, 2H), 7.25 – 7.19 (m, 2H), 3.62 (s, 3H), 3.28 (dd, *J* = 15.0, 7.0 Hz, 1H), 2.59 (m, 2H), 1.30 (d, *J* = 7.0 Hz, 3H); ^{13}C NMR (101 MHz, $CDCl_3$) δ 172.86, 145.71, 128.52, 126.72, 126.43, 51.51, 42.75, 36.44, 21.78.

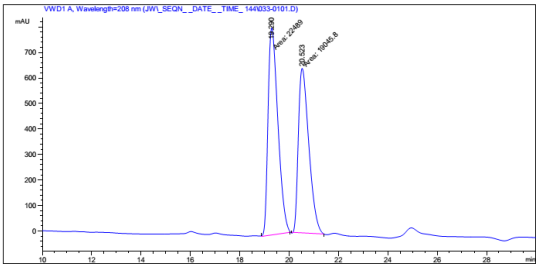

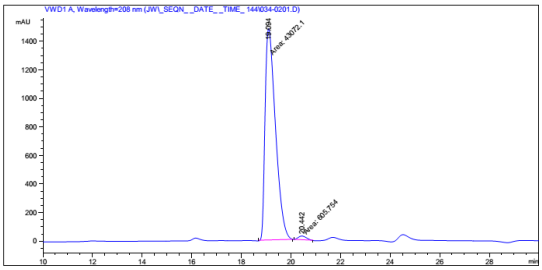

Signal 1: VWD1 A, Wavelength=208 nm

Peak #	RetTime [min]	Type	Width [min]	Area mAU *s	Height [mAU]	Area %
1	19.094	MM	0.4844	4.30721e4	1482.00610	98.6131
2	20.442	MM	0.3806	605.75427	26.52571	1.3869
Totals :				4.36778e4	1508.53181	

(*R*)-methyl 3-(4-bromophenyl)butanoate **4g**

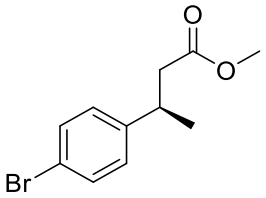

White solid; Yield: 51%, 94% ee; $[\alpha]_D^{22}$ = -16.5 (c = 0.2, $CHCl_3$); The enantiomeric excess was determined by HPLC on Chiralpak OJ-H column, hexane: isopropanol = 99:1; flow rate = 0.6 mL/min; UV detection at 208 nm; t_R = 19.5 min (major), 21.3 min (minor); ^{1}H NMR (400 MHz, $CDCl_3$) δ 7.34 – 7.27 (m, 2H), 7.21 (m, 2H), 3.62 (s, 3H), 3.28 (dd, *J* = 14.6, 7.2 Hz, 1H), 2.59 (m, 2H), 1.30 (d, *J* = 6.9 Hz, 3H); ^{13}C NMR (101 MHz, $CDCl_3$) δ 172.93, 145.72, 128.54, 126.75, 126.44, 51.62, 42.79, 36.46, 21.82.

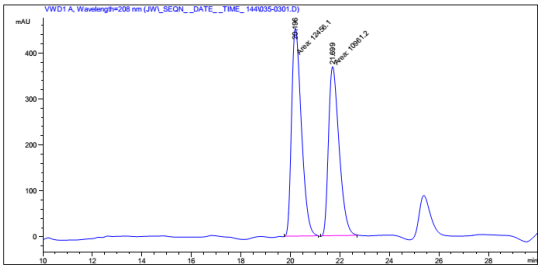

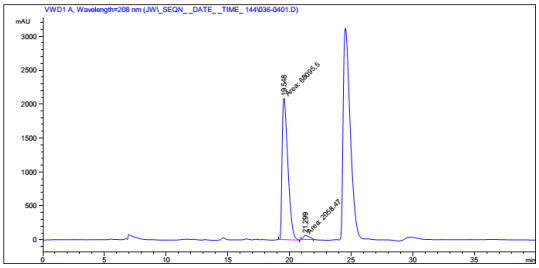

Signal 1: VWD1 A, Wavelength=208 nm

Peak #	RetTime [min]	Type	Width [min]	Area mAU *s	Height [mAU]	Area %
1	19.548	MM	0.5434	6.80955e4	2088.56860	97.0658
2	21.299	MM	0.5588	2058.47192	61.39164	2.9342

Totals : 7.01540e4 2149.96024

(*R*)-methyl 3-(4-(trifluoromethyl)phenyl)butanoate **4h**

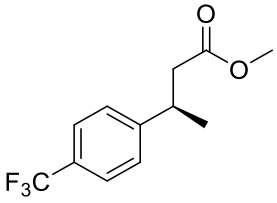

Colorless liquid; Yield: 97%, 96% ee; $[\alpha]_D^{22}$ = -12.2 (c = 0.2, $CHCl_3$); The enantiomeric excess was determined by HPLC on Chiralpak OJ-H column, hexane: isopropanol = 99:1; flow rate = 0.6 mL/min; UV detection at 208 nm; t_R = 11.5 min (major), 12.7 min (minor); ^{1}H NMR (400 MHz, $CDCl_3$) δ 7.56 (m, 2H), 7.34 (m, 2H), 3.62 (s, 3H), 3.35 (dd, *J* = 14.4, 7.2 Hz, 1H), 2.69 – 2.53 (m, 2H), 1.31 (d, *J* = 7.0 Hz, 3H); ^{13}C NMR (101 MHz, $CDCl_3$) δ 172.37, 149.71, 128.77 (dd, *J* = 65.3, 33.1 Hz), 127.14, 125.49 (q, *J* = 3.7 Hz), 51.61, 42.27, 36.29, 21.71.

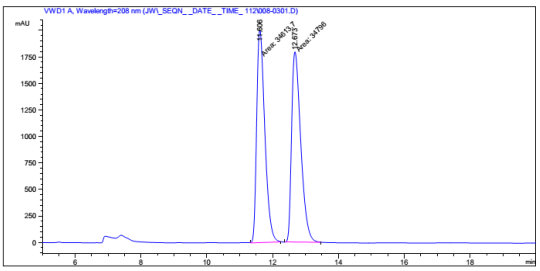

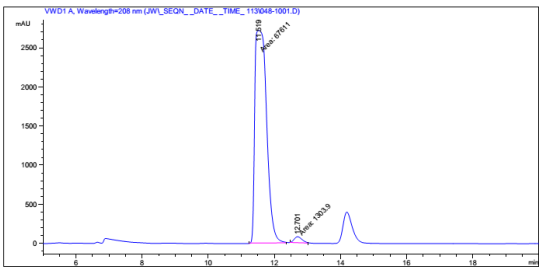

```
Signal 1: VWD1 A, Wavelength=208 nm

Peak RetTime Type  Width     Area      Height     Area
  #   [min]        [min]  mAU   *s   [mAU   ]      %
----|-------|----|-------|----------|----------|--------|
   1  11.519 MM    0.4144 6.76110e4  2719.33838  98.1080
   2  12.701 MM    0.2798 1303.90015   77.66666   1.8920

Totals :                 6.89149e4  2797.00504
```

(*R*)-methyl 3-(thiophen-2-yl)butanoate **4i**

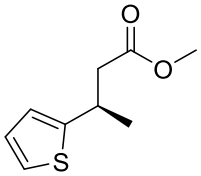

Colorless liquid; Yield: 95%, 96% ee; $[\alpha]_D^{22}$ = -7.2 (c = 0.2, $CHCl_3$); The enantiomeric excess was determined by HPLC on Chiralpak OJ-H column, hexane: isopropanol = 99:1; flow rate = 0.6 mL/min; UV detection at 208 nm; t_R = 22.6 min (major), 26.8 min (minor); ^{1}H NMR (400 MHz, $CDCl_3$) δ 7.13 (m, 1H), 7.00 – 6.70 (m, 2H), 3.78 – 3.52 (m, 4H), 2.63 (m, 2H), 1.38 (d, *J* = 6.9 Hz, 3H); ^{13}C NMR (101 MHz, $CDCl_3$) δ 172.37, 149.64, 126.61, 122.99, 122.88, 51.63, 43.67, 31.96, 22.63.

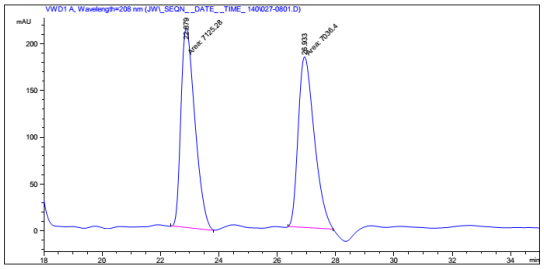

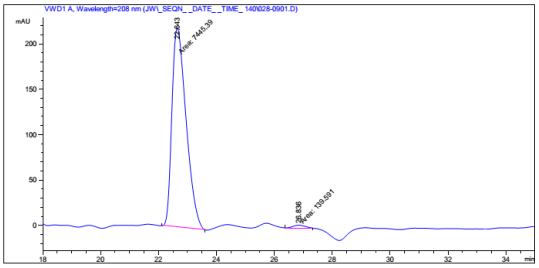

```
Signal 1: VWD1 A, Wavelength=208 nm

Peak RetTime Type  Width     Area      Height     Area
  #   [min]        [min]  mAU   *s   [mAU   ]      %
----|-------|----|-------|----------|----------|--------|
   1  22.643 MM    0.5665 7445.38916  219.05545  98.1596
   2  26.836 MM    0.5814  139.59059    4.00129   1.8404

Totals :                 7584.97975  223.05674
```

(*S*)-methyl 2-(1,2,3,4-tetrahydronaphthalen-1-yl)acetate **4j**

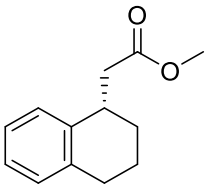

Colorless liquid; Yield: 72%, 96% ee; $[\alpha]_D^{22}$ = 2.1 (c = 0.2, $CHCl_3$); The enantiomeric excess was determined by HPLC on Chiralpak OJ-H column, hexane: isopropanol = 98:2; flow rate = 1.0 mL/min; UV detection at 208 nm; t_R = 7.9 min (major), 11.5 min (minor); ^{1}H NMR (400 MHz, $CDCl_3$) δ 7.20 – 7.01 (m, 4H), 3.71 (s, 3H), 3.35 (m, 1H), 2.84 – 2.66 (m, 3H), 2.60 – 2.49 (m, 1H), 1.95 – 1.64 (m, 4H); ^{13}C NMR (101 MHz, $CDCl_3$) δ 173.29, 139.24, 137.15, 129.31, 128.27, 126.05, 125.84, 51.61, 41.83, 34.55,

29.53, 28.12, 19.48.

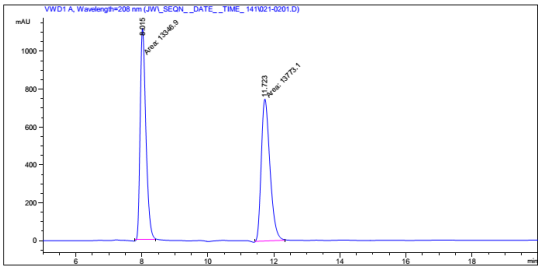

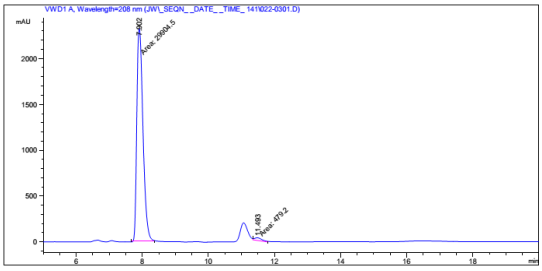

Signal 1: VWD1 A, Wavelength=208 nm

Peak #	RetTime [min]	Type	Width [min]	Area mAU *s	Height [mAU]	Area %
1	7.902	MM	0.2148	2.99045e4	2319.95996	98.4228
2	11.493	MM	0.2709	479.19977	29.47843	1.5772

Totals : 3.03837e4 2349.43839

(*R*)-methyl 3-(naphthalen-2-yl)butanoate **4k**

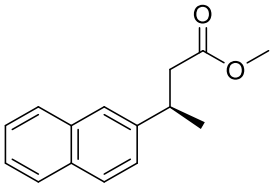

White solid; Yield: 97%, 96% ee; $[\alpha]_D^{22}$ = -19.1 (c = 0.2, $CHCl_3$); The enantiomeric excess was determined by HPLC on Chiralpak OJ-H column, hexane: isopropanol = 99:1; flow rate = 1 mL/min; UV detection at 208 nm; t_R = 42.7 min (major), 51.2 min (minor); ^{1}H NMR (400 MHz, $CDCl_3$) δ 7.94 – 7.75 (m, 3H), 7.65 (s, 1H), 7.52 – 7.33 (m, 3H), 3.61 (s, 3H), 3.45 (dd, *J* = 14.7, 7.2 Hz, 1H), 2.68 (m, 2H), 1.38 (d, *J* = 7.0 Hz, 3H); ^{13}C NMR (101 MHz, $CDCl_3$) δ 172.83, 143.17, 133.59, 132.35, 128.19, 127.68, 127.61, 126.00, 125.48, 125.42, 124.94, 51.55, 42.68, 36.57, 21.82.

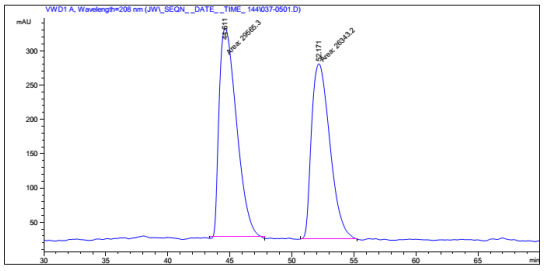

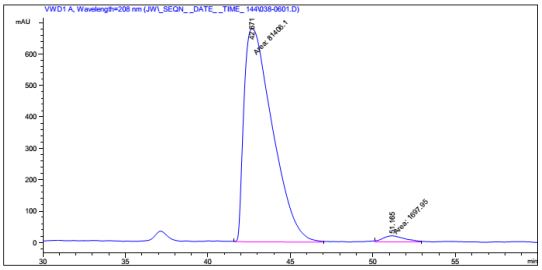

Signal 1: VWD1 A, Wavelength=208 nm

Peak #	RetTime [min]	Type	Width [min]	Area mAU *s	Height [mAU]	Area %
1	42.671	MM	1.9949	8.14061e4	680.13202	97.9568
2	51.165	MM	1.5042	1697.95483	18.81376	2.0432

Totals : 8.31041e4 698.94578

(*R*)-ethyl 3-phenylbutanoate **4l**

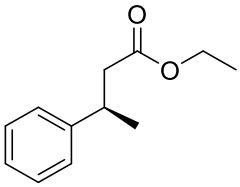

Colorless liquid; Yield: 81%, 95% ee; $[\alpha]_D^{22}$ = -9.0 (c = 0.2, $CHCl_3$); The enantiomeric excess was determined by HPLC on Chiralpak OJ-H column, hexane: isopropanol = 98:2; flow rate = 1.0 mL/min; UV detection at 208 nm; t_R = 11.0 min (major), 12.4 min (minor); ^{1}H NMR (400 MHz, $CDCl_3$) δ 7.40 – 7.12 (m, 5H), 4.07 (q, *J* = 7.1 Hz, 2H), 3.36 – 3.17 (m, 1H), 2.57 (m, 2H), 1.30 (d, *J* = 7.0 Hz, 3H), 1.18 (t, *J* = 7.1 Hz, 3H); ^{13}C NMR (101 MHz, $CDCl_3$) δ 172.41, 145.76, 128.48, 126.78, 126.39, 60.27, 43.01, 36.53, 21.82, 14.18.

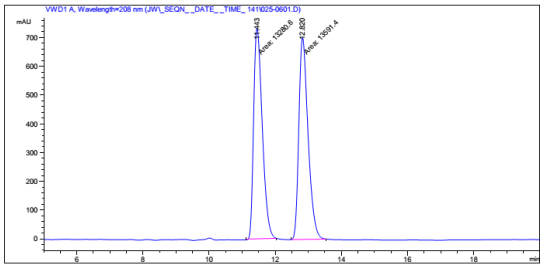

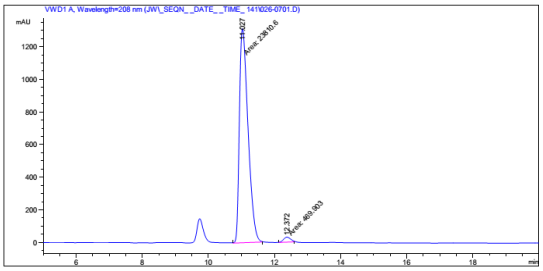

Signal 1: VWD1 A, Wavelength=208 nm

Peak #	RetTime [min]	Type	Width [min]	Area mAU *s	Height [mAU]	Area %
1	11.027	MM	0.3023	2.38106e4	1312.65613	98.0647
2	12.372	MM	0.2540	469.90295	30.83426	1.9353
Totals :				2.42805e4	1343.49039	

1. Pihko, P. M., *Hydrogen Bonding in Organic Synthesis*. Wiley: 2009.

2. Doyle, A. G.; Jacobsen, E. N., Small-Molecule H-Bond Donors in Asymmetric Catalysis. *Chemical Reviews* **2007,** *107* (12), 5713-5743.

3. Taylor, M. S.; Jacobsen, E. N., Asymmetric Catalysis by Chiral Hydrogen-Bond Donors. *Angewandte Chemie International Edition* **2006,** *45* (10), 1520-1543.

4. Schreiner, P. R.; Wittkopp, A., H-Bonding Additives Act Like Lewis Acid Catalysts. *Organic Letters* **2002,** *4* (2), 217-220.

5. Pihko, P. M., Activation of Carbonyl Compounds by Double Hydrogen Bonding: An Emerging Tool in Asymmetric Catalysis. *Angewandte Chemie International Edition* **2004,** *43* (16), 2062-2064.

6. Huynh, P. N. H.; Walvoord, R. R.; Kozlowski, M. C., Rapid Quantification of the Activating Effects of Hydrogen-Bonding Catalysts with a Colorimetric Sensor. *Journal of the American Chemical Society* **2012,** *134* (38), 15621-15623.

7. Walvoord, R. R.; Huynh, P. N. H.; Kozlowski, M. C., Quantification of Electrophilic Activation by Hydrogen-Bonding Organocatalysts. *Journal of the American Chemical Society* **2014,** *136* (45), 16055-16065.

8. Connon, S. J., Organocatalysis Mediated by (Thio)urea Derivatives. *Chemistry – A European Journal* **2006,** *12* (21), 5418-5427.

9. Connon, S. J., Asymmetric catalysis with bifunctional cinchona alkaloid-based urea and thiourea organocatalysts. *Chemical Communications* **2008,** (22), 2499-2510.

10. Fang, X.; Wang, C.-J., Recent advances in asymmetric organocatalysis mediated by bifunctional amine-thioureas bearing multiple hydrogen-bonding donors. *Chemical Communications* **2015,** *51* (7), 1185-1197.

11. Takemoto, Y., Development of Chiral Thiourea Catalysts and Its Application to Asymmetric Catalytic Reactions. *Chemical and Pharmaceutical Bulletin* **2010,** *58* (5), 593-601.

12. Khumsubdee, S.; Burgess, K., Comparison of Asymmetric Hydrogenations of Unsaturated Carboxylic Acids and Esters. *ACS Catalysis* **2013,** *3* (2), 237-249.

13. Kanazawa, Y.; Tsuchiya, Y.; Kobayashi, K.; Shiomi, T.; Itoh, J.-i.; Kikuchi, M.; Yamamoto, Y.; Nishiyama, H., Asymmetric Conjugate Reduction of α,β-Unsaturated Ketones and Esters with Chiral Rhodium(2,6-bisoxazolinylphenyl) Catalysts. *Chemistry – A European Journal* **2006,** *12* (1), 63-71.

14. von Matt, P.; Pfaltz, A., Enantioselective conjugate reduction of α,β-unsaturated carboxamides with semicorrin cobalt catalysts. *Tetrahedron: Asymmetry* **1991,** *2* (7), 691-700.

15. Shang, J.; Han, Z.; Li, Y.; Wang, Z.; Ding, K., Highly enantioselective asymmetric hydrogenation of (E)-[small beta],[small beta]-disubstituted [small alpha],[small beta]-unsaturated Weinreb amides catalyzed by Ir(i) complexes of SpinPhox ligands. *Chemical Communications* **2012,** *48* (42), 5172-5174.

16. Kelly, T. R.; Kim, M. H., Relative Binding Affinity of Carboxylate and Its Isosteres: Nitro, Phosphate, Phosphonate, Sulfonate, and .delta.-Lactone. *Journal of the American Chemical Society* **1994,** *116* (16), 7072-7080.

17. Li, P.; Zhou, M.; Zhao, Q.; Wu, W.; Hu, X.; Dong, X.-Q.; Zhang, X., Synthesis of Chiral β-Amino Nitroalkanes via Rhodium-Catalyzed Asymmetric Hydrogenation. *Organic Letters* **2016,** *18* (1), 40-43.

18. Wen, J.; Tan, R.; Liu, S.; Zhao, Q.; Zhang, X., Strong Bronsted acid promoted asymmetric hydrogenation of isoquinolines and quinolines catalyzed by a Rh-thiourea chiral phosphine complex via anion binding. *Chemical Science* **2016**.

19. Zhao, Q.; Li, S.; Huang, K.; Wang, R.; Zhang, X., A Novel Chiral Bisphosphine-Thiourea Ligand

for Asymmetric Hydrogenation of β,β-Disubstituted Nitroalkenes. *Organic Letters* **2013,** *15* (15), 4014-4017.

20. Zhao, Q.; Wen, J.; Tan, R.; Huang, K.; Metola, P.; Wang, R.; Anslyn, E. V.; Zhang, X., Rhodium-Catalyzed Asymmetric Hydrogenation of Unprotected NH Imines Assisted by a Thiourea. *Angewandte Chemie International Edition* **2014,** *53* (32), 8467-8470.

21. Duan, Y.; Li, L.; Chen, M.-W.; Yu, C.-B.; Fan, H.-J.; Zhou, Y.-G., Homogenous Pd-Catalyzed Asymmetric Hydrogenation of Unprotected Indoles: Scope and Mechanistic Studies. *Journal of the American Chemical Society* **2014,** *136* (21), 7688-7700.

22. Kita, Y.; Yamaji, K.; Higashida, K.; Sathaiah, K.; Iimuro, A.; Mashima, K., Enhancing Effects of Salt Formation on Catalytic Activity and Enantioselectivity for Asymmetric Hydrogenation of Isoquinolinium Salts by Dinuclear Halide-Bridged Iridium Complexes Bearing Chiral Diphosphine Ligands. *Chemistry – A European Journal* **2015,** *21* (5), 1915-1927.

23. de Vries, J. G.; Elsevier, C. J., *The handbook of homogeneous hydrogenation*. Wiley-VCH: 2007.

24. Guillaneux, D.; Zhao, S.-H.; Samuel, O.; Rainford, D.; Kagan, H. B., Nonlinear Effects in Asymmetric Catalysis. *Journal of the American Chemical Society* **1994,** *116* (21), 9430-9439.

25. Wu, R.; Beauchamps, M. G.; Laquidara, J. M.; Sowa, J. R., Ruthenium-Catalyzed Asymmetric Transfer Hydrogenation of Allylic Alcohols by an Enantioselective Isomerization/Transfer Hydrogenation Mechanism. *Angewandte Chemie International Edition* **2012,** *51* (9), 2106-2110.

26. Tang, W.; Wang, W.; Zhang, X., Phospholane–Oxazoline Ligands for Ir-Catalyzed Asymmetric Hydrogenation. *Angewandte Chemie International Edition* **2003,** *42* (8), 943-946.

27. Oi, S.; Taira, A.; Honma, Y.; Inoue, Y., Asymmetric 1,4-Addition of Organosiloxanes to α,β-Unsaturated Carbonyl Compounds Catalyzed by a Chiral Rhodium Complex. *Organic Letters* **2003,** *5* (1), 97-99.

Publications

J. Wen, J. Jiang, X. Zhang. Rhodium-Catalyzed Asymmetric Hydrogenation of α,β-Unsaturated Carbonyl Compounds via Thiourea Hydrogen Bonding. *Org. Lett.* **DOI:** 10.1021/acs.orglett.6b01812

J. Wen, R. Tan, S, Liu, Q. Zhao, X. Zhang. Strong brønsted acid promoted asymmetric hydrogenation of isoquinolines and quinolones catalyzed by a Rh-thiourea chiral phosphine complex via ainon binding. *Chem. Sci.* 2016,**7**, 3047-3051.

L. Yao, **J. Wen**, S. Liu, R. Tan, N. Wood, W. Chen, S. Zhang, X. Zhang. Highly enantioselective hydrogenation of a–oxy functionalized a, b-unsaturated acids catalyzed by a ChenPhos–Rh complex in CF_3CH_2OH. *Chem. Comm.* 2016,**52**, 2273-2276.

Q. Zhao, **J. Wen**, R. Tan, K. Huang, P. Metola, R. Wang, E. V. Anslyn, X. Zhang, Rhodium-Catalyzed Asymmetric Hydrogenation of Unprotected NH Imines Assisted by a Thiourea. *Angew. Chem. Int. Ed.* 2014, **53**, 8467.